論文 / 著書情報
Article / Book Information

題目(和文)	柔軟な立体配座をもつベンゾフェノン誘導体の迅速な不斉制御に基づく自己適応型不斉触媒
Title(English)	Asymmetric catalysts with self-adaptation via instant chirality control of conformetionally mobile (Tropos) benzophenone derivatives
著者(和文)	若林一樹
Author(English)	Kazuki Wakabayashi
出典(和文)	学位:博士（工学）, 学位授与機関:東京工業大学, 報告番号:甲第7169号, 授与年月日:2008年3月26日, 学位の種別:課程博士, 審査員:三上 幸一
Citation(English)	Degree:Doctor of Engineering, Conferring organization: Tokyo Institute of Technology, Report number:甲第7169号, Conferred date:2008/3/26, Degree Type:Course doctor, Examiner:
学位種別(和文)	博士論文
Type(English)	Doctoral Thesis

Asymmetric Catalysts with Self-Adaptation via Instant Chirality Control of Conformationally Mobile (*Tropos*) Benzophenone Derivatives

Department of Applied Chemistry
Graduate School of Science and Engineering
Tokyo institute of Technology

Kazuki Wakabayashi

Tokyo, Japan

Abbreviations

Å	angstrom
Ac	acetyl
aq.	aqueous
Ar	aryl
atm	atmosphere
BINAP	2,2’-bis(diphenylphosphino)-1,1’-binaphthyl
BINOL	1,1'-bi-2-naphthol
BIPHEP	2,2’-bis(diphenylphosphino)-1,1’-biphenyl
BIPOL	1,1'-bi-2-phenol
br	broad
Bu	butyl
Bn	benzyl
°C	degrees Celsius
C	carbon
cat.	catalytic amount
cod	1,5-cyclooctadiene
coe	cyclooctene
Cu	copper
δ	chemical shift in parts per million downfield
d	doublet
DABN	2,2’-diamino-1,1’-binaphthyl
DAIPEN	1,1-bis(4-methoxyphenyl)-3-methylbutane-1,2-diamine
DFT	density functional theory
DMF	*N*,*N*-dimethylformamide
DMSO	dimethylsulfoxide
DPEDA	*N*,*N*’-diphenylethylenediamine
DPEN	1,2-diphenylethylenediamine
DPPF	1,1'-bis(diphenylphosphino)-ferrocene
DuPhos	1,2-bis(phosopholano)benzene
ee	enantiomeric excess
eq.	equivalent
Et	ethyl
ether	diethyl ether
g	gram(s)
GC	gas chromatography
h	hour(s)
HMPT	hexamethylphosphorous triamide
HPLC	high performance liquid chromatography
Hz	hertz
i	iso
IPA	isopropyl alcohol
Ir	iridium
J	coupling constant (in NMR)
LAH	lithium aluminium hydride
m	multiplet (spectral)
M	moles per liter, metal
Me	methyl
min.	minute(s)
mL	milliliter
mol	mole(s)
n	normal
nbd	2,5-norbornadiene
NMR	nuclear magnetic resonance
Pd	palladium
Ph	phenyl
ppm	parts per million
Pr	propyl
Pt	platinum
q	quartet
quant.	quantitative
R	alkyl
Ref.	reference

Rh	rhodium
Ru	ruthenium
r.t.	room temperature
s	singlet
sat.	saturated
t	triplet (spectral)
tert (t)	tertiary
TADDOL	1,1,4,4-tetraphenyl-threitol
Tf	trifluoromethanesulfonyl
THF	tetrahydrofuran
TLC	thin layer chromatography
t_R	retention time
UV	ultraviolet
Xyl	xylyl

Table of Contents

1-1. Introduction

Homogeneity in chirality, either right- or left-handed biomolecules, has been recognized as a fundamental principle in Nature.[1] The scenario of successive evolution, proposed by Pearson, suggests that molecular formations at the beginning of evolution might involve a nonracemic composition via "symmetry breaking" of racemic primitive earth, and subsequent evolutional processes account for the appearance of an excess of molecules with homochirality.[2] A homogeneous chirality sense in Nature is the key for the quest of molecular evolution. The fundamental question about the generation of homo-chirality in Nature has long received widespread attention.

Although various theoretical models for spontaneous amplification of chirality have been proposed,[3] experimental evidence of that has been limited. In 1848, Pasteur found that a racemic mixture of sodium ammonium tartrate made up a conglomerate of 1 : 1 mixture of two enantiomers by a crystallization (Scheme 1-1).[4] The spontaneous resolution of racemic compounds was a pioneering work for spontaneous generation of optical activity without any chiral bias and was used as a method to resolve racemic amino acids synthesized.[5]

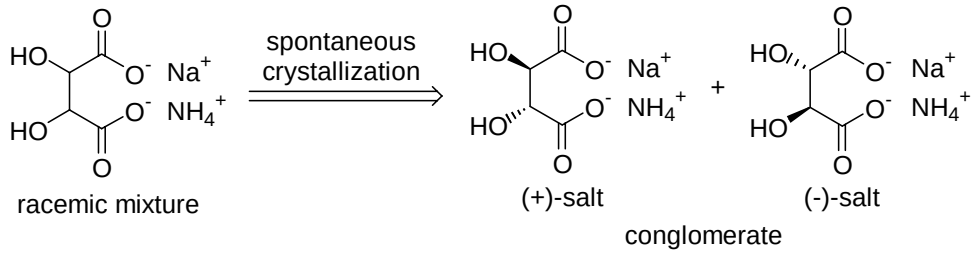

Scheme 1-1.

Crystallization of achiral compounds, not racemic compounds, has also been reported.[6] Phenol is one of the typical examples of the achiral compounds and can not adopt a chiral conformation in a solution phase. However, hydrogen bonding between phenols was formed in a crystalline phase, and the hydrogen bonding chain adopted a chiral helical conformation with a pitch of 5.97 Å (Scheme 1-2).[7] Similarly, Koshima and co-workers has reported that 3-indolepropionic acid adopt a helix conformation in a crystalline phase.[8] In the crystal lattice of 3-indolepropionic acid, hydrogen bonding between the N-H of indole ring and the O=C group of a next 3-indolepropionic acid was formed, and the hydrogen bonding chain adopted a chiral helical conformation. In addition,

3-indolepropionic acid was confirmed to form double helix in a crystalline phase.

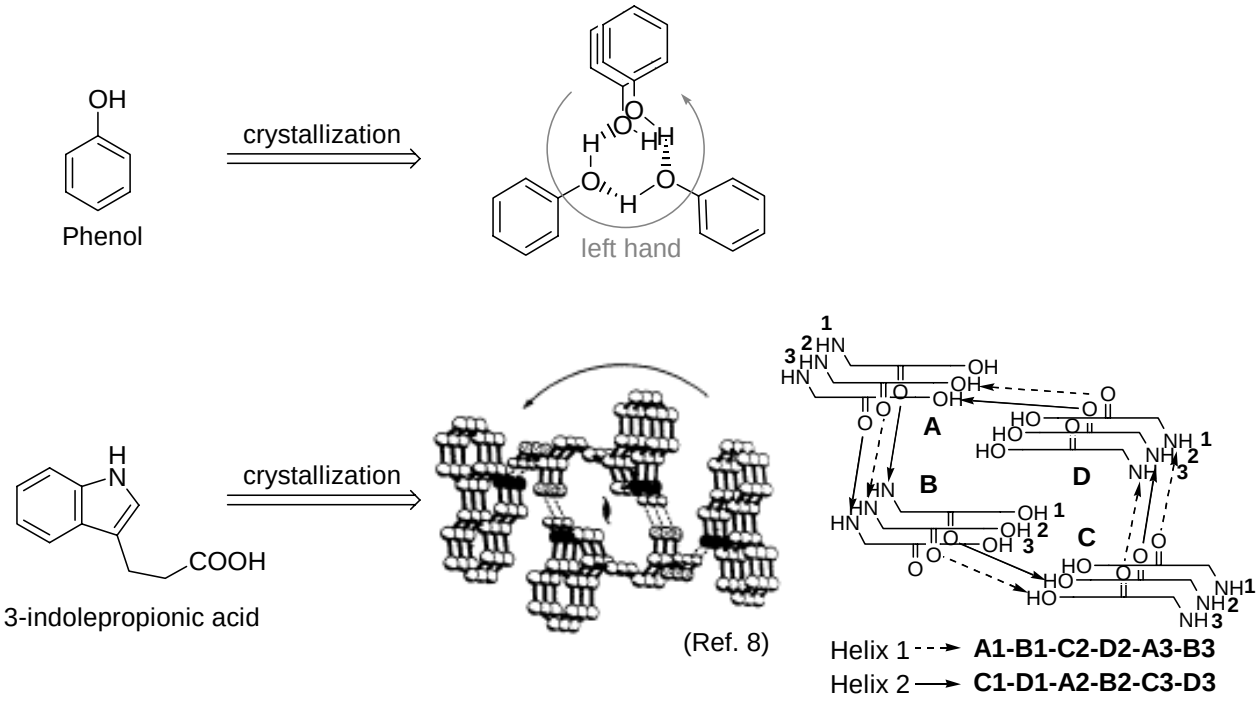

Scheme 1-2.

Pincock and co-workers have reported the spontaneous generation of optical activity in the crystallization of racemic 1,1'-binaphthyl (Scheme 1-3).[9] The rotation of 1,1'-binaphthyl which interconverts between enantiomers is only moderately hindered ($t_{1/2}$ = *ca*. 15 min at 50 °C). However, crystallization of melted (±)-1,1'-binaphthyl at 150 °C formed a chiral crystal with a specific rotation of 42°. At 150 °C, melted 1,1'-binaphthyl interconverts between the enantiomers, but the highly stereospecific character of the solid state promotes the development of optically active crystal. Similarly, Williams and co-workers have reported C_3-symmetry tri-*o*-thymolide to form a chiral crystal. At room temperature, tri-*o*-thymolide interconverts between the enantiomers slowly ($t_{1/2}$ = 2.4 min at 21 °C). Similar to melted (±)-1,1'-binaphthyl, achiral tri-*o*-thymolide adopted a chiral propeller conformation in a crystalline phase.[10]

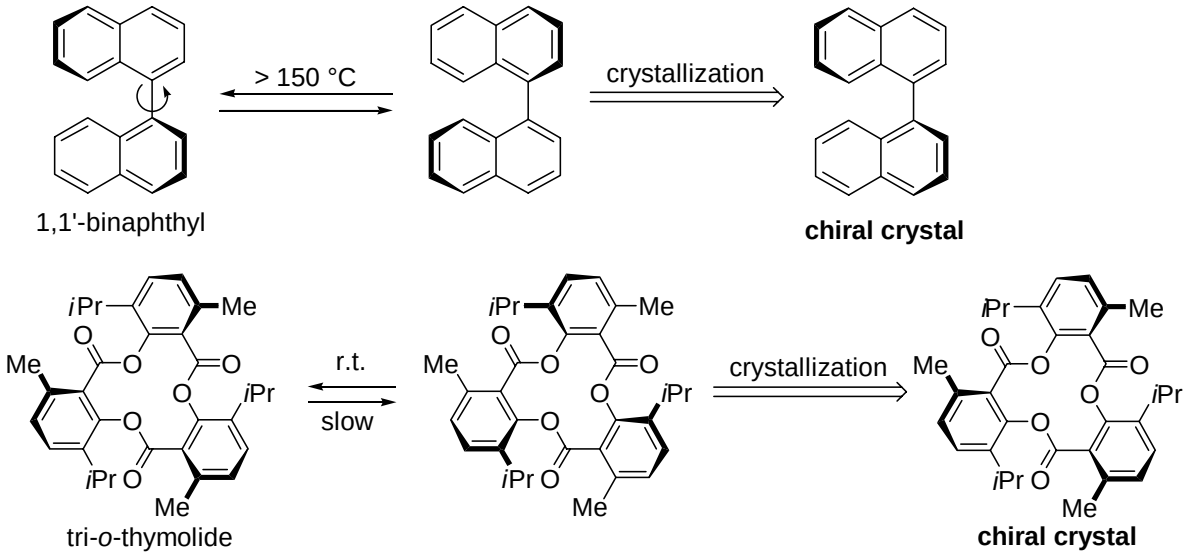

Scheme 1-3.

The chiral 1,1'-binaphthyl, which is obtained by crystallization, have moderately hindered rotations and the solution keeps the specific rotation at room temperature. On the other hand, molecules with free rotational single bond, such as butane and benzophenone, are conformationally mobile in a solution phase due to rapid interconversion between several conformations at room temperature (Scheme 1-4). Just like a gauche conformation of butane, however, some conformations of flexible compounds adopt chirality.

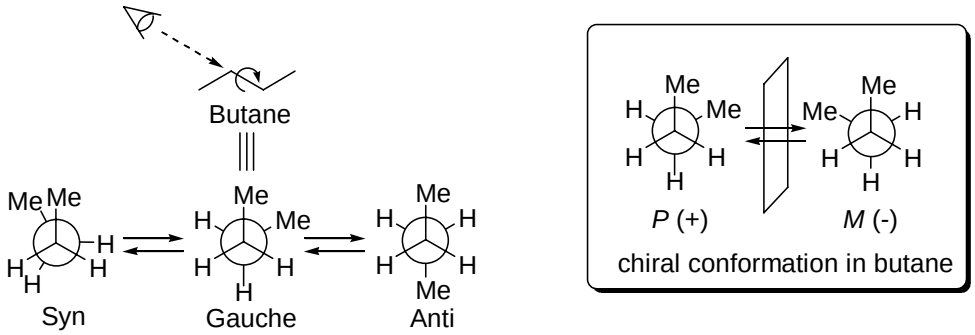

Scheme 1-4.

Different from 1,1'-binaphthyl with one single bond rotation, benzophenone has two free rotational single bonds and interconverts more rapidly between the chiral conformations (Scheme 1-5). In addition, benzophenone-derived compounds have been reported to adopt C_1, C_2-syn and C_2-anti conformations.[11] The most stable conformation of benzophenone-derived compounds depended on

functional groups (X and R) (Scheme 1-5).

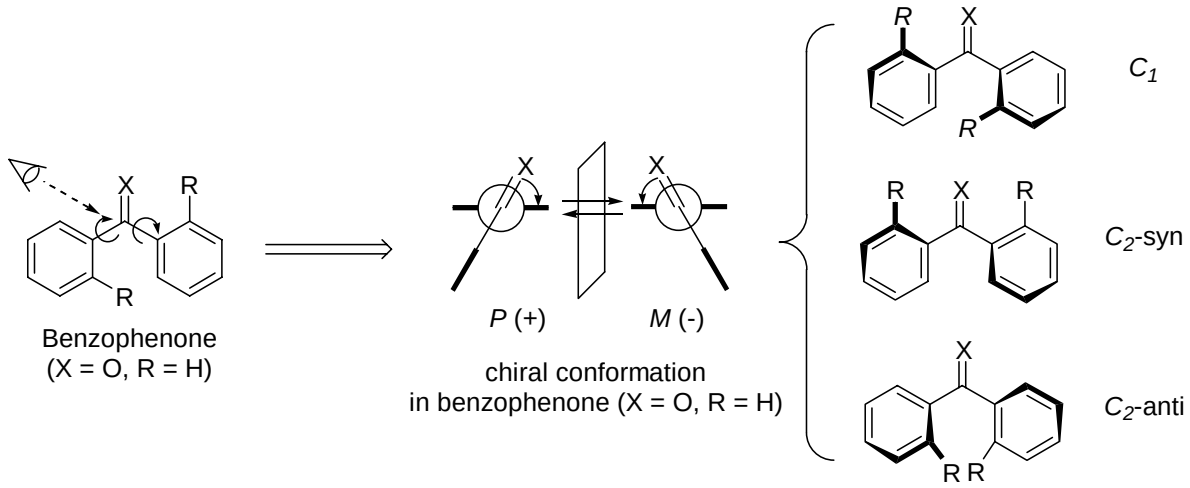

Scheme 1-5.

The optical activity in the crystallization of achiral molecules can generate an external chiral bias and evidence the symmetry breaking in Nature, categorized as abiotic. The abiotic theories are classified into a "chance mechanism" to generate an optically active molecule randomly, such as spontaneous resolution of racemic compounds, and a "determining mechanism" to favor one enantiomer by internal or external chiral bias. Based on the determining mechanism concept of the symmetry breaking, asymmetric catalysis with achiral compound to generate an optically activity by the internal or external chiral bias can be used as asymmetric catalysts. Therefore, generation of chirality in conformationally mobile compounds is considered as one of the most intriguing topics in asymmetric catalysts.

1-2. Chirality of conformationally mobile (*tropos*) compounds

As descried in Section 1-1, conformationally mobile compounds, such as butane- and benzophenone-derived compounds, possess chiral conformations. These compounds can be controlled to a single chiral conformation in a crystalline phase. Toda, Kuroda and co-workers have reported to obtain a chiral conformation of butane-derived compound by crystallization within host molecule.[12] The crystalline complex of 1,2-dichloroethane with (*S*)-2-bromo-3,3a,8-triphenyl-1,3a-

dihydrocyclopenta[α]indene-1-one could be obtained in a chiral gauche conformation of 1,2-dichloroethane (Scheme 1-6).

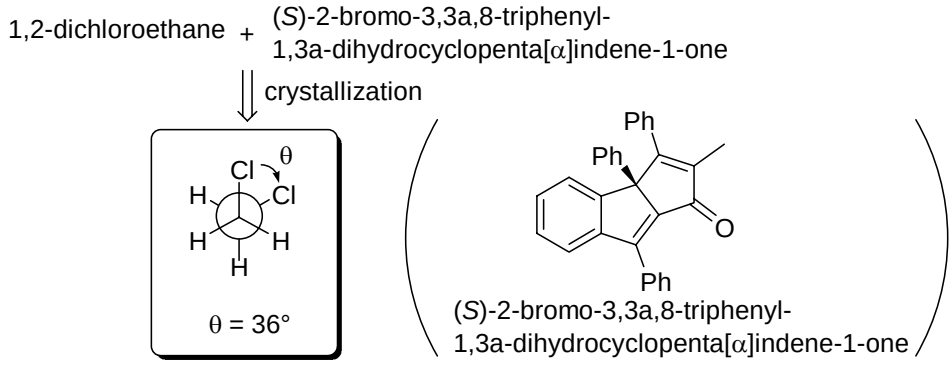

Scheme 1-6.

Similarly, benzophenone has been reported to form optically active crystals with component molecules frozen in a chiral conformation (Scheme 1-7).[13] The crystallization with cholic acid led benzophenone to three chiral conformations, because of two free rotational single bonds of benzophenone.

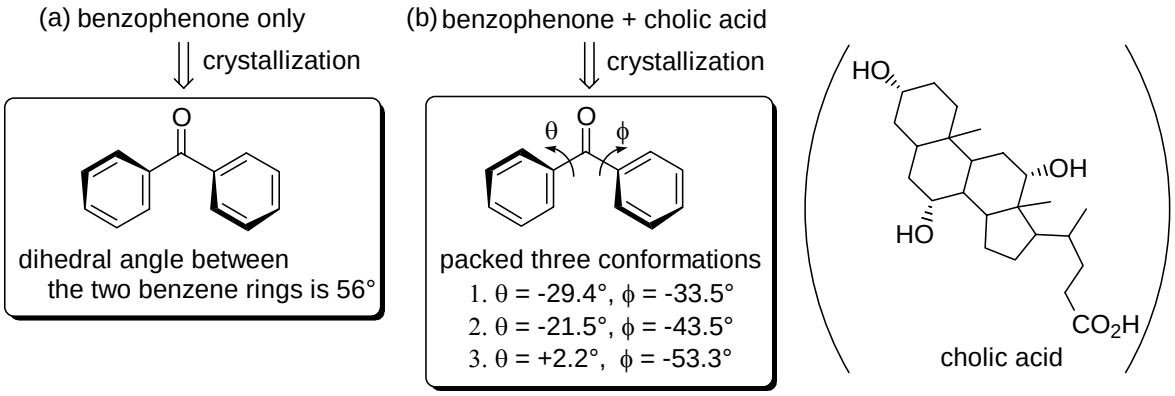

Scheme 1-7.

Flipping equilibrium of carbocyclic compounds can also be frozen in one optical conformer by crystallization. Toda and co-workers have reported that cycloocta-2,4-dien-1-one, which existed as an equilibrium mixture in a solution phase. Cycloocta-2,4-dien-1-one was controlled in a single conformation by crystallization with (-)-1,6-di(*o*-chlorophenyl)-1,6-diphenylhexa-2,4-diyne-1,6-diol (Scheme 1-8).[14] In addition, irradiation of the optically active crystal for 48 h gave

tricyclo[8.6.0.0^{2,9}]-hexadeca-7,11-diene-3,16-dione in 55% yield with 78% *ee* (-). Irradiation of cycloocta-2,4-dien-1-one in pentane for 1 h gave the racemic product in 10% yield along with polymeric materials. Compared to a solution phase, the photoreaction in a crystalline phase proceeded more efficiently and enantioselectivity.

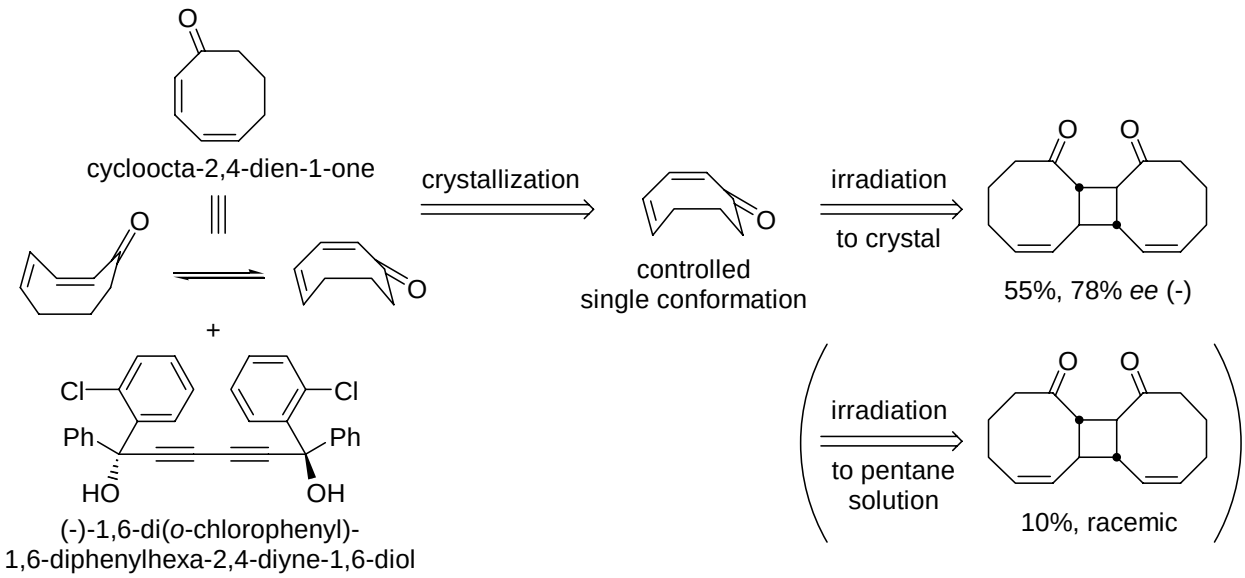

Scheme 1-8.

Molecules with a chiral conformation in a crystalline phase can be used in the synthesis of asymmetric catalysts. Balavoine and co-workers have reported that 1,1'-diphenyl-3,3',4,4'-tetramethyl-2,2'-biphosphole (BIPHOS), which has the instable axial chirality and central chiralities on phosphorous atoms, crystallizes as a conglomerate; each enantiomer crystallizes independently.[15] The single crystal in a rather large scale could be used in the synthesis of the optically pure complex $PdCl_2$(biphos) (Scheme 1-9).[15b,15c]

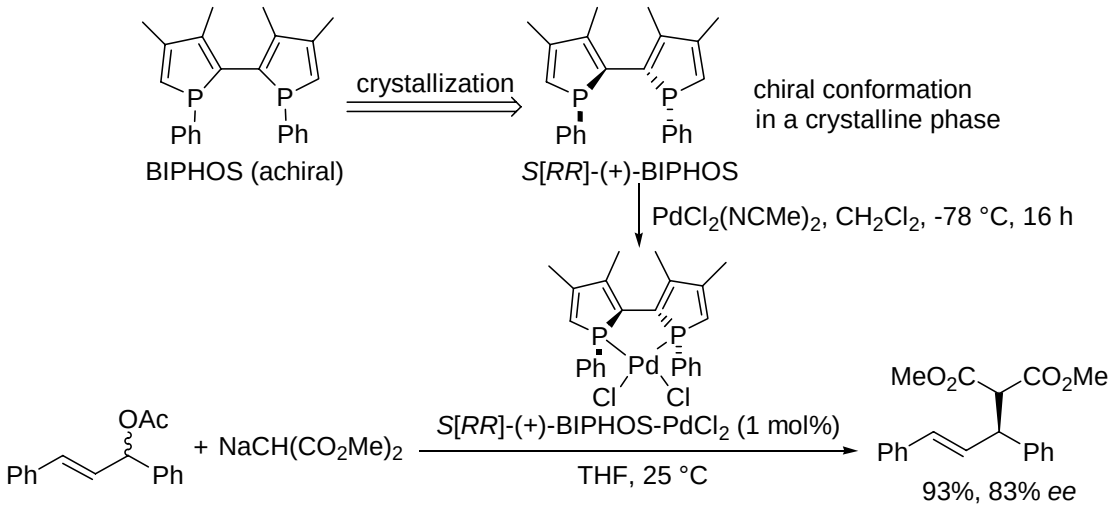

Scheme 1-9.

To prevent the racemization of the Pd complex, the complexation was carried out at -78 °C. The optical pure $PdCl_2$(biphos) complex was optically stable at room temperature to attain high enantioselectivity in asymmetric allylic substitution of 1,3-diphenyl-prop- 2-enyl acetate with sodium dimethyl malonate.

Helically chiral polymers obtained from achiral monomers can also be used as chiral catalysts. Reggelin and co-workers have reported asymmetric reactions with chiral polymer synthesized from achiral triaryl monomers and chiral initiator (Scheme 1-10).[16] Achiral monomers **1** and **2** rapidly isomerized, but chiral copolymer p(**1**-co-**2**) adopted a single-handed helical configuration initiated by a chiral lithium complex. The value of specific optical rotation decreased very slowly with time at room temperature, proving an almost stable helical conformation in a solution phase. The pyridine parts of **1** in copolymer had a chance to complex in a bidentate fashion. The Pd complex with the chiral copolymer p(**1**-co-**2**) was used in asymmetric allylic substitution to give the product in 99% yield with 60% *ee*.

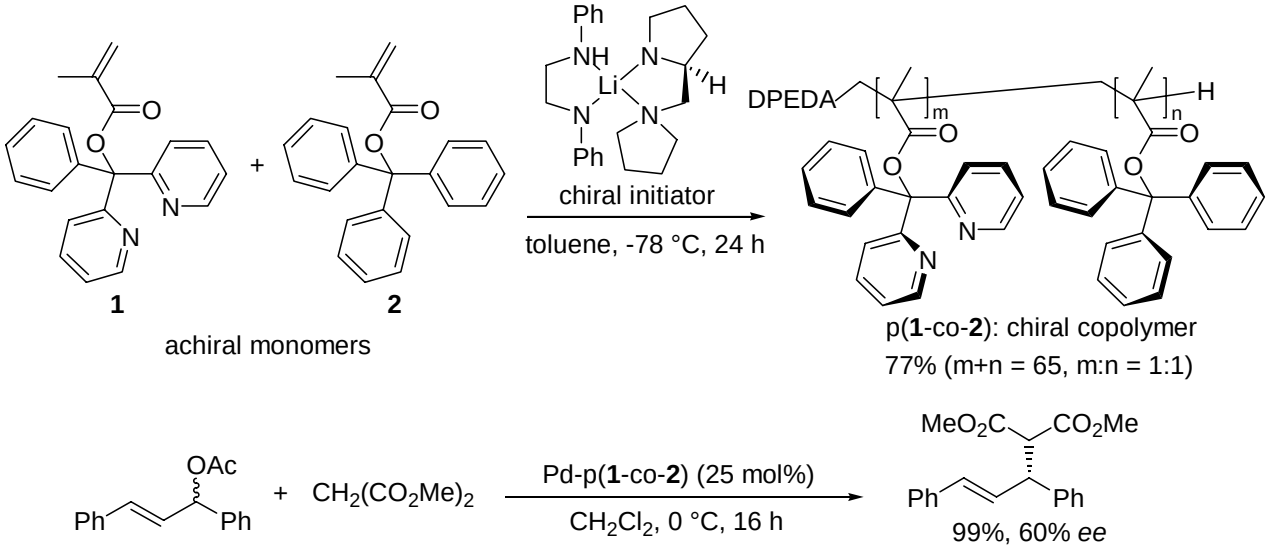

Scheme 1-10.

1-3. Chirality control of *tropos* ligands

BINOL and BINAP, which provide high catalytic activity and enantioselectivity in asymmetric catalysts, are enantiopure and atropisomeric ligands. "Atropisomerism" was coined by Kuhn[17] to cover isomerism caused by blocking the internal turn around a single bond. The word '*atropos*' originated from Greek word and consists of '*a*' meaning 'not' and '*tropos*' meaning 'turn' in Greek. The discovery of atropisomeric biphenyls antedated by several years the concept of conformation[18] and the discovery of the rotational barrier in ethane.[19]

As described in Section 1-2, conformationally mobile compounds can be controlled in a single chiral conformation in particular situations, such as in a crystalline phase or copolymer. The chirally controlled compounds can be used even as ligands for asymmetric catalysts. Including these ligands, the conformationally and chirally flexible nature of a ligand, such as BIPOL, BIPHEP, and DPPF, may be called '*tropos'* (Scheme 1-11).[20] Chiral conformations in *tropos* ligands rapidly interconvert.

Chirally flexible ligands (*tropos*)

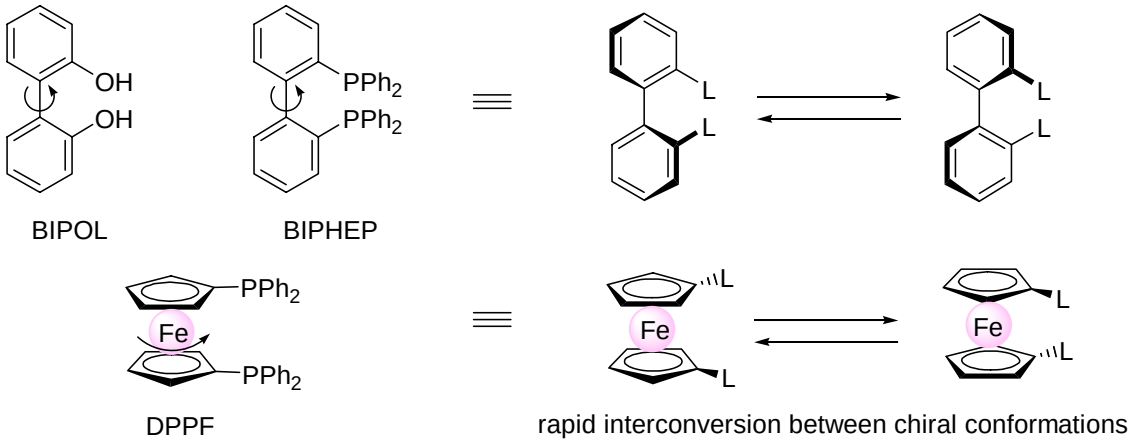

Scheme 1-11.

In terms of dynamic behavior of a ligand around chiral axis, planar, helix, and center, the conformationally and chirally rigid nature of a ligand may thus be called '*atropos*' (Scheme 1-12).

Chirally rigid ligands (*atropos*)

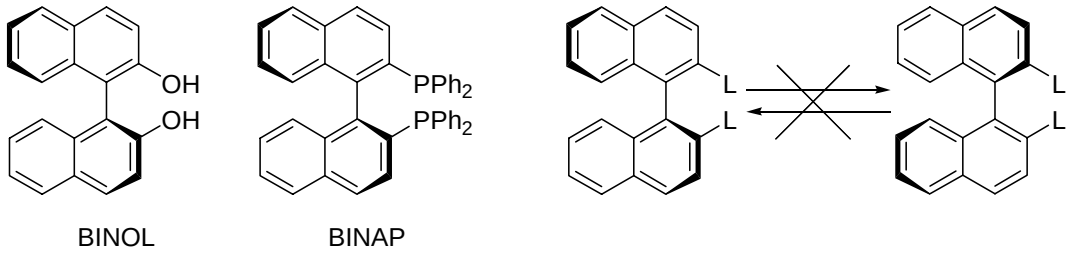

Scheme 1-12.

Generally, asymmetric catalysts are composed of metal complexes with chiral *atropos* ligands and provide high catalytic activity and enantioselectivity in asymmetric reactions.[21]

However, a *tropos* complex with a chiral additive, which we call a chiral activator[22] (Act* in Scheme 1-13); 1:1 ratio of diastereomers can be isomerized to a single diastereomer. The single diastereomer thus obtained can be used as an asymmetric catalyst even in a solution phase (Scheme 1-13, chirality control). A chiral activator also increases the catalytic activity and enantioselectivity of the parent catalyst in asymmetric reactions. That is to say, a chiral activator plays two roles of (1) chirality control and (2) increase in the catalytic activity and enantioselectivity of parent catalysts.

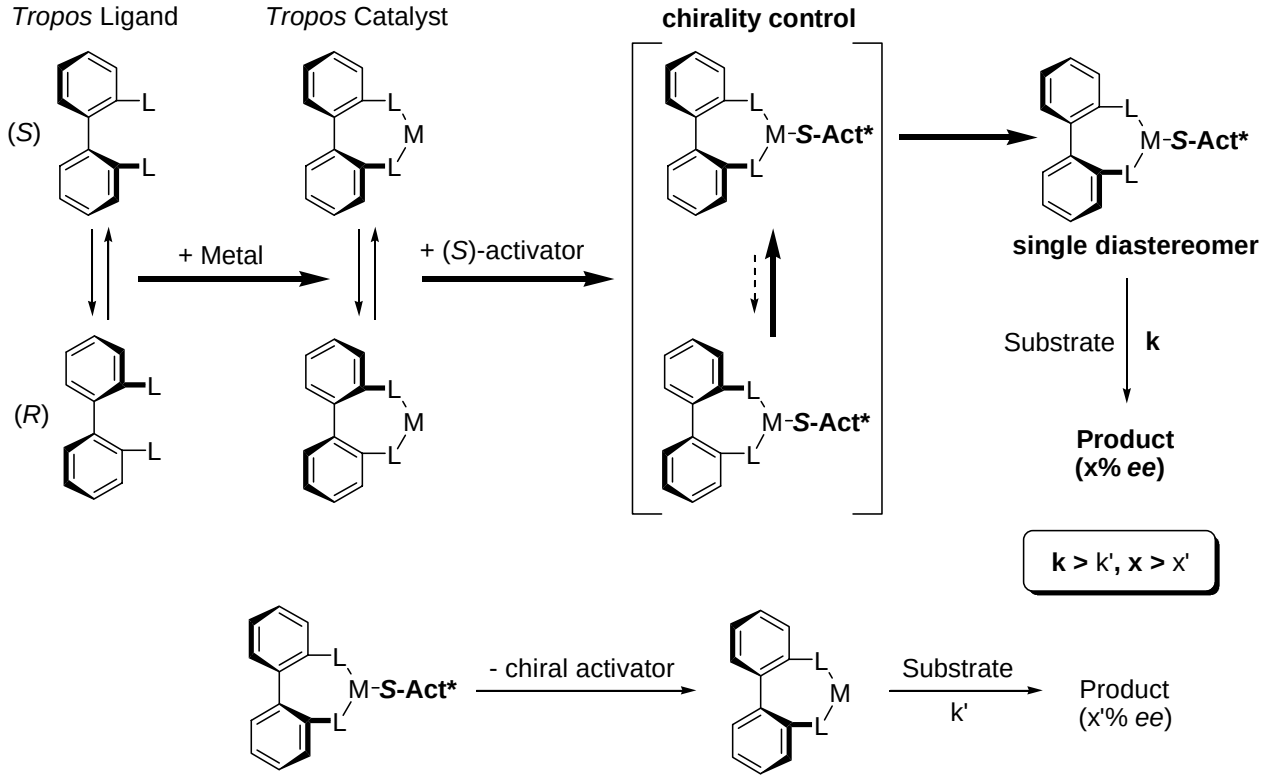

Scheme 1-13.

Mikami and co-workers have reported catalytic asymmetric reactions with *tropos* biphenol (BIPOL) that replaced the enantiopure form of *atropos* BINOL. The chiral titanium catalysts by self-assembly of TADDOL-BINOL combination exhibited the high catalytic activity and enantioselectivity through asymmetric activation.[23] In the *tropos* BIPOLate-Ti catalyst, chiral TADDOL controls the chirality of the *tropos* BIPOL ligand to give high enantioselectivity. Actually, the chirality of BIPOLate-Ti/TADDOL catalyst could be controlled and the chirally controlled catalyst gave alcohol product in methylation with high enantiomeric excess (Scheme 1-14).[24] The introduction of sterically bulky 3,3'-substituents led to an increase in enantioselectivity. Particularly, 3,3'-dimethoxy derivative provided virtually complete enantioselectivity (>99% *ee*).

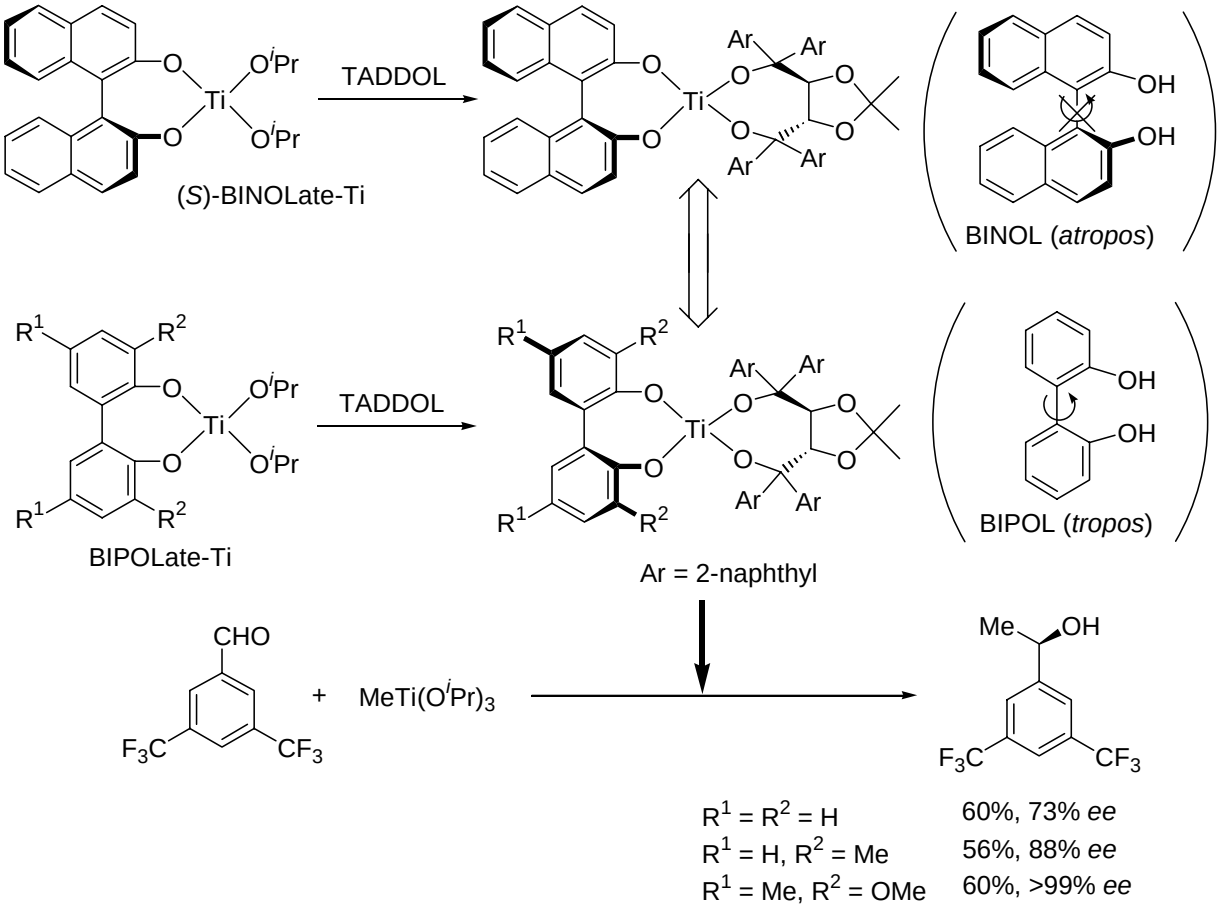

Scheme 1-14.

Mikami and co-workers have also reported that metal complexes with *tropos* BIPHEP[25] could be controlled in chiral conformations upon addition of chiral activators. Chiral activators can control the conformation of BIPHEP complexes in a solution phase and stabilize the chirality of BIPHEP. The BIPHEP complexes chirally controlled attained higher catalytic activity and enantioselectivity in asymmetric reactions. Some of the BIPHEP complexes chirally controlled kept the chirality even after dissociation of chiral activators.

Aikawa in Mikami's group has reported the chirality control of BIPHEP-Pd complex. The complexation of racemic BIPHEP-Pd complex with one equivalent of (*S*)-DABN resulted in the formation of diastereomer mixture of (*S*)-BIPHEP-Pd/ (*S*)-DABN and (*R*)-BIPHEP-Pd/(*S*)-DABN complexes in a 1 : 1 ratio. The BIPHEP-Pd/(*S*)-DABN complex did not isomerize at room temperature even after 3 days, but did at 80 °C after 8 h to afford the favorable (*S*)-BIPHEP-Pd/(*S*)-DABN complex exclusively.[26] The single diastereomer (*S*)-BIPHEP-Pd/(*S*)-DABN complex

thus obtained could be used as an activated asymmetric catalyst for C-C bond forming reactions such as the hetero Diels-Alder reactions at room temperature (Scheme 1-15). In case of the hetero Diels-Alder reaction with (*S*)-BIPHEP-Pd catalyst dissociated (*S*)-DABN, the catalytic activity and enantioselectivity of the Pd catalyst were decreased.

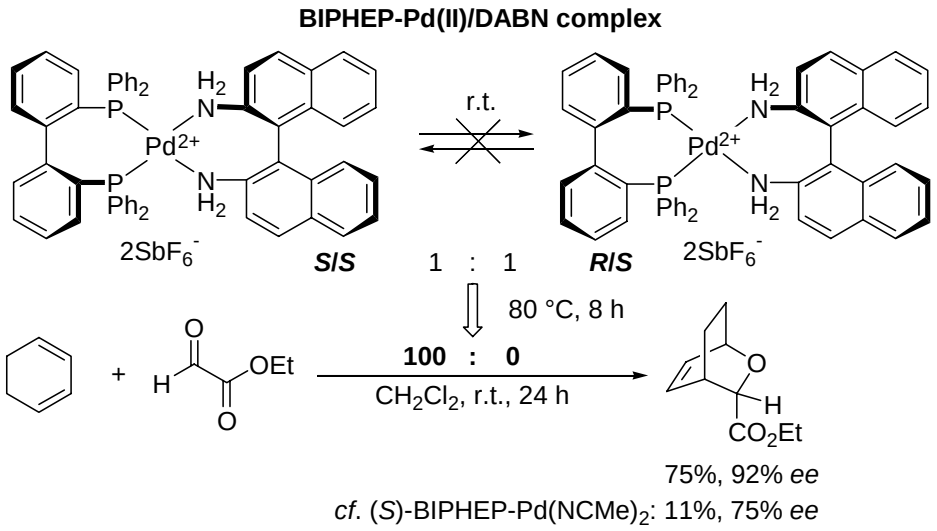

Scheme 1-15.

Not only Pd complex, but also Pt, Rh and Ru complexes with BIPHEPs were examined in their chirality control for catalytic asymmetric reactions. BIPHEP-Rh complex isomerized to a single diastereomer upon addition of (*S*)-DABN.[27a] The diastereopure (*S*)-DM-BIPHEP-Rh/(*S*)-DABN complex could be used as an asymmetric catalyst for ene-type cyclizations of 1,6-enyne substrates by addition of trifluoromethanesulfonic acid (TfOH) to protonate the (*S*)-DABN (Scheme 1-16). During the ene-type cyclizations at 5 °C, racemization of DM-BIPHEP-Rh complex did not proceed at all.

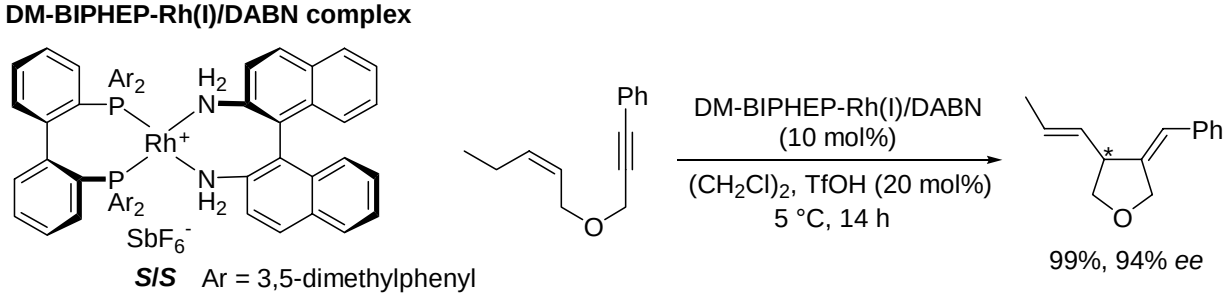

Scheme 1-16.

(*S*)-NOBIN has also been reported to control the chirality of BIPHEP-Rh complex (Scheme 1-17).[28b] BIPHEP-Rh complex could be instantly controlled by (*S*)-NOBIN to give the (*R*)-BIPHEP-Rh/(*S*)-NOBIN diastereomer (82% selectivity) at room temperature. The (*R*)-BIPHEP-Rh/(*S*)-NOBIN complex thus obtained could be used as an asymmetric catalyst for ene-type cyclizations of 1,6-enyne substrates without protonation of (*S*)-NOBIN. In case of (*S*)-DM-BIPHEP-Rh/(*S*)-DABN catalyst with TfOH, asymmetric cyclization of acid-labile *p*-methoxy substrate afforded low yield (22%, 93% *ee*). In sharp contrast the cyclization with BIPHEP-Rh/(*S*)-NOBIN catalyst proceeded without TfOH to give 70% yield and 98% *ee*.

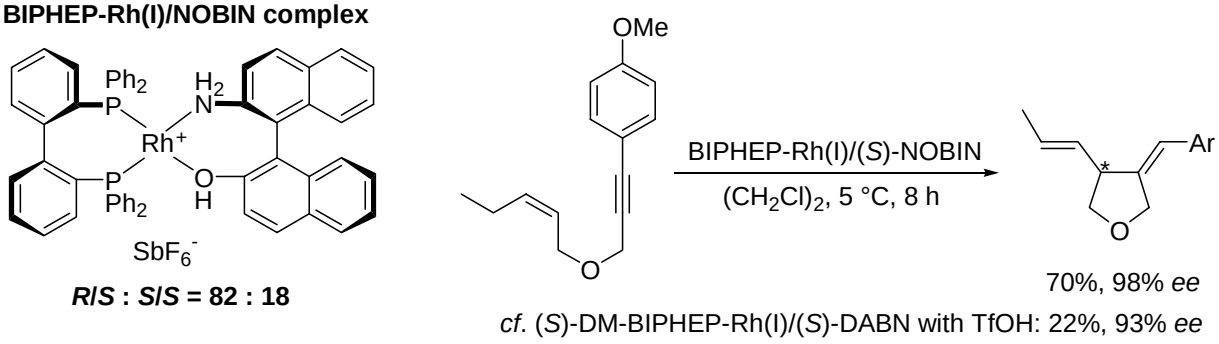

Scheme 1-17.

Korenaga and co-workers in the Mikami group has reported the chirality control of BIPHEPs-Ru complex with (*S*,*S*)-DPEN.[28] 1:1 Diastereomer ratio of (*S*)- and (*R*)-DM-BIPHEP-Ru/(*S*,*S*)-DPEN complexes changed to 3:1 at room temperature. The 3:1 complex gave a high enantioselectivity in asymmetric hydrogenation of ketone substrates (Scheme 1-18).

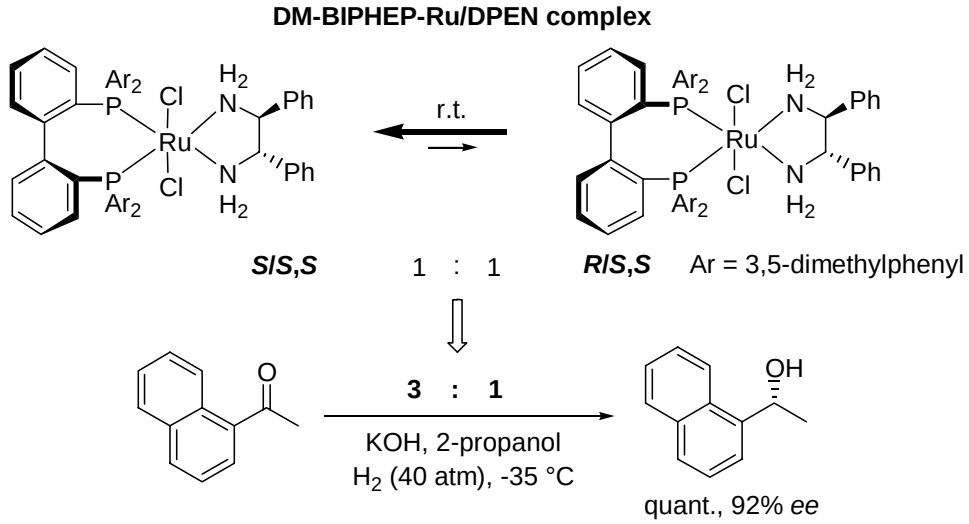

Scheme 1-18.

In 2001, Gagné and co-workers reported a very similar approach.[29] The reaction of racemic BIPHEP-Pt(CO_3) with (*S*)-BINOL yielded (±)-BIPHEP-Pt/(*S*)-BINOL complexes as a 1:1 mixture of diastereomers. Through the isomerization of BIPHEP moiety, the thermodynamically favored (*S*)/(*S*)-diastereomer could be obtained in a 95:5 ratio at 90 °C after 3 days. The thermodynamically disfavored (*R*)/(*S*)-diastereomer could be obtained by recrystallization (Scheme 1-19). The reaction of (*R*)-BIPHEP-Pt/(*S*)-BINOL obtained from recrystallization gave enantiopure (*R*)-BIPHEP-Pt via treatment with TfOH without racemization of the BIPHEP. In hetero Diels-Alder reactions, the enantiopure BIPHEP-Pt afforded the desired products in high enantioselectivity.

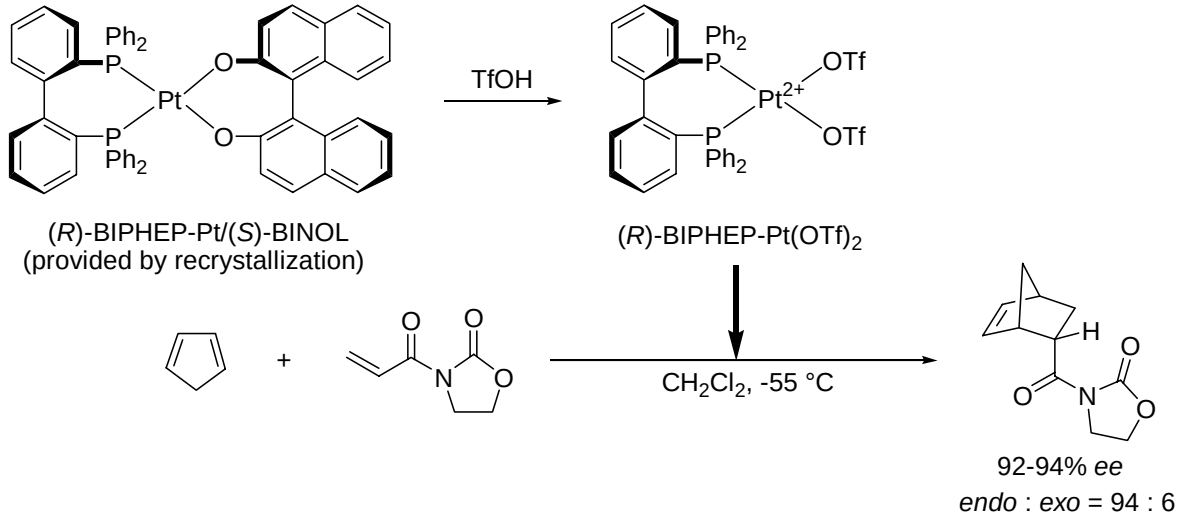

Scheme 1-19.

On the other hand, Aikawa and co-workers in the Mikami group have reported that BIPHEP-Pt complex isomerized to a single diastereomer upon addition of (*R*)-DABNTf or (*R*)-DABN.[30] The Pt complex with *tropos* BIPHEP ligand can be resolved as the *atropos* complex even at 50 °C. However, The BIPHEP-Pt/(*R*)-DABNTf complex isomerized at 110 °C after 12 h to afford the enantiopure (*S*)-BIPHEP-Pt/(*R*)-DABNTf complex. Similarly, the BIPHEP-Pt/(*R*)-DABN complex afforded the enantiopure (*R*)-BIPHEP-Pt/(*R*)-DABN complex at 80 °C after 30 h. Upon addition of concentrated HCl at room temperature, the chirally controlled (*S*)-BIPHEP-Pt/(*R*)-DABNTf complex provided the enantiopure (*S*)-BIPHEP-$PtCl_2$ complex. The enantiopure (*S*)-BIPHEP-$PtCl_2$ complex attained high catalytic activity and enantioselectivity in hetero Diels-Alder reactions at room temperature after treatment with $AgSbF_6$ (Scheme 1-20).

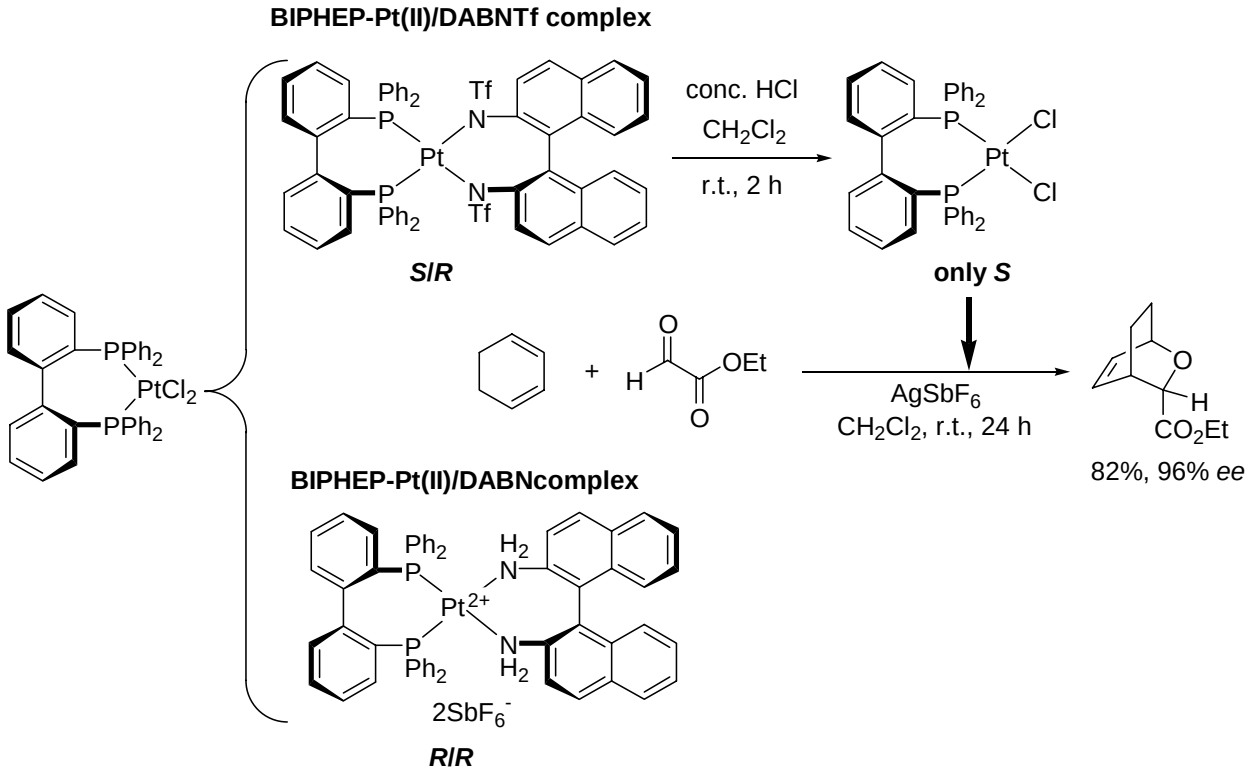

Scheme 1-20.

In 2003, Doherty, Knight and co-workers reported a novel *tropos* ligand, NUPHOS, which had been already proposed[20] to possess a structural similarity to *tropos* BIPHEP ligands (Scheme 1-21).[31] It was revealed that enantiopure BINOL could be used as an effective resolving reagent for Pt complexes bearing NUPHOS ligands. The isomerization of (±)-NUPHOS-Pt/(*S*)-BINOL complexes

proceeded at high temperature to afford a diastereo-enriched mixture that could be crystallized to give a diastereopure (*R*)-NUPHOS-Pt/(*S*)-BINOL. Reaction with the diastereopure (*R*)-NUPHOS-Pt/(*S*)-BINOL complexes with TfOH gave the corresponding enantiopure (*R*)-NUPHOS-Pt$(OTf)_2$ complexes. The enantiopure (*R*)-NUPHOS- Pt$(OTf)_2$ complexes could be used as highly efficient catalysts for hetero Diels-Alder reactions.

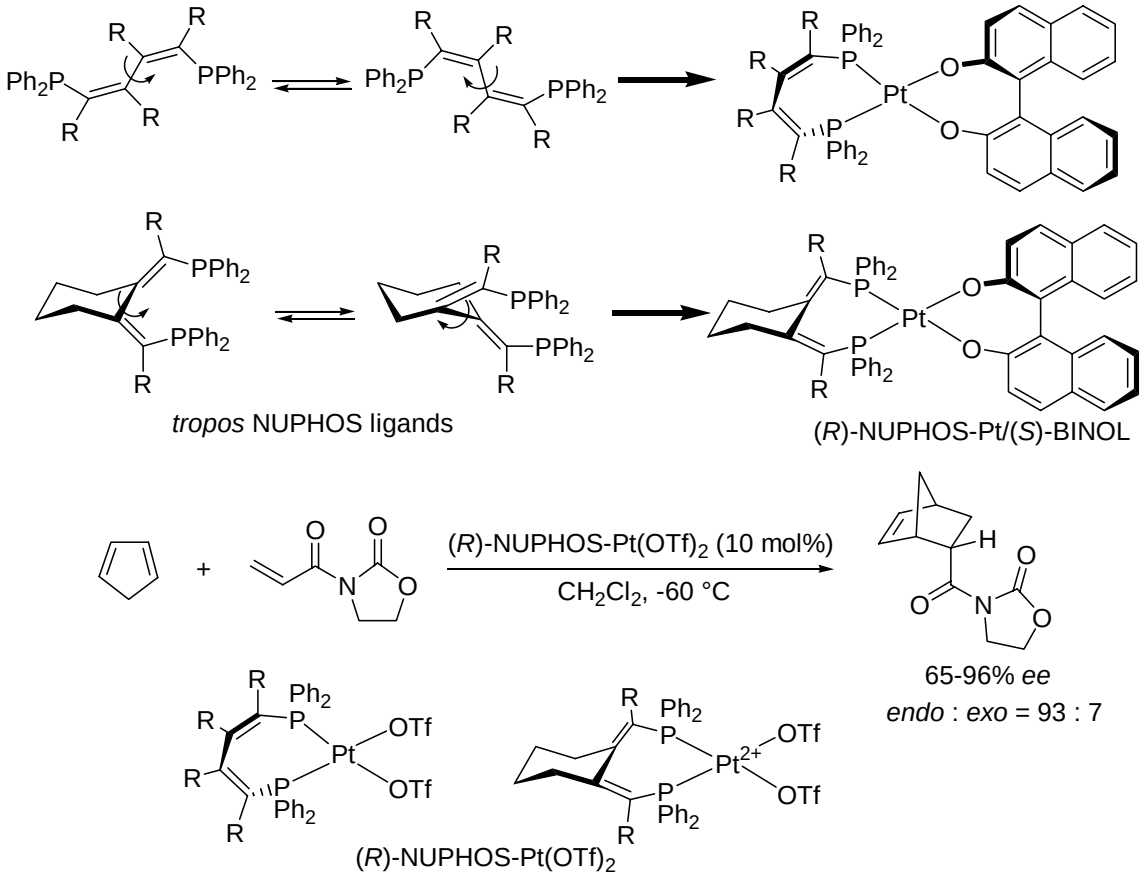

Scheme 1-21.

1-4. Thesis works

As described in Sections 1-2 and 3, conformationally mobile (*tropos*) compounds that rapidly interconvert between the chiral conformations can be controlled in a single chiral conformation, and the chirally controlled compounds can be used as asymmetric catalysts.

The addition of chiral activator is one of the most useful methods to chirally control *tropos* catalysts. Indeed, chiral activators controlled the BIPHEP complexes to a single chiral conformation. However,

the chirality control of BIPHEP complex often needs heat for several hours (Table 1-1). BIPHEP-Pt and Pd complexes with DABN could not be controlled to a single conformation at room temperature but isomerized at 80 °C after several hours. The chirality control of BIPHEP-Rh and Ir complexes isomerized more quickly than BIPHEP-Pd and Pt complexes and the isomerization proceeded at room temperature. However, the isomerization of BIPHEP-Rh and Ir complexes finished at room temperature after several days. In case of BIPHEP-Ru complex with DPEN, the ratio of diastereomers could be changed at room temperature, but the complex did not isomerize to a single diastereomer.

Table 1-1. Chirality control of BIPHEP complexes with DABN or DPEN

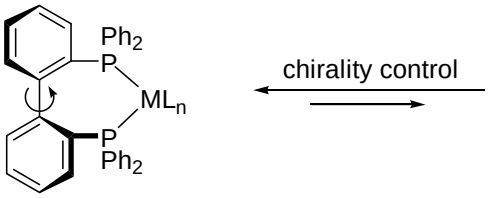

M	L_n	Time (h)	Temp. (°C)	Diastereomer ratio
Pd	DABN	8	80	100 : 0
Pt	DABN	30	80	100 : 0
Rh	DABN	17 (days)	r.t.	100 : 0
Rh	DABN	5	80	100 : 0
Ir	DABN	3(days)	r.t.	100 : 0
Ir	DABN	1	100	100 : 0
Ru	DPEN	3	r.t.	3 : 1

Chiral Activator (L_n):

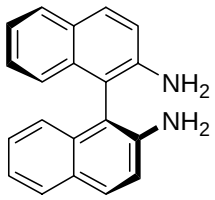

DABN

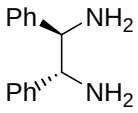

DPEN

Ru **DABN: *tropos*** **DPEN: *tropos***	**Rh** **DABN: *tropos*** DPEN: *atropos*	**Pd** DABN: *atropos* DPEN: *atropos*
Os	**Ir** **DABN: *tropos***	**Pt** DABN: *atropos* DPEN: *atropos*

Yamanaka in the Mikami group has reported the issue of the *tropos* or *atropos* nature of the BIPHEP-Ru, Rh and Pd complexes with chiral diamines by theoretical calculation;[20] the results show that the *atropos* nature of the BIPHEP-M/diamine complexes (M = Pd) can be traced back to the quite larger interaction energy between the BIPHEP and the M-diamine fragments than that in the *tropos* BIPHEP-M/diamine complex, such as BIPHEP-$RuCl_2$/DPEN. The slow isomerization is caused by steric repulsion of the single bond rotation in BIPHEP.

The chirality control of more flexible *tropos* ligands, such as benzophenone-derived ligands, is thus considered to proceed faster than that of BIPHEP (e.g. at room temperature within minutes). In addition, biphenyl- and binaphthyl-derived ligands, such as BIPHEP and BINAP, adopt only C_2-conformation, but benzophenone-derived ligands adopt various chiral conformations (Scheme 1-22). Scheme 1-7 shows the various chiral conformations of benzophenone in a crystalline phase.

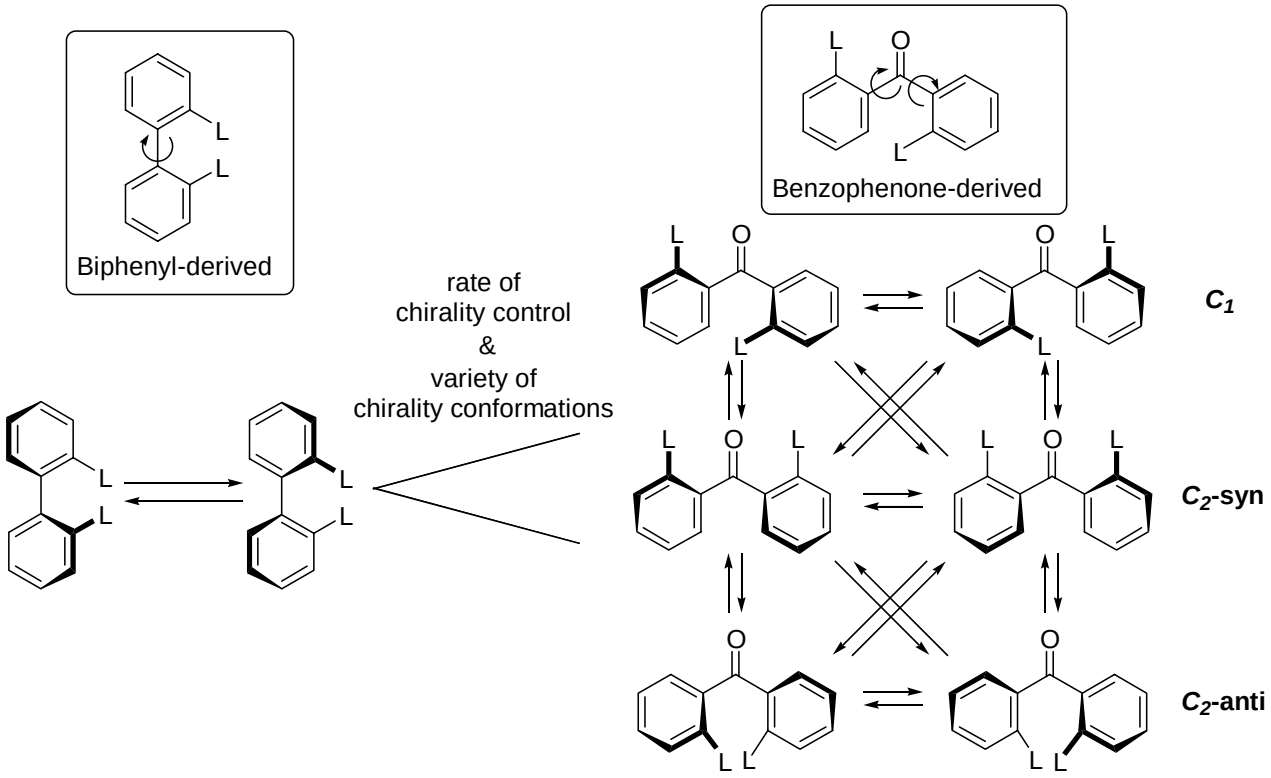

Scheme 1-22.

The addition of chiral activator was considered to control the various conformations of *tropos* complexes to a single conformation even in a solution phase (Scheme 1-23). The author was thus interested with chirality control of *tropos* complexes.

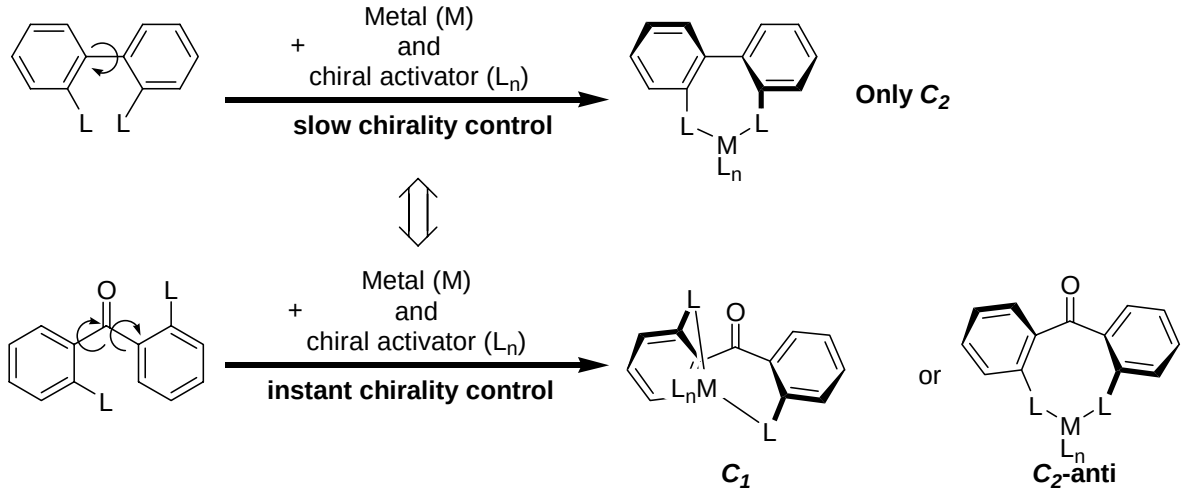

Scheme 1-23.

It is expected that these *tropos* benzophenone-derived complexes can be chirally controlled instantly to provide a great advantage over the *atropos* BINAP complexes. The chelate bite angle of the complex with benzophenone-derived ligands is larger than those of binaphthyl counterparts to attain the more effective shielding over metal center, and hence, to afford higher catalytic activity and enantioselectivity in asymmetric catalyses. In case of *atropos* BINAP catalysts, the dihedral angle between the naphthalene rings can be tuned by changing the metal and counter anion. More significantly, *tropos* benzophenone-derived complexes can be controlled not only in their dihedral angles but also in their chirality by external factors, such as the metal, counter anion, chiral activator and substrate etc. Therefore, the *tropos* benzophenone-derived catalysts have a great possibility to adopt the chiral conformation to fit well with the stereoelectronic effects of substrates, reagents and chiral activators. The *tropos* catalysts attain high catalytic activity and enantioselectivity irrespective of the substrates and reagents. The optimization of chiral conformation in catalysts caused by the stereoelectronic effects of substrates and activators is thus called "self-adaptation" of catalysts. The self-adaptable *tropos* ligands and catalysts is advantageous over *atropos* ligands and catalysts which can not self-adapt in their chirality.

Therefore, the author started the research project on the chirality control of the complexes with benzophenone-derived ligands and asymmetric catalysis with the complexes chirally controlled. The author believe in the efficiency of these *tropos* compounds as the new paradigm, namely self-adaptable asymmetric catalysts.

In Chapter 2, the author describes the chirality control of complexes with benzophenone-derived diphenylphosphine ligand upon addition of chiral activators. Compared to one single bond rotation of BIPHEP complex, two single bond rotations of the benzophenone-derived complex seem to be more facile and the conformation of the complex can be controlled instantaneously (Scheme 1-24). In sharp contrast to the corresponding BIPHEP complexes, the benzophenone-derived complexes chirally controlled were expected to possess several conformations. The conformation of benzophenone-derived complex was thus analyzed by X-ray structural analysis. In addition, the complexes chirally controlled with benzophenone-derived ligand were also examined to use as asymmetric catalysts.

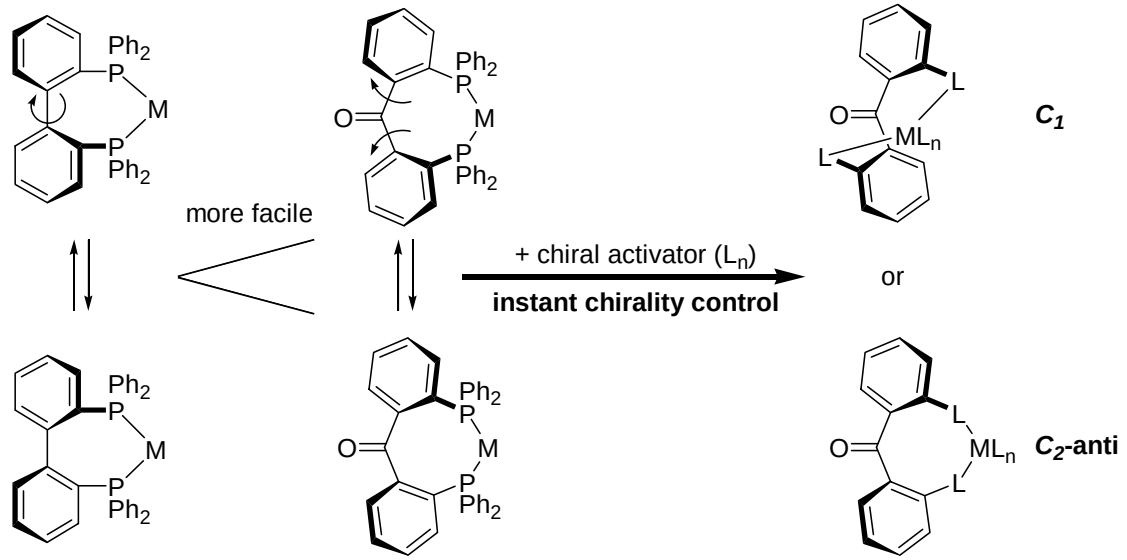

Scheme 1-24.

In Chapter 3, the author describes the asymmetric catalysis with benzophenone-like monodentate ligands chirally controlled by a chiral activator (Scheme 1-25). Achiral phosphoramidites in metal complexes were controlled in a single conformation by the chiral dienes. The chirally controlled complexes were used in asymmetric Michael additions (Scheme 1-25).

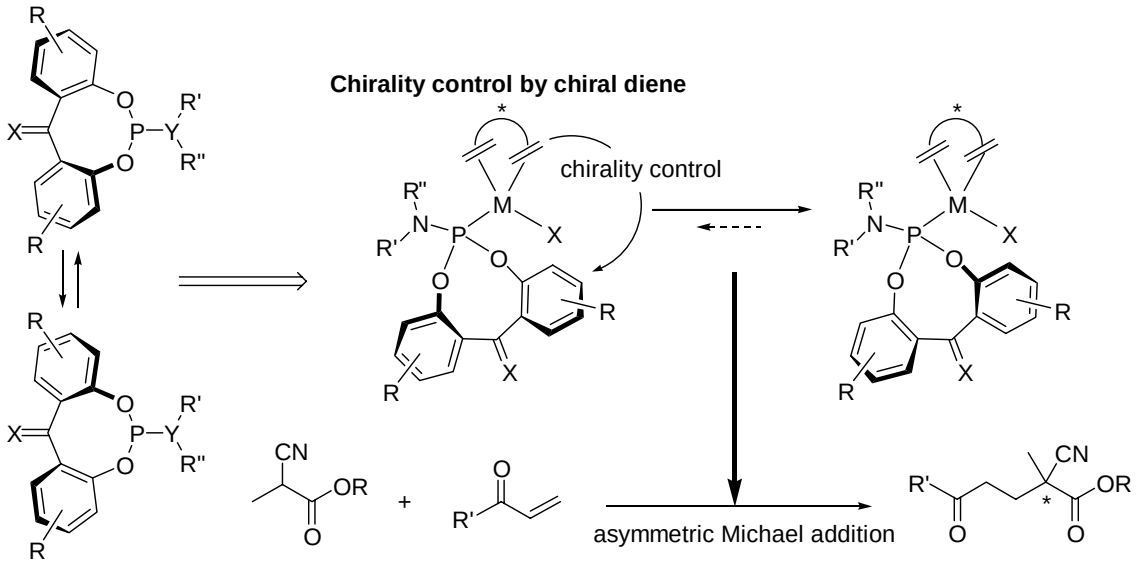

Scheme 1-25.

In Chapter 4, the author describes the benzophenone-like monodentate ligands chirally controlled by chiral part built therein (Scheme 1-26). The complexes with the benzophenone-like phosphoramidite ligands adopted a single conformation and were used as catalysts for asymmetric conjugate additions.

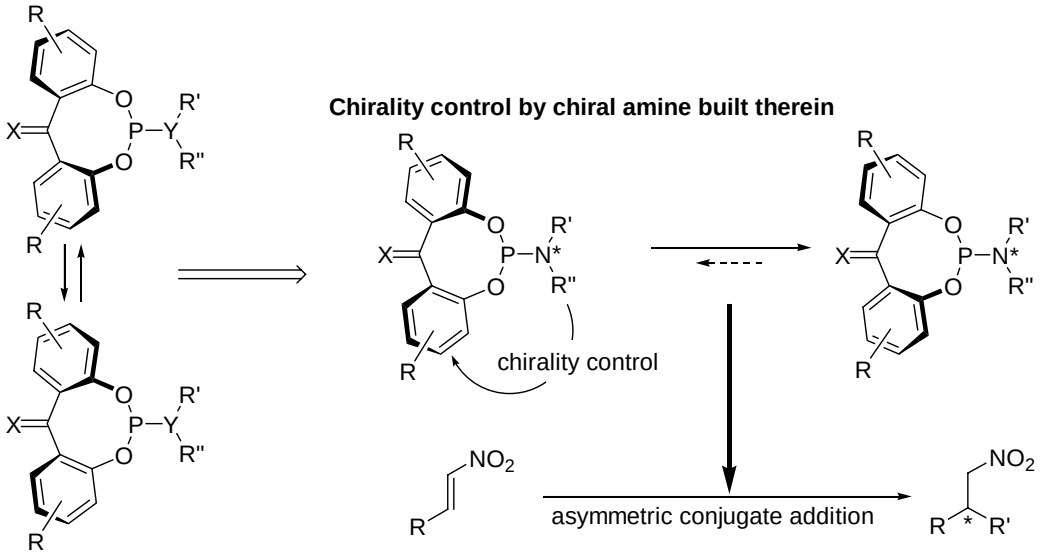

Scheme 1-26.

In Chapter 5, the author describes the summary of this thesis and the outlook of the chirality control of *tropos* compounds.

References for Chapter 1

1 Pasteur, L. *Proc. R. Soc. London* **1857**, *8*, 254.

2 Person, K. *Nature* **1898**, *58*, 495. Also see: Japp, F. R. *Nature* **1898**, *58*, 452.

3 For example see: (a) Seelig, F. F. J. *Theor. Biol.* **1971**, *31*, 355. (b) Seelig, F. F. J. *Theor. Biol.* **1972**, *32*, 93. (c) Decker, P. *J. Mol. Evol*. **1973**, *2*, 137. (d) Decker, P. *J. Mol. Evol.* **1974**, *4*, 49. (e) Decker, P. In *Origins of Optical Activity in Nature*; Walker, D. C., Ed.; Elsevier: Amsterdam, 1979; pp 109. (f) Iwamoto, K.; Seno, M. *J. Chem. Phys*. **1979**, *70*, 5851. (g) Iwamoto, K.; Seno, M. *J. Chem. Phys*. **1979**, *70*, 5858. (h) Iwamoto, K.; Seno, M. *J. Chem. Phys*. **1982**, *76*, 2347. (i) Kondepudi, D. K.; Nelson, G. W. *Phys. Rev. Lett*. **1983**, *50*, 1023; *Nature* **1985**, *314*, 438. (j) Goldanskii, V. I.; Kuz'min, V. V. Z. *Phys. Chem. Leipzig* **1988**, *269*, 216. (k) Czege, J.; Fajszi, C. *Origins Life* **1977**, *8*, 271. (l) Fajszi, C.; Czege, J. *Origins Life* **1981**, *11*, 143.

4 Pasteur, L. *C. R. Acad. Sci.* **1848**, *26*, 535.

5 Collet, A.; Brienne, M.-J.; Jacques, J. *Chem. Rev.* **1980**, *80*, 215.

6 Review: Matsuura, T.; Koshima, H. *J. Photochem. Photobiol. C Photochem. Rev.* **2005**, *6*, 7.

7 (a) Gillier-Pandraud, H. *Bull. Chim. Soc. Fr.* **1967**, 1988. (b) Scheringer, S. *Kristallogr*. **1963**, *119*, 273.

8 Koshima, H.; Hayashi, E.; Matsuura, T.; Tanaka, K.; Toda, F.; Kato, M.; Kiguchi, M. *Tetrahedron lett.* **1997**, *38*, 5009.

9 (a) Pincock, R. E.; Wilson, K. R. *J. Am. Chem. Soc.* **1971**, *93*, 1291. (b) Pincock, R. E.; Perkins R. R.; Ma, A. S.; Wilson, K. R. *Science* **1971**, *174*, 1018.

10 Williams, D. J.; Lawton, D. *Tetrahedron Lett*. **1975**, *16*, 111.

11 Lunazzi, L.; Mazzanti, A.; Minzoni, M. *J. Org. Chem.* **2005**, *70*, 456.

12 Toda, F.; Tanaka, K.; Kuroda, R. *Chem. Commun.* **1997**, 1227.

13 (a) Fleischer, E. B.; Sung, N.; Hawkinson, S. *J. Phys. Chem.* **1968**, *72*, 4311. (b) Rappoport, Z.; Biali, S. E.; Kaftory, M. *J. Am. Chem. Soc.* **1990**, *112*, 7742. (c) Szyrszyng, M.; Nowak, E.; Gdaniec, M.; Milewska, M. J.; Połonski, T. *Tetahedron: Asymmetry* **2004**, *15*, 103.

14 Toda, F.; Tanaka, K.; Oda, M. *Tetrahedron Lett.* **1988**, *29*, 653.

15 (a) Mercier, F.; Holand, S.; Mathey, F. *J. Organomet. Chem.* **1986**, *316*, 271. (b) Tissot, O.; Gouygou, M.; Daran, J.-C.; Balavoine, G. G. A. *Chem. Commun.* **1996**, 2287. (c) Tissot, O.;

Gouygou, M.; Dallemer, F.; Daran, J.-C.; Balavoine, G. G. A. *Angew. Chem. Int. Ed.* **2001**, *40*, 1076.

16 Reggelin, M.; Doerr, S.; Klussmann, M.; Schultz, M.; Holbach, M. *Proc. Nat. Acad. Sci. U.S.A.* **2004**, *101*, 5461.

17 Kuhn, W.; *Stereochemie*; Freudenberg, K. Ed.; Franz Deuticke: Leipzig, 1933; pp. 803.

18 Haworth, W. H. *The Constitution of the Sugars*; Edward Arnold & C.: London, 1929, p. 90.

19 (a) Kemp, J. D.; Pitzer, K. S. *J. Chem. Phys*. **1936**, *4*, 749. (b) Kemp, J. D.; Pitzer, K. S. *J. Am. Chem. Soc*. **1937**, *59*, 276.

20 Mikami, K.; Aikawa, K.; Yusa, Y.; Jodry, J. J.; Yamanaka, M. *Synlett* **2002**, 1561.

21 (a) *Catalytic Asymmetric Synthesis*; Ojima, I., Ed.; VCH: New York, 1993, 2000; Vol. I and II. (b) Brunner, H.; Zettlmeier, W. *Handbook of Enantioselective Catalysis*; VCH: Weinheim, 1993. (c) Noyori, R.; *Asymmetric Catalysis in Organic Synthesis*; Wiley: New York, 1994. (d) *Transition Metals for Organic Synthesis*; Beller, M.; Bolm, C., Eds.; VCH: Weinheim, 1998. (e) *Comprehensive Asymmetric Catalysis*; Jacobsen, E. N.; Pfaltz, A.; Yamamoto, H., Eds.; Springer: Berlin, 1999; Vol. 1-3. (f) *New Frontiers in Asymmetric catalysis*; Mikami, K.; Lantens, M., Eds; Wiley: New York, 2007.

22 Mikami, K.; Matsukawa, S. *Nature* **1997**, *385*, 613.

23 (a) Mikami, K.; Matsukawa, S.; Volk, T.; Terada, M. *Angew. Chem. Int. Ed. Engl.* **1997**, *36*, 2768. (b) Chavarot, M.; Byrne, J. J.; Chavant, P. Y.; Pardillos-Guindet, J.; Vallee, Y. *Tetrahedron: Asymmetry* **1998**, *9*, 3889.

24 Ueki, M.; Matsumoto, Y.; Jodry, J. J.; Mikami, K. *Synlett* **2001**, 1889.

25 BIPHEP ((2,2'-bis(diphenylphosphino)-1,1'-biphenyl): This ligand was also named BPBP, but contrarily to what was claimed in the publication, it was unsuccessfully synthesized to give instead the monophosphine derivative: (a) Uehara, A.; Bailar, Jr, J. C. *J. Organomet. Chem.* **1982**, *239*, 1. (b) Bennett, M. A.; Bhargava, S. K.; Griffiths, K. D.; Robertson, G. B. *Angew. Chem. Int. Ed. Engl.* **1987**, *26*, 260. (c) Desponds, O.; Schlosser, M. *J. Organomet. Chem.* **1996**, *507*, 257. (d) Desponds, O.; Schlosser, M. *Tetrahedron Lett*. **1996**, *37*, 47.

For more details see: "BIPHEMP" (2,2'-bis(diphenylphosphanyl)-6,6'-dimethyl-1,1'-biphenyl): (e) Svensson, G.; Albertsson, J.; Frejd, T.; Klingstedt, T. *Acta Crystallogr., Sect. C* **1986**, *42*, 1324. (f)

Schmid, R.; Cereghetti, M.; Heiser, B.; Schonholzer, P.; Hansen, H.-J. *Helv. Chim. Acta* **1988**, *71*, 897. "BICHEPs" (2,2'-bis(dicyclohexylphosphanyl)-6,6'-dimethyl-1,1'-biphenyl): (g) Chiba, T.; Miyashita, A.; Nohira, H. *Tetrahedron Lett.* **1991**, *32*, 4745. "MeO-BIPHEP" (2,2'-bis(diphenyl-phosphanyl)-6,6'-dimethoxy-1,1'-biphenyl): (h) Schmid, R.; Foricher, J.; Cereghetti, M.; Schönholzer, P. *Helv. Chim. Acta* **1991**, *74*, 370. (i) Schmid, R.; Broger, E. A.; Cereghetti, M.; Crameri, Y.; Foricher, J.; Lalonde, M.; Müller, R. K.; Scalone, M.; Schoettel, G.; Zutter, U. *Pure Appl. Chem.* **1996**, *68*, 131. (j) Trabesinger, G.; Albinati, A.; Feiken, N.; Kunz, R. W.; Pregosin, P. S.; Tschoerner, M. *J. Am. Chem. Soc.* **1997**, *119*, 6315. (2,2'-bis(diphenylphosphanyl)-6,6'-difluoro-1,1'-biphenyl): (k) Jendralla, H.; Li, C.-H.; Paulus, E. *Tetrahedron: Asymmetry* **1994**, *5*, 1297.

26 (a) Mikami, K.; Aikawa, K.; Yusa, Y.; Hatano, M. *Org. Lett.* **2002**, *4*, 91. (b) Mikami, K.; Aikawa, K.; Yusa, Y. *Org. Lett.* **2002**, *4*, 95. (c) Aikawa, K. *Ph.D. Thesis*, Tokyo Institute of Technology, **2005**.

27 (a) Mikami, K.; Kataoka, S.; Yusa, Y.; Aikawa, K. *Org. Lett.* **2004**, *6*, 3699. (b) Mikami, K.; Kataoka, S.; Wakabayashi, K.; Aikawa, K. *Tetrahedron* **2006**, *47*, 6361.

28 (a) Mikami, K.; Korenaga, T.; Terada, M.; Ohkuma, T.; Pham, T.; Noyori, R. *Angew. Chem. Int. Ed.* **1999**, *38*, 495. (b) Korenaga, T. *Ph.D. Thesis*, Tokyo Institute of Technology, **2000**.

29 Becker, J. J.; White, P. S.; Gagné, M. R. *J. Am. Chem. Soc.* **2001**, *123*, 9478.

30 Mikami, K.; Kakuno, H.; Aikawa, K. *Angew. Chem. Int. Ed.* **2005**, *44*, 7257.

31 (a) Doherty, S.; Newman, C. R.; Rath, R. K.; Luo, H.; Nieuwenhuyzen, M.; Knight, J. G. *Org. Lett.* **2003**, *5*, 3863. (b) Doherty, S.; Newman, C. R.; Rath, R. K.; Berg, J.; Hardacre, C.; Nieuwenhuyzen, M.; Knight, J. G. *Organometallics* **2004**, *23*, 1055. (c) Doherty, S.; Knight, J. G.; Hardacre, C.; Lou, H.; Newman, C. R.; Rath, R. K.; Campbell, S.; Nieuwenhuyzen, M. *Organometallics* **2004**, *23*, 6127.

2-1. Introduction

As described in Chapter 1, the generation of chirality in conformationally mobile compounds can be considered one of the most intriguing topics. Molecules with free rotational bonds, such as benzophenone and butane, are conformationally mobile in a solution phase due to rapid interconversion between right- and left-handed enantiomers ((*P*) and (*M*) configuration, respectively) (Scheme 2-1). However, optically active crystals are obtained even from conformationally mobile compounds, when frozen in a chiral conformation.[1,2] For example, the crystalline 1:2 inclusion complex of benzophenone with cholic acid has been reported to possess C_1-conformation of benzophenone.[2d]

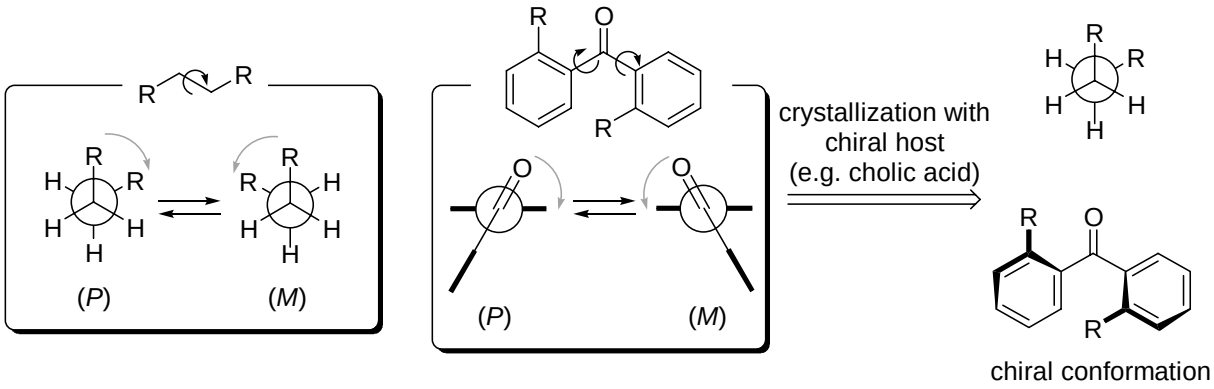

Scheme 2-1.

At low temperature, NMR spectra also show the chiral conformation of benzophenone-derived substrates in a solution phase. Minzoni and co-workers have reported that 2,2'-diisopropyl-benzophenone has three stable conformations, C_1, C_2-syn and C_2-anti; It mainly adopts C_2-syn conformation at low temperature (Scheme 2-2).[3] The most stable conformation of 2,2'-diisopropylbenzophenone is indicated by DFT calculation to be C_2-syn.

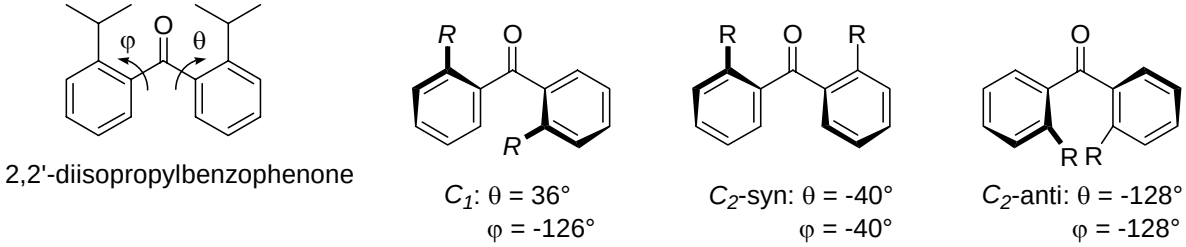

Scheme 2-2.

^{13}C NMR of 2,2'-diisopropylbenzophenone shows the C_2-syn conformation at low temperature (Figure 2-1). The broad methyl signal of isopropyl group splits into two equally intense lines at -139 °C.

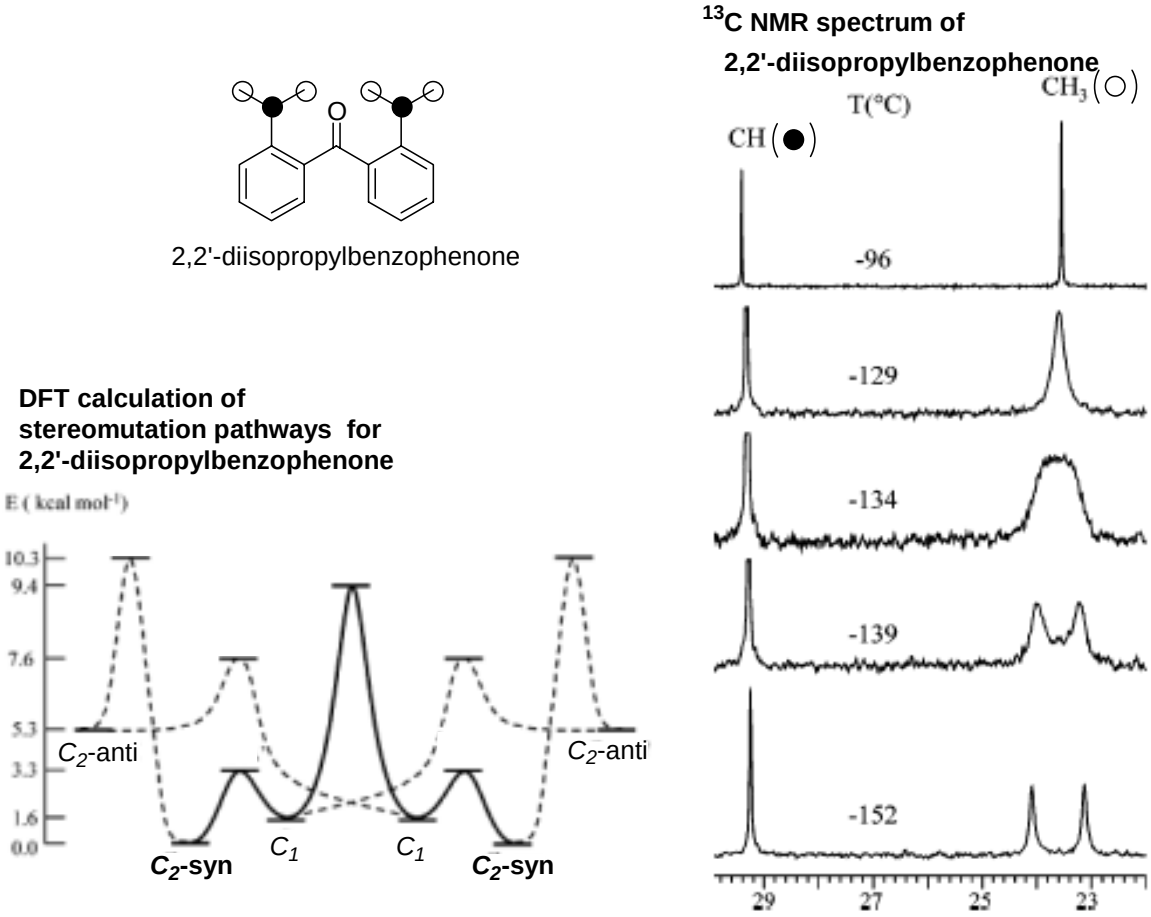

Figure 2-1. DFT calculation and ^{13}C NMR of 2,2'-diisopropylbenzophenone (Ref. 3)

In the previous reports, benzophenone-derived compounds have been reported to adopt their chiral conformation in particular situations. Even in a solution phase at room temperature, chiral conformation of benzophenone can be observed upon addition of chiral activators. Mikami and co-workers have already reported the chirality control of achiral BIPHEPs-M complexes (M = Pd, Pt, Rh, Ir, Ru) by chiral aminoalcohols or diamines.[4,5,6,7,8] For example, BIPHEP-Pd(II) complex with (*S*)-DABN isomerized at 80 °C after 8 h to afford the favorable (*S*)-BIPHEP-Pd/(*S*)-DABN complex exclusively (Scheme 2-3). The single diastereomer (*S*)-BIPHEP-Pd/(*S*)-DABN complex thus obtained could be used as an activated asymmetric catalyst for C-C bond forming reactions such as the hetero Diels-Alder reactions at room temperature (75% yield, 92% *ee*).[4b]

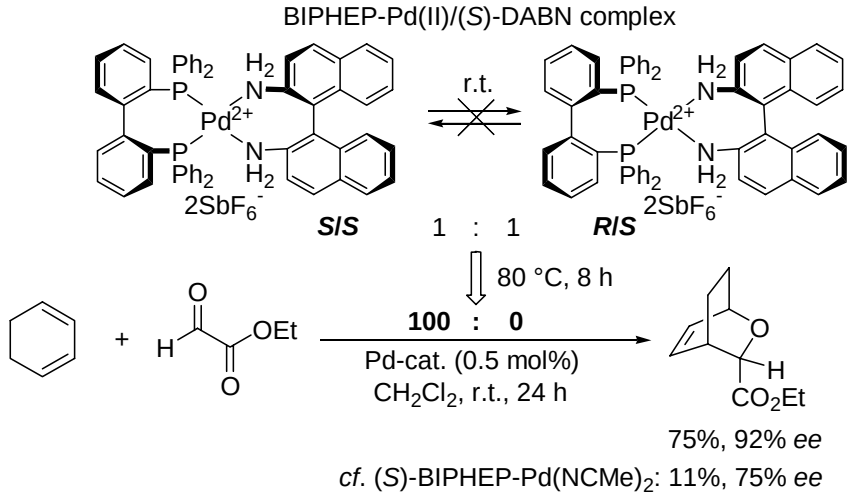

Scheme 2-3.

Chirality control of BIPHEP complexes is useful to afford single diastereomer but often needs treatment of heat for several hours. Compared to one single bond rotation of BIPHEP, two single bond rotations of a benzophenone-derived ligand **2a** seem to be more facile.[3,9] The chirality control of complexes with **2a** can be confirmed to finish instantaneously (Scheme 2-4). The chirality control of complexes with benzophenone-derived diphenylphosphine ligand **2a** was thus examined upon addition of chiral activators.[10]

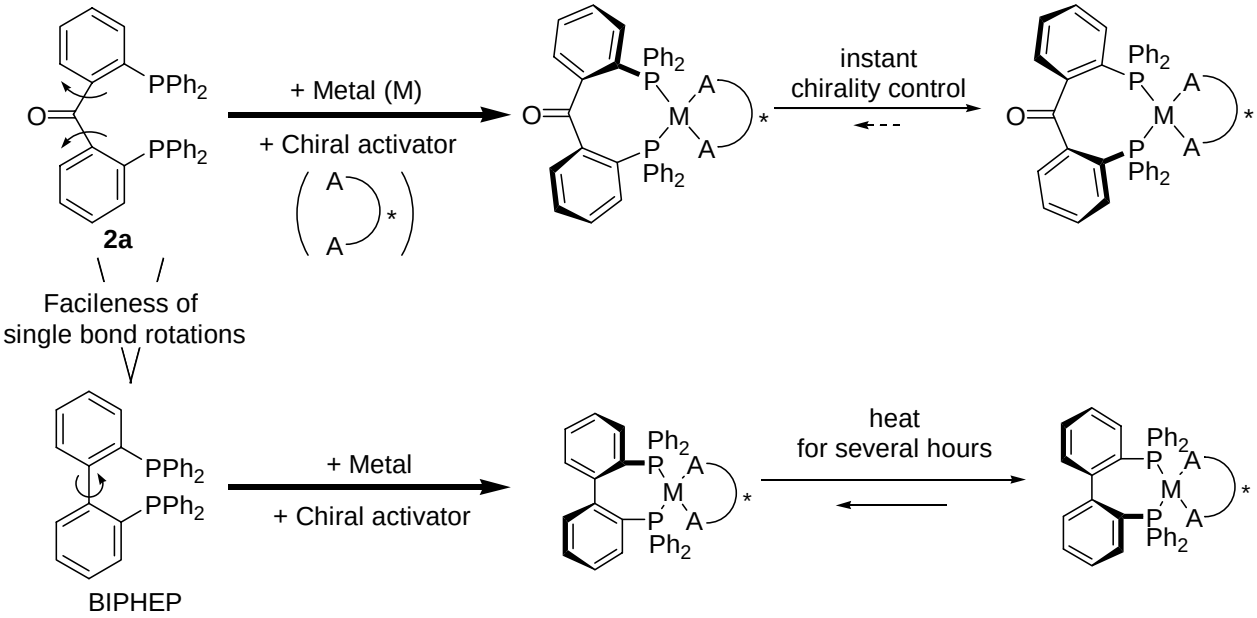

Scheme 2-4.

As shown in Scheme 2-2, the benzophenone-derived ligand **2a** can be adopted several chiral conformations. Especially, C_1-conformation can not be obtained with biphenyl- and binaphthyl-derived ligands, so that the complex with **2a** chirally controlled has a possibility to show higher catalytic activity and enantioselectivity in asymmetric reactions.

In Chapter 2, the author reports the instant chirality control of complexes with benzophenone-derived diphenylphosphine ligand compared with that of BIPHEP complexes. Similar to the BIPHEP complexes, the benzophenone-derived complexes chirally controlled can be used as activated asymmetric catalysts. Therefore, the catalyzed reactions with benzophenone-derived complexes were also examined, in comparison with biphenyl- and binaphthyl-derived complexes.

2-2. Synthesis of benzophenone-derived diphosphine ligand

First, benzophenone-derived diphenylphosphine ligand **2a** was synthesized. A synthetic method without reduction was chosen to prevent the reduction of the carbonyl group. The reaction with palladium acetate to replace iodide by diphenylphosphine group was thus used.[11] By the Pd catalyzed replacement and the Grignard reaction of 2-bromo-diphenylphosphinobenzene and 2-iodo-benzoylchloride, 2,2'-bis(diphenylphosphino)benzophenone **2a** was synthesized (Scheme 2-5). On the other hand, benzhydrol- and diphenylmethane-derived diphenylphosphine ligands were synthesized by the reduction of benzophenone-derived diphenylphosphinoyl compound.

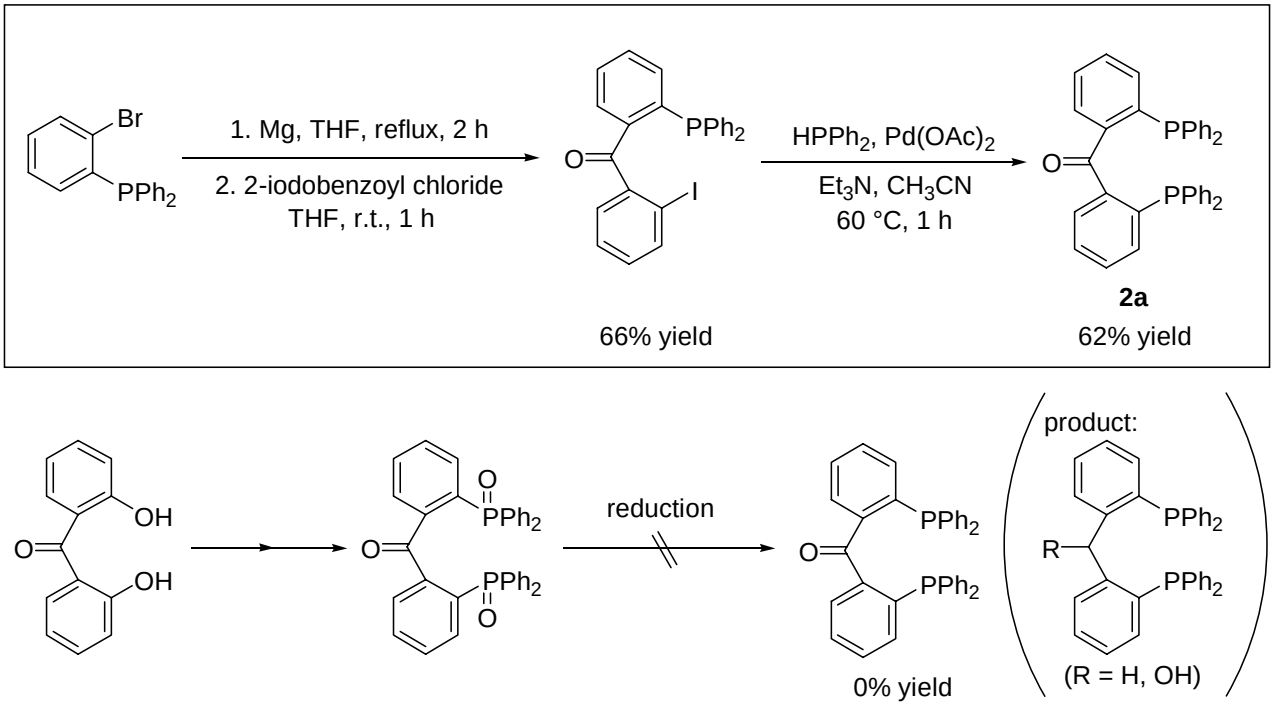

Scheme 2-5.

Metal complexes with **2a** were easily synthesized. $PtCl_2$ complex with **2a** was synthesized from $PtCl_2$(cod) complex and **2a** (Scheme 2-6). Similarly, [Rh(**2a**)(cod)]SbF_6 and $RuCl_2$(**2a**)$(dmf)_n$ complexes were synthesized from $[Rh(cod)_2]SbF_6$ and $[RuCl_2(benzene)]_2$ complexes.

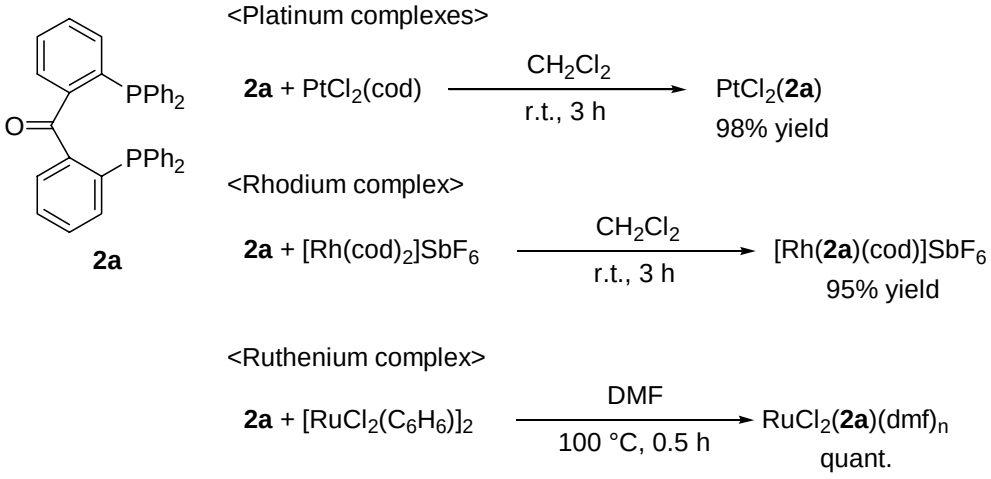

Scheme 2-6.

2-3. Chirality control of metal complexes with benzophenone-derived ligand

2-3-1. X-ray structural analysis of Pt complex

As described in Section 2-1, benzophenone-derived compounds are conformationally mobile but adopt a chiral conformation in a crystalline phase. X-ray analysis of a single crystal of $PtCl_2$(**2a**) showed the chiral conformation of **2a** in the metal complex (Figure 2-2). Figure 2-2 shows the C_1-conformation of benzophenone skeleton of **2a**, which adopts a helical propeller conformation.

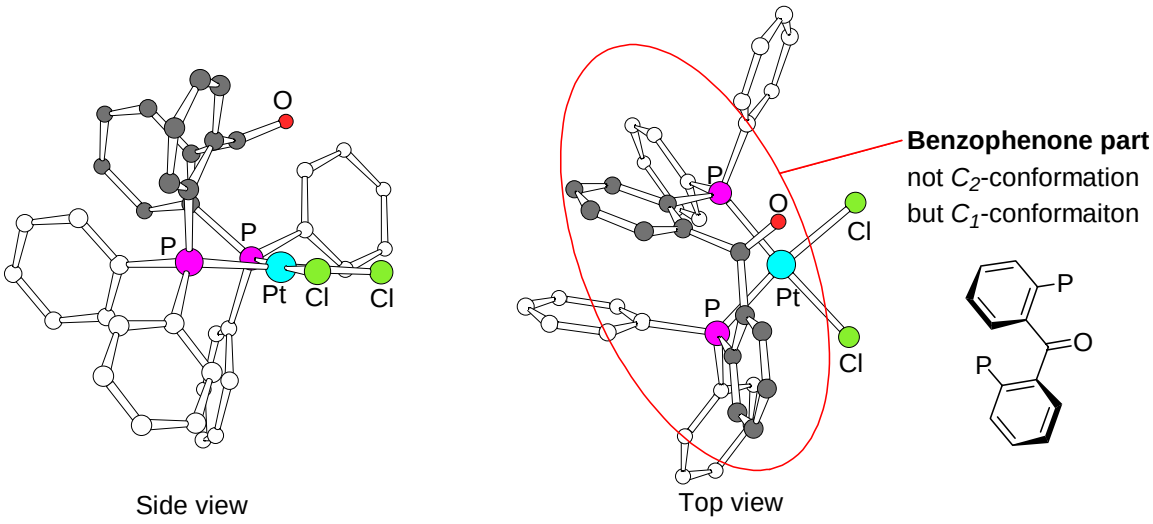

Figure 2-2. X-ray structural analysis of $PtCl_2$(**2a**)

^{31}P NMR spectrum of $PtCl_2$(**2a**) showed one peak (14.6 ppm) at room temperature. However, ^{31}P NMR spectrum showed two doublet peaks (12.6 and 16.2 ppm) at -80 °C (Figure 2-3). These VT-NMR analyses show that $PtCl_2$(**2a**) adopts C_1-conformation at -80 °C, but interconverts rapidly between the conformations at room temperature. In contrast, one singlet of ^{31}P NMR spectrum shows that ligand **2a** itself interconverts rapidly between the conformations even at -80 °C.

From VT-NMR analyses of $PtCl_2$(**2a**) (25 °C to -80 °C), the rotational barrier ($\Delta G^{\#}$) of $PtCl_2$(**2a**) was calculated at 11.9 kcal/mol (Tc = -40 °C), on the basis of the following equation[9]: $\Delta G^{\#} = 4.57\ Tc[10.32+\log_{10}(Tc/\Delta\delta^2+\sigma J^2)]$. Compared to *tropos* Ru-BIPHEP complex ($\Delta G^{\#}$ = 22.0 kcal/mol)[12], the rotational barrier of $PtCl_2$(**2a**) is low. The lower energy of $PtCl_2$(**2a**) shows that the single bond rotation of the complexes with **2a** is more facile than BIPHEP complexes.

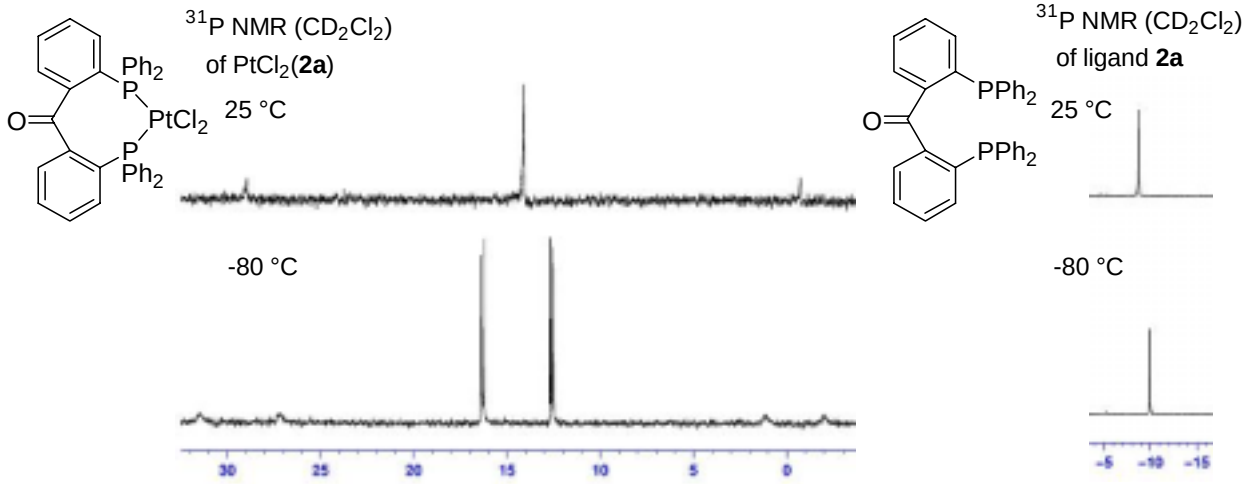

Figure 2-3. ^{31}P NMR of $PtCl_2$(**2a**) complex and ligand **2a**

In order to obtain the chiral C_1-conformation even in a solution phase, chirality control of **2a** complexes was examined upon addition of chiral diamines, as compared with the chirality control of BIPHEP complexes.

2-3-2. Chirality control of Ru and Rh complexes

Chirality control of Ru-BIPHEP complex was examined upon addition of DPEN (Scheme 2-7). (*P*)- and (*M*)-DM-BIPHEP-Ru/(*S*,*S*)-DPEN complexes are initially obtained as a 1:1 diastereomer mixture. However, even at room temperature, diastereomer ratio changes to 3:1.[5a]

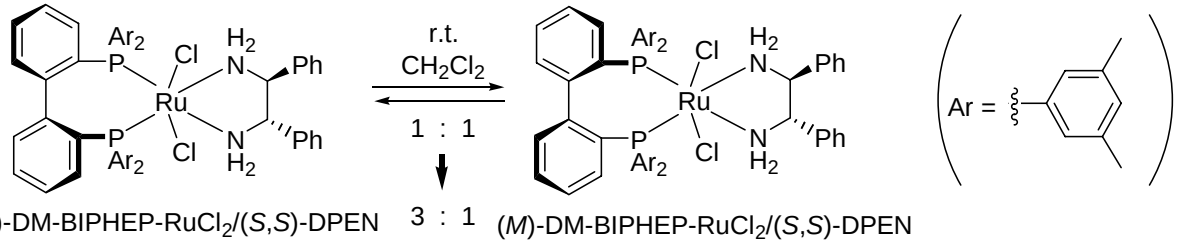

(*P*)-DM-BIPHEP-$RuCl_2$/(*S*,*S*)-DPEN (*M*)-DM-BIPHEP-$RuCl_2$/(*S*,*S*)-DPEN

Scheme 2-7.

Chirality control of $RuCl_2$(**2a**)$(dmf)_n$ complex with (*S*,*S*)-DPEN led to the formation of enantiomerically pure complex $RuCl_2$(**2a**)[(*S*,*S*)-dpen] within minutes (Scheme 2-8). ^{31}P NMR spectrum of $RuCl_2$(**2a**)[(*S*,*S*)-dpen] shows two doublets. Two doublets imply that two phosphorus atoms in $RuCl_2$(**2a**)[(*S*,*S*)-dpen] are non-equivalent and the Ru-**2a** complex chirally controlled adopts C_1-conformation.

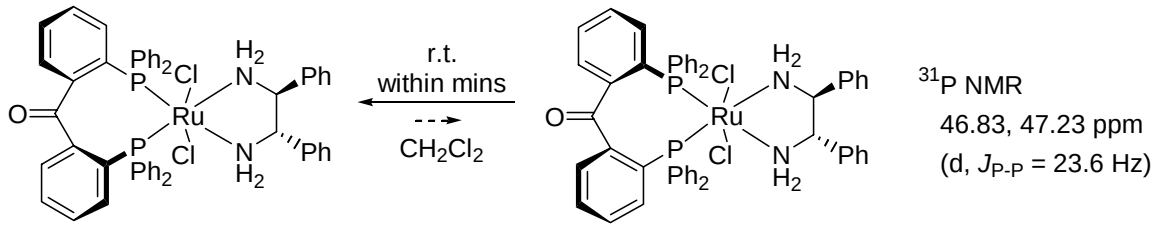

(*P*)-**2a**-$RuCl_2$/(*S*,*S*)-DPEN (*M*)-**2a**-$RuCl_2$/(*S*,*S*)-DPEN

***C*$_1$-conformation**

Scheme 2-8.

^1H NMR spectrum of $RuCl_2$(**2a**)[(*S*,*S*)-dpen] also indicates the C_1-conformation (Figure 2-4). In ^1H NMR spectrum of C_2-$RuCl_2$[(*S*)-binap][(*S*,*S*)-dpen] complex, four protons of diamine showed two multiplet peaks (axial and equatorial protons) and two protons of benzyl parts showed one multiplet peak. On the other hand, ^1H NMR spectrum of C_1-$RuCl_2$(**2a**)[(*S*,*S*)-dpen] showed three sets of multiplet peaks of amine parts and two multiplet peaks of benzylic parts. In addition, ^1H and ^{31}P NMR spectra at 80 ˚C showed that the C_1-conformation of $RuCl_2$(**2a**)[(*S*,*S*)-dpen] was kept at high temperature (Figure 2-5).

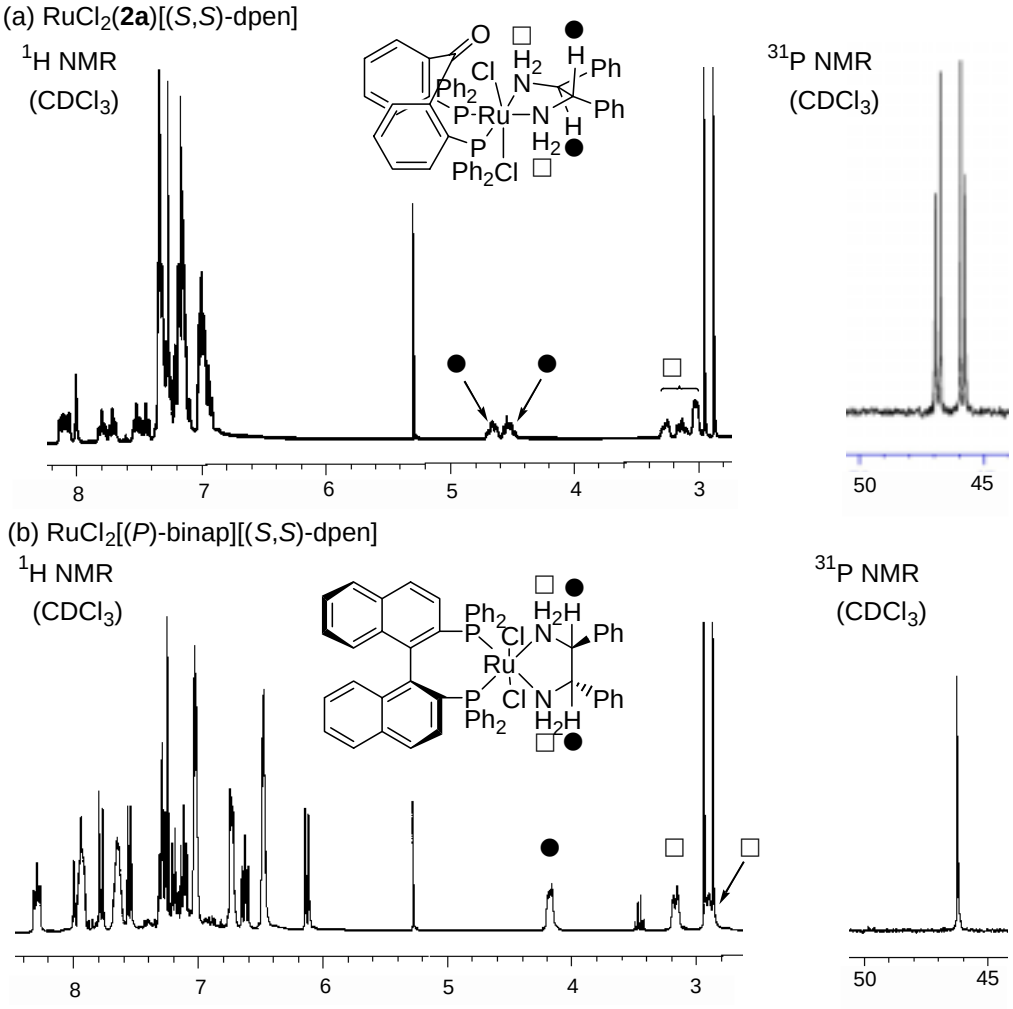

Figure 2-4. NMR spectra of Ru-**2a** and Ru-BINAP complexes with DPEN

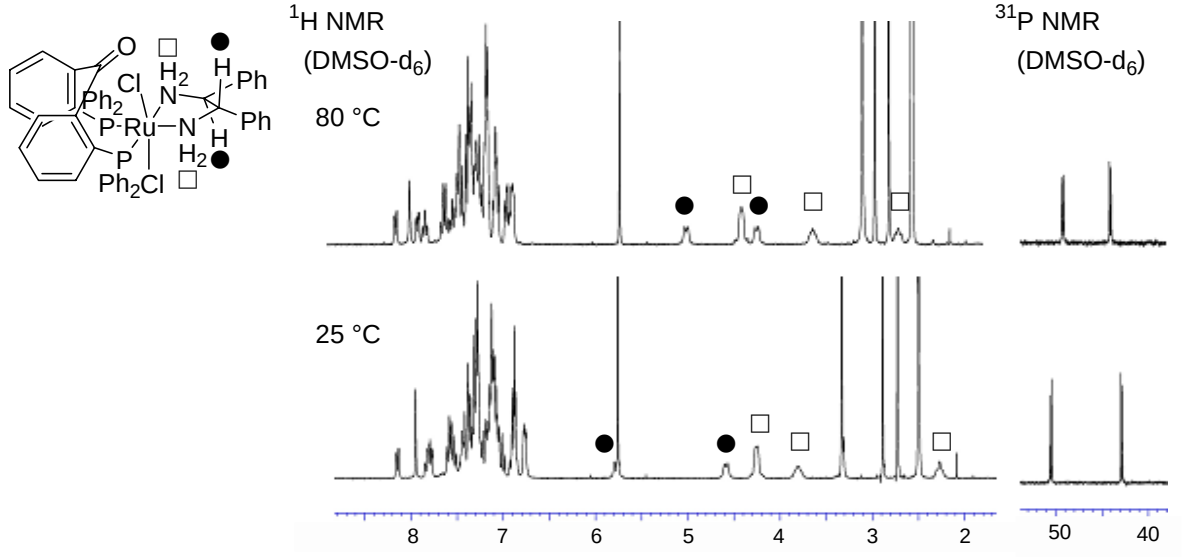

Figure 2-5. VT NMR spectra of Ru-**2a** complexes with DPEN

The single crystal of $RuCl_2$(**2a**)[(*S*,*S*)-dpen] was not obtained. Fortunately however, the single crystal of the monotriflate derivative, [RuCl(OTf)(**2a**){(*S*,*S*)-dpen}]$_2$AgOTf was obtained (Figure 2-6). The X-ray structural analysis of [RuCl(OTf)(**2a**){(*S*,*S*)-dpen}]$_2$AgOTf showed the enantiopure structure of the benzophenone-derived diphenylphosphine-metal complex. Top view of Figure 2-6 shows that the benzophenone skeleton of **2a** adopts a chiral propeller conformation.

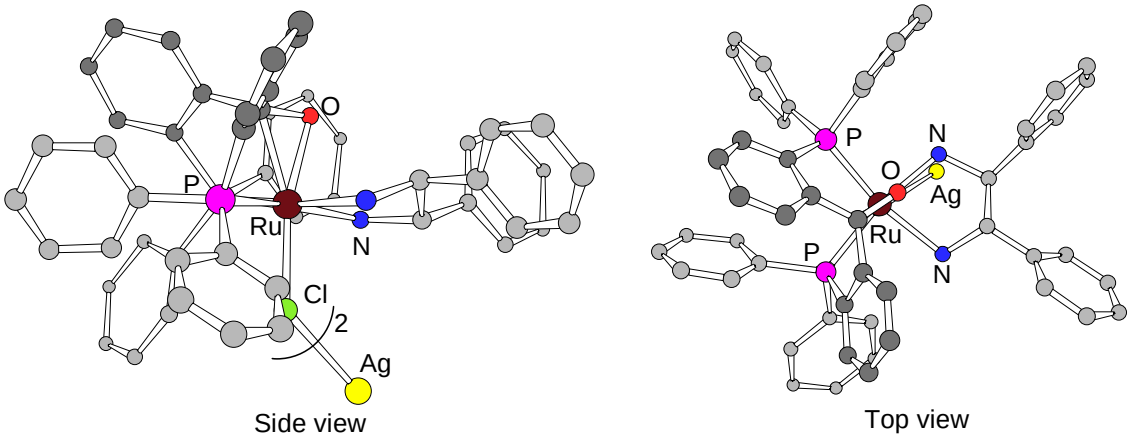

Figure 2-6. X-ray structural analysis of [RuCl(OTf)(**2a**){(*S*,*S*)-dpen}]$_2$AgOTf

The chiral conformation of **2a** in metal complexes is determined by the steric interaction between the phenyl groups of **2a** painted in black (Figure 2-7), and equatorial amine protons of DPEN painted in green. Figure 2-7 shows that disfavored (*P*)-**2a**-Ru/(*R*,*R*)-dpen complex has steric repulsion between phenyl groups of **2a** and equatorial amine protons of DPEN.

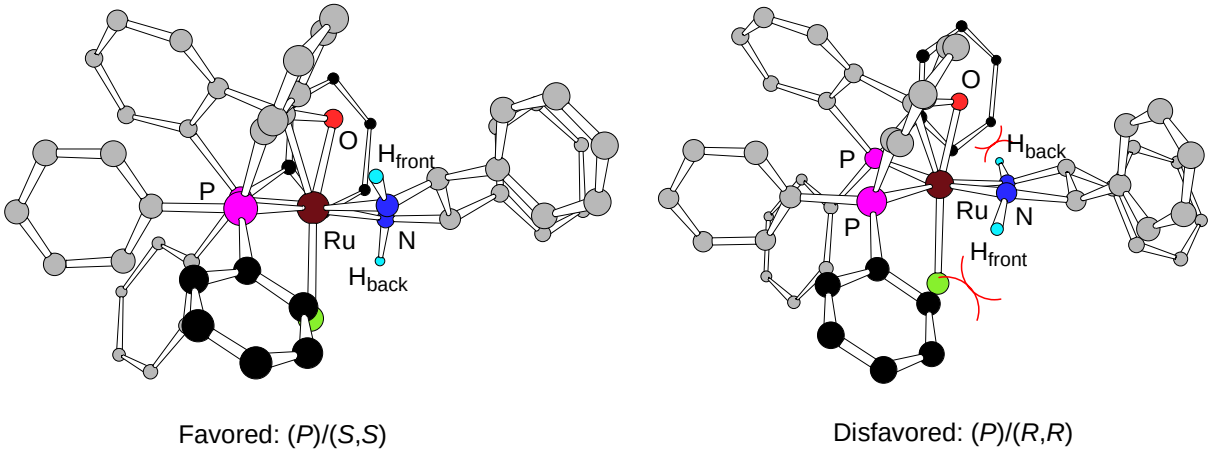

Figure 2-7. Steric repulsion between 2a and DPEN in metal complex

In case of chirality control of Rh complexes, BIPHEP-Rh/(*S*)-DABN was allowed to heat in dichloroethane at 80 °C for 5 h, or at room temperature over 17 days, (*P*)-BIPHEP-Rh/(*S*)-DABN diastereomer was only formed (Scheme 2-9).[6a] On the other hand, BIPHEP-Rh/(*S*,*S*)-DPEN did not isomerize even at 80 °C.

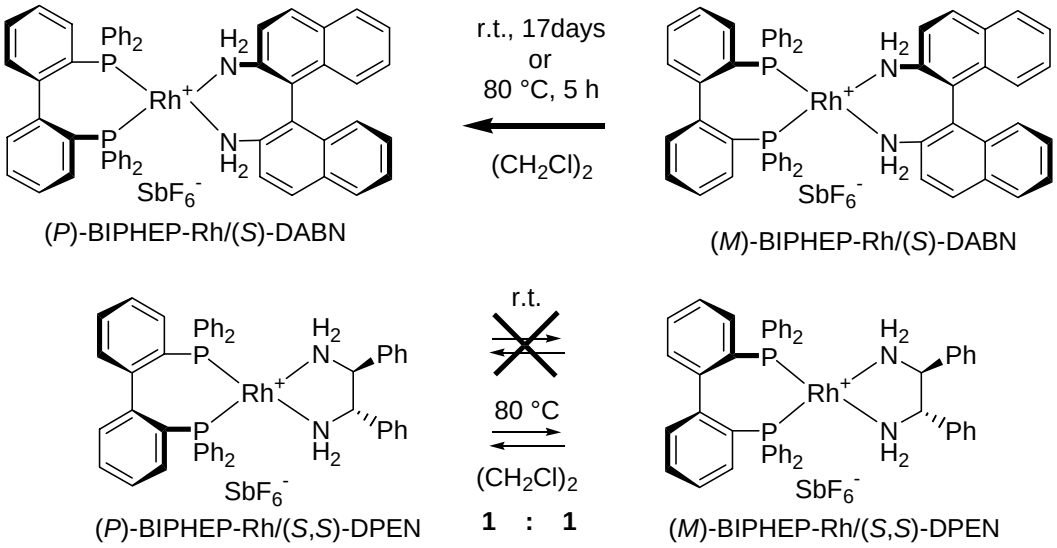

Scheme 2-9.

The chirality control of [Rh(**2a**)(cod)]SbF_6 complex by (*S*,*S*)-DPEN led to the formation of enantiomerically pure complex [Rh(**2a**){(*S*,*S*)-dpen}]SbF_6 at room temperature within minutes (Scheme 2-10). ^{31}P NMR spectrum of [Rh(**2a**){(*S*,*S*)-dpen}]SbF_6 shows two sets of doublets. These peaks indicate that two phosphorus atoms in the Rh-**2a** complex chirally controlled are non-equivalent as well as the Ru-**2a** complex chirally controlled. On the other hand, Rh-**2a** complex with (*S*)-DABN shows four broad peaks in ^{31}P NMR spectrum. Compared to DPEN, coordination ability of DABN is weak and, hence, (*S*)-DABN does not coordinate tightly to Rh-**2a** complex.

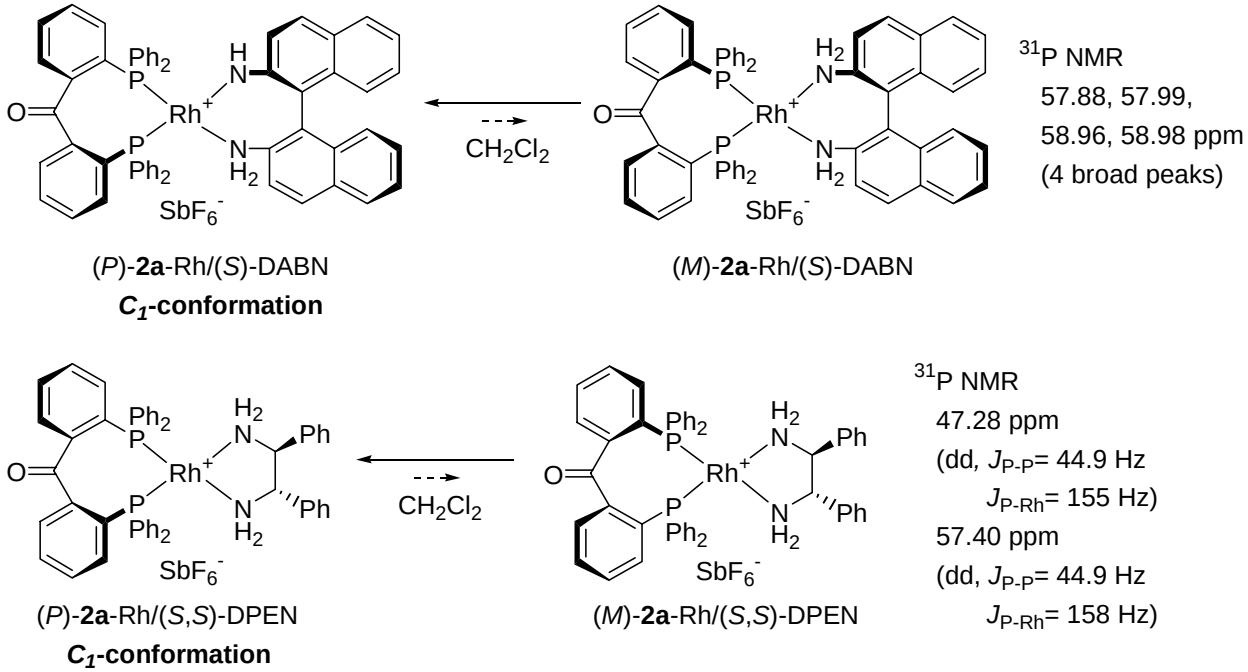

Scheme 2-10.

Compared to the $PtCl_2$-**2a** complex, the Ru- and Rh-**2a** complexes with (*S*)-DABN or (*S*,*S*)-DPEN adopted C_1- conformation at room temperature. In case of the Ru- and Rh-**2a** complexes, the carbonyl group of **2a** can be coordinated to Ru and Rh metals (Scheme 2-11). The coordination of carbonyl group is suggested by ^{13}C NMR spectrum of carbonyl group. In ^{13}C NMR spectrum, the carbonyl group of **2a** showed one single at 197.99 ppm, but the carbonyl group of Ru-**2a** complexes with (*S*,*S*)-DPEN showed two doublet at 149.89 ppm ($J_{C\text{-}P}$ = 24.8, 18.8 Hz). The coordinated carbonyl group of **2a** shifts upfield and splits into two doublet due to two phosphorus atoms of **2a**. The coordination of carbonyl group of **2a** retards the interconversion of **2a**, so that the Ru- and Rh-**2a** complexes with (*S*,*S*)-DPEN or (*S*)-DABN adopt a single chiral C_1-conformation.

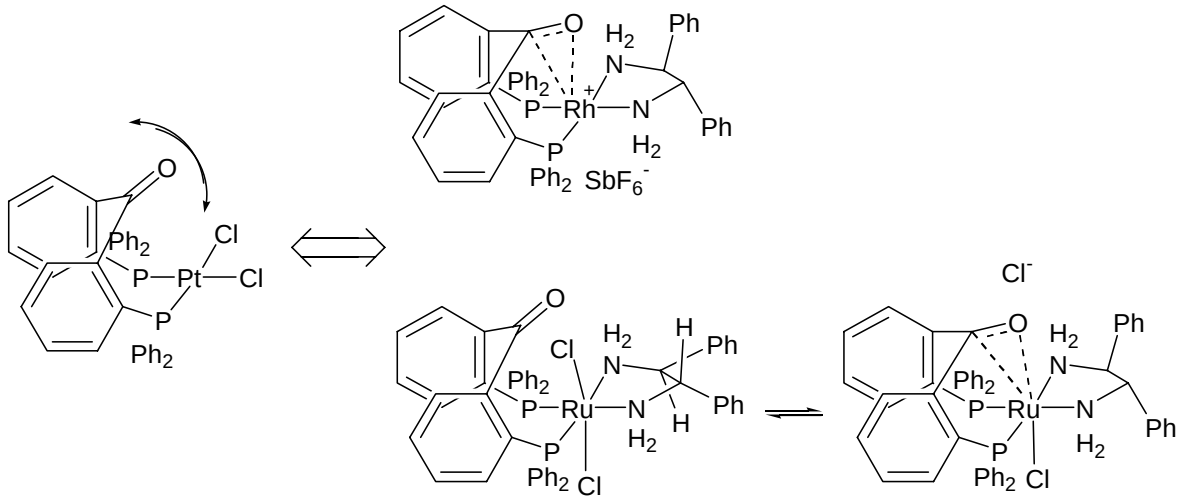

Scheme 2-11.

Two possible mechanisms can be envisaged for isomerization of the complex with **2a** or BIPHEP (Scheme 2-12).[9] Path (1) involves internal rotation between the two phenyl rings, and path (2) needs dissociation of one P-M (phosphine-metal) bond followed by rotation back leading to the enantiomeric complex. In case of BIPHEP-metal complex, the single diastereomer was obtained *via* path (2).[12] In contrast, metal complex with **2a** was estimated to obtain in a diastereomerically pure form at room temperature *via* path (1). The isomerization of 2,2'-diisopropylbenzophenone proceeded with internal rotation between the two phenyl rings (Scheme 2-13, path (1')).[3]

In the transition state of path (1), 2- and 2'-P go through each other. In the transition state of path (2), 2-P goes through 6'-H, in terms of the so-called "cog-wheel effect".[13] It is clear that the complexes with **2a** has longer distance between 2-P and 2'-P or 2-P and 6'-H than BIPHEP complexes, and has lower activation energies of two isomerization paths. Because of the lower rotational barrier, the complex with **2a** adopts a single conformation instantaneously.

Compared to BIPHEP complexes, Ru and Rh complexes with **2a** instantly adopted a single conformation upon addition of chiral activators. The chirality control of BIPHEP complexes did not proceed at room temperature (except for Ru complex). In sharp contrast, the complexes of **2a** controlled the conformation at room temperature within minutes. The flexibility of benzophenone backbone attains the instant chirality control.

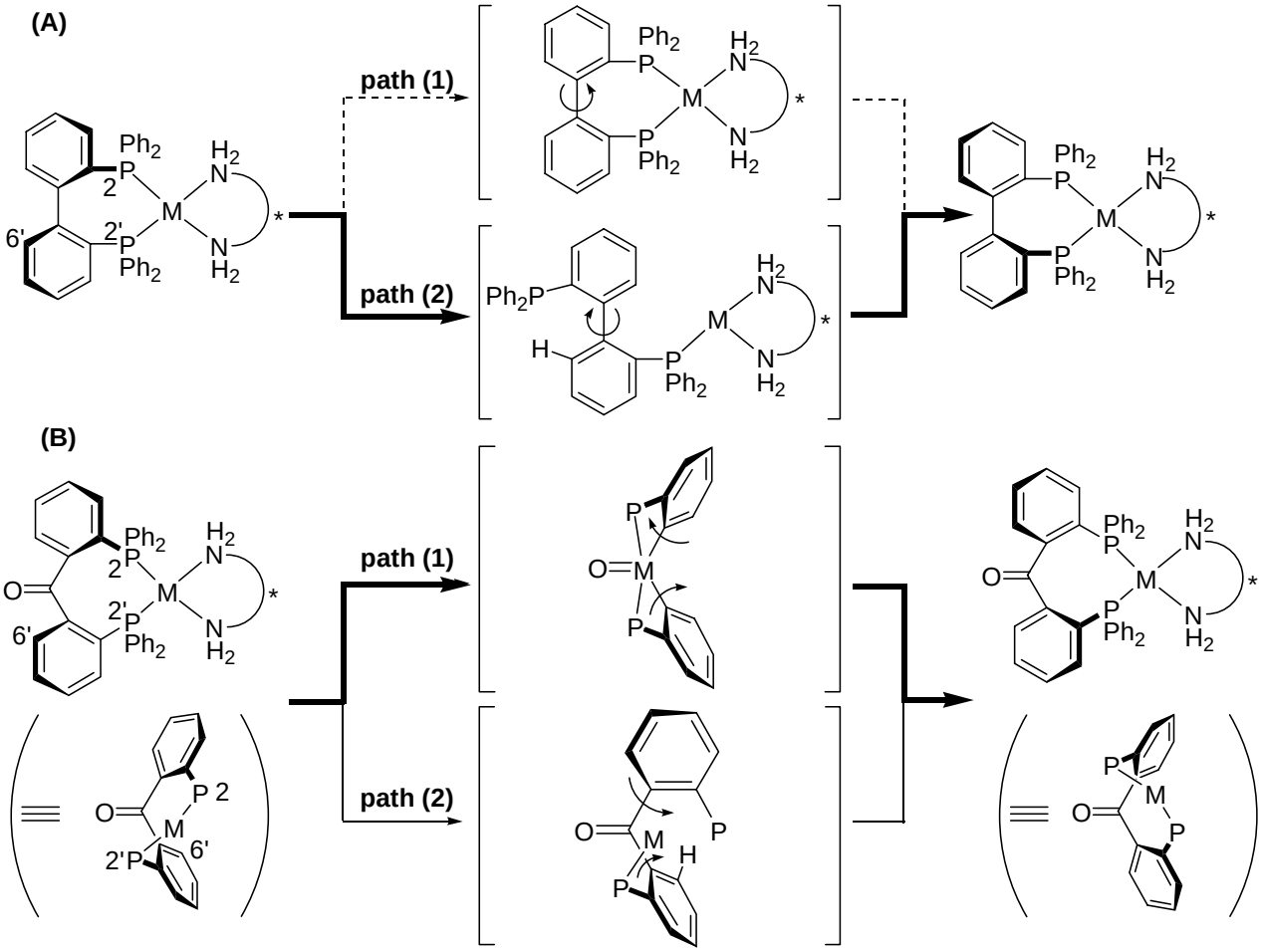

Scheme 2-12.

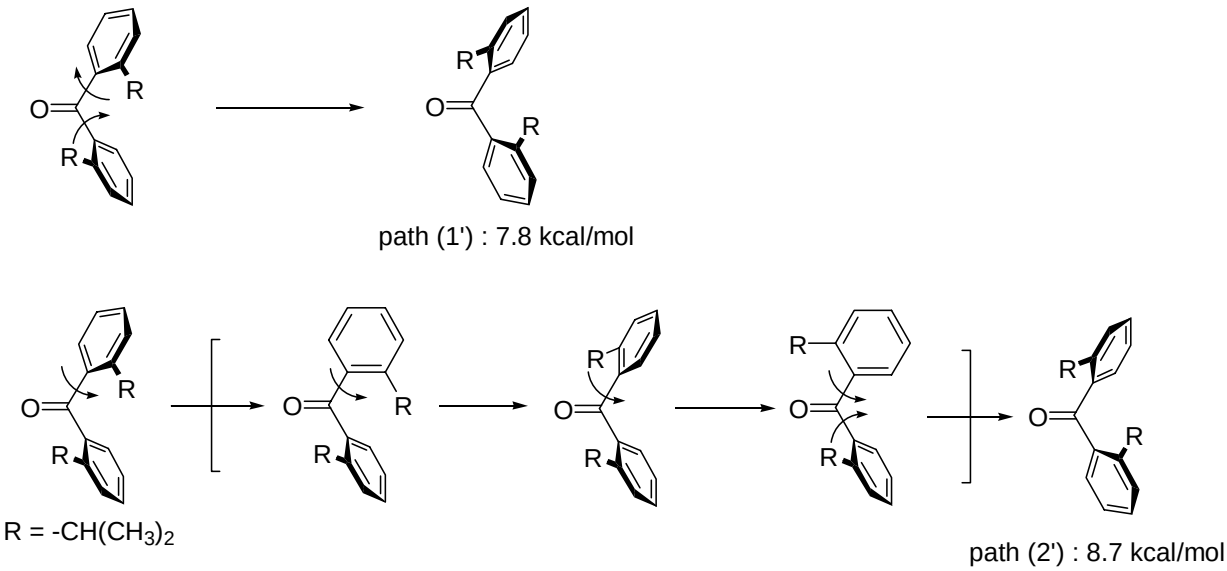

Scheme 2-13.

2-4. Catalytic asymmetric reactions with chirally controlled benzophenone-derived ligand

Section 2-3 shows that the benzophenone-derived ligand **2a** in Ru and Rh complexes instantly adopted a single chiral conformation upon addition of chiral activators. This section is referred to asymmetric reactions with **2a** complexes chirally controlled. The metal complexes with **2a** can be controlled to a single chiral conformation by chiral activators. Therefore, catalytic reactions with Ru and Rh complexes of **2a** that proceeded without desorption of chiral activators were first examined.

2-4-1. Ru-catalyzed asymmetric hydrogenation

Ru-diphosphine and diamine complexes have been used as asymmetric catalysts of hydrogenation of ketone substrates.[14,15] For example, Noyori and co-workers have reported that Ru-(*S*)-BINAP complexes with (*S*,*S*)-DPEN and (*S*)-DAIPEN attained high catalytic activity and enantioselectivity in asymmetric hydrogenation of acetophenone-derived substrates (Table 2-1).

Table 2-1. Asymmetric hydrogenation with BINAP-Ru complex and chiral diamines[6c,14,15a]

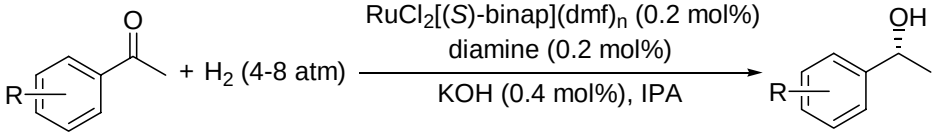

Diamine:

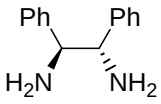

(*S*,*S*)-DPEN

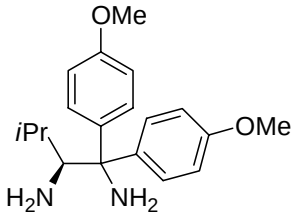

(*S*)-DAIPEN

Entry	Diamine	R	*Ee* (%)
1[a]	(*S*)-DAIPEN	H	87
2[b]	(*S*,*S*)-DPEN	*o*-CH_3	95
3[b]	(*S*)-DAIPEN	*p*-CH_3	94
4[a]	(*S*)-DAIPEN	*m*-OCH_3	88
5[a]	(*S*)-DAIPEN	*p*-OCH_3	92
6[b]	(*S*)-DAIPEN	*p*-Br	84
7[a]	(*S*,*S*)-DPEN	1-Naphthyl	97
8[c]	(*S*,*S*)-DPEN	2-Naphthyl	79

a. Ref 15a
b. Ref 14
c. Ref 6c

The advantage of benzophenone-derived ligand **2a** for asymmetric catalysis can be seen in hydrogenation of 1-acetonaphthone (Table 2-2).[10a] A virtually complete enantioselectivity was attained (99% *ee*, entry 1). The enantioselectivity (99% *ee*) thus obtained was higher than 97% *ee* obtained with enantiopure (*S*)-BINAP counterpart (entries 1 *vs*. 6). Hydrogenated **2a**, namely 2,2'-bis(diphenylphosphino)benzhydrol **2b**, might involve in the present hydrogenation of 1-acetonaphthone. However, the hydrogenation with **2b** was confirmed to be much lower in enantioselectivity than that with **2a** (entries 1 *vs*. 2). Not only ligand **2b**, diphenylmethane- and diphenylether-derived diphenylphosphine ligands (**2c** and **2d**) also decreased enantioselectivity (entries 3 and 4).

Table 2-2. Asymmetric hydrogenation of 1-acetonaphthone with Ru-**2a** complex

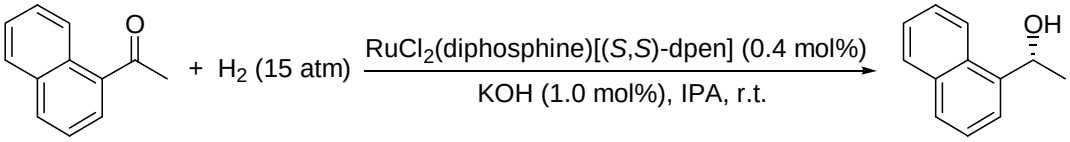

Entry	Diphosphine	Conv. (%)	*Ee* (%)
1	**2a**	**>99**	**99**
2	2b	67	66
3	2c	>99	70
4	2d	>99	29
5 [a]	DM-BIPHEP	>99	92
6 [b]	(*S*)-BINAP	>99	97

a. Ref 6c: reaction temperature was at -35 °C, H_2 pressure was 40 atm.
b. Ref 15a: H_2 pressure was 4 atm.

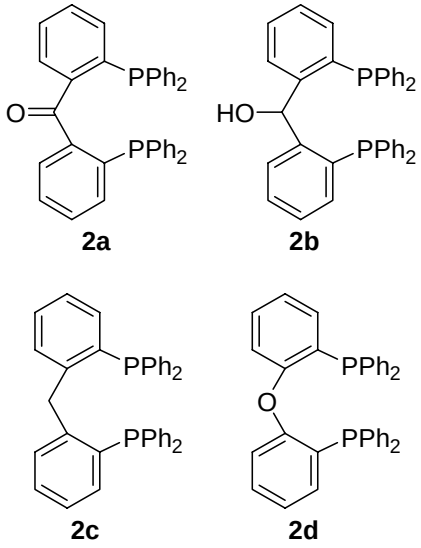

The hydrogenation by Ru-**2a** was also effective even in the case of *o*-, *m*-, or *p*-substituted acetophenones (Table 2-3). Ru-**2a** complex gave *o*-, *m*-, or *p*-substituted phenethyl alcohols with high enantiomeric excess (up to 98% *ee*).* Unfortunately, Ru-**2a** complex attained low catalytic activity and enantioselectivity in asymmetric hydrogenation of 9-acetylanthracene (entry 13).

Table 2-3. Asymmetric hydrogenation of acetophenone-derived substrates

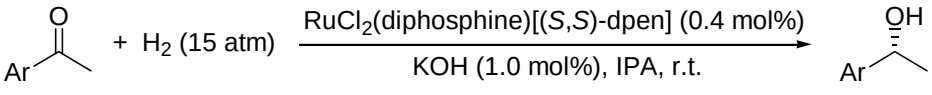

Entry	Substrate	Diphosphine	Conv. (%)	*Ee* (%)
1	**1**	**2a**	**>99**	**90**
2	1	(*S*)-BINAP	>99	86
3	**2A**	**2a**	**>99**	**98**
4[a]	2A	(*S*)-tolBINAP	>99	94
5	**2B**	**2a**	**>99**	**92**
6	2B	(*S*)-BINAP	>99	89
7	**2C**	**2a**	**>99**	**91**
8	2C	(*S*)-BINAP	>99	87
9	**3**	**2a**	**>99**	**99**
10[a]	3	(*S*)-BINAP	>99	97
11	**4**	**2a**	**99**	**87**
12[b]	4	(*S*)-BINAP	99	79
13[c]	**5**	**2a**	**3**	**40**

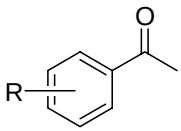

1: R = H
2A: R = *o*-Me
2B: R = *m*-Me
2C: R = *p*-Me

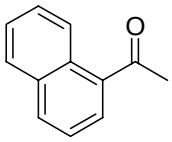

3

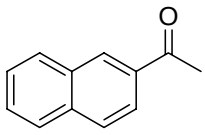

4

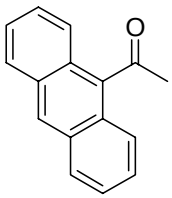

5

a. Ref 15a: H_2 pressure was 4 atm.
b. Ref 6c: H_2 pressure was 8 atm.
c. Reaction temperature was at 60 °C, H_2 pressure was 20 atm.

---

* After finished up our research project (*Bachelor Presentation* in 2003, Tokyo Institute of Technology et al)[10], Ding and co-workers (2006) reported the asymmetric hydrogenation with Ru-**2a** complexes and various chiral diamines in ethanol solution.[16] In this report, (*R*,*R*)-DPEN shows the best performance in asymmetric hydrogenation of acetophenone (>99%, 90% *ee*).

In the transition state of asymmetric hydrogenation with Ru-**2a** complex, $RuCl_2$(**2a**)[(*S*,*S*)-dpen] is transformed to RuX_2(**2a**)[(*S*,*S*)-dpen] (X = Cl or H).[16,17,18] Because of C_1-conformation of $RuCl_2$(**2a**)-[(*S*,*S*)-dpen], upper and lower hydrides of RuX_2(**2a**)[(*S*,*S*)-dpen] are non-equivalent (Scheme 2-14). The carbonyl group of **2a** blocks the approach of ketone substrates to the upper side, so that RuHCl(**2a**)[(*S*,*S*)-dpen] catalyzed hydrogenation proceeds in lower side. In the transition state, the H^--Ru-N-H_{ax}^+ group of the Ru-**2a** catalyst forms a 1,4-dipole which fits with the C^+=O^- dipole of ketone substrates. A comparison of two transition structures (Ts-*Si* and Ts-*Re* in Scheme 2-14) show that Ts-*Si* is less hindered in terms of the repulsion between aryl group of substrates and phenyl group of **2a** (painted in grey) and give (*R*)-enriched products, which is consistent with the outcome observed. In hydrogenation of 9-acetylanthracene, the huge anthryl group prevented the approach of the ketone substrate to the Ru-**2a** catalyst and showed low catalytic activity and enantioselectivity.

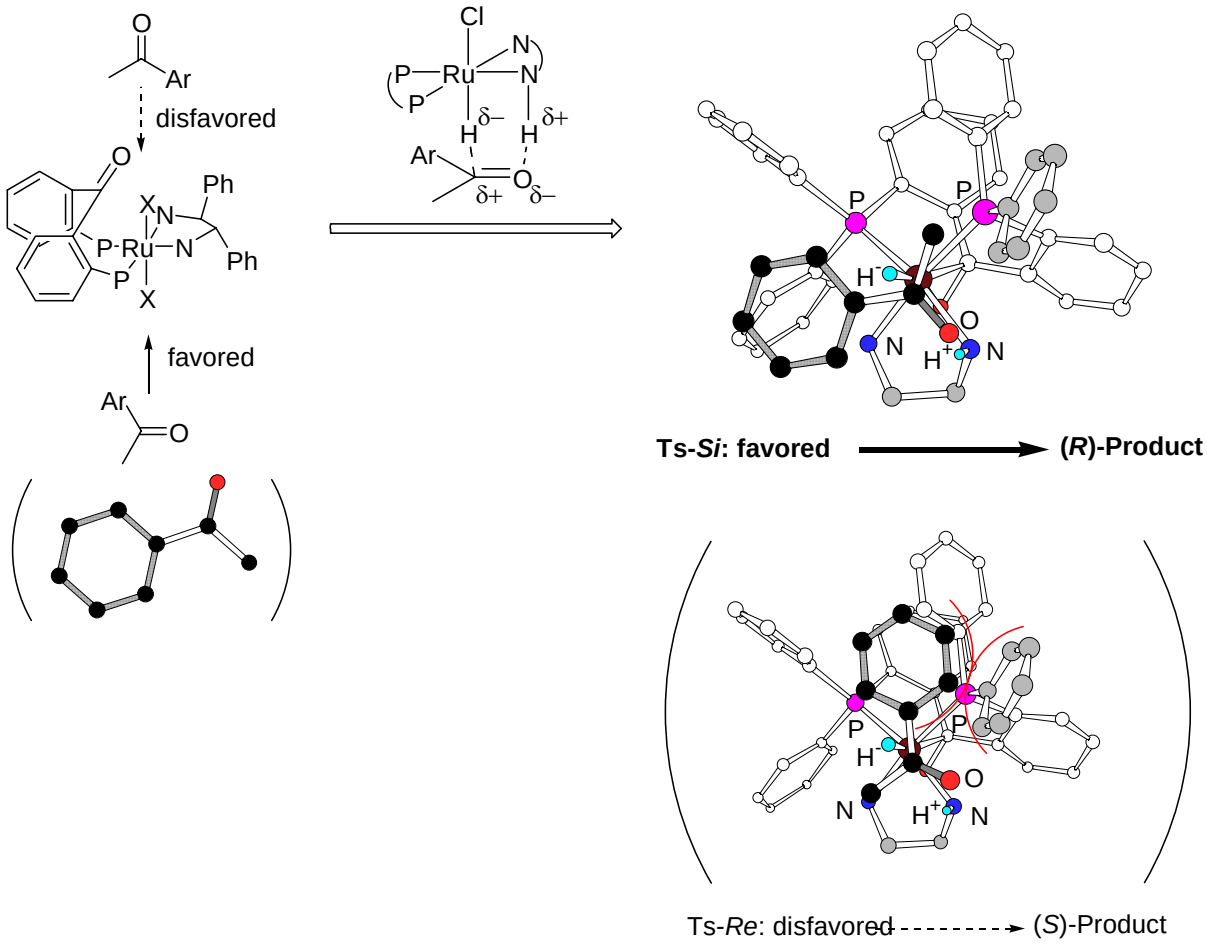

Scheme 2-14.

Compared to the asymmetric hydrogenation of 1-acetonaphthone with (*S*)-BINAP-Ru/(*S*,*S*)-DPEN catalyst, the asymmetric hydrogenation of 9-acetylanthracene required the change in the absolute configuration of BINAP counterpart.[6c,15e] (*S*)-BINAP-$RuCl_2$/(*S*,*S*)-DPEN attained high catalytic activity and enantioselectivity in hydrogenation of 1-acetonaphthone (Table 2-4). On the other hand, (*R*)-BINAP-$RuCl_2$/(*S*,*S*)-DPEN attained low catalytic activity and enantioselectivity in asymmetric hydrogenation of 1-acetonaphthone, but asymmetric hydrogenation of 9-acetylanthracene with (*R*)-tolBINAP-$RuCl_2$/(*S*,*S*)-DPEN gave the product in high yield and enantiomeric excess.

$RuCl_2$(**2a**)[(*S*,*S*)-dpen] and one equivalent of AgOTf attained high catalytic activity and enantioselectivity in asymmetric hydrogenation of both 1-acetonaphthone and 9-acetylanthracene irrespective of the ketonic substrates (Table 2-4). These results are in sharp contrast to the different matched pair of BINAP and DPEN opposite between asymmetric hydrogenations of 1-acetonaphthone and 9-acetylanthracene. The asymmetric hydrogenation of 9-acetylanthracene with $RuCl_2$(**2a**)-[(*S*,*S*)-dpen] and silver salt was examined with several conditions (Table 2-5). The variety of silver salts did not affect the catalytic activity and enantioselectivity (entries 2-5). Remarkably, the addition of silver salt quite increased the catalytic activity. The hydrogenation of 9-acetylanthracene with (*R*)-tolBINAP-$RuCl_2$/ (*S*,*S*)-DPEN proceeded at 80 °C, but the hydrogenation with the Ru-**2a** complex and silver salt proceeded even at room temperature and attained higher enantioselectivity than at 60 ˚C (entries 5 *vs.* 7).

Table 2-4. Asymmetric hydrogenation of 1-acetonaphthone and 9-acetylanthracene

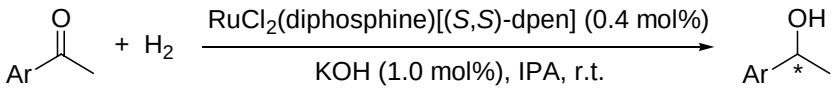

Yield/*Ee*	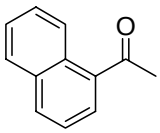	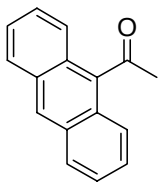
2a + AgOTf (1.0 eq.)	**>99%/96% *ee* (*R*)**	**95%/91% *ee* (*R*)**
(*S*)-BINAP [a]	>99%/97% *ee* (*R*)	91%/41% *ee* (*R*)[b]
(*R*)-BINAP [a]	>99%/14% *ee* (*S*)	99%/81% *ee* (*R*)[b]

a. Ref 6c
b. Reaction temperature was 80 °C. tolBINAP was used instead of BINAP.

Table 2-5. Asymmetric hydrogenation of 9-acetylanthracene with Ru-**2a** and silver salt

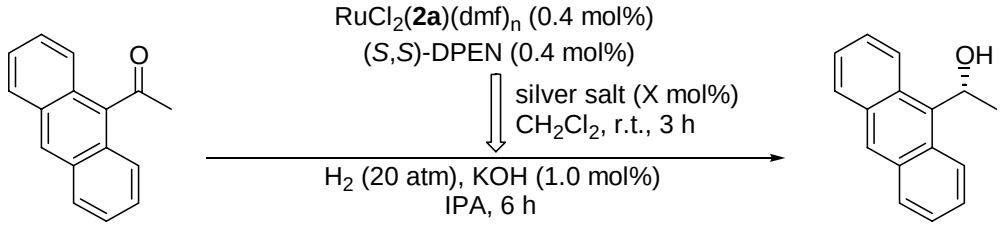

Entry	Silver solt	X (mol%)	Temp. (°C)	Yield (%)	*Ee* (%)
1 [a]	-	-	60	3	40
2	$AgSbF_6$	0.4	60	92	86
3	$AgPF_6$	0.4	60	99	85
4	$AgBF_4$	0.4	60	98	87
5	AgOTf	0.4	60	99	86
6	AgOTf	1.0	60	91	85
7 [a]	**AgOTf**	**0.4**	**r.t.**	**95**	**91**
cf. [b]	$RuCl_2$\{(*R*)-tolbinap\}\{(*S*,*S*)-dpen\}		80	99	81

a. Reaction time was 24 h.

b. Ref 6c

Based on the X-ray structural analysis of [RuCl(OTf)(**2a**){(*S*,*S*)-dpen}]$_2$AgOTf, the addition of silver salt to the $RuCl_2$(**2a**)[(*S*,*S*)-dpen] complex led to the coordination of the carbonyl group of **2a** to the Ru metal. It is estimated that the coordination of carbonyl group changes the conformation of the ruthenium-hydride complex with **2a** and (*S*,*S*)-DPEN, which was the active species of the asymmetric hydrogenation.

Noyori, Ohkuma and co-workers have reported that *trans*-RuH(η^1-BH_4)(binap)(dpen) was synthesized from BINAP-$RuCl_2$/DPEN complex and $NaBH_4$. [18] Following the report, the RuHX(**2a**)[(*S*,*S*)-dpen] (X = η^1-BH_4 or TfO) complexes were synthesized. Compared with $RuCl_2$(**2a**)[(*S*,*S*)-dpen] and [RuCl(**2a**){(*S*,*S*)-dpen}](OTf) complexes, ^{31}P NMR spectra of the RuHX(**2a**)[(*S*,*S*)-dpen] complexes showed different peaks depending on silver salt (Figure 2-8). In addition, hydride peaks of ^{1}H NMR spectra were different from those of RuHX(**2a**)[(*S*,*S*)-dpen] complexes. The one triplet peak of ^{1}H NMR spectrum (a') showed that reaction with $RuCl_2$(**2a**)[(*S*,*S*)-dpen] complex and $NaBH_4$ synthesized *trans*-RuH(η^1-BH_4)(**2a**)[(*S*,*S*)-dpen] complex. Compared with the *trans*-RuH(η^1-BH_4)(**2a**)[(*S*,*S*)-dpen] complex, the hydride peak of

[RuH(**2a**){(*S*,*S*)-dpen}](OTf) shifts downfield (-2.8 ppm) and splits into two doublets. The two doublets peak of [RuH(**2a**){(*S*,*S*)-dpen}](OTf) showed that the *trans* position of hydride possessed carbonyl group of **2a** and the octahedral conformation around Ru metal was distorted.

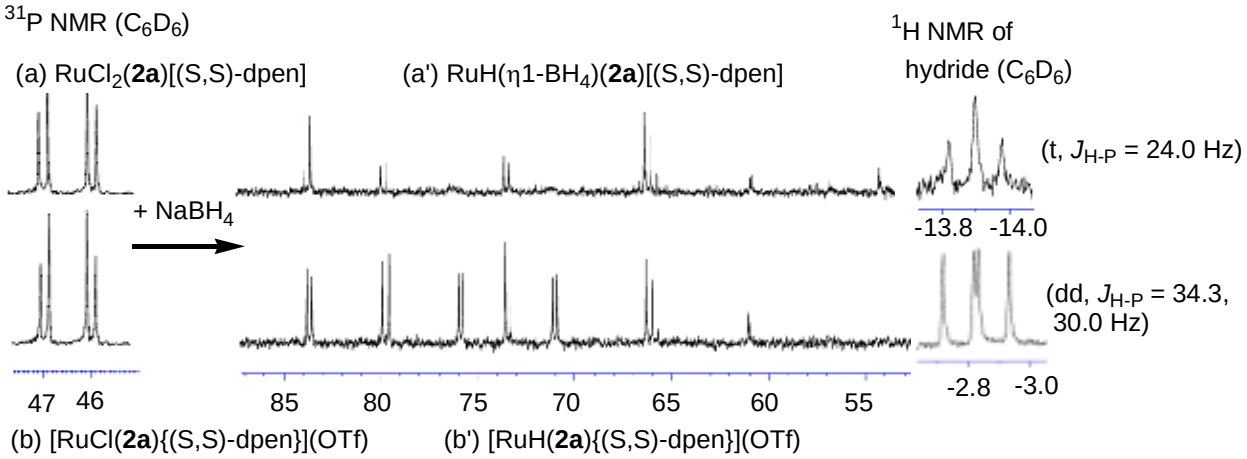

Figure 2-8. ^{1}H and ^{31}P NMR spectra of Ru-**2a** complexes reacted with $NaBH_4$

In the transition state of asymmetric hydrogenation, it is estimated that the distorted conformation of [RuH(**2a**){(*S*,*S*)-dpen}](OTf) transforms *trans* conformation to *cis* conformation depending on the steric electronic effect of ketonic substrates. The transformation affects the catalytic activity and enantioselectivity of the asymmetric hydrogenation, the so-called "induced fit catalysis".[19] The dihedral angle of 9-acetylanthracene between carbonyl group and anthryl group is about 90°. In hydrogenation with *trans*-$RuCl_2$(**2a**)[(*S*,*S*)-dpen], the huge anthryl group prevents the approach to the Ru-**2a** complex.. Probably, the transformation between *trans* and *cis* conformation provided high catalytic activity and enantioselectivity in asymmetric hydrogenation of both 1-acetonaphthone (via the *trans* conformation) and 9-acetylanthracene (via the *cis* conformation) (Scheme 2-15).

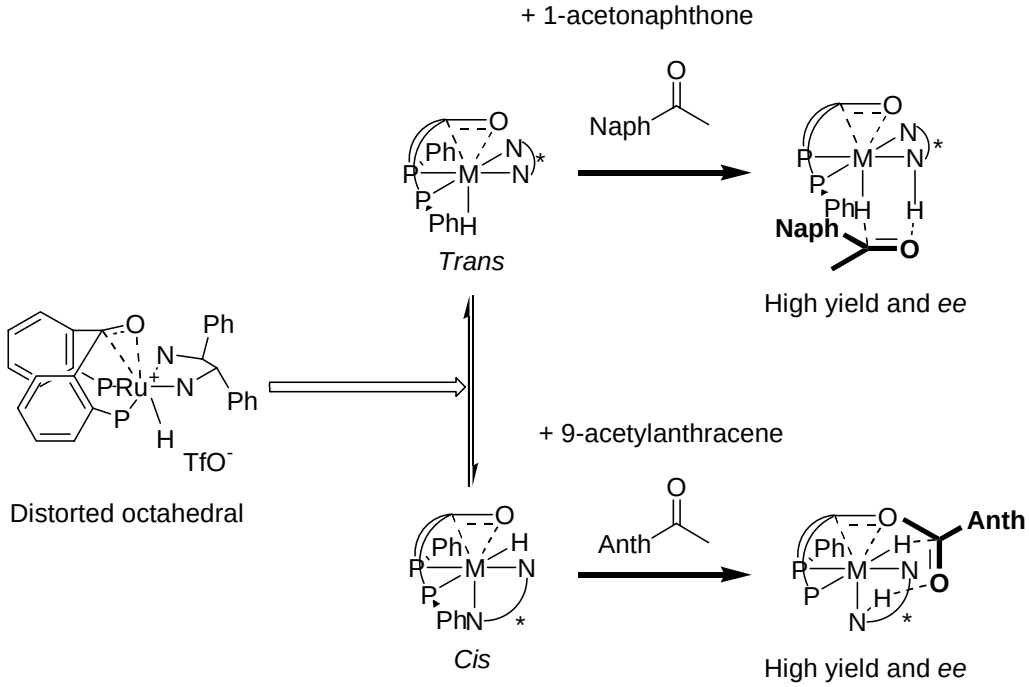

Scheme 2-15.

Figure 2-9 shows the transition structures (Ts) of the *trans* and *cis* conformations on the basis of the X-ray structural analysis. In case of *trans* conformation, enantioselectivity of hydrogenation depends on the steric interaction between substrates and phenyl group of **2a** (painted in grey). On the other hand, steric interaction between substrates and phenyl group of **2a** (painted in yellow) determines the enantioselectivity of hydrogenation with *cis*-Ru-**2a** complex.

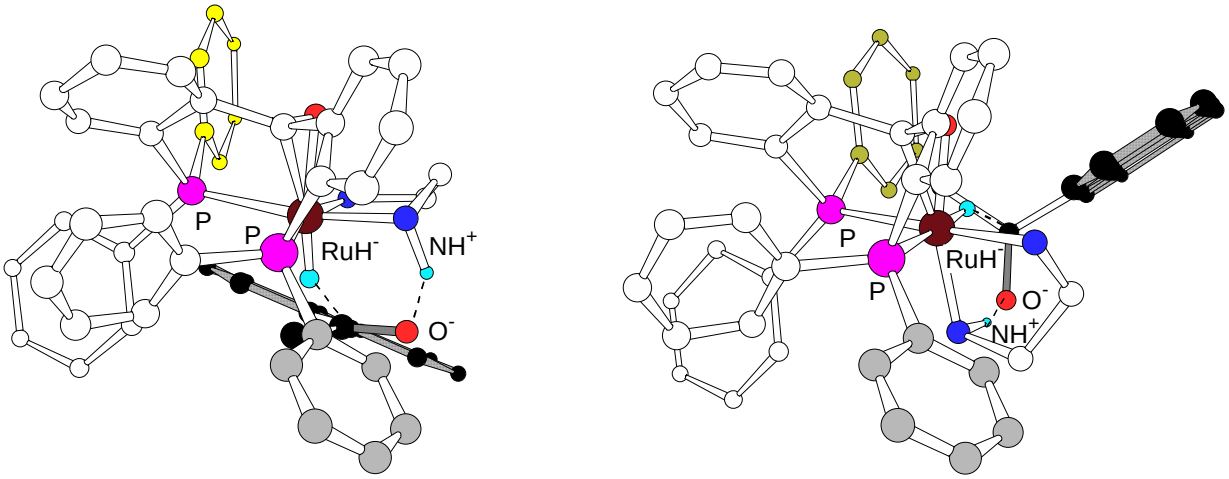

Ts: *trans* conformation　　Ts: *cis* conformation

Figure 2-9. transition structures of the *trans* and *cis* conformations of Ru-**2a** complex

2-4-2. Rh-catalyzed asymmetric transfer hydrogenation

Not only asymmetric hydrogenations with Ru catalysts, benzophenone-derived ligand **2a** attained high catalytic activity and enantioselectivity in transfer hydrogenations with Rh complex.

Asymmetric transfer hydrogenations have been reported to use Rh complexes with chiral diamine ligands[20] or chiral PNNP-type ligands.[21] Lemaire and co-workers have reported that the Rh complex with (*S*,*S*)-DM-DPEN attains high catalytic activity and enantioselectivity in asymmetric transfer hydrogenation of phenyl glyoxylate substrate, but the catalytic activity and enentioselectivity were quite decreased in the transfer hydrogenation of acetophenone (Table 2-6).[20d]

Table 2-6. Asymmetric transfer hydrogenation with Rh-DM-DPEN complex[20d]

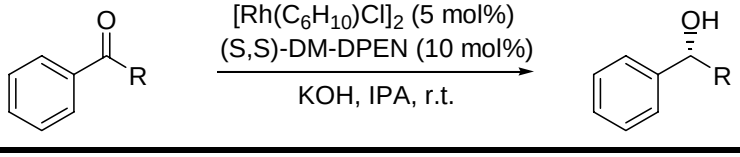

(*S*,*S*)-DM-DPEN

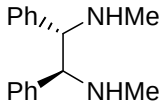

Entry	R	Time	Conv. (%)	*Ee* (%)
1	CO_2CH_3	1 h	99	>99
2	CH_3	7 days	100	67

Yusa in the Mikami group has previously reported the transfer hydrogenation with BINAP-Rh-chiral diamine complexes. BINAP-Rh complexes were examined by changing the chirality and aliphatic or aromatic nature of diamines (Table 2-7). Among diamines examined, DPEN afforded the highest enantioselectivity, though at a moderate level (96%, 71% *ee*, entry 6). It should be noted here that the matched enantiomer of DPEN for acetophenone is changed from $RuCl_2$[(*R*)-binap][(*R*,*R*)-dpen] to [Rh{(*R*)-binap}{(*S*,*S*)-dpen}]SbF_6.[22]

Table 2-7. Asymmetric transfer hydrogenation with BINAP-Rh complexes

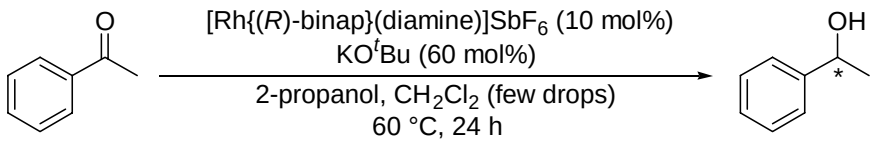

Diamine:

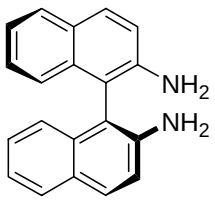

(*S*)-DABN

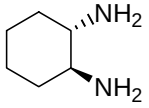

(*S*,*S*)-DACH

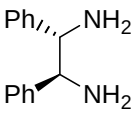

(*S*,*S*)-DPEN

Entry	Diamine	Conv. (%)	*Ee* (%)
1	(*R*)-DABN	58	12 (*S*)
2	(*S*)-DABN	73	0 -
3	(*R*,*R*)-DACH	37	10 (*S*)
4	(*S*,*S*)-DACH	81	57 (*R*)
5	(*R*,*R*)-DPEN	93	0 -
6	**(*S*,*S*)-DPEN**	**96**	**71 (*R*)**

cf.

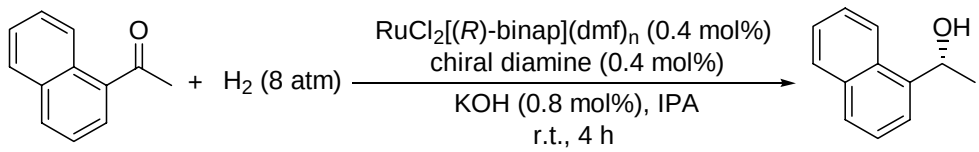

Chiral Diamine = **(*R*,*R*)-DPEN : >99%, 98% *ee*[a]**
= (*S*,*S*)-DPEN : >99%, 16% *ee*[a] a. Ref 15a

The advantage of achiral benzophenone-derived ligand **2a** over the enantiopure BINAP for asymmetric catalysis can be seen in asymmetric transfer hydrogenation of acetophenone (Table 2-8).[10b] At the outset, the reaction conditions were optimized using the BINAP catalysts. Transfer hydrogenation with [Rh(**2a**){(*S*,*S*)-dpen}]SbF_6 was first examined with respect to the reaction temperature and co-solvent using the best diamine for the Rh-BINAP complex (entry 1). 1,2-Dichloroethane rather than dichloromethane was found to be the best co-solvent and room temperature was preferable to give the highest enantioselectivity (entry 8). 1,2-dichloroethane attained high enantioselectivity, but an excess amount of 1,2-dichloroethane decreased catalytic activity (entries 6 *vs.* 7). Rh-BINAP complex with 1,2-dichloroethane did not catalyze the transfer hydrogenation (entry 10).

Table 2-8. Asymmetric transfer hydrogenation of acetophenone with Rh-**2a** complex

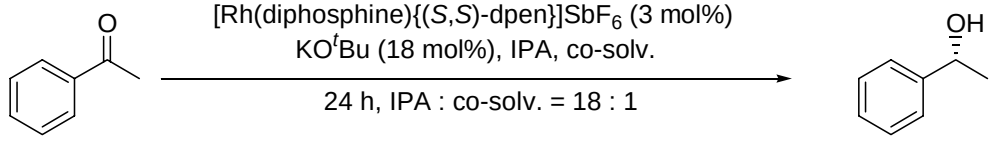

Entry	Diphosphine	Co-solv.	Temp. (°C)	Conv. (%)	*Ee* (%)
1	2a	dichloromethane[a]	60	99	68
2	2a	-	60	98	63
3	2a	toluene	60	99	37
4	2a	THF	60	>99	48
5	2a	*o*-dichlorobenzene	60	>99	72
6	2a	1,2-dichloroethane	60	96	86
7	2a	1,2-dichloroethane[b]	60	47	86
8	**2a**	**1,2-dichloroethane**	**25**	**97**	**89**
9	(*R*)-BINAP	dichloromethane[a]	60	96	71
10	(*R*)-BINAP	1,2-dichloroethane	60	trace	-

a. Co-solvent was added few drops.
b. IPA : co-solv. = 4 : 1

Virtually complete enantioselectivities were obtained for 1-acetonaphthone and *o*-methyl-acetophenone under the optimized reaction conditions (Table 2-9, entries 4 and 11). The [Rh(**2a**){(*S*,*S*)-dpen}]SbF_6 catalyst gave (*R*)-1-(1'-naphthyl)ethanol and (*R*)-*o*-methyl-phenethylalcohol in 99% yield with 99% *ee*,* which is significantly higher than 72% *ee* and 57% *ee* respectively obtained with enantiopure [Rh{(*R*)-binap}{(*S*,*S*)-dpen}]SbF_6.

*Compared to other ketone substrates, transfer hydrogenations of 1-acetonaphthone and *o*-methyl-acetophenone with Rh-**2a** complex attained high catalytic activity and enantioselectivity without 1,2-dichloroethane (Table 2-9, entries 3 and 10).

Table 2-9. Asymmetric transfer hydrogenation with Rh-**2a** complex.

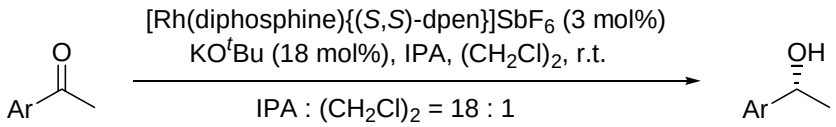

Entry	Substrate	Diphosphine	Time (h)	Conv. (%)	*Ee* (%)
1	**1**	**2a**	**24**	**97**	**89**
2 [a]	1	(*R*)-BINAP	24	96	71
3	**2A**	**2a**	**48**	**67**	**97**
4 [b]	**2A**	**2a**	**24**	**99**	**99**
5 [a]	2A	(*R*)-BINAP	24	61	57
6	**2B**	**2a**	**48**	**95**	**91**
7 [a]	2B	(*R*)-BINAP	24	97	68
8	**2C**	**2a**	**48**	**97**	**85**
9 [a]	2C	(*R*)-BINAP	24	99	55
10	**3**	**2a**	**48**	**92**	**97**
11 [b]	**3**	**2a**	**24**	**99**	**99**
12 [a]	3	(*R*)-BINAP	24	98	72
13	**4**	**2a**	**24**	**97**	**84**
14 [a]	4	(*R*)-BINAP	24	73	59
15	**5**	**2a**	**48**	**8**	**90**

a. co-solvent was CH_2Cl_2 (fewdrops), reaction temperature was 60 °C.
b. only IPA sovent

Substrate:

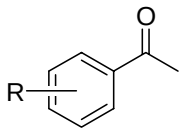

1: R = H
2A: R = *o*-Me
2B: R = *m*-Me
2C: R = *p*-Me

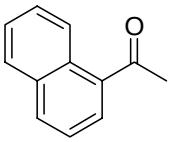

3

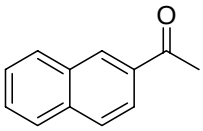

4

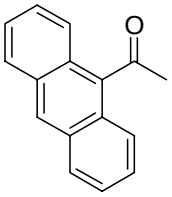

5

2-5. Conclusion

In summary, the Ru and Rh complexes with benzophenone-derived ligand **2a** can instantly adopt a single chiral conformation upon addition of chiral diamines. The BIPHEP complexes isomerized into a single diastereomer at high temperature for several hours, but the complexes with **2a** isomerized into a single conformation even at room temperature within minutes (Scheme 2-16). Compared to one single bond rotation of a biphenyl compound, two single bond rotations of a benzophenone-derived compound are more facile and the chirality in the complexes with **2a** could be controlled instantaneously.

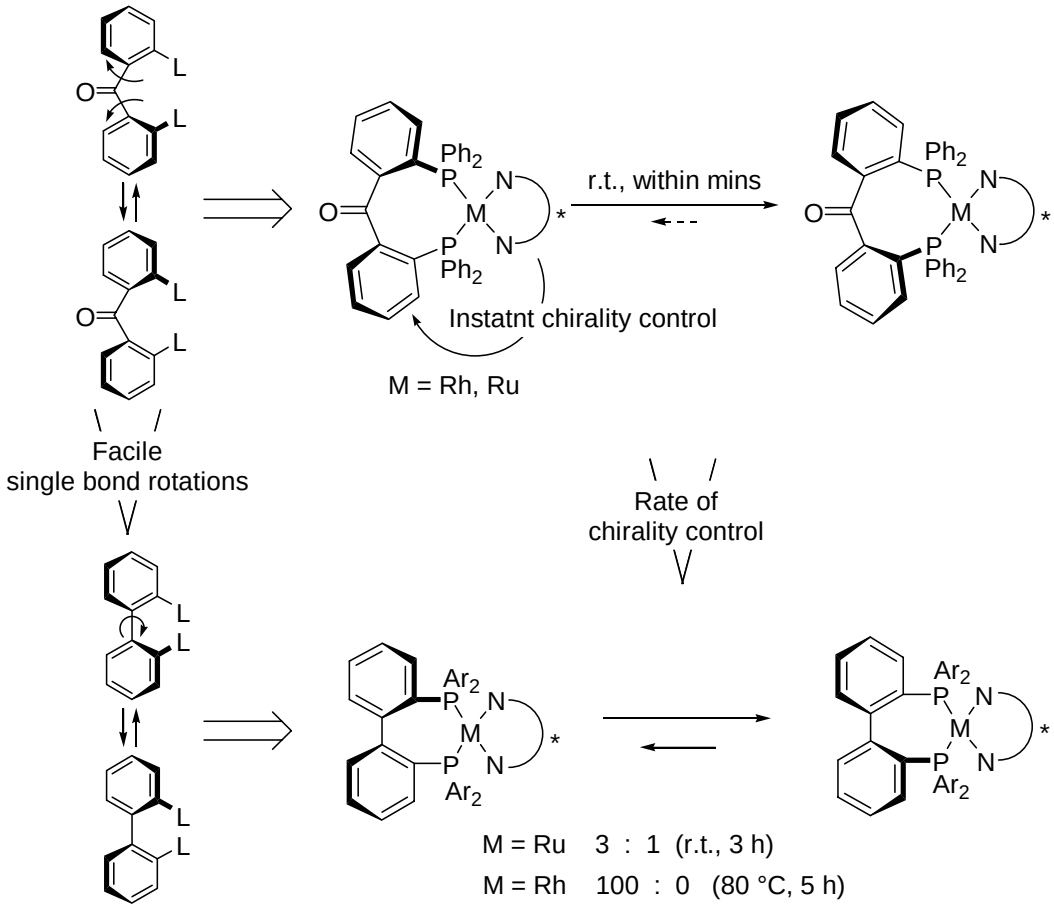

Scheme 2-16.

The complexes chirally controlled with **2a** showed high catalytic activity and enantioselectivity in catalytic asymmetric reactions (Scheme 2-17). In case of the hydrogenation and transfer hydrogenation of ketone substrates, the Ru- and Rh-**2a** complexes with (*S*,*S*)-DPEN afforded higher

enantioselectivity than those attained by the enantiopure BINAP counterpart (up to >99%, 99% *ee*).

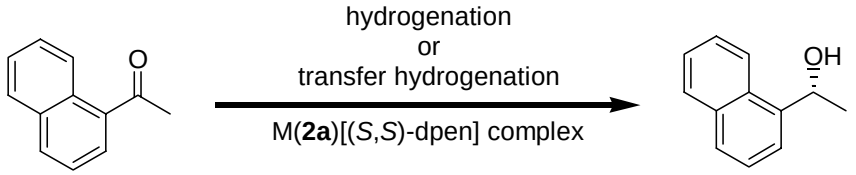

M = $RuCl_2$: >99%, 99% *ee*
M = $RhSbF_6$: >99%, 99% *ee*

cf. $RuCl_2$[(*S*)-binap][(*S*,*S*)-dpen] : >99%, 97% *ee* (Ref 16a)
[Rh{(*R*)-binap}{(*S*,*S*)-dpen}]SbF_6: 98%, 72% *ee*

Scheme 2-17.

In addition, the Ru-**2a** complex with silver salt attained high catalytic activity and enantioselectivity in asymmetric hydrogenations of 1-acetonaphthone and 9-acetylanthracene (Table 2-10). In sharp contrast, the BINAP-Ru/DPEN complexes have to be changed in the absolute configuration of BINAP to attain high enantioselectivities for both ketonic substrates.

Table 2-10. Asymmetric hydrogenation of 1-acetonaphthone and 9-acetylanthracene

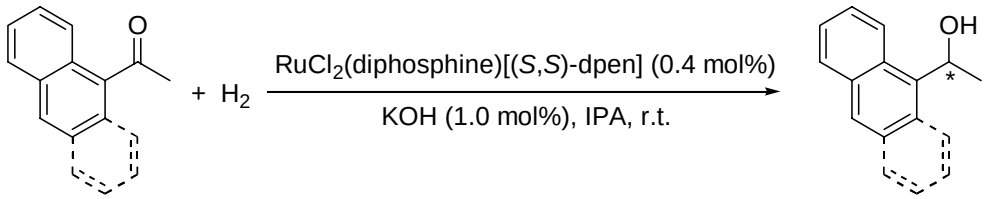

yield/*ee*	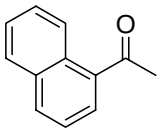	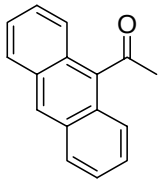
2a + AgOTf (1.0 eq.)	**>99%/96% *ee* (*R*)**	**95%/91% *ee* (*R*)**
(*S*)-BINAP[a]	>99%/97% *ee* (*R*)	91%/41% *ee* (*R*)[b]
(*R*)-BINAP[a]	>99%/14% *ee* (*S*)	99%/81% *ee* (*R*)[b]

a. Ref 6c
b. Reaction temperature was 80 °C. tolBINAP was used instead of BINAP.

The Ru-**2a** complex chirally controlled is estimated to interconvert between *cis* conformation and *trans* conformation. Each conformation was instantly controlled in a single chiral conformation and attained high catalytic activity and enantioselectivity to fit well with the substrate change (Scheme 2-18). The high enantioselectivities with **2a** complexes exemplifies the advantage of the instant chirally controlled catalysts.

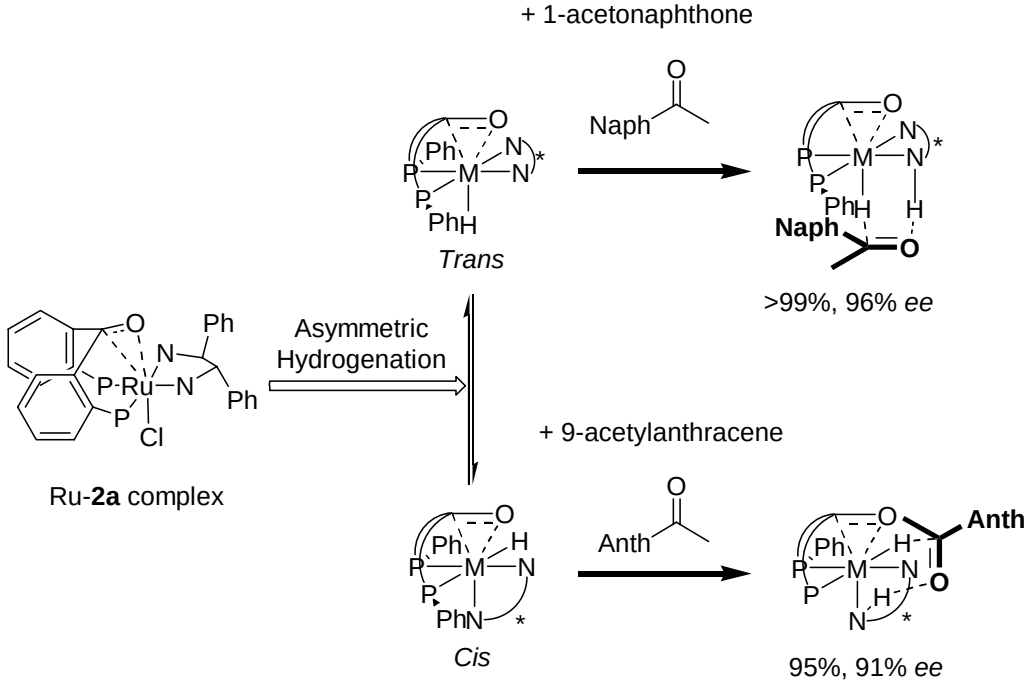

Scheme 2-18.

Experimental section

General

^{1}H NMR and ^{13}C NMR spectra were measured on Varian Gemini 300 (300 MHz), Varian Inova-400 (400 MHz) and Bruker AV300M (300 MHz) spectrometers, ^{31}P NMR and ^{19}F NMR spectra were measured on Varian Inova-400 (400 MHz) and Bruker AV300M (300 MHz) spectrometers. Chemical shift of ^{1}H NMR was expressed in parts per million downfield from tetramethylsilane as an internal standard (δ = 0) in $CDCl_3$. Significant ^{1}H NMR data were tabulated in the following order: multiplicity (s: singlet; d: doublet; t: triplet; q: quartet; br: broad; m: multiplet) and coupling constants (*J*) are reported (Hz). Chemical shifts of ^{13}C NMR were expressed in parts per million downfield from $CDCl_3$ as an internal standard (δ = 77.0) in $CDCl_3$. Chemical shifts of ^{19}F NMR were expressed in parts per million downfield from BTF as an external standard (δ = -63.24) in $CDCl_3$. Chemical shifts of ^{31}P NMR were expressed in parts per million downfield from 85% H_3PO_4 as an external standard (δ = 0) in $CDCl_3$.

Analytical thin layer chromatography (TLC) was performed on a glass plates pre-coated with silica-gel (Merck Kieselgal 60 F_{254}, layer thickness 0.25 mm). Visualization was accomplished by UV light (254 nm), anisaldehyde, $KMnO_4$. Column chromatography was performed on KANTO Silica Gel 60N (spherical, neutral) or ICN Alumina N (neutral, Activity Super I).

High performance liquid chromatographic (HPLC) was conducted on JASCO PU-980, LG-980-02, DG-980-50, and CO-966 instrument equipped with model UV-975 spectrometers as an ultra violet light. Peak areas were calculated by JASCO-BORWIN (Windows NT) as an automatic integrator. DAICEL Chemical-AS, OD-H, OB-H and AD-H were used as chiral columns.

Capillary gas chromatographic analysis (GC) was conducted on Shimadzu GC-14B instrument equipped with FID detector and capillary column coated with PEG-20 M by using N_2 as a carrier gas. Peak area was calculated by Shimadzu C-R6A as an automatic integrator. CP-Chirasil-Dex CB (i.d. 0.25 mm x 25 m, CHROMPACK; GL Science), CP-Cyclodextrin-β-2,3,6-M-19 (i.d. 0.25 mm x 25 m, CHROMPACK; GL Science) and ChiralDex GTA (i.d. 0.25 mm x 25 m, CHROMPACK; TCI) were used as chiral columns.

Optical rotations were measured on a JASCO DIP-370.

TOF Mass spectra were measured on a JEOL JMS-T100LC.

IR spectra were measured on a JASCO FT/IR-4200 spectrometer.

Elemental analyses were measured on a LECO CHNS-932 (Center for Advanced Materials Analysis in Tokyo Institute of Technology).

X-ray crystal analyses were measured on Bruker APEXII and Bruker SMART CCD area detector (MoKα radiation, graphite monochrometer, λ = 0.71073 Å) (Nippon Bruker AXS K.K.). The structures ($PtCl_2$(**2a**) and [RuCl(OTf)(**2a**){(*S*,*S*)-dpen}]$_2$AgOTf: see page 67 and 71) were solved by direct methods (SHELXS-97) and refined by full-matrix least-squares methods based on F^2 with all measured unique reflections. All non-hydrogen atoms were given anisotropic displacement parameters.

Hydrogen atoms were input at calculated positions and refined with a riding model.

Computational calculations were executed on Sun Fire X4600 (Tokyo Institute of Technology).

All experiments were carried out under an argon atmosphere otherwise noted. Tetrahydrofuran and Et_2O (these were purchased from Kanto Chemical Co., Inc) were distilled from sodium benzophenone ketyl immediately prior to use. Acetonitrile (dehydrate), benzene (dehydrate), dichloromethane (dehydrate), *N*,*N*-dimethylformamide (dehydrate), 2-propanol (dehydrate) and toluene (dehydrate) were purchased from Kanto Chemical Co., Inc. 1,2-Dichloroethane (dehydrate) was purchased from Sigma-Aldrich Co., Inc.

Experimental section for Chapter 2

2-Bromo(diphenylphosphino)benzene was prepared by previously reported method.[11]

2-Diphenylphosphino-2'-iodobenzophenone

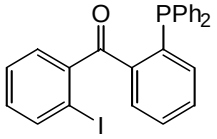

To a mixture of magnesium turnings (72.9 mg, 3.0 mmol) in THF (1 mL) was added carefully 2-bromo(diphenylphosphino)benzene (921.2 mg, 2.7 mmol) and 1,2-dibromoethane (few drops) in THF (5 mL) at 80 ºC under an argon atmosphere and stirred for 2 h at 80 ºC. After cooled down to 0 ºC, to the solution was added 2-iodobenzoyl chloride (799.4 mg, 3.0 mmol). After stirred for 1 h at room temperature, the reaction mixture was poured into 1*N* aq. HCl and extracted with CH_2Cl_2 twice. The organic layer was washed with water and dried over $MgSO_4$. After concentration under reduced pressure, the residue was purified by silica-gel chromatography (hexane/ethyl acetate = 18/1) to give 2-diphenylphosphino- 2'-iodobenzophenone (877.6 mg, 66% yield).

^{1}H NMR ($CDCl_3$, 300 MHz) δ 7.08-7.16 (m, 2H), 7.23 (dd, *J* = 7.8, 1.5 Hz, 1H), 7.26-7.49 (m, 13H), 7.53 (ddd, *J* = 7.8, 3.6, 1.2 Hz, 1H), 7.87 (d, *J* = 6.9 Hz, 1H).
^{13}C NMR ($CDCl_3$, 75 MHz) δ 92.92, 127.76, 128.10, 128.40, 128.49, 128.61, 129.36, 129.37, 131.27, 132.21, 132.69, 133.05, 133.09, 133.89, 134.16, 135.02, 137.71, 137.85, 139.46, 139.70, 139.76, 141.31, 141.57, 141.93, 144.14, 197.22.
^{31}P NMR ($CDCl_3$, 162 MHz) δ -3.37.

2,2'-Bis(diphenylphosphino)benzophenone (2a)

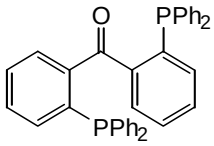

To a solution of 2-diphenylphosphino-2'-iodobenzophenone (886.1 mg, 1.8 mmol) and palladium(II) acetate (33.7 mg, 0.15 mmol) in acetonitrile (8 mL) were added successively diphenylphosphine (330 μL, 1.9 mmol) and triethylamine (270 μL, 1.9 mmol) at room temperature under an argon atmosphere. After stirred for 1 h at 60 ºC, the reaction mixture was poured into 1*N* aq. HCl and extracted with CH_2Cl_2 twice. The organic layer was washed with water and dried over $MgSO_4$. After concentration under reduced pressure, the residue was purified by silica-gel chromatography (hexane/ethyl acetate = 18/1) to give 2,2'-bis(diphenylphosphino)benzophenone (603.1 mg, 62% yield).

^{1}H NMR ($CDCl_3$, 300 MHz) δ 7.16 (dd, *J* = 7.5, 3.0 Hz, 2H), 7.14-7.39 (m, 26H).
^{13}C NMR ($CDCl_3$, 75 MHz) δ 127.95, 128.25, 128.29, 128.34, 128.39, 130.82, 133.75, 133.88, 134.02, 134.65, 137.57, 137.60, 137.63, 139.08, 139.11, 139.14, 139.41, 139.44, 139.47, 137.57, 137.60, 137.63, 143.42, 143.74, 197.99.
^{31}P NMR ($CDCl_3$, 162 MHz) δ -7.83.
TOF-HRMS (ESI), Calcd for $C_{37}H_{28}OP_2Na$ $[M+Na]^+$: 573.1513, Found: 573.1538.
FT-IR (KBr pellet, cm^{-1}) 3070, 3049, 3003, 1651 (*C=O*), 1433, 1266, 928, 744, 700, 694, 427.

2,2'-Bis(diphenylphosphino)benzhydrol (2b)

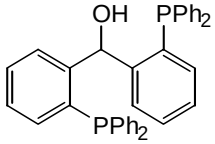

To a solution of $LiAlH_4$ (22.6 mg, 0.6 mmol) in THF (3 mL) was added 2,2'-bis-(diphenylphosphino)benzophenone (82.6 mg, 0.15 mmol) in THF (3 mL) at room temperature under an argon atmosphere and stirred for 3 h. After cooled down to 0 ºC, to the reaction mixture was added saturated aq. $NaHCO_3$ (few drops) and dried over $MgSO_4$. The reaction mixture was filtered through Celite® to remove gray solid. After concentration under reduced pressure, the residue was purified by silica-gel chromatography (hexane/ethyl acetate = 6/1) to give 2,2'-bis(diphenylphosphino)benzhydrol (73.5 mg, 89% yield).

^{1}H NMR ($CDCl_3$, 300 MHz) δ 2.38 (s, 1H), 7.03-7.07 (m, 2H), 7.12-7.35 (m, 26H), 7.51 (t, *J* = 6.6 Hz, 1H).

^{13}C NMR ($CDCl_3$, 75 MHz) δ 71.20, 71.53, 71.86, 127.64, 127.74, 127.79, 127.84, 128.16, 128.21, 128.25, 128.38, 128.51, 128.56, 128.60, 129.06, 133.52, 133.66, 133.80, 133.93, 134.08, 134.57, 135.68, 135.75, 135.78, 135.87, 136.29, 136.35, 136.37, 136.43, 137.36, 137.44, 137.50, 147.31, 147.43, 147.60, 147.77, 147.89.
^{31}P NMR ($CDCl_3$, 162 MHz) δ -17.72.
TOF-HRMS (ESI), Calcd for $C_{37}H_{30}P_2Na$ $[M+Na]^+$: 575.1670, Found: 575.1659.

Bis(2-trifluoromethanesulfonyloxybenzyl)methane

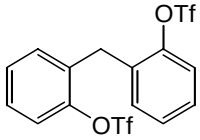

To a solution of bis(2-hydroxyphenyl)methane (300.3 mg, 1.5 mmol), 4-dimethylaminopyridine (12.2 mg, 0.1 mmol), and 2,6-lutidine (465 μL, 4.0 mmol) in CH_2Cl_2 (10 mL) was added anhydrous trifluoromethanesulfonic acid (670 μL, 4.0 mmol) at 0 °C under an argon atmosphere. After stirred for 8 h at room temperature, the reaction mixture was poured into 1*N* aq. HCl and extracted with CH_2Cl_2 twice. The organic layer was washed with brine and dried over $MgSO_4$. After concentration under reduced pressure, the residue was purified by silica-gel chromatography (hexane/ethyl acetate = 7/1) to give bis(2-trifluoromethanesulfonyloxybenzyl)methane (557.2 mg, 81% yield).

^{1}H NMR (300 MHz, $CDCl_3$) δ 4.22 (s, 2H), 7.18 (d, J = 6.9 Hz, 2H), 7.31-7.38 (m, 6H).
^{13}C NMR (75 MHz, $CDCl_3$) δ 29.89, 118.55 (q, $J_{C\text{-}F}$ = 320.0 Hz), 120.67, 128.58, 128.85, 131.34, 131.76, 147.98.
^{19}F NMR (282 MHz, $CDCl_3$) δ -73.7.

Bis(2-diphenylphosphinoylbenzyl)methane

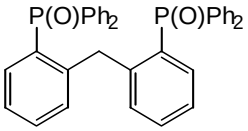

To a solution of bis(2-trifluoromethanesulfonyloxybenzyl)methane (464.4 mg, 1.0 mmol), diphenylphosphine oxide (505.5 mg, 2.5 mmol), 1,4-bis(diphenylphosphino)butane (42.6 mg, 0.1 mmol), and palladium(II) acetate (22.4 mg, 0.1 mmol) in DMSO (8 mL) was added diisopropylethylamine (540 μL, 4.0 mmol) at room temperature under an argon atmosphere. After stirred for 18 h at 100 ºC, the reaction mixture was poured into CH_2Cl_2 at room temperature. The organic layer washed with 1*N* aq. HCl and brine and dried over $MgSO_4$. After concentration under reduced pressure, the residue was purified by silica-gel chromatography (ethyl acetate, then methanol/dichloromethane = 1/19) to give bis(2-diphenylphosphinoylbenzyl)methane (523.1 mg, 92%

yield).

^{1}H NMR (300 MHz, $CDCl_3$) δ 4.43 (s, 2H), 7.03-7.07 (m, 4H), 7.24-7.44 (m, 16H), 7.51-7.54 (m, 8H).
^{13}C NMR (75 MHz, $CDCl_3$) δ 37.82, 37.89, 125.31, 125.48, 128.34, 128.50, 130.15, 131.58, 131.61, 131.80, 131.91, 132.20, 132.23, 132.81, 132.99, 133.62, 146.20, 146.31.
^{31}P NMR (121 MHz, $CDCl_3$) δ 31.1.

Bis(2-diphenylphosphinobenzyl)methane (2c)

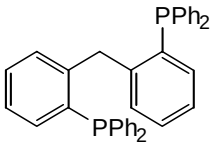

To a solution of bis(2-diphenylphosphinoylbenzyl)methane (511.7 mg, 0.9 mmol) in toluene (10 mL) were added *N*,*N*-dimethylaniline (3.8 mL, 30 mmol) and trichlorosilane (1.0 mL, 10 mmol) at 0 ºC under an argon atmosphere. The reaction mixture was refluxed for 3 h, and then was poured into 30% aq. KOH (20 mL) and CH_2Cl_2 (20 mL). After filtered through Celite® to remove white solid, the filtrate was washed with 1*N* aq. HCl three times and brine and dried over $MgSO_4$. After concentration under reduced pressure, the residue was purified by silica-gel chromatography (hexane/ethyl acetate = 10/1) to give bis(2-diphenylphosphinobenzyl)methane (313.9 mg, 65% yield).

^{1}H NMR (300 MHz, $CDCl_3$) δ 4.60 (s, 2H), 7.02-7.06 (m, 4H), 7.17 (dt, *J* = 7.2, 1.5 Hz, 2H), 7.24 (dt, *J* = 7.2, 1.5 Hz, 2H), 7.31-7.42 (m, 20H).
^{13}C NMR (75 MHz, $CDCl_3$) δ 38.16, 38.46, 38.77, 126.46, 128.49, 128.53, 128.58, 128.64, 128.94, 130.13, 130.17, 130.21, 133.53, 133.92, 134.05, 134.19, 136.60, 136.43, 136.46, 136.57, 136.60, 136.63, 136.72, 136.75, 136.78, 136.86, 136.89, 136.92, 145.15, 145.51.
^{31}P NMR (121 MHz, $CDCl_3$) δ -14.6.
TOF-HRMS (ESI), Calcd for $C_{37}H_{31}P_2$ $[M+H]^+$: 537.1901, Found: 537.1919.

$PtCl_2$(2a): 2a-$PtCl_2$

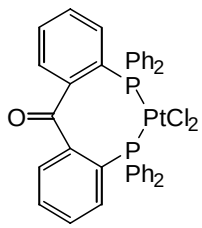

To a mixture of 2,2'-bis(diphenylphosphino)benzophenone (**2a**) (5.5 mg, 0.01 mmol) and

$PtCl_2$(cod) (2.8 mg, 0.01 mmol) was added CH_2Cl_2 (1 mL) at room temperature under an argon atmosphere. After stirred for 2 h, the reaction mixture was concentrated under reduced pressure. The residue was washed with Et_2O three times and then dried to give $PtCl_2$(**2a**) (8.0 mg, 98% yield).

^{1}H NMR ($CDCl_3$, 300 MHz) δ 7.14-7.28 (m, 16H), 7.42-7.57 (m, 12H); 5.23 (s, 1/2H, dichloromethane).
^{31}P NMR ($CDCl_3$, 162 MHz) δ 14.56 (d, $J_{P\text{-}Pt}$ = 3.62 kHz).
Anal. Calcd for $C_{37}H_{28}Cl_2OP_2Pt{\cdot}1/4CH_2Cl_2$: C, 53.40; H, 3.43%. Found: C, 53.35; H, 3.84%. $1/4CH_2Cl_2$ was derived from solvent. The sample was evacuated at 100 ºC for 12 h.
FT-IR (KBr pellet, cm^{-1}) 3075, 3057, 3046, 1666 (*C=O*), 1438, 1236, 1093, 746, 700, 696, 510.
X-ray analysis (*vide infla*): A single crystal used for X-ray analysis was prepared from the CH_2Cl_2 and hexane solution of $PtCl_2$(**2a**) stored at room temperature.

$RuCl_2$(2a)$(dmf)_n$: 2a-$RuCl_2$/$(DMF)_n$

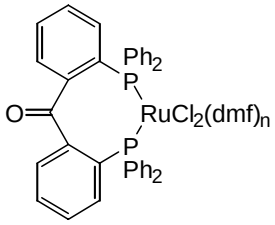

To a mixture of 2,2'-bis(diphenylphosphino)benzophenone (**2a**) (55.0 mg, 0.1 mmol) and $[RuCl_2(C_6H_6)]_2$ (25.0 mg, 0.05 mmol) was added DMF (2 mL) at room temperature under an argon atmosphere in a Schlenk tube. After stirred for 20 min at 100 ºC, the reaction mixture was concentrated under reduced pressure to give $RuCl_2$(**2a**)$(dmf)_n$. $RuCl_2$(**2a**)$(dmf)_n$ is air sensitive oligomer.

^{31}P NMR ($CDCl_3$, 162 MHz) δ 31.55, 32.01, 46.64, 49.56, 59.33, 59.47, 60.21.

$RuCl_2$(2a)[(*S*,*S*)-dpen]: 2a-$RuCl_2$/(*S*,*S*)-DPEN

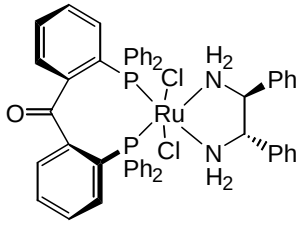

To a mixture of $RuCl_2$(**2a**)$(dmf)_n$ (8.7 mg, 0.01 mmol) and (*S*,*S*)-DPEN (2.1 mg, 0.01 mmol) was added CH_2Cl_2 (1 mL) at room temperature under an argon atmosphere in a Schlenk tube. After stirred for 10 min, the reaction mixture was concentrated under reduced pressure to give

$RuCl_2$(**2a**)[(*S*,*S*)-dpen].

^{1}H NMR ($CDCl_3$, 300 MHz) δ 2.94-3.15 (m, 4H), 4.45-4.64 (m, 2H), 6.91-7.33 (m, 32H), 7.42-7.54 (m, 2H), 7.68-7.80 (m, 2H), 8.03-8.11 (m, 2H); 5.23 (s, 2H, dichloromethane), 2.97 (s, 3H, DMF), 3.02 (s, 3H, DMF), 8.00 (s, 1H, DMF).
^{13}C NMR ($CDCl_3$, 75 MHz) δ 63.37, 64.39, 126.74, 126.86, 128.33, 128.45, 128.86, 129.00, 129.10, 129.19, 129.26, 129.41, 129.57, 129.60, 129.77, 130.13, 130.19, 130.22, 130.27, 130.30, 130.35, 130.51, 130.55, 130.72, 131.00, 131.04, 131.13, 131.17, 131.36, 132.24, 132.35, 132.47, 132.59, 132.71, 132.77, 132.89, 133.14, 133.77, 134.23, 134.47, 134.89, 135.22, 137.29, 137.52, 149.89 (dd, $J_{C\text{-}P}$ = 24.8, 18.8 Hz, *C*=O); 53.2 (dichloromethane), 30.91 (DMF), 35.85 (DMF), 162.24 (DMF).
^{31}P NMR ($CDCl_3$, 162 MHz) δ 46.38 (d, *J* = 23.6 Hz, 1P), 47.23 (d, *J* = 23.6 Hz, 1P).
$[\alpha]_D^{27}$ = -88 (c = 0.15 in $CHCl_3$).
Anal. Calcd for $C_{51}H_{44}Cl_2N_2OP_2Ru{\cdot}CH_2Cl_2{\cdot}$DMF: C, 60.45; H, 4.89; N, 3.84%. Found: C, 60.08; H, 5.23; N, 3.75%. CH_2Cl_2 was derived from solvent and DMF was derived from $RuCl_2$(**2a**)$(dmf)_n$. The sample was evacuated at 100 ºC for 12 h.
FT-IR (KBr pellet, cm^{-1}) 3314, 3205, 3058, 1671 (*C*=*O*), 1633, 1435, 1096, 748, 721, 696, 525.

[RuCl(2a){(*S*,*S*)-dpen})]OTf: 2a-RuCl(OTf)/(*S*,*S*)-DPEN

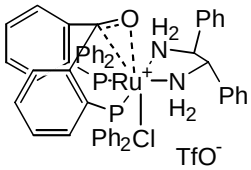

To a mixture of $RuCl_2$(**2a**)$(dmf)_n$ (8.7 mg, 0.01 mmol) and (*S*,*S*)-DPEN (2.1 mg, 0.01 mmol) was added CH_2Cl_2 (1 mL) at room temperature under an argon atmosphere in a Schlenk tube. After stirred for 15 min, to the reaction mixture was added AgOTf (2.6 mg, 0.01 mmol). After stirred for 3 h, the reaction mixture was filtered through Celite® to remove AgCl. The filtrate was concentrated under reduced pressure to give [RuCl(**2a**){(*S*,*S*)-dpen}]OTf.

^{1}H NMR ($CDCl_3$, 300 MHz) δ 2.97-3.16 (m, 4H), 4.42-4.59 (m, 2H), 6.89-7.29 (m, 32H), 7.39-7.52 (m, 2H), 7.64-7.78 (m, 2H), 8.04-8.11 (m, 2H); 5.24 (s, 2H, dichloromethane).
^{13}C NMR ($CDCl_3$, 75 MHz) δ 63.30, 64.43, 126.71, 126.79, 128.28, 128.45, 128.75, 128.81, 128.94, 129.11, 129.21, 129.51, 129.58, 129.70, 129.78, 130.06, 130.14, 130.27, 130.49, 130.85, 130.97, 131.09, 132.24, 132.35, 132.45, 132.56, 132.68, 132.79, 132.91, 133.10, 133.70, 133.75, 134.14, 134.44, 134.80, 135.66, 137.33, 137.35, 137.50, 137.52, 149.98 (dd, $J_{C\text{-}P}$ = 24.8, 12.0 Hz, *C*=O); 53.2 (dichloromethane).
^{19}F NMR ($CDCl_3$, 376 MHz) δ -78.45.
^{31}P NMR ($CDCl_3$, 162 MHz) δ 46.51 (d, *J* = 22.9 Hz, 1P), 47.03 (d, *J* = 22.9 Hz, 1P).

$[\alpha]_D^{27}$ = -68 (c = 0.20 in $CHCl_3$).

Anal. Calcd for $C_{52}H_{44}ClF_3N_2O_4P_2RuS \cdot CH_2Cl_2$: C, 56.17; H, 4.09; N, 2.47; S, 2.83%. Found: C, 56.67; H, 4.54; N, 2.42; S, 2.68%. CH_2Cl_2 was derived from solvent. The sample was evacuated at 100 ºC for 12 h.

[RuCl(OTf)(2a){(*S*,*S*)-dpen}]$_2$AgOTf: [2a-RuCl(OTf)/(*S*,*S*)-DPEN]$_2$AgOTf

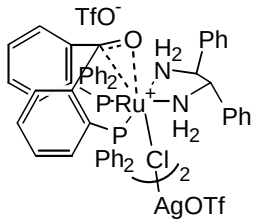

To a mixture of $RuCl_2$(**2a**)$(dmf)_n$ (8.7 mg, 0.01 mmol) and (*S*,*S*)-DPEN (2.1 mg, 0.01 mmol) was added CH_2Cl_2 (1 mL) at room temperature under an argon atmosphere in a Schlenk tube. After stirred for 15 min, to the reaction mixture was added AgOTf (5.2 mg, 0.02 mmol). After stirred for 3 h, the reaction mixture was filtered through Celite® to remove AgCl. The filtrate was concentrated under reduced pressure to give [RuCl(OTf)(**2a**){(*S*,*S*)-dpen}]$_2$AgOTf.

^{1}H NMR ($CDCl_3$, 300 MHz) δ 2.86-2.94 (m, 2H), 3.29-3.45 (m, 2H), 4.50-4.63 (m, 2H), 6.91-7.51 (m, 34H), 7.65-7.77 (m, 2H), 7.99-8.07 (m, 2H).

^{19}F NMR ($CDCl_3$, 376 MHz) δ -78.12.

^{31}P NMR ($CDCl_3$, 162 MHz) δ 46.51 (d, *J* = 22.9 Hz, 1P), 47.03 (d, *J* = 22.9 Hz, 1P).

X-ray analysis (*vide infla*): A single crystal used for X-ray analysis was prepared from the CH_2Cl_2, $CHCl_3$ and toluene solution of [RuCl(OTf)(**2a**){(*S*,*S*)-dpen}]$_2$AgOTf stored at room temperature.

[Rh(2a)(cod)]SbF$_6$: 2a-RhSbF$_6$/COD

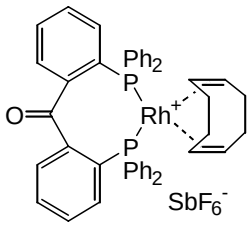

To a mixture of $[Rh(cod)_2]SbF_6$ (52.3 mg, 0.1 mmol) and 2,2'-bis(diphenylphosphino)-benzophenone (**2a**) (55.0 mg, 0.1 mmol) was added CH_2Cl_2 (2 mL) at room temperature under an argon atmosphere in a Schlenk tube. After stirred for 3 h, the reaction mixture was concentrated under reduced pressure. The orange residue was washed with ether three times under an argon atmosphere to give [Rh(**2a**)(cod)]SbF_6 (9.8 mg 95% yield).

^{1}H NMR ($CDCl_3$, 300 MHz) δ 1.58 (s, 2H), 3.90 (br, 2H), 4.44 (d, *J* = 2.4 Hz, 4H), 6.92-7.52 (m,

28H); 1.45 (s, 2H, water), 5.24 (s, 1H, dichloromethane).
^{31}P NMR ($CDCl_3$, 162 MHz) δ 18.21 (d, $J_{P\text{-}Rh}$ = 154.0 Hz).
Anal. Calcd for $C_{45}H_{40}F_6OP_2RhSb \cdot 1/2CH_2Cl_2 \cdot H_2O$: C, 51.66; H, 4.10%. Found: C, 51.53; H, 3.83%. $1/2CH_2Cl_2$ was derived from solvent and H_2O was derived from ether that washed the orange residue. The sample was evacuated at 50 ºC for 12 h.

[Rh(2a){(*S*,*S*)-dpen}]SbF_6: 2a-RhSbF_6/(*S*,*S*)-DPEN

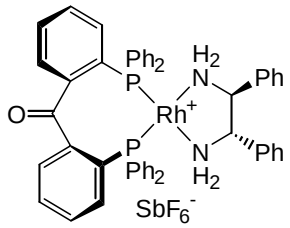

To [Rh(**2a**)(cod)]SbF_6 (9.8 mg, 0.01 mmol) was added $(CH_2Cl)_2$ (1 mL) at room temperature under an argon atmosphere in a Schlenk tube. The reaction mixture was frozen and charged with hydrogen using balloon (ab. 1 atm). After stirred for 30 min at room temperature, to the reaction mixture was added (*S*,*S*)-DPEN (2.1 mg, 0.01 mmol) and concentrated under reduced pressure to give [Rh(**2a**){(*S*,*S*)-dpen}]SbF_6. [Rh(**2a**){(*S*,*S*)-dpen}]SbF_6 is air sensitive.

^{1}H NMR ($CDCl_3$, 300 MHz) δ 1.67 (br, 1H), 1.89 (br, 1H), 2.84 (br, 1H), 3.23 (br, 1H), 3.94 (br, 1H), 4.39 (br, 1H), 5.98-6.05 (m, 2H), 6.48-6.52 (m, 2H), 6.88-8.30 (m, 34H).
^{31}P NMR ($CDCl_3$, 162 MHz) δ 47.28 (dd, $J_{P\text{-}P}$ = 44.9 Hz, $J_{P\text{-}Rh}$ = 155.2 Hz, 1P), 57.40 (dd, $J_{P\text{-}P}$ = 44.9 Hz, $J_{P\text{-}Rh}$ = 157.6 Hz, 1P).
Anal. Calcd for $C_{51}H_{44}F_6N_2OP_2RhSb$: C, 55.61; H, 4.03; N, 2.54%. Found: C, 55.48; H, 4.31; N, 2.19%. The sample was evacuated at 100 ºC for 12 h.

[Rh(2a){(*S*)-dabn}]SbF_6: 2a-RhSbF_6/(*S*)-DABN

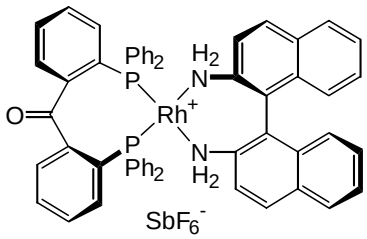

[Rh(**2a**){(*S*)-dabn}]SbF_6 was prepared from [Rh(**2a**)(cod)]SbF_6 and (*S*)-DABN in a similar to manner as [Rh(**2a**){(*S*,*S*)-dpen}]SbF_6. [Rh(**2a**){(*S*)-dabn}]SbF_6 is air sensitive.

^{1}H NMR ($CDCl_3$, 300 MHz) δ 3.29 (br, 1H), 3.79 (br, 2H), 4.41(br, 1H), 6.30-8.05 (m, 40H); 1.32 (s,

16H, peak of cyclooctane).
^{31}P NMR ($CDCl_3$, 162 MHz) δ 57.88 (br), 57.99 (br), 58.96 (br), 58.98 (br).
Anal. Calcd for $C_{57}H_{44}F_6N_2OP_2RhSb{\cdot}C_8H_{16}$: C, 60.72; H, 4.70; N, 2.18%. Found: C, 60.48; H, 4.48; N, 2.45%. Cyclooctane was derived from hydrogenation of 1,5-cyclooctadiene of [Rh(**2a**)(cod)]SbF_6. The sample was evacuated at 100 ºC for 12 h.

Asymmetric hydrogenation with Ru complexes

Hydrogenation of 1-acetonaphthone

To a mixture of $RuCl_2$(**2a**)$(dmf)_n$ (10.4 mg, 0.012 mmol) and (*S*,*S*)-DPEN (2.5 mg, 0.012 mmol) was added CH_2Cl_2 (1 mL) at room temperature under an argon atmosphere in a Schlenk tube. After stirred for 10 min, the reaction mixture was concentrated under reduced pressure. To the residue were added 2-propanol (3.3 mL) and 1-acetonaphthone (0.46 mL, 3.0 mmol), and 100-mL autoclave was charged with this reaction mixture under a stream of argon. After addition of KOH/2-propanol (0.5 M, 60 μL, 0.03 mmol), hydrogen was introduced at a pressure of 15 atm. The solution was vigorously stirred for 4 h at room temperature. After concentration under reduced pressure, the residue was filtered through a short column of silica-gel chromatography (hexane/ethyl acetate = 3/1) to give 1-(1'-naphthyl)ethanol.

Hydrogenation of 2-acetonaphthone

To a mixture of $RuCl_2$(**2a**)$(dmf)_n$ (10.4 mg, 0.012 mmol) and (*S*,*S*)-DPEN (2.5 mg, 0.012 mmol) was added CH_2Cl_2 (1 mL) at room temperature under an argon atmosphere in a Schlenk tube. After stirred for 10 min, the reaction mixture was concentrated under reduced pressure. To the residue and 2-acetonaphthone (510.6 mg, 3.0 mmol) was added 2-propanol (3.3 mL), and 100-mL autoclave was charged with this reaction mixture under a stream of argon. After addition of KOH/2-propanol (0.5 M, 60 μL, 0.03 mmol), hydrogen was introduced at a pressure of 15 atm. The solution was vigorously stirred for 4 h at room temperature. After concentration under reduced pressure, the residue was filtered through a short column of silica-gel chromatography (hexane/ethyl acetate = 3/1) to give 1-(2'-naphthyl)ethanol.

Hydrogenation of 9-acetylanthracene

To a mixture of [RuCl(**2a**){(*S*,*S*)-dpen})]OTf (12.6 mg, 0.012 mmol) and 9-acetylanthracene (660.8 mg, 3.0 mmol) were added 2-propanol (3.3 mL) and toluene (1.5 mL) under an argon atmosphere in a Schlenk tube. 100-mL autoclave was charged with this reaction mixture under a stream of argon. After addition of KOH/2-propanol (0.5 M, 60 μL, 0.03 mmol), hydrogen was introduced at a pressure of 20 atm. The solution was vigorously stirred for 24 h at room temperature. After concentration under reduced pressure, the residue was filtered through a short column of silica-gel chromatography (hexane/ethyl acetate = 3/1) to give 1-(9'-anthryl)ethanol.

Asymmetric transfer hydrogenation with Rh complexes

Transfer hydrogenation of acetophenone with BINAP-Rh complex

A well concentrated CH_2Cl_2 solution of [Rh{(*R*)-binap}{(*S*,*S*)-dpen}]SbF_6 (0.01 mmol) was prepared under an argon atmosphere in a Schlenk tube. To the solution were added 2-propanol (4 mL) and 0.1 M of *t*BuOK/2-propanol (0.6 mL, 0.06 mmol) and stirred for 1 h at room temperature. Then, to the reaction mixture was added acetophenone (38 μL, 0.33 mmol) and stirred for 24 h at 60 ºC. After concentration under reduced pressure, the residue was filtered through a short column of silica-gel chromatography (hexane/ethyl acetate = 3/1) to give 1-phenylethanol.

Transfer hydrogenation of acetophenone with Rh-2a complex

(a) Without co-solvent

To the solution of [Rh(**2a**){(*S*,*S*)-dpen}]SbF_6 (0.01 mmol) in 2-propanol (3.6 mL) was added 0.1 M of *t*BuOK/2-propanol (0.6 mL, 0.06 mmol) at room temperature under an argon atmosphere in a Schlenk tube and stirred for 20 min. To the reaction mixture was added acetophenone (38 μL, 0.33 mmol) and stirred for 24 h at room temperature. After concentration under reduced pressure, the residue was filtered through a short column of silica-gel chromatography (hexane/ethyl acetate = 3/1) to give 1-phenylethanol.

(b) With co-solvent

To a solution of [Rh(**2a**){(*S*,*S*)-dpen}]SbF_6 (0.01 mmol) in $(CH_2Cl)_2$ (0.23 mL) were added 2-propanol (3.6 mL) and 0.1 M of *t*BuOK/2-propanol (0.6 mL, 0.06 mmol) at room temperature under an argon atmosphere in a Schlenk tube and stirred for 20 min at room temperature. To the reaction mixture was added acetophenone (38 μL, 0.33 mmol) and stirred for 24 h at room temperature. After concentration under reduced pressure, the residue was filtered through a short column of silica-gel chromatography (hexane/ethyl acetate = 3/1) to give 1-phenylethanol.

(*R*)-1-Phenylethanol[15a]

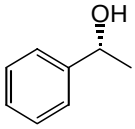

GC (column, CP-Cyclodextrin-β-2,3,6-M-19, i.d. 0.25 mm x 25 m, Chrompack; carrier gas, N_2 (75 kPa); column temp, 105 ºC; injection and detection temp, 135 ºC; split rate, 100:1), t_R = 21.7 min (*R*)/23.5 min (*S*), t_R = 13.4 min (ketone).

(*R*)-1-(2-Methylphenyl)ethanol[15a]

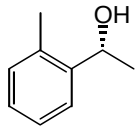

GC (column, CP-Cyclodextrin-β-2,3,6-M-19, i.d. 0.25 mm x 25 m, Chrompack; carrier gas, N_2 (75 kPa); column temp, 130 ºC; injection and detection temp, 160 ºC; split rate, 100:1), t_R = 16.1 min (*R*)/18.1 min (*S*), t_R = 8.94 min (ketone).

(*R*)-1-(3-Methylphenyl)ethanol[15f]

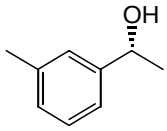

GC (column, CP-Cyclodextrin-β-2,3,6-M-19, i.d. 0.25 mm x 25 m, Chrompack; carrier gas, N_2 (75 kPa); column temp, 115 ºC; injection and detection temp, 145 ºC; split rate, 100:1), t_R = 23.7 min (*R*)/25.7 min (*S*), t_R = 16.4 min (ketone).

(*R*)-1-(4-Methylphenyl)ethanol[15a]

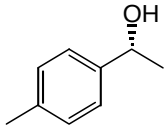

GC (column, CP-Cyclodextrin-β-2,3,6-M-19, i.d. 0.25 mm x 25 m, Chrompack; carrier gas, N_2 (75 kPa); column temp, 120 ºC; injection and detection temp, 150 ºC; split rate, 100:1), t_R = 17.4 min (*R*)/19.1 min (*S*), t_R = 14.8 min (ketone).

(*R*)-1-(1-Naphthyl)ethanol[15a]

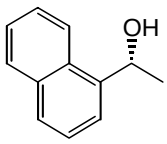

GC (column, CP-Cyclodextrin-β-2,3,6-M-19, i.d. 0.25 mm x 25 m, Chrompack; carrier gas, N_2 (75 kPa); column temp, 160 ºC; injection and detection temp, 190 ºC; split rate, 100:1), t_R = 37.6 min (*S*)/38.9 min (*R*), t_R = 25.9 min (ketone).

(*R*)-1-(2-Naphthyl)ethanol[15a]

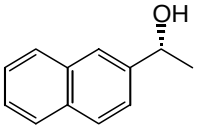

HPLC (column, CHIRALPAK AS, hexane/2-propanol = 98 : 2, flow rate, 1.0 mL/min, detection UV =

254 nm), t_R = 15.9 min (*R*)/17.9 min (*S*).

(*R*)-1-(9-Anthryl)ethanol[15e]

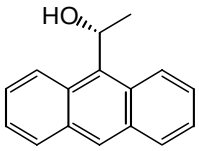

HPLC (column, CHIRALPAK AS, hexane/2-propanol = 98 : 2, flow rate, 1.0 mL/min, detection UV = 254 nm), t_R = 19.0 min (*S*)/24.3 min (*R*).

NMR analyses of RuHX(2a)(dpen) complexes (X=BH_4 or TfO) (see page 44)[18]

To a solution of [RuCl(**2a**){(*S*,*S*)-dpen})]OTf (10.5 mg, 0.01 mmol) in degassed ethanol (1 mL) and benzene (1 mL) was added $NaBH_4$ (9.5 mg, 0.25 mmol) at room temperature under an argon atmosphere in a Schlenk tube. After stirred for 5 min at 60 °C, the reaction mixture was cooled down to room temperature and stirred for 30 min. After concentration under reduced pressure, the residue was dissolved in degassed benzene. The solution filtered through Celite® under an argon atmosphere to remove white solid. The filtrate was evaporated under reduced pressure and dissolved in C_6D_6.

Crystal data of $PtCl_2$(2a)

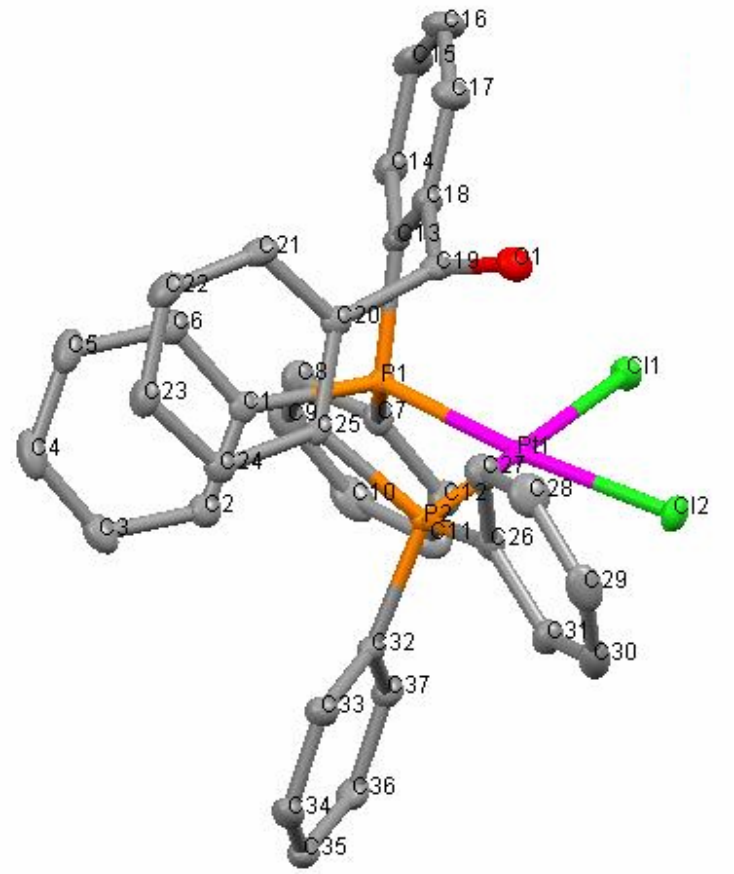

Empirical formula	$C_{39}H_{32}Cl_6OP_2Pt$	
Formula weight	986.38	
Temperature	100 K	
Wavelength	0.71073 Å ($Mo_{K\alpha}$)	
Crystal system	Triclinic	
Space group	P-1	
Unit cell dimensions	a = 11.1806(4) Å	α = 83.7820(10)°
	b = 11.2602(4) Å	β = 85.7920(10)°
	c = 16.3715(5) Å	γ = 67.1050(10)°
Volume	1886.46(11) $Å^3$	
Z	2	
Density (calculated)	1.736 Mg/m^3	
Diffractometer	Bruker APEXII	
Absorption coefficient	4.261 mm^{-1}	
F(000)	968	
Crystal size	0.17 x 0.07 x 0.07 mm^3	
Theta range for data collection	1.97 to 27.84°	

Index ranges	-14<=h<=14, -14<=k<=14, -21<=l<=21
Reflections collected	22364
Independent reflections	8833 [R(int) = 0.0164]
Completeness to theta = 27.84°	98.2 %
Absorption correction	Empirical
Max. and min. transmission	0.7547 and 0.5312
Refinement method	Full-matrix least-squares on F^2
Data / restraints / parameters	8833 / 117 / 471
Goodness-of-fit on F^2	1.067
Final R indices [I>2sigma(I)]	R1 = 0.0199, wR2 = 0.0510
R indices (all data)	R1 = 0.0204, wR2 = 0.0513
Largest diff. peak and hole	2.233 and -1.313 e.Å^{-3}

Bond lengths (Å)

C(1)-C(2) 1.396(4)	C(13)-C(14) 1.391(3)	C(25)-P(2) 1.825(2)
C(1)-C(6) 1.396(4)	C(13)-C(18) 1.411(4)	C(26)-C(27) 1.391(4)
C(1)-P(1) 1.824(3)	C(13)-P(1) 1.826(3)	C(26)-C(31) 1.400(4)
C(2)-C(3) 1.389(4)	C(14)-C(15) 1.397(4)	C(26)-P(2) 1.825(2)
C(2)-H(2) 0.9500	C(14)-H(14) 0.9500	C(27)-C(28) 1.398(4)
C(3)-C(4) 1.382(4)	C(15)-C(16) 1.378(4)	C(27)-H(27) 0.9500
C(3)-H(3) 0.9500	C(15)-H(15) 0.9500	C(28)-C(29) 1.380(5)
C(4)-C(5) 1.383(4)	C(16)-C(17) 1.392(4)	C(28)-H(28) 0.9500
C(4)-H(4) 0.9500	C(16)-H(16) 0.9500	C(29)-C(30) 1.389(5)
C(5)-C(6) 1.393(4)	C(17)-C(18) 1.394(4)	C(29)-H(29) 0.9500
C(5)-H(5) 0.9500	C(17)-H(17) 0.9500	C(30)-C(31) 1.389(4)
C(6)-H(6) 0.9500	C(18)-C(19) 1.515(3)	C(30)-H(30) 0.9500
C(7)-C(12) 1.394(4)	C(19)-O(1) 1.210(3)	C(31)-H(31) 0.9500
C(7)-C(8) 1.402(4)	C(19)-C(20) 1.516(4)	C(32)-C(37) 1.400(3)
C(7)-P(1) 1.822(3)	C(20)-C(21) 1.400(4)	C(32)-C(33) 1.400(3)
C(8)-C(9) 1.389(4)	C(20)-C(25) 1.402(3)	C(32)-P(2) 1.816(3)
C(8)-H(8) 0.9500	C(21)-C(22) 1.384(4)	C(33)-C(34) 1.387(4)
C(9)-C(10) 1.383(5)	C(21)-H(21) 0.9500	C(33)-H(33) 0.9500
C(9)-H(9) 0.9500	C(22)-C(23) 1.386(4)	C(34)-C(35) 1.390(4)
C(10)-C(11) 1.384(5)	C(22)-H(22) 0.9500	C(34)-H(34) 0.9500
C(10)-H(10) 0.9500	C(23)-C(24) 1.387(4)	C(35)-C(36) 1.384(4)
C(11)-C(12) 1.395(4)	C(23)-H(23) 0.9500	C(35)-H(35) 0.9500
C(11)-H(11) 0.9500	C(24)-C(25) 1.402(3)	C(36)-C(37) 1.392(4)
C(12)-H(12) 0.9500	C(24)-H(24) 0.9500	C(36)-H(36) 0.9500

C(37)-H(37) 0.9500
C(1S)-Cl(2S) 1.732(2)
C(1S)-Cl(1S) 1.732(2)
C(1S)-H(38) 0.9900
C(1S)-H(39) 0.9900
C(2S)-Cl(3S) 1.731(2)
C(2S)-Cl(4S) 1.731(2)
C(2S)-H(41) 0.9900
C(2S)-H(40) 0.9900
C(3S)-Cl(5S) 1.731(2)
C(3S)-Cl(6S) 1.979(9)
C(3S)-H(43) 0.9900
C(3S)-H(42) 0.9900
Cl(1)-Pt(1) 2.3643(6)
Cl(2)-Pt(1) 2.3407(6)
P(1)-Pt(1) 2.2607(6)
P(2)-Pt(1) 2.2321(6)

Bond angles (^{o})

C(2)-C(1)-C(6) 119.2(2)
C(2)-C(1)-P(1) 118.4(2)
C(6)-C(1)-P(1) 122.3(2)
C(3)-C(2)-C(1) 120.3(3)
C(3)-C(2)-H(2) 119.9
C(1)-C(2)-H(2) 119.9
C(4)-C(3)-C(2) 120.4(3)
C(4)-C(3)-H(3) 119.8
C(2)-C(3)-H(3) 119.8
C(3)-C(4)-C(5) 119.8(3)
C(3)-C(4)-H(4) 120.1
C(5)-C(4)-H(4) 120.1
C(4)-C(5)-C(6) 120.5(3)
C(4)-C(5)-H(5) 119.7
C(6)-C(5)-H(5) 119.7
C(5)-C(6)-C(1) 119.9(3)
C(5)-C(6)-H(6) 120.1
C(1)-C(6)-H(6) 120.1
C(12)-C(7)-C(8) 119.2(2)
C(12)-C(7)-P(1) 119.79(19)
C(8)-C(7)-P(1) 120.2(2)
C(9)-C(8)-C(7) 120.0(3)
C(9)-C(8)-H(8) 120.0
C(7)-C(8)-H(8) 120.0
C(10)-C(9)-C(8) 120.5(3)
C(10)-C(9)-H(9) 119.7
C(8)-C(9)-H(9) 119.7
C(9)-C(10)-C(11) 119.9(3)
C(9)-C(10)-H(10) 120.1
C(11)-C(10)-H(10) 120.1
C(10)-C(11)-C(12) 120.3(3)
C(10)-C(11)-H(11) 119.9
C(12)-C(11)-H(11) 119.9
C(7)-C(12)-C(11) 120.1(3)
C(7)-C(12)-H(12) 120.0
C(11)-C(12)-H(12) 120.0
C(14)-C(13)-C(18) 118.9(2)
C(14)-C(13)-P(1) 121.9(2)
C(18)-C(13)-P(1) 118.80(18)
C(13)-C(14)-C(15) 120.7(3)
C(13)-C(14)-H(14) 119.6
C(15)-C(14)-H(14) 119.6
C(16)-C(15)-C(14) 120.1(3)
C(16)-C(15)-H(15) 120.0
C(14)-C(15)-H(15) 120.0
C(15)-C(16)-C(17) 120.1(3)
C(15)-C(16)-H(16) 119.9
C(17)-C(16)-H(16) 119.9
C(16)-C(17)-C(18) 120.3(3)
C(16)-C(17)-H(17) 119.8
C(18)-C(17)-H(17) 119.8
C(17)-C(18)-C(13) 119.8(2)
C(17)-C(18)-C(19) 115.0(2)
C(13)-C(18)-C(19) 125.2(2)
O(1)-C(19)-C(18) 120.9(2)
O(1)-C(19)-C(20) 120.8(2)
C(18)-C(19)-C(20) 117.1(2)
C(21)-C(20)-C(25) 119.6(2)
C(21)-C(20)-C(19) 114.6(2)
C(25)-C(20)-C(19) 125.8(2)
C(22)-C(21)-C(20) 120.5(2)
C(22)-C(21)-H(21) 119.7
C(20)-C(21)-H(21) 119.7
C(21)-C(22)-C(23) 119.9(2)
C(21)-C(22)-H(22) 120.1
C(23)-C(22)-H(22) 120.1
C(22)-C(23)-C(24) 120.3(2)
C(22)-C(23)-H(23) 119.9
C(24)-C(23)-H(23) 119.9
C(23)-C(24)-C(25) 120.4(2)
C(23)-C(24)-H(24) 119.8
C(25)-C(24)-H(24) 119.8
C(24)-C(25)-C(20) 119.1(2)
C(24)-C(25)-P(2) 121.87(19)
C(20)-C(25)-P(2) 119.01(18)
C(27)-C(26)-C(31) 119.2(2)
C(27)-C(26)-P(2) 121.3(2)
C(31)-C(26)-P(2) 119.5(2)
C(26)-C(27)-C(28) 120.2(3)
C(26)-C(27)-H(27) 119.9
C(28)-C(27)-H(27) 119.9
C(29)-C(28)-C(27) 120.0(3)
C(29)-C(28)-H(28) 120.0
C(27)-C(28)-H(28) 120.0
C(28)-C(29)-C(30) 120.2(3)
C(28)-C(29)-H(29) 119.9
C(30)-C(29)-H(29) 119.9
C(31)-C(30)-C(29) 120.1(3)
C(31)-C(30)-H(30) 120.0
C(29)-C(30)-H(30) 120.0
C(30)-C(31)-C(26) 120.2(3)
C(30)-C(31)-H(31) 119.9
C(26)-C(31)-H(31) 119.9

C(37)-C(32)-C(33) 118.9(2)
C(37)-C(32)-P(2) 119.31(19)
C(33)-C(32)-P(2) 121.62(19)
C(34)-C(33)-C(32) 120.5(2)
C(34)-C(33)-H(33) 119.8
C(32)-C(33)-H(33) 119.8
C(33)-C(34)-C(35) 120.1(2)
C(33)-C(34)-H(34) 120.0
C(35)-C(34)-H(34) 120.0
C(36)-C(35)-C(34) 120.1(2)
C(36)-C(35)-H(35) 120.0
C(34)-C(35)-H(35) 120.0
C(35)-C(36)-C(37) 120.2(3)
C(35)-C(36)-H(36) 119.9
C(37)-C(36)-H(36) 119.9
C(36)-C(37)-C(32) 120.3(2)
C(36)-C(37)-H(37) 119.8
C(32)-C(37)-H(37) 119.8

Cl(2S)-C(1S)-Cl(1S) 113.5(2)
Cl(2S)-C(1S)-H(38) 108.9
Cl(1S)-C(1S)-H(38) 108.9
Cl(2S)-C(1S)-H(39) 108.9
Cl(1S)-C(1S)-H(39) 108.9
H(38)-C(1S)-H(39) 107.7
Cl(3S)-C(2S)-Cl(4S) 115.4(6)
Cl(3S)-C(2S)-H(41) 108.4
Cl(4S)-C(2S)-H(41) 108.4
Cl(3S)-C(2S)-H(40) 108.4
Cl(4S)-C(2S)-H(40) 108.4
H(41)-C(2S)-H(40) 107.5
Cl(5S)-C(3S)-Cl(6S) 101.9(4)
Cl(5S)-C(3S)-H(43) 111.4
Cl(6S)-C(3S)-H(43) 111.4
Cl(5S)-C(3S)-H(42) 111.4
Cl(6S)-C(3S)-H(42) 111.4
H(43)-C(3S)-H(42) 109.3

C(7)-P(1)-C(1) 98.47(11)
C(7)-P(1)-C(13) 112.26(12)
C(1)-P(1)-C(13) 104.96(12)
C(7)-P(1)-Pt(1) 113.32(9)
C(1)-P(1)-Pt(1) 123.97(8)
C(13)-P(1)-Pt(1) 103.76(8)
C(32)-P(2)-C(25) 110.29(11)
C(32)-P(2)-C(26) 101.98(11)
C(25)-P(2)-C(26) 102.02(11)
C(32)-P(2)-Pt(1) 112.70(8)
C(25)-P(2)-Pt(1) 110.71(8)
C(26)-P(2)-Pt(1) 118.33(8)
P(2)-Pt(1)-P(1) 96.49(2)
P(2)-Pt(1)-Cl(2) 90.33(2)
P(1)-Pt(1)-Cl(2) 173.10(2)
P(2)-Pt(1)-Cl(1) 175.97(2)
P(1)-Pt(1)-Cl(1) 85.91(2)
Cl(2)-Pt(1)-Cl(1) 87.22(2)

Crystal data of [RuCl(OTf)(2a){(*S*,*S*)-dpen}]$_2$AgOTf

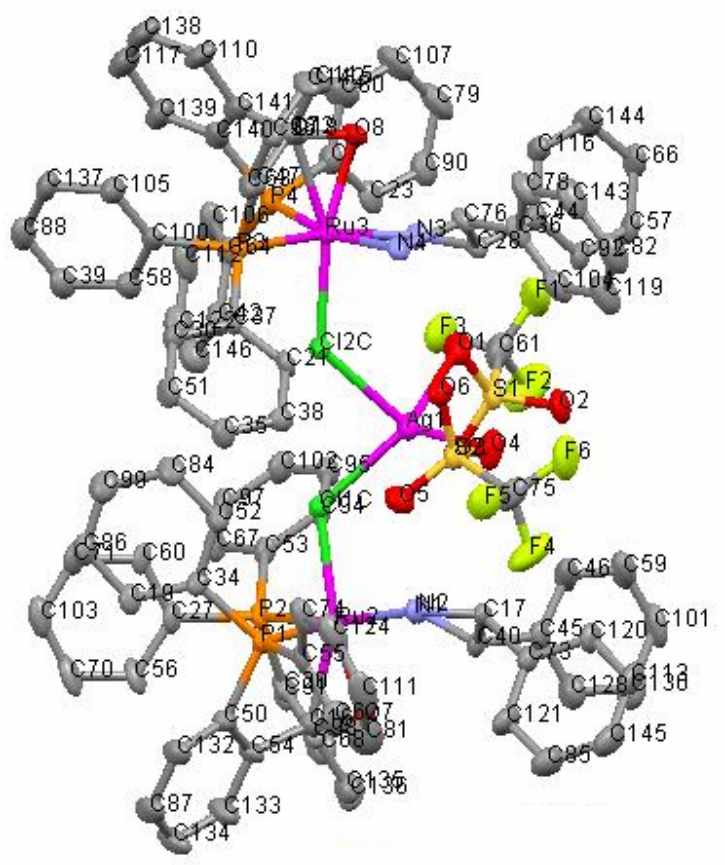

Empirical formula	$C_{107}H_{90.50}AgCl_{9.50}F_{7.50}N_4O_{9.50}P_4\ Ru_2S_{2.50}$	
Formula weight	2577.65	
Temperature	90 K	
Wavelength	0.71073 Å ($Mo_{K\alpha}$)	
Crystal system	Orthorhombic	
Space group	P2(1)2(1)2	
Unit cell dimensions	a = 20.9715(16) Å	α = 90°
	b = 39.437(3) Å	β = 90°
	c = 13.8177(10) Å	γ = 90°
Volume	11428.0(15) $Å^3$	
Z	4	
Density (calculated)	1.498 Mg/m^3	
Absorption coefficient	0.823 mm^{-1}	
F(000)	5202	
Crystal size	0.29 x 0.27 x 0.13 mm^3	
Theta range for data collection	1.47 to 27.93°	
Index ranges	-27<=h<=26, -51<=k<=50, -18<=l<=18	

Reflections collected	135463
Independent reflections	26825 [R(int) = 0.0511]
Completeness to theta = 27.84°	99.2 %
Absorption correction	Empirical
Max. and min. transmission	0.9006 and 0.7963
Refinement method	Full-matrix least-squares on F^2
Data / restraints / parameters	26825 / 2307 / 1448
Goodness-of-fit on F^2	1.145
Final R indices [I>2sigma(I)]	R1 = 0.0754, wR2 = 0.2099
R indices (all data)	R1 = 0.0821, wR2 = 0.2145
Largest diff. peak and hole	10.390 and -1.310 e.Å^{-3}

Bond lengths (Å)

Ag(1)-O(4) 2.389(5)
Ag(1)-O(1) 2.445(6)
Ag(1)-Cl(1C) 2.5060(17)
Ag(1)-Cl(2C) 2.5578(18)
C(7)-C(23) 1.387(13)
C(7)-C(80) 1.383(13)
C(7)-P(4) 1.831(8)
C(16)-O(7) 1.301(9)
C(16)-C(98) 1.493(11)
C(16)-C(54) 1.519(11)
C(16)-Ru(2) 2.182(7)
C(17)-C(73) 1.525(10)
C(17)-N(1) 1.531(10)
C(17)-C(40) 1.540(11)
C(17)-H(17A) 1.0000
C(18)-O(8) 1.332(9)
C(18)-C(141) 1.485(13)
C(18)-C(72) 1.493(12)
C(18)-Ru(3) 2.196(7)
C(19)-C(34) 1.397(11)
C(19)-C(86) 1.412(12)
C(19)-H(19A) 0.9500
C(20)-C(91) 1.382(12)
C(20)-C(98) 1.400(12)
C(20)-P(2) 1.823(8)
C(21)-C(37) 1.369(10)
C(21)-C(38) 1.408(11)
C(21)-H(21A) 0.9500
C(23)-C(90) 1.392(12)
C(23)-H(23A) 0.9500
C(27)-C(60) 1.394(12)
C(27)-C(56) 1.404(12)
C(27)-P(2) 1.808(7)
C(28)-C(44) 1.507(9)
C(28)-N(3) 1.511(9)
C(28)-C(76) 1.515(10)
C(28)- H(28A) 1.0000
C(30)-C(37) 1.389(10)
C(30)-C(51) 1.393(11)
C(30)-H(30A) 0.9500
C(34)-C(52) 1.426(11)
C(34)-P(1) 1.815(7)
C(35)-C(38) 1.336(11)
C(35)-C(51) 1.401(11)
C(35)-H(35A) 0.9500
C(36)-C(78) 1.368(12)
C(36)-C(104) 1.368(14)
C(36)-C(76) 1.525(11)
C(37)-P(3) 1.839(7)
C(38)-H(38A) 0.9500
C(39)-C(88) 1.377(14)
C(39)-C(58) 1.394(11)
C(39)-H(39A) 0.9500
C(40)-C(45) 1.511(11)
C(40)-N(2) 1.516(9)
C(40)-H(40A) 1.0000
C(42)-C(64) 1.375(13)
C(42)-C(146) 1.400(13)
C(42)-H(42A) 0.9500
C(44)-C(92) 1.353(10)
C(44)-C(116) 1.396(11)
C(45)-C(128) 1.376(13)
C(45)-C(46) 1.388(13)
C(46)-C(59) 1.374(15)
C(46)-H(46A) 0.9500
C(47)-C(72) 1.377(11)
C(47)-C(63) 1.403(11)
C(47)-P(3) 1.832(8)
C(50)-C(132) 1.398(11)
C(50)-C(54) 1.416(11)
C(50)-P(1) 1.812(8)
C(51)-H(51A) 0.9500
C(52)-C(84) 1.379(12)
C(52)-H(52A) 0.9500
C(53)-C(67) 1.395(10)
C(53)-C(94) 1.407(11)
C(53)-P(2) 1.829(7)
C(54)-C(133) 1.381(12)

C(55)-C(62) 1.375(13)
C(55)-C(74) 1.395(13)
C(55)-P(1) 1.846(7)
C(56)-C(70) 1.384(12)
C(56)-H(56A) 0.9500
C(57)-C(66) 1.362(13)
C(57)-C(92) 1.408(11)
C(57)-H(57A) 0.9500
C(58)-C(100) 1.370(11)
C(58)-H(58A) 0.9500
C(59)-C(101) 1.361(17)
C(59)-H(59A) 0.9500
C(60)-C(71) 1.409(11)
C(60)-H(60A) 0.9500
C(61)-F(1) 1.323(3)
C(61)-F(2) 1.323(3)
C(61)-F(3) 1.323(3)
C(61)-S(1) 1.827(6)
C(62)-C(81) 1.376(13)
C(62)-H(62A) 0.9500
C(63)-C(96) 1.388(11)
C(63)-H(63A) 0.9500
C(64)-C(106) 1.419(12)
C(64)-P(4) 1.838(9)
C(66)-C(144) 1.389(13)
C(66)-H(66A) 0.9500
C(67)-C(97) 1.364(12)
C(67)-H(67A) 0.9500
C(68)-C(136) 1.398(16)
C(68)-C(91) 1.409(14)
C(68)-H(68A) 0.9500
C(70)-C(103) 1.375(16)
C(70)-H(70A) 0.9500
C(71)-C(103) 1.383(15)
C(71)-H(71A) 0.9500
C(72)-C(115) 1.390(12)
C(73)-C(121) 1.387(13)
C(73)-C(120) 1.397(11)
C(74)-C(124) 1.382(12)
C(74)-H(74A) 0.9500
C(75)-F(4) 1.323(3)
C(75)-F(6) 1.323(3)
C(75)-F(5) 1.323(3)
C(75)-S(2) 1.827(6)
C(76)-N(4) 1.514(9)
C(76)-H(76A) 1.0000
C(78)-C(143) 1.405(14)
C(78)-H(78A) 0.9500
C(79)-C(107) 1.386(18)
C(79)-C(90) 1.392(15)
C(79)-H(79A) 0.9500
C(80)-C(107) 1.416(14)
C(80)-H(80A) 0.9500
C(81)-C(111) 1.388(18)
C(81)-H(81A) 0.9500
C(82)-C(119) 1.315(16)
C(82)-C(143) 1.400(17)
C(82)-H(82A) 0.950
C(84)-C(99) 1.402(13)
C(84)-H(84A) 0.9500
C(85)-C(145) 1.371(15)
C(85)-C(121) 1.416(12)
C(85)-H(85A) 0.9500
C(86)-C(99) 1.363(13)
C(86)-H(86A) 0.9500
C(87)-C(132) 1.375(13)
C(87)-C(134) 1.400(15)
C(87)-H(87A) 0.9500
C(88)-C(137) 1.397(14)
C(88)-H(88A) 0.9500
C(90)-H(90A) 0.9500
C(91)-H(91A) 0.9500
C(92)-H(92A) 0.9500
C(94)-C(95) 1.363(11)
C(94)-H(94A) 0.9500
C(95)-C(102) 1.374(11)
C(95)-H(95A) 0.9500
C(96)-C(142) 1.381(13)
C(96)-H(96A) 0.9500
C(97)-C(102) 1.403(12)
C(97)-H(97A) 0.9500
C(98)-C(135) 1.400(12)
C(99)-H(99A) 0.9500
C(100)-C(105) 1.368(12)
C(100)-P(3) 1.840(8)
C(101)-C(130) 1.425(16)
C(101)-H(10A) 0.9500
C(102)-H(10B) 0.9500
C(103)-H(10C) 0.9500
C(104)-C(119) 1.392(12)
C(104)-H(10D) 0.9500
C(105)-C(137) 1.396(12)
C(105)-H(10E) 0.9500
C(106)-C(112) 1.405(15)
C(106)-H(10F) 0.9500
C(107)-H(10G) 0.9500
C(110)-C(138) 1.406(15)
C(110)-C(141) 1.434(12)
C(110)-H(11A) 0.9500
C(111)-C(124) 1.379(17)
C(111)-H(11B) 0.9500
C(112)-C(122) 1.348(16)
C(112)-H(11C) 0.9500
C(113)-C(145) 1.360(17)
C(113)-C(120) 1.405(12)
C(113)-H(11D) 0.9500
C(115)-C(142) 1.371(14)
C(115)-H(11E) 0.9500
C(116)-C(144) 1.388(12)
C(116)-H(11F) 0.9500
C(117)-C(138) 1.372(18)
C(117)-C(139) 1.409(15)
C(117)-H(11G) 0.9500
C(119)-H(11H) 0.9500
C(120)-H(12A) 0.9500
C(121)-H(12B) 0.9500
C(122)-C(146) 1.380(16)
C(122)-H(12C) 0.9500
C(124)-H(12D) 0.9500
C(128)-C(130) 1.405(13)

C(128)-H(12E) 0.9500
C(130)-H(13A) 0.9500
C(132)-H(13B) 0.9500
C(133)-C(134) 1.349(14)
C(133)-H(13C) 0.9500
C(134)-H(13D) 0.9500
C(135)-C(136) 1.358(15)
C(135)-H(13E) 0.9500
C(136)-H(13F) 0.9500
C(137)-H(13G) 0.9500
C(138)-H(13H) 0.9500
C(139)-C(140) 1.396(13)
C(139)-H(13I) 0.9500
C(140)-C(141) 1.414(14)
C(140)-P(4) 1.821(10)
C(142)-H(14A) 0.9500
C(143)-H(14B) 0.9500
C(144)-H(14C) 0.9500
C(145)-H(14D) 0.9500
C(146)-H(14E) 0.9500
C(1U)-Cl(3U) 1.729(4)
C(1U)-Cl(1U) 1.729(4)
C(1U)-Cl(2U) 1.729(4)
C(1U)-H(1UA) 1.0000
C(1V)-Cl(3V) 1.729(4)
C(1V)-Cl(2V) 1.729(4)
C(1V)-Cl(1V) 1.729(4)
C(1V)-H(1VA) 1.0000
C(1T)-Cl(2T) 1.729(4)
C(1T)-Cl(1T) 1.729(4)
C(1T)-Cl(3T) 1.729(4)
C(1T)-H(1TA) 1.0000
C(1W)-Cl(1W) 1.729(4)
C(1W)-Cl(3W) 1.729(4)
C(1W)-Cl(2W) 1.729(4)
C(1W)-H(1WA) 1.0000
Cl(1C)-Ru(2) 2.3702(17)
Cl(2C)-Ru(3) 2.3646(17)
N(1)-Ru(2) 2.149(6)
N(1)-H(1A) 0.9200
N(1)-H(1B) 0.9200
N(2)-Ru(2) 2.199(6)
N(2)-H(2A) 0.9200
N(2)-H(2B) 0.9200
N(3)-Ru(3) 2.128(6)
N(3)-H(3A) 0.9200
N(3)-H(3B) 0.9200
N(4)-Ru(3) 2.207(6)
N(4)-H(4A) 0.9200
N(4)-H(4B) 0.9200
O(1)-S(1) 1.447(2)
O(2)-S(1) 1.446(2)
O(3)-S(1) 1.446(2)
O(4)-S(2) 1.446(2)
O(5)-S(2) 1.446(2)
O(6)-S(2) 1.446(2)
O(7)-Ru(2) 2.070(5)
O(8)-Ru(3) 2.084(5)
P(1)-Ru(2) 2.3047(19)
P(2)-Ru(2) 2.3590(17)
P(3)-Ru(3) 2.3579(18)
P(4)-Ru(3) 2.318(2)
S(1G)-S(1G) 1.032(7)
S(1G)-O(1G) 1.231(11)
S(1G)-O(1G) 1.446(2)
S(1G)-O(2G) 1.446(2)
S(1G)-O(3G) 1.446(2)
S(1G)-C(1G) 1.514(7)
S(1G)-F(3G) 1.753(13)
S(1G)-C(1G) 1.827(6)
S(1G)-O(2G) 1.850(10)
O(1G)-O(2G) 0.50(2)
O(1G)-S(1G) 1.231(11)
O(2G)-O(1G) 0.50(2)
O(2G)-S(1G) 1.850(10)
O(3G)-F(3G) 0.569(15)
O(3G)-C(1G) 1.577(16)
C(1G)-C(1G) 1.175(16)
C(1G)-F(2G) 1.323(3)
C(1G)-F(3G) 1.323(3)
C(1G)-F(1G) 1.323(3)
C(1G)-F(1G) 1.419(15)
C(1G)-S(1G) 1.514(7)
C(1G)-O(3G) 1.577(16)
C(1G)-F(2G) 1.837(18)
F(1G)-F(2G) 0.821(16)
F(1G)-C(1G) 1.419(15)
F(2G)-F(1G) 0.821(16)
F(2G)-C(1G) 1.837(18)
F(3G)-O(3G) 0.569(15)
F(3G)-S(1G) 1.753(13)
C(1X)-Cl(3X) 1.729(4)
C(1X)-Cl(2X) 1.729(4)
C(1X)-Cl(1X) 1.729(4)
C(1X)-H(1XA) 1.0000
Cl(1X)-Cl(3X) 0.35(3)
Cl(1X)-C(1X) 1.88(2)
Cl(2X)-Cl(2X) 0.000(12)
Cl(2X)-C(1X) 1.729(4)
Cl(3X)-Cl(1X) 0.35(3)
Cl(3X)-C(1X) 1.552(15)

Bond angles (º)

O(4)-Ag(1)-O(1) 105.75(14)
O(4)-Ag(1)-Cl(1C) 123.23(11)
O(1)-Ag(1)-Cl(1C) 124.18(11)
O(4)-Ag(1)-Cl(2C) 112.24(10)
O(1)-Ag(1)-Cl(2C) 96.05(9)
Cl(1C)-Ag(1)-Cl(2C) 89.24(6)
C(23)-C(7)-C(80) 119.0(8)
C(23)-C(7)-P(4) 118.8(7)
C(80)-C(7)-P(4) 122.0(7)

O(7)-C(16)-C(98) 119.9(7)
O(7)-C(16)-C(54) 115.9(7)
C(98)-C(16)-C(54) 117.7(7)
O(7)-C(16)-Ru(2) 67.6(4)
C(98)-C(16)-Ru(2) 110.1(5)
C(54)-C(16)-Ru(2) 115.0(5)
C(73)-C(17)-N(1) 110.4(6)
C(73)-C(17)-C(40) 108.4(6)
N(1)-C(17)-C(40) 110.0(6)
C(73)-C(17)-H(17A) 109.4
N(1)-C(17)-H(17A) 109.4
C(40)-C(17)-H(17A) 109.4
O(8)-C(18)-C(141) 119.3(8)
O(8)-C(18)-C(72) 117.8(8)
C(141)-C(18)-C(72) 117.2(7)
O(8)-C(18)-Ru(3) 67.3(4)
C(141)-C(18)-Ru(3) 114.1(6)
C(72)-C(18)-Ru(3) 109.8(5)
C(34)-C(19)-C(86) 118.2(8)
C(34)-C(19)-H(19A) 120.9
C(86)-C(19)-H(19A) 120.9
C(91)-C(20)-C(98) 120.6(8)
C(91)-C(20)-P(2) 127.8(7)
C(98)-C(20)-P(2) 110.5(6)
C(37)-C(21)-C(38) 120.3(7)
C(37)-C(21)-H(21A) 119.9
C(38)-C(21)-H(21A) 119.9
C(7)-C(23)-C(90) 121.0(9)
C(7)-C(23)-H(23A) 119.5
C(90)-C(23)-H(23A) 119.5
C(60)-C(27)-C(56) 118.9(7)
C(60)-C(27)-P(2) 117.8(6)
C(56)-C(27)-P(2) 123.0(7)
C(44)-C(28)-N(3) 108.3(6)
C(44)-C(28)-C(76) 116.1(6)
N(3)-C(28)-C(76) 108.4(6)
C(44)-C(28)-H(28A) 107.9
N(3)-C(28)-H(28A) 107.9
C(76)-C(28)-H(28A) 107.9
C(37)-C(30)-C(51) 120.2(7)
C(37)-C(30)-H(30A) 119.9
C(51)-C(30)-H(30A) 119.9
C(19)-C(34)-C(52) 119.6(7)
C(19)-C(34)-P(1) 123.8(6)
C(52)-C(34)-P(1) 116.6(6)
C(38)-C(35)-C(51) 121.8(8)
C(38)-C(35)-H(35A) 119.1
C(51)-C(35)-H(35A) 119.1
C(78)-C(36)-C(104) 118.3(8)
C(78)-C(36)-C(76) 118.4(8)
C(104)-C(36)-C(76) 123.2(7)
C(21)-C(37)-C(30) 119.7(7)
C(21)-C(37)-P(3) 121.5(5)
C(30)-C(37)-P(3) 118.7(6)
C(35)-C(38)-C(21) 119.6(8)
C(35)-C(38)-H(38A) 120.2
C(21)-C(38)-H(38A) 120.2
C(88)-C(39)-C(58) 119.5(9)
C(88)-C(39)-H(39A) 120.3
C(58)-C(39)-H(39A) 120.3
C(45)-C(40)-N(2) 112.4(6)
C(45)-C(40)-C(17) 112.9(6)
N(2)-C(40)-C(17) 107.3(6)
C(45)-C(40)-H(40A) 108.0
N(2)-C(40)-H(40A) 108.0
C(17)-C(40)-H(40A) 108.0
C(64)-C(42)-C(146) 118.8(9)
C(64)-C(42)-H(42A) 120.6
C(146)-C(42)-H(42A) 120.6
C(92)-C(44)-C(116) 120.1(7)
C(92)-C(44)-C(28) 121.3(7)
C(116)-C(44)-C(28) 118.3(7)
C(128)-C(45)-C(46) 118.8(8)
C(128)-C(45)-C(40) 118.6(8)
C(46)-C(45)-C(40) 122.6(8)
C(59)-C(46)-C(45) 121.1(11)
C(59)-C(46)-H(46A) 119.5
C(45)-C(46)-H(46A) 119.5
C(72)-C(47)-C(63) 121.2(7)
C(72)-C(47)-P(3) 110.5(6)
C(63)-C(47)-P(3) 127.5(6)
C(132)-C(50)-C(54) 120.0(7)
C(132)-C(50)-P(1) 126.3(6)
C(54)-C(50)-P(1) 113.6(6)
C(30)-C(51)-C(35) 118.3(7)
C(30)-C(51)-H(51A) 120.8
C(35)-C(51)-H(51A) 120.8
C(84)-C(52)-C(34) 120.0(7)
C(84)-C(52)-H(52A) 120.0
C(34)-C(52)-H(52A) 120.0
C(67)-C(53)-C(94) 117.6(7)
C(67)-C(53)-P(2) 119.7(6)
C(94)-C(53)-P(2) 122.2(5)
C(133)-C(54)-C(50) 117.4(8)
C(133)-C(54)-C(16) 121.2(8)
C(50)-C(54)-C(16) 121.3(7)
C(62)-C(55)-C(74) 119.0(8)
C(62)-C(55)-P(1) 118.0(7)
C(74)-C(55)-P(1) 122.9(7)
C(70)-C(56)-C(27) 120.4(10)
C(70)-C(56)-H(56A) 119.8
C(27)-C(56)-H(56A) 119.8
C(66)-C(57)-C(92) 120.7(8)
C(66)-C(57)-H(57A) 119.6
C(92)-C(57)-H(57A) 119.6
C(100)-C(58)-C(39) 119.5(8)
C(100)-C(58)-H(58A) 120.3
C(39)-C(58)-H(58A) 120.3
C(101)-C(59)-C(46) 120.6(10)
C(101)-C(59)-H(59A) 119.7
C(46)-C(59)-H(59A) 119.7
C(27)-C(60)-C(71) 120.1(8)
C(27)-C(60)-H(60A) 119.9
C(71)-C(60)-H(60A) 119.9
F(1)-C(61)-F(2) 107.9(3)
F(1)-C(61)-F(3) 107.9(3)
F(2)-C(61)-F(3) 107.9(3)
F(1)-C(61)-S(1) 111.1(4)
F(2)-C(61)-S(1) 111.2(4)
F(3)-C(61)-S(1) 110.5(4)

C(55)-C(62)-C(81) 121.2(11)
C(55)-C(62)-H(62A) 119.4
C(81)-C(62)-H(62A) 119.4
C(96)-C(63)-C(47) 117.8(8)
C(96)-C(63)-H(63A) 121.1
C(47)-C(63)-H(63A) 121.1
C(42)-C(64)-C(106) 120.9(9)
C(42)-C(64)-P(4) 122.4(7)
C(106)-C(64)-P(4) 116.5(7)
C(57)-C(66)-C(144) 118.7(8)
C(57)-C(66)-H(66A) 120.7
C(144)-C(66)-H(66A) 120.7
C(97)-C(67)-C(53) 121.2(8)
C(97)-C(67)-H(67A) 119.4
C(53)-C(67)-H(67A) 119.4
C(136)-C(68)-C(91) 120.8(9)
C(136)-C(68)-H(68A) 119.6
C(91)-C(68)-H(68A) 119.6
C(103)-C(70)-C(56) 120.3(10)
C(103)-C(70)-H(70A) 119.9
C(56)-C(70)-H(70A) 119.9
C(103)-C(71)-C(60) 119.4(9)
C(103)-C(71)-H(71A) 120.3
C(60)-C(71)-H(71A) 120.3
C(47)-C(72)-C(115) 119.8(8)
C(47)-C(72)-C(18) 116.1(7)
C(115)-C(72)-C(18) 124.0(7)
C(121)-C(73)-C(120) 120.5(8)
C(121)-C(73)-C(17) 119.9(7)
C(120)-C(73)-C(17) 119.6(7)
C(124)-C(74)-C(55) 120.5(10)
C(124)-C(74)-H(74A) 119.8
C(55)-C(74)-H(74A) 119.8
F(4)-C(75)-F(6) 108.0(3)
F(4)-C(75)-F(5) 107.9(3)
F(6)-C(75)-F(5) 107.9(3)
F(4)-C(75)-S(2) 111.4(4)
F(6)-C(75)-S(2) 111.2(4)
F(5)-C(75)-S(2) 110.3(4)
N(4)-C(76)-C(28) 107.2(5)
N(4)-C(76)-C(36) 112.4(6)
C(28)-C(76)-C(36) 114.7(7)
N(4)-C(76)-H(76A) 107.4
C(28)-C(76)-H(76A) 107.4
C(36)-C(76)-H(76A) 107.4
C(36)-C(78)-C(143) 121.9(11)
C(36)-C(78)-H(78A) 119.1
C(143)-C(78)-H(78A) 119.1
C(107)-C(79)-C(90) 119.3(9)
C(107)-C(79)-H(79A) 120.3
C(90)-C(79)-H(79A) 120.3
C(7)-C(80)-C(107) 120.3(11)
C(7)-C(80)-H(80A) 119.9
C(107)-C(80)-H(80A) 119.9
C(62)-C(81)-C(111) 119.1(11)
C(62)-C(81)-H(81A) 120.4
C(111)-C(81)-H(81A) 120.4
C(119)-C(82)-C(143) 119.4(10)
C(119)-C(82)-H(82A) 120.3
C(143)-C(82)-H(82A) 120.3
C(52)-C(84)-C(99) 120.5(8)
C(52)-C(84)-H(84A) 119.8
C(99)-C(84)-H(84A) 119.8
C(145)-C(85)-C(121) 118.5(10)
C(145)-C(85)-H(85A) 120.8
C(121)-C(85)-H(85A) 120.8
C(99)-C(86)-C(19) 122.3(8)
C(99)-C(86)-H(86A) 118.8
C(19)-C(86)-H(86A) 118.8
C(132)-C(87)-C(134) 120.7(9)
C(132)-C(87)-H(87A) 119.7
C(134)-C(87)-H(87A) 119.7
C(39)-C(88)-C(137) 121.4(8)
C(39)-C(88)-H(88A) 119.3
C(137)-C(88)-H(88A) 119.3
C(79)-C(90)-C(23) 120.2(10)
C(79)-C(90)-H(90A) 119.9
C(23)-C(90)-H(90A) 119.9
C(20)-C(91)-C(68) 118.0(9)
C(20)-C(91)-H(91A) 121.0
C(68)-C(91)-H(91A) 121.0
C(44)-C(92)-C(57) 120.3(8)
C(44)-C(92)-H(92A) 119.9
C(57)-C(92)-H(92A) 119.9
C(95)-C(94)-C(53) 120.3(7)
C(95)-C(94)-H(94A) 119.9
C(53)-C(94)-H(94A) 119.9
C((94)-C(95)-C(102) 122.2(8)
C(94)-C(95)-H(95A) 118.9
C(102)-C(95)-H(95A) 118.9
C(142)-C(96)-C(63) 120.5(9)
C(142)-C(96)-H(96A) 119.7
C(63)-C(96)-H(96A) 119.7
C(67)-C(97)-C(102) 120.8(7)
C(67)-C(97)-H(97A) 119.6
C(102)-C(97)-H(97A) 119.6
C(135)-C(98)-C(20) 120.4(8)
C(135)-C(98)-C(16) 122.2(8)
C(20)-C(98)-C(16) 117.4(7)
C(86)-C(99)-C(84) 119.4(8)
C(86)-C(99)-H(99A) 120.3
C(84)-C(99)-H(99A) 120.3
C(105)-C(100)-C(58) 121.1(7)
C(105)-C(100)-P(3) 122.3(6)
C(58)-C(100)-P(3) 116.5(6)
C(59)-C(101)-C(130) 120.5(9)
C(59)-C(101)-H(10A) 119.7
C(130)-C(101)-H(10A) 119.7
C(95)-C(102)-C(97) 117.8(8)
C(95)-C(102)-H(10B) 121.1
C(97)-C(102)-H(10B) 121.1
C(70)-C(103)-C(71) 120.8(8)
C(70)-C(103)-H(10C) 119.6
C(71)-C(103)-H(10C) 119.6
C(36)-C(104)-C(119) 119.5(9)
C(36)-C(104)-H(10D) 120.2
C(119)-C(104)-H(10D) 120.2
C(100)-C(105)-C(137) 120.8(9)
C(100)-C(105)-H(10E) 119.6
C(137)-C(105)-H(10E) 119.6

C(112)-C(106)-C(64) 116.9(10)
C(112)-C(106)-H(10F) 121.6
C(64)-C(106)-H(10F) 121.6
C(79)-C(107)-C(80) 120.0(10)
C(79)-C(107)-H(10G) 120.0
C(80)-C(107)-H(10G) 120.0
C(138)-C(110)-C(141) 119.2(11)
C(138)-C(110)-H(11A) 120.4
C(141)-C(110)-H(11A) 120.4
C(124)-C(111)-C(81) 120.7(8)
C(124)-C(111)-H(11B) 119.6
C(81)-C(111)-H(11B) 119.6
C(122)-C(112)-C(106) 123.0(10)
C(122)-C(112)-H(11C) 118.5
C(106)-C(112)-H(11C) 118.5
C(145)-C(113)-C(120) 120.7(9)
C(145)-C(113)-H(11D) 119.7
C(120)-C(113)-H(11D) 119.7
C(142)-C(115)-C(72) 119.3(8)
C(142)-C(115)-H(11E) 120.3
C(72)-C(115)-H(11E) 120.3
C(144)-C(116)-C(44) 119.0(8)
C(144)-C(116)-H(11F) 120.5
C(44)-C(116)-H(11F) 120.5
C(138)-C(117)-C(139) 122.5(10)
C(138)-C(117)-H(11G) 118.8
C(139)-C(117)-H(11G) 118.8
C(82)-C(119)-C(104) 122.9(12)
C(82)-C(119)-H(11H) 118.5
C(104)-C(119)-H(11H) 118.5
C(73)-C(120)-C(113) 118.4(9)
C(73)-C(120)-H(12A) 120.8
C(113)-C(120)-H(12A) 120.8
C(73)-C(121)-C(85) 120.0(9)
C(73)-C(121)-H(12B) 120.0
C(85)-C(121)-H(12B) 120.0
C(112)-C(122)-C(146) 118.8(10)
C(112)-C(122)-H(12C) 120.6
C(146)-C(122)-H(12C) 120.6
C(111)-C(124)-C(74) 119.3(10)
C(111)-C(124)-H(12D) 120.3
C(74)-C(124)-H(12D) 120.3
C(45)-C(128)-C(130) 121.8(10)
C(45)-C(128)-H(12E 119.1
C(130)-C(128)-H(12E 119.1
C(128)-C(130)-C(101) 117.2(11)
C(128)-C(130)-H(13A) 121.4
C(101)-C(130)-H(13A) 121.4
C(87)-C(132)-C(50) 119.3(8)
C(87)-C(132)-H(13B) 120.4
C(50)-C(132)-H(13B) 120.4
C(134)-C(133)-C(54) 123.3(10)
C(134)-C(133)-H(13C) 118.4
C(54)-C(133)-H(13C) 118.4
C(133)-C(134)-C(87) 118.9(9)
C(133)-C(134)-H(13D) 120.5
C(87)-C(134)-H(13D) 120.5
C(136)-C(135)-C(98) 119.5(10)
C(136)-C(135)-H(13E) 120.3
C(98)-C(135)-H(13E) 120.3
C(135)-C(136)-C(68) 120.6(9)
C(135)-C(136)-H(13F) 119.7
C(68)-C(136)-H(13F) 119.7
C(88)-C(137)-C(105) 117.7(8)
C(88)-C(137)-H(13G) 121.1
C(105)-C(137)-H(13G) 121.1
C(117)-C(138)-C(110) 120.3(10)
C(117)-C(138)-H(13H) 119.8
C(110)-C(138)-H(13H) 119.8
C(140)-C(139)-C(117) 117.5(11)
C(140)-C(139)-H(13I) 121.2
C(117)-C(139)-H(13I) 121.2
C(139)-C(140)-C(141) 122.1(9)
C(139)-C(140)-P(4) 126.1(8)
C(141)-C(140)-P(4) 111.8(7)
C(140)-C(141)-C(110) 118.3(9)
C(140)-C(141)-C(18) 122.9(8)
C(110)-C(141)-C(18) 118.6(9)
C(115)-C(142)-C(96) 121.1(8)
C(115)-C(142)-H(14A) 119.5
C(96)-C(142)-H(14A) 119.5
C(78)-C(143)-C(82) 117.9(10)
C(78)-C(143)-H(14B) 121.0
C(82)-C(143)-H(14B) 121.0
C(66)-C(144)-C(116) 121.2(8)
C(66)-C(144)-H(14C) 119.4
C(116)-C(144)-H(14C) 119.4
C(113)-C(145)-C(85) 122.0(9)
C(113)-C(145)-H(14D) 119.0
C(85)-C(145)-H(14D) 119.0
C(122)-C(146)-C(42) 121.5(11)
C(122)-C(146)-H(14E) 119.2
C(42)-C(146)-H(14E) 119.2
Cl(3U)-C(1U)-Cl(1U) 111.2(3)
Cl(3U)-C(1U)-Cl(2U) 111.2(3)
Cl(1U)-C(1U)-Cl(2U) 111.2(3)
Cl(3U)-C(1U)-H(1UA) 107.7
Cl(1U)-C(1U)-H(1UA) 107.7
Cl(2U)-C(1U)-H(1UA) 107.7
Cl(3V)-C(1V)-Cl(2V) 111.2(3)
Cl(3V)-C(1V)-Cl(1V) 111.2(3)
Cl(2V)-C(1V)-Cl(1V) 111.2(3)
Cl(3V)-C(1V)-H(1VA) 107.7
Cl(2V)-C(1V)-H(1VA) 107.7
Cl(1V)-C(1V)-H(1VA) 107.7
Cl(2T)-C(1T)-Cl(1T) 111.2(3)
Cl(2T)-C(1T)-Cl(3T) 111.2(3)
Cl(1T)-C(1T)-Cl(3T) 111.2(3)
Cl(2T)-C(1T)-H(1TA) 107.7
Cl(1T)-C(1T)-H(1TA) 107.7
Cl(3T)-C(1T)-H(1TA) 107.7
Cl(1W)-C(1W)-Cl(3W) 111.2(3)
Cl(1W)-C(1W)-Cl(2W) 111.2(3)
Cl(3W)-C(1W)-Cl(2W) 111.2(3)
Cl(1W)-C(1W)-H(1WA) 107.7
Cl(3W)-C(1W)-H(1WA) 107.7
Cl(2W)-C(1W)-H(1WA) 107.7
Ru(2)-Cl(1C)-Ag(1) 124.07(7)
Ru(3)-Cl(2C)-Ag(1) 129.24(8)
C(17)-N(1)-Ru(2) 114.2(4)

C(17)-N(1)-H(1A) 108.7
Ru(2)-N(1)-H(1A) 108.7
C(17)-N(1)-H(1B) 108.7
Ru(2)-N(1)-H(1B) 108.7
H(1A)-N(1)-H(1B) 107.6
C(40)-N(2)-Ru(2) 106.8(4)
C(40)-N(2)-H(2A) 110.4
Ru(2)-N(2)-H(2A) 110.4
C(40)-N(2)-H(2B) 110.4
Ru(2)-N(2)-H(2B) 110.4
H(2A)-N(2)-H(2B) 108.6
C(28)-N(3)-Ru(3) 115.0(4)
C(28)-N(3)-H(3A) 108.5
Ru(3)-N(3)-H(3A) 108.5
C(28)-N(3)-H(3B) 108.5
Ru(3)-N(3)-H(3B) 108.5
H(3A)-N(3)-H(3B) 107.5
C(76)-N(4)-Ru(3) 108.0(4)
C(76)-N(4)-H(4A) 110.1
C(76)-N(4)-H(4B) 110.1
Ru(3)-N(4)-H(4A) 110.1
Ru(3)-N(4)-H(4B) 110.1
H(4A)-N(4)-H(4B) 108.4
S(1)-O(1)-Ag(1) 98.2(3)
S(2)-O(40)-Ag(1) 103.2(2)
C(16)-O(7)-Ru(2) 76.9(4)
C(18)-O(8)-Ru(3) 76.5(4)
C(50)-P(1)-C(34) 108.5(4)
C(50)-P(1)-C(55) 100.0(4)
C(34)-P(1)-C(55) 104.6(4)
C(50)-P(1)-Ru(2) 105.6(3)
C(34)-P(1)-Ru(2) 121.7(2)
C(55)-P(1 Ru(2) 114.3(2)
C(27)-P(2)-C(20) 110.5(4)
C(27)-P(2)-C(53) 101.6(4)
C(20)-P(2)-C(53) 100.9(4)
C(27)-P(2)-Ru(2) 119.2(2)
C(20)-P(2)-Ru(2) 101.1(3)
C(53)-P(2)-Ru(2) 121.9(2)
C(47)-P(3)-C(37) 103.8(4)
C(47)-P(3)-C(100) 107.4(4)
C(37)-P(3)-C(100) 100.9(3)
C(47)-P(3)-Ru(3) 100.6(2)
C(37)-P(3)-Ru(3) 121.1(2)
C(100)-P(3)-Ru(3) 121.3(2)
C(140)-P(4)-C(7) 103.6(4)
C(140)-P(4)-C(64) 110.1(4)
C(140)-P(4)-Ru(3) 104.2(3)
C(7)-P(4)-C(64) 100.3(4)
C(7)-P(4)-Ru(3) 106.5(3)
C(64)-P(4)-Ru(3) 129.3(3)
O(7)-Ru(2)-N(1) 79.4(2)
O(7)-Ru(2)-C(16) 35.5(3)
N(1)-Ru(2)-C(16) 114.6(3)
O(7)-Ru(2)-N(2) 86.3(2)
N(1)-Ru(2)-N(2) 78.0(2)
C(16)-Ru(2)-N(2) 98.1(3)
O(7)-Ru(2)-P(1) 87.37(15)
N(1)-Ru(2)-P(1) 90.79(18)
C(16)-Ru(2)-P(1) 82.4(2)
N(2)-Ru(2)-P(1) 167.97(16)
O(7)-Ru(2)-P(2) 108.58(16)
N(1)-Ru(2)-P(2) 166.70(18)
C(16)-Ru(2)-P(2) 74.9(2)
N(2)-Ru(2)-P(2) 91.69(16)
P(1)-Ru(2)-P(2) 100.02(6)
O(7)-Ru(2)-Cl(1C) 167.78(15)
N(1)-Ru(2)-Cl(1C) 88.41(17)
C(16)-Ru(2)-Cl(1C) 156.7(2)
N(2)-Ru(2)-Cl(1C) 90.11(17)
P(1)-Ru(2)-Cl(1C) 93.97(6)
P(2)-Ru(2)-Cl(1C) 83.17(6)
O(8)-Ru(3)-N(3) 78.9(2)
O(8)-Ru(3)-C(18) 36.1(2)
N(3)-Ru(3)-C(18) 114.9(3)
O(8)-Ru(3)-N(4) 85.7(2)
N(3)-Ru(3)-N(4) 78.0(2)
C(18)-Ru(3)-N(4) 96.4(3)
O(8)-Ru(3)-P(4) 84.25(18)
N(3)-Ru(3)-P(4) 90.70(16)
C(18)-Ru(3)-P(4) 81.0(3)
N(4)-Ru(3)-P(4) 166.11(18)
O(8)-Ru(3)-P(3) 107.66(15)
N(3)-Ru(3)-P(3) 166.42(17)
C(18)-Ru(3)-P(3) 73.1(2)
N(4)-Ru(3)-P(3) 90.51(18)
P(4)-Ru(3)-P(3) 101.65(7)
O(8)-Ru(3)-Cl(2C) 165.75(16)
N(3)-Ru(3)-Cl(2C) 86.84(18)
C(18)-Ru(3)-Cl(2C) 158.1(2)
N(4)-Ru(3)-Cl(2C) 90.62(17)
P(4)-Ru(3)-Cl(2C) 96.81(7)
P(3)-Ru(3)-Cl(2C) 86.11(6)
O(2)-S(1)-O(3) 114.52(11)
O(2)-S(1)-O(1) 114.49(11)
O(3)-S(1)-O(1) 114.48(11)
O(2)-S(1)-C(61) 104.0(3)
O(3)-S(1)-C(61) 105.5(3)
O(1)-S(1)-C(61) 101.9(3)
O(6)-S(2)-O(5) 114.59(11)
O(6)-S(2)-O(4) 114.57(11)
O(5)-S(2)-O(4) 114.56(11)
O(6)-S(2)-C(75) 103.2(3)
O(5)-S(2)-C(75) 104.1(3)
O(4)-S(2)-C(75) 103.8(3)
S(1G)-S(1G)-O(1G) 78.9(6)
S(1G)-S(1G)-O(1G) 56.7(6)
O(1G)-S(1G)-O(1G) 96.2(12)
S(1G)-S(1G)-O(2G) 95.1(6)
O(1G)-S(1G)-O(2G) 19.6(10)
O(1G)-S(1G)-O(2G) 114.56(12)
S(1G)-S(1G)-O(3G) 148.5(6)
O(1G)-S(1G)-O(3G) 132.2(7)
O(1G)-S(1G)-O(3G) 114.55(12)
O(2G)-S(1G)-O(3G) 114.55(12)
S(1G)-S(1G)-C(1G) 89.7(4)
O(1G)-S(1G)-C(1G) 137.4(8)
O(1G)-S(1G)-C(1G) 111.4(8)
O(2G)-S(1G)-C(1G) 127.6(8)
O(3G)-S(1G)-C(1G) 64.4(7)

S(1G)-S(1G)-F(3G) 134.1(4)
O(1G)-S(1G)-F(3G) 141.1(9)
O(1G)-S(1G)-F(3G) 118.3(8)
O(2G)-S(1G)-F(3G) 121.6(7)
O(3G)-S(1G)-F(3G) 17.3(6)
C(1G)-S(1G)-F(3G) 47.1(3)
S(1G)-S(1G)-C(1G) 55.9(3)
O(1G)-S(1G)-C(1G) 104.5(7)
O(1G)-S(1G)-C(1G) 102.3(7)
O(2G)-S(1G)-C(1G) 105.4(7)
O(3G)-S(1G)-C(1G) 103.5(6)
C(1G)-S(1G)-C(1G) 39.8(6)
F(3G)-S(1G)-C(1G) 86.2(5)
S(1G)-S(1G)-O(2G) 51.1(4)
O(1G)-S(1G)-O(2G) 102.4(6)
O(1G)-S(1G)-O(2G) 10.5(11)
O(2G)-S(1G)-O(2G) 121.6(10)
O(3G)-S(1G)-O(2G) 114.2(6)
C(1G)-S(1G)-O(2G) 101.5(6)
F(3G)-S(1G)-O(2G) 114.5(7)
C(1G)-S(1G)-O(2G) 92.5(5)
O(2G)-O(1G)-S(1G) 105(2)
O(2G)-O(1G)-S(1G) 138(3)
S(1G)-O(1G)-S(1G) 44.5(4)
O(1G)-O(2G)-S(1G) 55.3(16)
O(1G)-O(2G)-S(1G) 32(2)
S(1G)-O(2G)-S(1G) 33.8(3)
F(3G)-O(3G)-S(1G) 113.6(17)
F(3G)-O(3G)-C(1G) 53.8(15)
S(1G)-O(3G)-C(1G) 59.9(4)
C(1G)-C(1G)-F(2G) 94.5(10)
C(1G)-C(1G)-F(3G) 156.9(8)
F(2G)-C(1G)-F(3G) 107.9(3)
C(1G)-C(1G)-F(1G) 68.9(9)
F(2G)-C(1G)-F(1G) 107.9(3)
F(3G)-C(1G)-F(1G) 107.9(3)
C(1G)-C(1G)-F(1G) 60.4(6)
F(2G)-C(1G)-F(1G) 34.6(7)
F(3G)-C(1G)-F(1G) 142.4(8)
F(1G)-C(1G)-F(1G) 88.8(10)
C(1G)-C(1G)-S(1G) 84.6(4)
F(2G)-C(1G)-S(1G) 133.2(8)
F(3G)-C(1G)-S(1G) 76.0(8)
F(1G)-C(1G)-S(1G) 115.1(8)
F(1G)-C(1G)-S(1G) 127.7(8)
C(1G)-C(1G)-O(3G) 138.9(6)
F(2G)-C(1G)-O(3G) 119.5(8)
F(3G)-C(1G)-O(3G) 20.3(6)
F(1G)-C(1G)-O(3G) 115.6(8)
F(1G)-C(1G)-O(3G) 152.2(11)
S(1G)-C(1G)-O(3G) 55.7(4)
C(1G)-C(1G)-S(1G) 55.6(3)
F(2G)-C(1G)-S(1G) 111.5(7)
F(3G)-C(1G)-S(1G) 108.9(7)
F(1G)-C(1G)-S(1G) 112.4(8)
F(1G)-C(1G)-S(1G) 94.3(7)
S(1G)-C(1G)-S(1G) 34.4(3)
O(3G)-C(1G)-S(1G) 88.8(5)
C(1G)-C(1G)-F(2G) 45.9(6)
F(2G)-C(1G)-F(2G) 110.1(8)
F(3G)-C(1G)-F(2G) 126.3(6)
F(1G)-C(1G)-F(2G) 23.7(6)
F(1G)-C(1G)-F(2G) 81.0(6)
S(1G)-C(1G)-F(2G) 102.4(7)
O(3G)-C(1G)-F(2G) 126.7(9)
S(1G)-C(1G)-F(2G) 90.6(6)
F(2G)-F(1G)-C(1G) 116.0(14)
F(2G)-F(1G)-C(1G) 66.2(9)
C(1G)-F(1G)-C(1G) 50.6(8)
F(1G)-F(2G)-C(1G) 79.1(12)
F(1G)-F(2G)-C(1G) 40.3(10)
C(1G)-F(2G)-C(1G) 39.6(6)
O(3G)-F(3G)-C(1G) 105.9(18)
O(3G)-F(3G)-S(1G) 49.1(13)
C(1G)-F(3G)-S(1G) 56.9(6)
C(l3X)-C(1X)-Cl(2X) 111.2(3)
C(l3X)-C(1X)-Cl(1X) 111.2(3)
C(l2X)-C(1X)-Cl(1X) 111.2(3)
C(l3X)-C(1X)-H(1XA) 107.7
Cl(2X)-C(1X)-H(1XA) 107.7
Cl(1X)-C(1X)-H(1XA) 107.7
Cl(3X)-Cl(1X)-C(1X) 54.6(15)
Cl(3X)-Cl(1X)-C(1X) 59(3)
C(1X)-Cl(1X)-C(1X) 32.5(9)
Cl(2X)-Cl(2X)-C(1X) 0(10)
Cl(2X)-Cl(2X)-C(1X) 0(10)
C(1X)-Cl(2X)-C(1X) 34.4(11)
Cl(1X)-Cl(3X)-C(1X) 115(2)
Cl(1X)-Cl(3X)-C(1X) 111(2)
C(1X)-Cl(3X)-C(1X) 35.8(11)

References for Chapter 2

1 Review: (a) Green, B. S.; Lahav, M.; Rabinovich, D. *Acc. Chem. Res.* **1969**, *12*, 191. (b) Collet, A.; Brienne, M.-J.; Jacques, J. *Chem. Rev.* **1980**, *80*, 214. (c) Koshima, H.; Ding, Y.; Chisaka, T.; Matsuura, T. *J. Am. Chem. Soc.* **1996**, *118*, 12059. (d) Matsuura, T.; Koshima, H. *J. Photochem. Photobiol. C Photochem. Rev.* **2005**, *6*, 7.

2 (a) Fleischer, E. B.; Sung, N.; Hawkinson, S. *J. Phys. Chem.* **1968**, *72*, 4311. (b) Rappoport, Z.; Biali, S. E.; Kaftory, M. *J. Am. Chem. Soc.* **1990**, *112*, 7742. (c) Koshima, H.; Hayashi, E.; Matsuura, T.; Tanaka, K.; Toda, F.; Kato, M.; Kiguchi, M. *Tetrahedron lett.* **1997**, *38*, 5009. (d) Szyrszyng, M.; Nowak, E.; Gdaniec, M.; Milewska, M. J.; Połoński, T. *Tetahedron: Asymmetry* **2004**, *15*, 103.

3 Lunazzi, L.; Mazzanti, A.; Minzoni, M. *J. Org. Chem.* **2005**, *70*, 456.

4 BIPHEP-Pd: (a) Mikami, K.; Aikawa, K.; Yusa, Y.; Hatano, M. *Org. Lett.* **2002**, *4*, 91. (b) Mikami, K.; Aikawa, K.; Yusa, Y. *Org. Lett.* **2002**, *4*, 95. (c) Aikawa, K. *Ph.D. Thesis*, Tokyo Institute of Technology, **2005**.

5 BIPHEP-Pt: (a) Becker, J. J.; White, P. S.; Gagné, M. R. *J. Am. Chem. Soc.* **2001**, *123*, 9478. (b) Mikami, K.; Kakuno, H.; Aikawa, K. *Angew. Chem. Int. Ed.* **2005**, *44*, 7257.

6 BIPHEP-Ru: (a) Mikami, K.; Korenaga, T.; Terada, M.; Ohkuma, T.; Pham, T.; Noyori, R. *Angew. Chem. Int. Ed. Engl.* **1999**, *38*, 495. (b) Mikami, K.; Aikawa, K.; Korenaga, T. *Org. Lett.* **2001**, *3*, 243. (c) Korenaga, T. *Ph.D. Thesis*, Tokyo Institute of Technology, **2000**.

7 BIPHEP-Rh: (a) Mikami, K.; Kataoka, S.; Yusa, Y.; Aikawa, K. *Org. Lett.* **2004**, *6*, 3699. (b) Mikami, K.; Kataoka, S.; Wakabayashi, K.; Aikawa, K. *Tetrahedron* **2006**, *47*, 6361.

8 BIPHEP-Ir: Kataoka, S. *Master*'s *Thesis*, Tokyo Institute of Technology, **2006**.

9 Mikami, K.; Aikawa, K.; Yusa, Y.; Jodry, J. J.; Yamanaka, M. *Synlett* **2002**, 1561.

10 (a) Mikami, K.; Wakabayashi, K.; Aikawa, K. *Org. Lett.* **2006**, *8*, 1517. (b) Mikami, K.; Wakabayashi, K.; Yusa, Y.; Aikawa, K. *Chem. Commun.* **2006**, 2365. (c) Mikami, K.; Sayo, N. *PCT Int. Appl.* 2005; p. 107. (d) Wakabayashi, K. *Bachelor Presentation*, Merch 3rd 2003, Tokyo Institute of Technology. (e) Mikami, K.; Wakabayashi, K.; Aikawa, K. *84th Spring Meeting* 2004, 3 B8-31. (f) Mikami, K.; Wakabayashi, K.; Aikawa, K. *85th Spring Meeting* 2005, 1 A6-28.

11 Brauer, D. J.; Hingst, M.; Kottsieper, K. W.; Liek, C.; Nichel, T.; Tepper, M.; Stelzer, O.; Sheldrick,

W. S. *J. Organomet. Chem.* **2002**, *645*, 14.

12 (a) Korenaga, T.; Aikawa, K.; Terada, M.; Kawauchi S.; Mikami, K. *Adv. Synth. Cat.* **2001**, *343*, 284. (b) Yamanaka, M.; Mikami, K. *Organometallics* **2002**, *21*, 5847.

13 (a) Nilsson, B.; Martinson, P.; Olsson, K.; Carter, R. E. *J. Am. Chem. Soc.* **1974**, *96*, 3190. (b) Rousel, C.; Liden, A.; Chanon, M.; Metzger, J.; Sandstrom, J. *J. Am. Chem. Soc.* **1976**, *98*, 2847. (c) Bott, G.; Field, L. D.; Sternhell, S. *J. Am. Chem. Soc.* **1980**, *102*, 5618.

14 Review: Noyori, R.; Ohkuma, T. *Angew. Chem. Int. Ed.* **2001**, *40*, 40.

15 (a) Ohkuma, T.; Ooka, H.; Ikariya, T.; Noyori, R. *J. Am. Chem. Soc.* **1995**, *117*, 2675. (b) Ohkuma, T.; Ooka, H.; Yamakawa, M.; Ikariya, T.; Noyori, R. *J. Am. Chem. Soc.* **1995**, *117*, 10417. (c) Ohkuma, T.; Ikehira, H.; Ikariya, T.; Noyori, R. *Synlett* **1996**, 467. (d) Fujii, A.; Hashiguti, S.; Ooka, H.; Uematsu, N.; Ikariya, T.; Noyori, R. *J. Am. Chem. Soc.* **1996**, *118*, 2521. (e) Ohkuma, T.; Doucet, H.; Pham, T.; Mikami, K.; Korenaga, T.; Terada, M.; Noyori, R. *J. Am. Chem. Soc.* **1998**, *120*, 1086. (f) Ohkuma, T.; Koizumi, M.; Doucet, H.; Pham, T.; Kozawa, M.; Murata, K.; Katayama, E.; Yokozawa, T.; Ikariya, T.; Noyori, R. *J. Am. Chem. Soc.* **1998**, *120*, 13529. (g) Xie, J.-H.; Wang, L.-X.; Fu, Y.; Zhu, S.-F.; Fan, B.-M.; Duan, H.-F.; Zhou, Q.-L. *J. Am. Chem. Soc.* **2003**, *125*, 4404.

16 Jing, Q.; Sandoval, C. A.; Wang, Z.; Ding, K. *Eur. J. Org. Chem.* **2006**, 3606.

17 Review: Sandoval, C. A.; Ohkuma, T.; Muñiz, K.; Noyori, R. *J. Am. Chem. Soc.* **2003**, *125*, 13490.

18 Ohkuma, T.; Koizumi, M.; Muñiz, K.; Hilt, G.; Kabuto, C.; Noyori, R. *J. Am. Chem. Soc.* **2002**, *124*, 6508.

19 Reviews: (a) Carrillo, N.; Ceccarelli, E. A. *Eur. J. Biochem.* **2003**, *270*, 1900. (b) Pingoud, A.; Jeltsch, A. *Eur. J. Biochem.* **1997**, *246*, 1. (c) Schulz, G. E. *Faraday Discussions* **1992**, *93*, 85.

20 (a) Gladiali, S.; Pinna, L.; Delogu, G.; De Martin, S.; Zassinovich, G.; Mestroni, G. *Tetrahedron: Asymmetry* **1990**, *1*, 635. (b) Gamez, P.; Fache, F.; Mangeney, P.; Lemaire, M. *Tetrahedron Lett.* **1993**, *34*, 6897. (c) Gamez, P.; Dunjic, B.; Fache, F.; Lemaire, M.; *J. Chem. Soc., Chem. Commun.* **1994**, 1417. (d) Gamez, P.; Fache, F.; Lemaire, M. *Tetrahedron: Asymmetry* **1995**, *6*, 705.

21 (a) Gao, J. X.; Yi, X. D.; Xu, P. P.; Tang, C. L.; Wan, H. L.; Ikariya, T. *J. Organomet. Chem.* **1999**, *592*, 290. (b) Gao, J. X.; Yi, X. D.; Xu, P. P.; Tang, C. L.; Wan, H. L.; Ikariya, T. *J. Molecular Catalysis* **2000**, *159*, 3.

22 (a) Miyashita, A.; Yasuda, A.; Takaya, H.; Toriumi, K.; Ito, T.; Souchi, T.; Noyori R. *J. Am. Chem. Soc.* **1980**, *102*, 7932. (b) Tani, K.; Yamagata, T.; Akutagawa, S.; Kumobayashi, H.; Taketomi, T.; Takaya, H.; Miyashita, A.; Noyori R.; Otsuka, S. *J. Am. Chem. Soc.* **1984**, *106*, 5208. (c) Miyashita, A.; Takaya, H.; Souchi, T.; Noyori R. *Tetrahedron* **1984**, *40*, 1245. (d) Noyori, K.; Kitamura, M.; Ohkuma, T. *Proc. Nat. Acad. Sci. U.S.A.* **2004**, *101*, 5356. (e) Ohkuma, T.; Kitamura, M.; Noyori, K. *New Frontiers in Asymmetric catalysis*; Mikami, K.; Lantens, M., Eds; Wiley: New York, 2007, pp 1.

3-1. Introduction

As described in Chapter 2, metal complexes with benzophenone-derived diphosphine ligand could be controlled instantaneously in a single conformation upon addition of chiral activators and hence attained high catalytic activity and enantioselectivity (Scheme 3-1). Compared to biphenyl-derived ligands, chirality control of the benzophenone-derived ligand was so fast to afford single conformation within minutes even at room temperature. The instant chirality control and high enantioselectivity show the great advantage of highly *tropos* benzophenone-derived ligands over biphenyl-derived ligands.

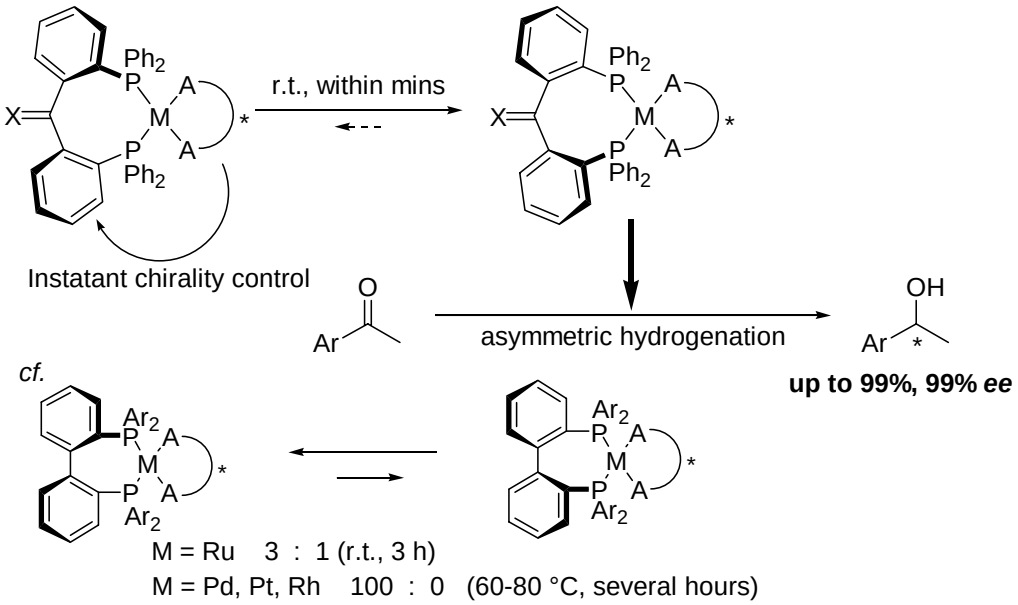

Scheme 3-1.

For further application of the benzophenone-derived compounds, benzophenone-like monodentate ligands were synthesized, and chirality control and catalytic asymmetric reactions using the monodentate ligands were examined.

Recently, not only bidentete ligands but also monodentate ligands have been reported to attain high catalytic activity and enantioselectivity in asymmetric reactions. For example, BINOL-derived monodentate phosphites, phosphonites and phosphoramidites have been reported to attain high catalytic activity and enantioselectivity in Rh-catalyzed asymmetric olefin hydrogenation (Scheme 3-2).[1]

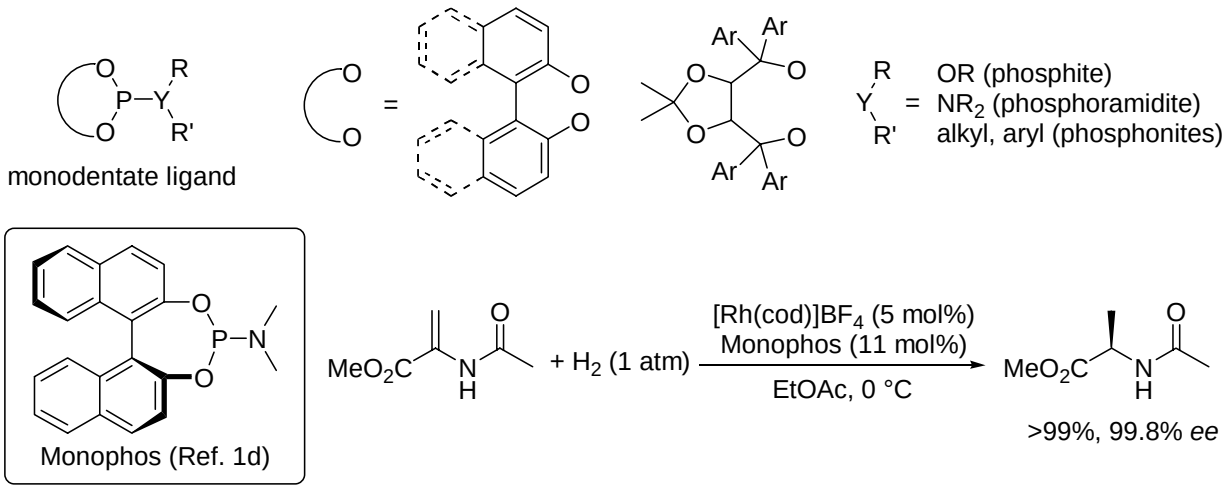

Scheme 3-2.

Similar to the benzophenone-derived diphenylphosphine ligand, it was considered that the chirality control of benzophenone-like monodentate ligands proceeded so fast to fit well with the substrate change (Scheme 3-3). Therefore, the chirality controls of monodentate ligands and asymmetric reactions with chirally controlled monodentate ligands were examined.

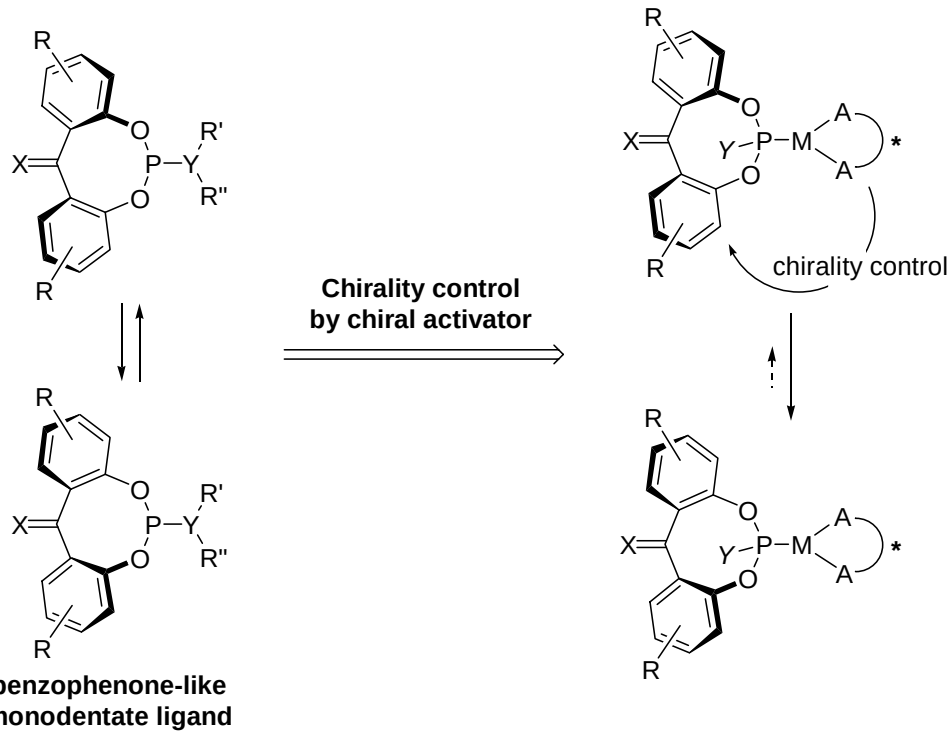

Scheme 3-3.

The synthesis of the metal complexes with a single phosphoramidite and diene has been reported.[2] In the metal complex with phosphoramidite and diene, chirality control of phosphoramidite can be attained by a chiral diene (Schema 3-4). The complexes with phosphoramidites and dienes could be used as asymmetric catalysts. The asymmetric catalyst could be used particularly in the asymmetric Michael additions.[3] The reaction proceeded at a low temperature by the synergistic effect of both phosphoramidite and diene. Therefore, the asymmetric Michael additions were examined with several benzophenone-like phosphoramidites and dienes.

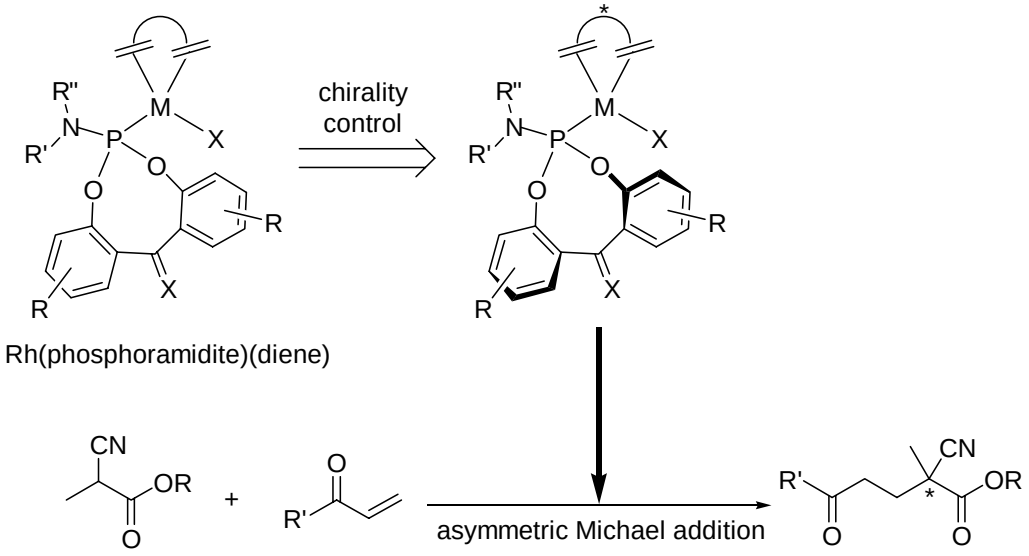

Scheme 3-4.

Previously, Aikawa and co-workers in Mikami's group have reported that Rh-duphos complex with chiral diene **A** attains quite higher enantioselectivity than with achiral 1,5-cyclooctadiene (cod) (Scheme 3-5).[4] This is a typical example of asymmetric synergy between diphosphines and chiral dienes. The complex of phosphoramidite bearing chiral amine part and chiral diene could also show asymmetric synergy effect. Asymmetric reactions with benzophenone-like phosphoramidites and chiral dienes were thus examined.

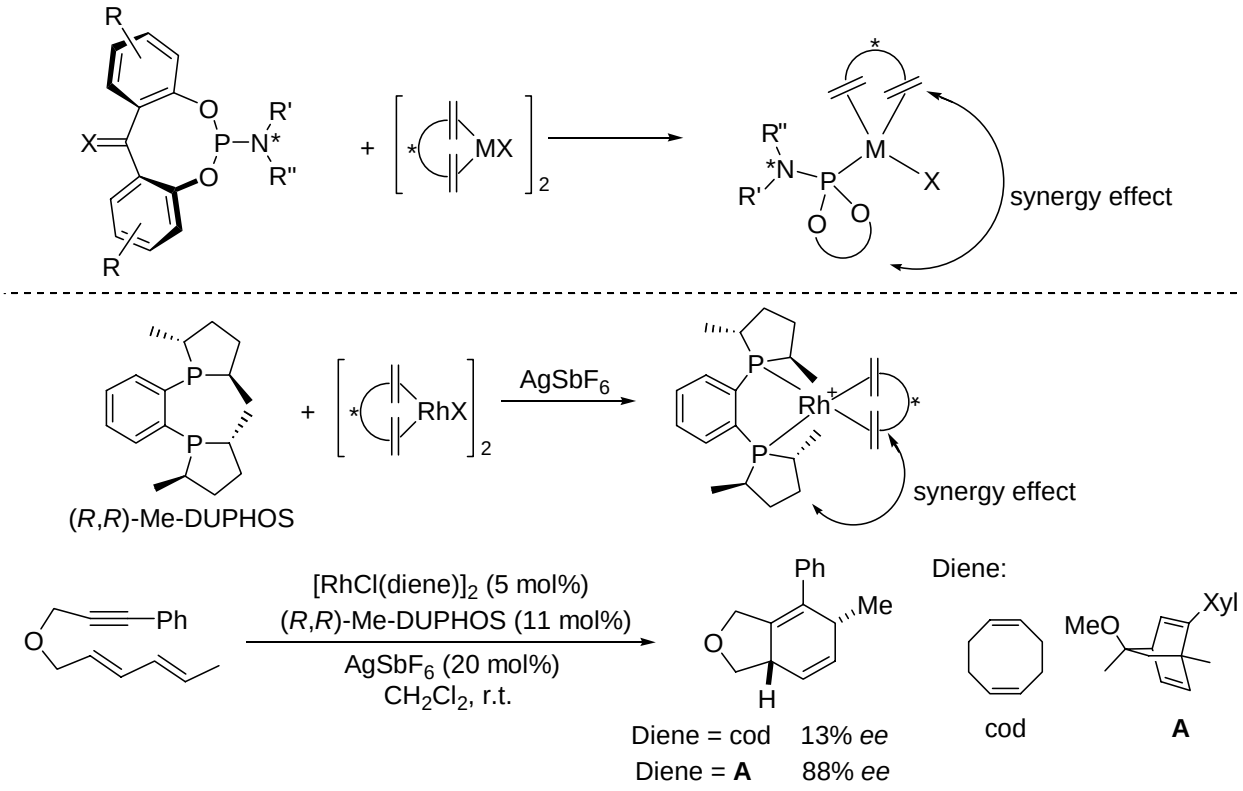

Scheme 3-5.

In Chapter 3, the author reports benzophenone-like phosphoramidite ligands in which the chirality can be controlled instantaneously by a chiral diene. The phosphoramidites chirally controlled attain high catalytic activity and enantioselectivity in the asymmetric Michael addition.

3-2. Synthesis of benzophenone-like phosphoramidite

First, benzophenone-like phosphoramidites **3a** were synthesized (Scheme 3-6). As prepared previously,[5] phosphoramidites **3a** could be synthesized. Unfortunately, benzophenone-derived phosphoramidite (X = CO) could not be synthesized, because carbonyl group reacted with phosphorus reagents ($P(NMe_2)_3$ or PCl_3).

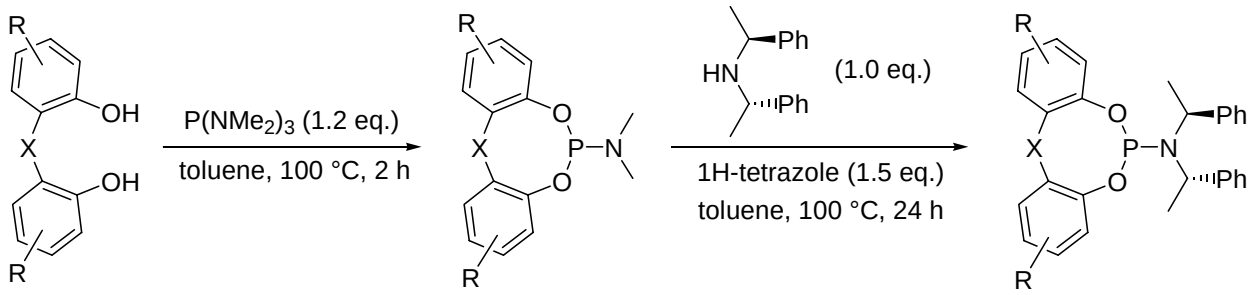

Scheme 3-6.

$Rh(nbd)(phosphoramidite)_2$ complexes have been reported as asymmetric catalysts with high catalytic activity and enantioselectivity.[1] However, $Rh(nbd)(\mathbf{3a})_2$ complexes could not be synthesized, even though excess **3a** was added (an excess amount of **3a** was remained). Only RhCl(nbd) complexes with single phosphoramidite **3a** were synthesized (Scheme 3-7).

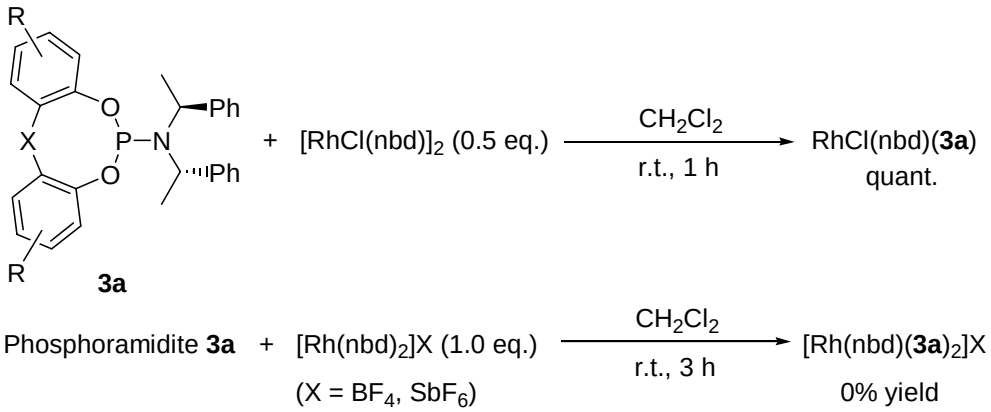

Scheme 3-7.

Figure 3-1 shows the ^{1}H and ^{31}P NMR spectra of RhCl(nbd)(**3a^{1}**) complex. One doublet peak of ^{31}P NMR spectrum showed that RhCl(nbd)(**3a^{1}**) possessed a single conformation. In addition, ^{1}H NMR spectrum of 4-methylphenyl group in phosphoramidite exhibited two singlets of methyl group and six peaks of phenyl groups.

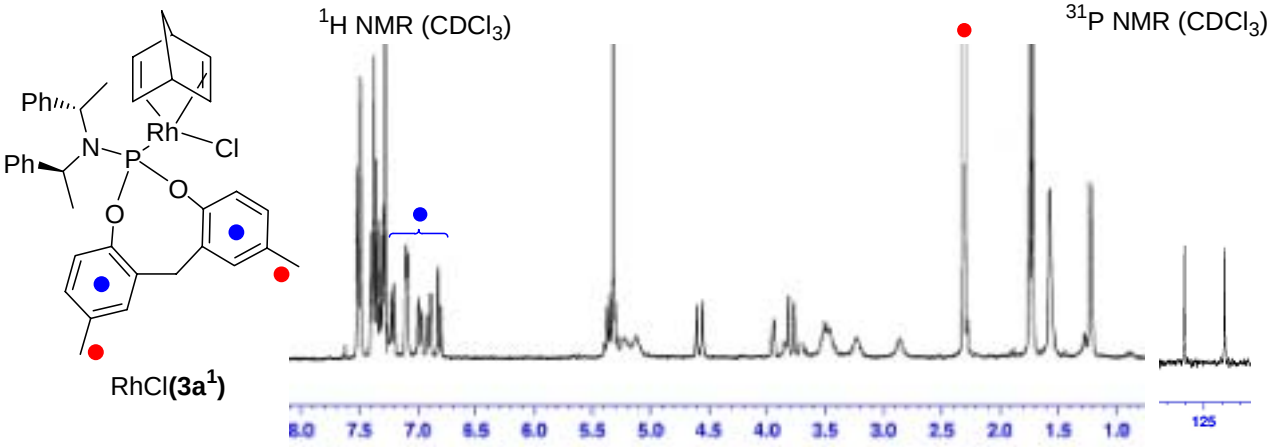

Figure 3-1. ^{1}H and ^{31}P NMR spectra of RhCl(nbd) complex with phosphoramidite **3a^{1}**

Recently, de Vries and co-workers have reported that iridium complex with single phosphoramidite **3b** attains high catalytic activity and enantioselectivity in asymmetric hydrogenations (Scheme 3-8).[6] Catalytic activity and enantioselectivity of the asymmetric hydrogenation were increased by a bulky phosphoramidite ligand. The bulky phosphoramidite is necessary to stabilize the complex with single phosphoramidite and to prevent dimerization, which causes deactivation of iridium hydrogenation catalysts.[7]

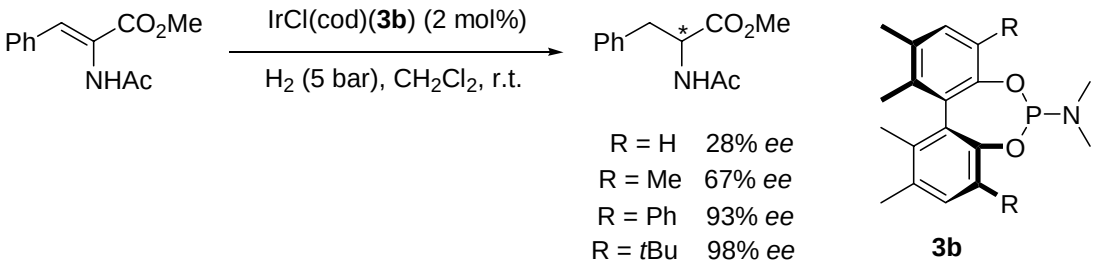

Scheme 3-8.

In case of the asymmetric hydrogenation with **3a**[1], both Ir and Rh complexes gave the product with low enantiomeric excess (Table 3-1). However, it was found that the RhCl(diene) complex with single benzophenone-like phosphoramidite attained high catalytic activity and enantioselectivity in asymmetric Michael additions.

Table 3-1. Asymmetric hydrogenation with RhCl- and IrCl-**3a**[1] complexes

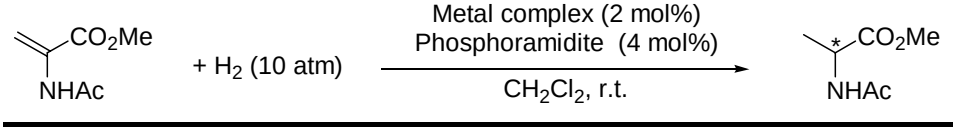

Entry	Metal	Phosphoramidite	Time (h)	Yield (%)	*Ee* (%)
1	$[IrCl(cod)]_2$	3a[1]	3	86	11
2	$[RhCl(nbd)]_2$	3a[1]	12	6	5
3[a]	$[RhCl(nbd)]_2$	3a[1]	12	75	3
4[b]	$[IrCl(cod)]_2$	3b (R = *t*Bu)	< 1	>99	50

a. with $AgSbF_6$ (5 mol%)
b. Ref. 6

Phosphoramidite:

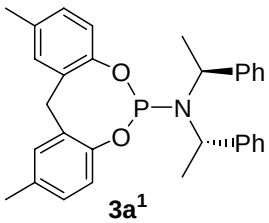

3a[1]

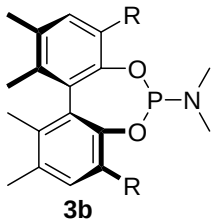

3b

3-3. Rh-Catalyzed asymmetric Michael addition

RhCl(nbd) complex with **3a**[1] showed high catalytic activity in asymmetric Michael addition of α-cyano carboxylate (Table 3-2). RhCl(nbd)(**3a**[1]) reacted even at -78 °C and gave the product in 96% yield with 48% *ee* (entry 1). This reaction did not proceed without a catalytic amount of iPr_2NEt (entry 2). Entries 1 and 3 show that 4-methyl group of **3a**[1] does not affect catalytic activity and enantioselectivity. On the other hand, diphenylether-derived phosphoramidite **3a**[3] decreased the catalytic activity and enantioselectivity (entries 1 *vs.* 4). Not only phosphoramidite but also achiral diene influenced enantioselectivity. Table 3-2 shows that 1,5-cycloocatadiene and 1,5-dimethyl-cycloocatadiene (cod and DM-cod) decreased enantioselectivity (entries 6 and 7) and that 1,2-dibromonorbiornadiene (Br-nbd), in contrast, increased enantioselectivity (entry 5).

Table 3-2. Asymmetric Michael addition of α-cyano carboxylate

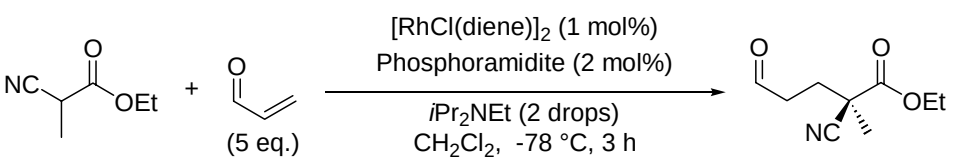

Diene:

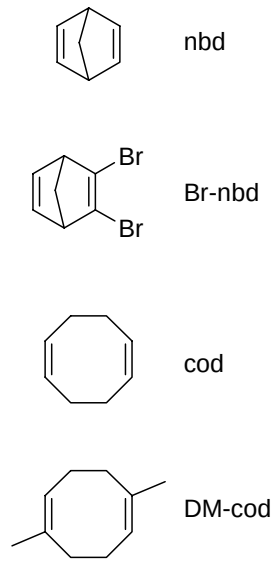

Entry	Phosphoramidite	Diene	Yield (%)	*Ee* (%)
1	3a[1]	nbd	96	48
2[a]	3a[1]	nbd	n.r.	-
3	3a[2]	nbd	95	49
4	3a[3]	nbd	94	22
5	3a[1]	Br-nbd	95	56
6	3a[1]	cod	96	39
7	3a[1]	DM-cod	95	2

a. without iPr$_2$NEt

The asymmetric Michael addition with RhCl(nbd)(**3a**[1]) complex was also examined with other electrophiles (Table 3-3). Compared to acrolein, other electrophiles, such as formaldehyde and methyl vinyl ketone, decreased catalytic activity and enantioselectivity.

Table 3-3. Asymmetric Michael addition with several electrophiles

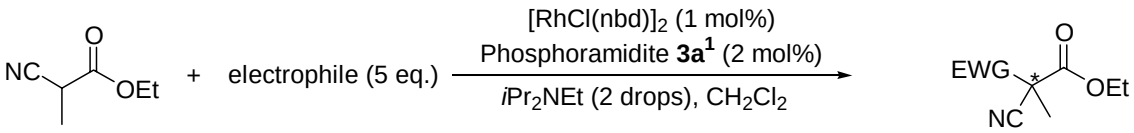

Entry	Electrophile	Temp. (°C)	Time (h)	EWG	Yield (%)	*Ee* (%)
1		-78	3	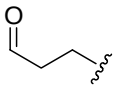	96	48 (*R*)
2		-78	12	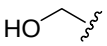	45	1
3	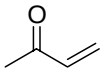	r.t.	12	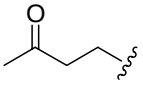	n.r.	-
4	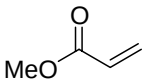	r.t.	12	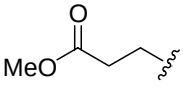	n.r.	-
5	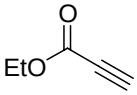	r.t.	12	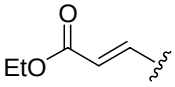	30 (only (*E*))	0

In the Michael addition with the RhCl(diene)(phosphoramidite) complex, even the achiral diene group in the Rh complex influenced enantioselectivity. For chirality control of achiral phosphoramidites, achiral dienes in Rh complexes were replaced with chiral dienes. Chiral dienes were synthesized to use in asymmetric catalyses, such as asymmetric 1,4-addition of boronic reagents and kinetic resolution of allylic carbonates (Scheme 3-9).[8] Table 3-2 shows that dienes in six-membered rings attained higher enantioselectivity than dienes in eight-membered rings. Therefore, the Rh complexes with chiral six-membered diene **A** was mainly used as asymmetric catalysts.

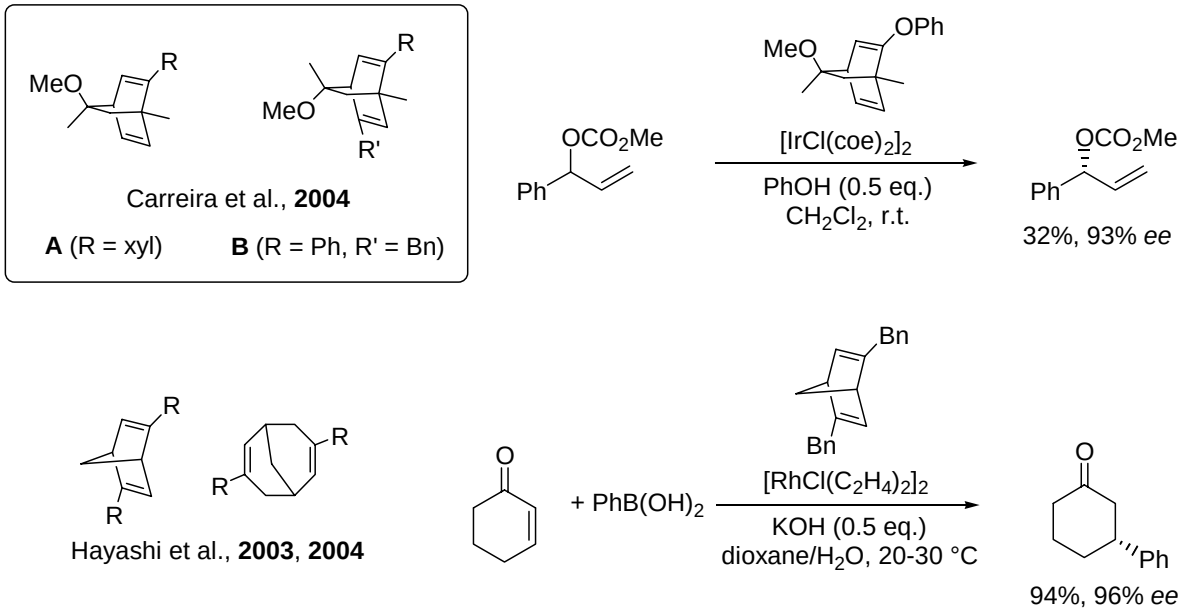

Scheme 3-9.

Similar to the chirality control by chiral diamines (see Chapter 2), chiral dienes controlled the conformation of achiral phosphoramidite to attain high enantioselectivity in the asymmetric Michael addition (Table 3-4). Low enantiomeric excesses of reactions obtained with [RhCl(chiral diene)]$_2$ complexes (entries 1 and 2) shows that both phosphoramidite and chiral diene synergistically worked in the asymmetric Michael addition. Rh-chiral diene **A** complexes with achiral phosphoramidites **3c** and **3e**[1] attained higher enantioselectivity than Rh-chiral diene **B** complexes did. In addition, the sence of enantioselectivities of products was reversed even by the type of chiral dienes. Phosphoramidite **3e**[3] bearing chiral amine was too bulky to decrease the catalytic activity and enantioselectivity. However, asymmetric Michel addition of 2-cyanopropionic acid *tert*-butyl ester with RhCl(diene **A**)(**3e**[1]) gave

the product in 95% yield with 86% *ee* (entry 8).

Table 3-4. Asymmetric Michael addition with RhCl(chiral dienes)(achiral phosphoramidites)

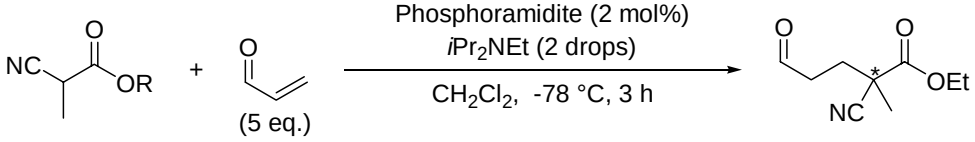

Entry	OR	Phosphoramidite	Diene	Yield (%)	*Ee* (%)
1	OEt	-	A	92	15 (*S*)
2	OEt	-	B	90	32 (*S*)
3	OEt	3c	A	95	54 (*S*)
4	OEt	3c	B	92	43 (*R*)
5	OEt	3d	A	94	38 (*S*)
6	OEt	3e[1]	A	95	63 (*S*)
7	OEt	3e[1]	B	94	41 (*R*)
8	**O*t*Bu**	**3e[1]**	**A**	**95**	**86 (*S*)**
9	O*t*Bu	3e[2]	A	81	78 (*S*)
10	O*t*Bu	(*R*)-3e[3]	A	85	56 (*S*)

Phosphoramidite:

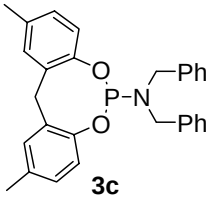

3c

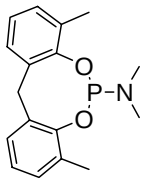

3d

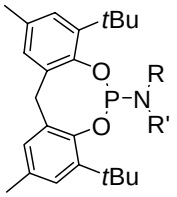

3e[1] (R = R' = Me)
3e[2] (R = R' = Bn)
3e[3] (R = H, R' = α-methylbenzyl)

Table 3-5 shows that the absolute configuration of products was determined not by the absolute configuration of phosphoramidites but by that of chiral dienes. Chiral diene **A** with (*R*,*R*)-**3a[1]** gave (*S*)-enriched product with 39% *ee* and with (*S*,*S*)-**3a[1]** also gave the (*S*)-enriched product with 32% *ee*. On the other hand, the chiral diene **B** with (*S*,*S*)-**3a[1]** gave the (*R*)-enriched product with 50% *ee* and with (*R*,*R*)-**3a[1]** also gave the (*R*)-enriched product with 16% *ee*.

Table 3-5. Asymmetric Michael addition with Rh-chiral diene complexes

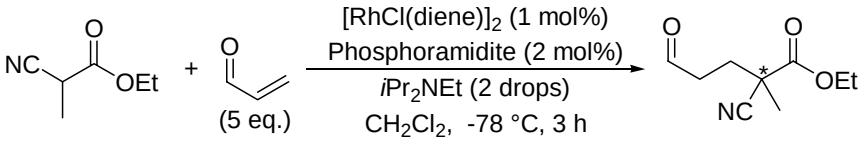

Entry	Phosphoramidite	Diene	Yield (%)	*Ee* (%)
1	(*S*,*S*)-3a[1]	nbd	96	48 (*R*)
2	(*S*,*S*)-3a[1]	A	92	32 (*S*)
3	(*R*,*R*)-3a[1]	A	93	39 (*S*)
4	(*S*,*S*)-3a[1]	B	96	50 (*R*)
5	(*R*,*R*)-3a[1]	B	66	16 (*R*)

In case of asymmetric [4+2] cycloaddition, the RhCl(diene **A**)(**3a**[1]) complex gave the product with 26% *ee*. The enantiomeric excess was equal to that in the reaction with [RhCl(diene **A**)]$_2$ complex (Scheme 3-10). In sharp contrast to the asymmetric Michael addition of α-cyano carboxylates, enyne substrates dissociated **3a**[1] from the Rh complex.

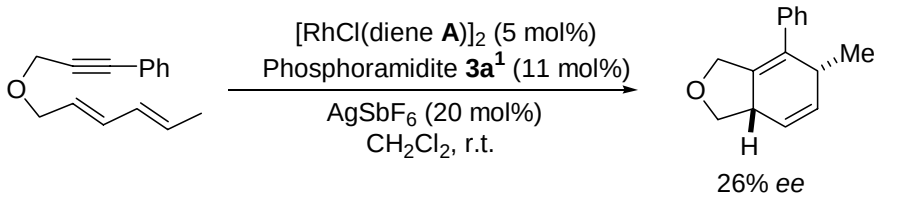

26% *ee*

Without phosphoramidite **3a**[1]: 26% *ee* (Ref. 4)

Scheme 3-10.

3-4. Reaction mechanism

RhCl(diene **A**)(**3e**[1]) attained high catalytic activity and enantioselectivity in the asymmetric Michael addition. ^{31}P NMR spectrum of RhCl(diene **A**)(**3e**[1]) showed a doublet peak and the ^{1}H NMR spectrum of 4-methyl-6-*tert*-butylphenyl groups in phosphoramidite **3e**[1] showed four singlet peaks of methyl and *tert*-butyl groups (Figure 3-2). Similar to RhCl(nbd)(**3a**[1]), these peaks show that the phosphoramidite in RhCl(diene **A**)(**3e**[1]) adopts a single chiral conformation by the chiral diene **3e**[1].

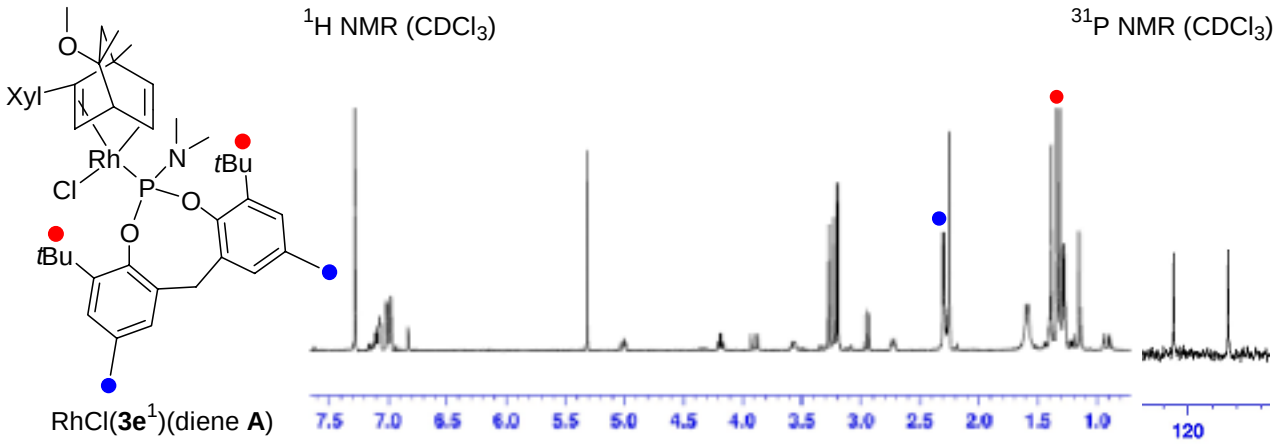

Figure 3-2. ^{1}H and ^{31}P NMR spectra of RhCl(diene **A**)(**3e^{1}**) complex

The most stable conformation of RhCl(diene **A'**)(**3e'**) as the model of RhCl(diene **A**)(**3e^{1}**) was deduced by DFT calculation (B3LYP/631SDD level: SDD for Rh, 6-31G for others) (Figure 3-3). The side view of Figure 3-3 shows that the achiral benzopheonone-like phosphoramidite **3e'** adopts a chiral conformation. The front view shows that dimethylamine group of **3e'** stays away from xylyl group of the chiral diene **A'**. The conformation of phosphoramidite **3e'** can be controlled by the chiral diene **A'** to give the high enantioselectivity in the asymmetric Michael addition.

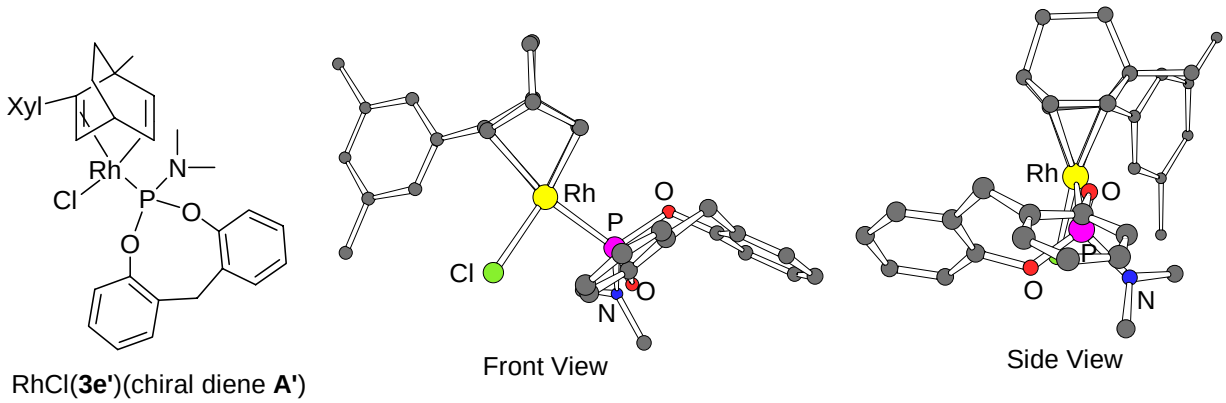

Figure 3-3. DFT calculation of simplified RhCl(diene **A'**)(**3e'**) complex

In case of the Rh-catalyzed Michael addition of α-cyano carboxylate, the active intermediate has been reported *N*-bonded enolate complex that is formed by coordination of α-cyanoester to rhodium (Scheme 3-11).[3c,9] Figure 3-4 (a) shows two types of coordination of α-cyanoester from the left side or right side. In the right of the Rh complex, there exist the xylyl group of diene **A'** and dimethylamine group of phosphoramidite **3e'** and hence the bulky groups prevent the approach of the α-cyano carboxylate.

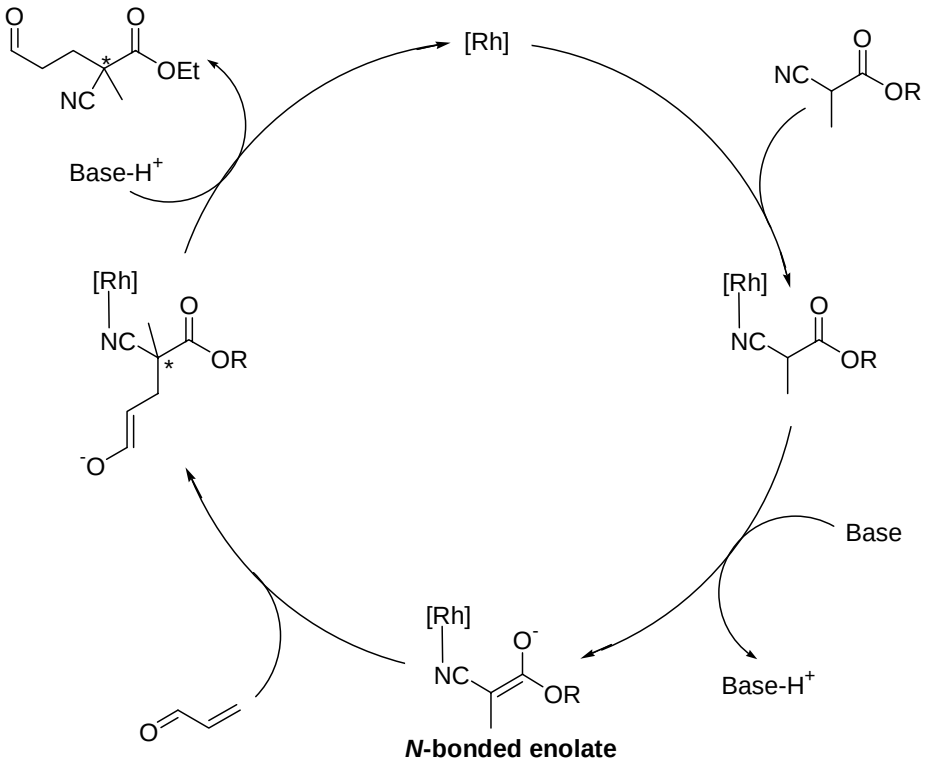

Scheme 3-11.

After the coordination of α-cyanoester, the *N*-bonded enolate complex is generated by deprotonation of α-cyanoester. The conformation of the *N*-bonded enolate complex can be estimated to be stabilized by hydrogen bonding between enolate and hydrogen of phosphoramidite (Figure 3-4(b)).[10] The *N*-bonded enolate complex is attacked by an electrophile. Figure 3-4(b) shows that the phosphoramidite of the *N*-bonded enolate complex prevents the approach of electrophile from the bottom side. Therefore, the attack of an electrophile is suitable from the less hindered upper side of the *N*-bonded enolate complex to give (*S*)-enriched products, which is consistent with the outcome actually observed (see Table 3-5, entry 6).

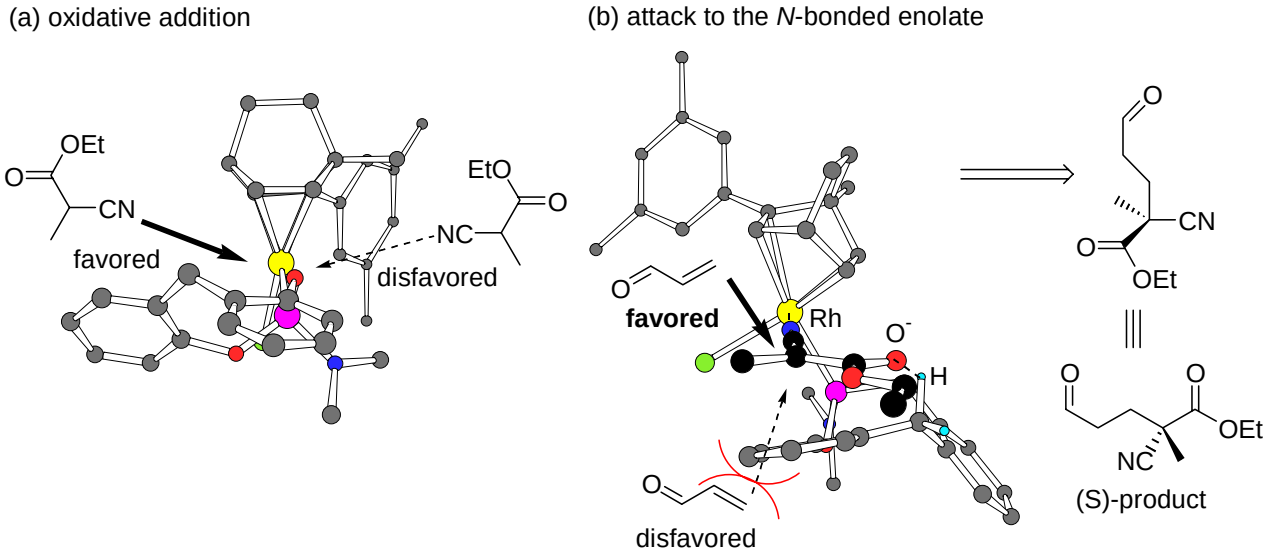

Figure 3-4. The reaction mechanism of Michael addition with Rh-phosphoramidite complex

Following the reaction mechanism involving the *N*-bonded enolate complex, the reversal of absolute configuration of the products by changing the catalyst from RhCl(**3e**[1])(chiral diene **A**) to RhCl(**3e**[1])(chiral diene **B**) (see Table 3-5, entries 6 *vs.* 7) can be illustrated. The conformation of phosphoramidite in RhCl(**3e'**)(chiral diene **A'**) is determined by the steric repulsion between dimethylamine group of **3e'** and xylyl group of **A'**. Different from RhCl(**3e'**)(chiral diene **A'**), the conformation of phosphoramidite in RhCl(**3e'**)(chiral diene **B'**) as the model of RhCl(**3e**[1])(chiral diene **B**) complex is determined by the steric repulsion between diphenylmethane group of **3e'** and benzyl group of **B'**. Figure 3-5 shows the different conformation of phosphoramidite between two Rh complexes RhCl(**3e**[']) (chiral diene **A'**) (right side) and RhCl(**3e**[']) (chiral diene **B'**) (left side).

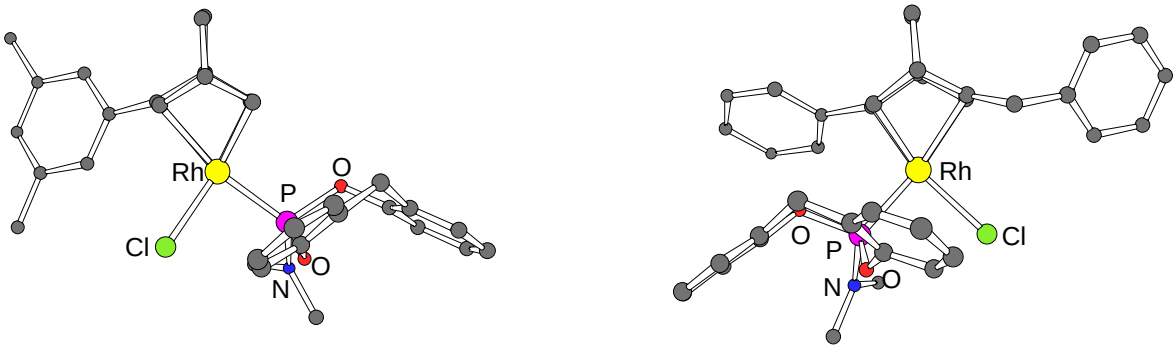

RhCl(**3e'**)(chiral diene **A'**)
Phosphoramidite: right side

RhCl(**3e'**)(chiral diene **B'**)
Phosphoramidite: left side

Figure 3-5. The conformation of phosphoramidite in two Rh complexes

The conformation of α-cyanoester in *N*-bonded enolate complexes is determined by the conformation of phosphoramidite because of steric repulsion between methyl group of the α-cyanoester and phosphoramidite and stabilization by hydrogen bonding between the enolate and phosphoramidite. Figure 3-6 shows that the enantioface of cyanoester is reversed by changing from RhCl(**3e'**)(chiral diene **A'**) to RhCl(**3e'**)(chiral diene **B'**). Both the *N*-bonded enolate complexes are attacked by electrophile from the opposite side of phosphoramidite. Therefore, RhCl(**3e'**)(chiral diene **A'**) gives (*S*)-enriched products and RhCl(**3e'**)(chiral diene **B'**) does (*R*)-enriched products.

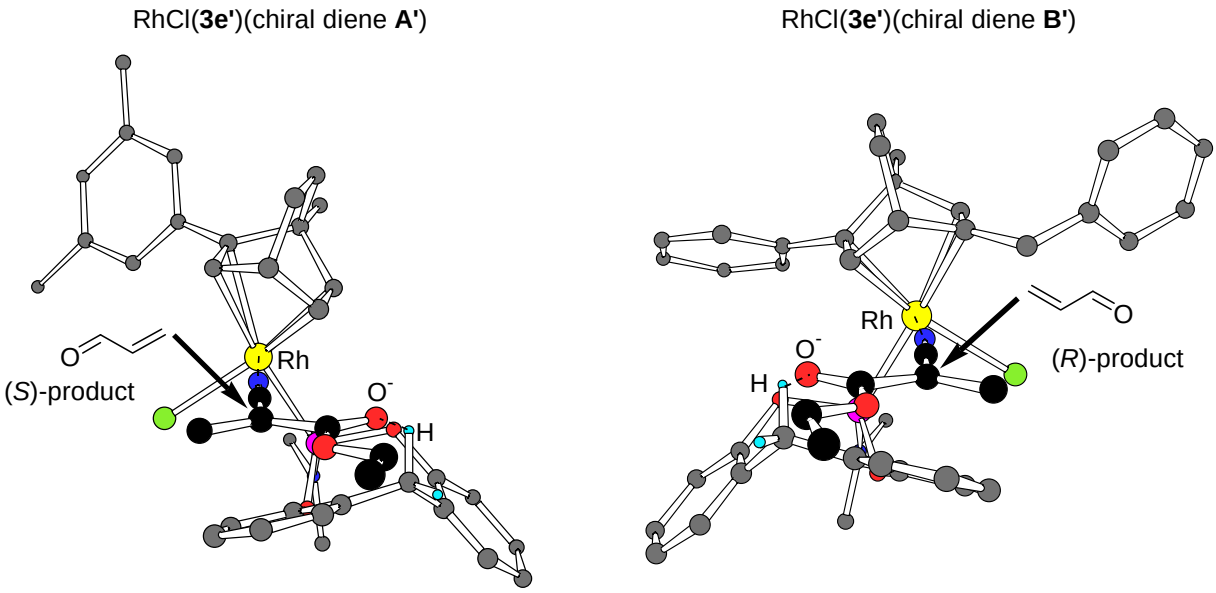

Figure 3-6. The conformation of cyanoester in two *N*-bonded enolate complexes

3-5. Conclusion

In summary, the monodentate benzophenone-like phosphoramidite can be controlled by an external chiral dienes to possess a single chiral conformation, just like a chirality control of benzophenone-derived diphenylphosphine ligand by external chiral diamines. In Rh complexes with phosphoramidite and diene, the chiral diene could control the conformation of phosphoramidite so fast at room temperature (Scheme 3-12).

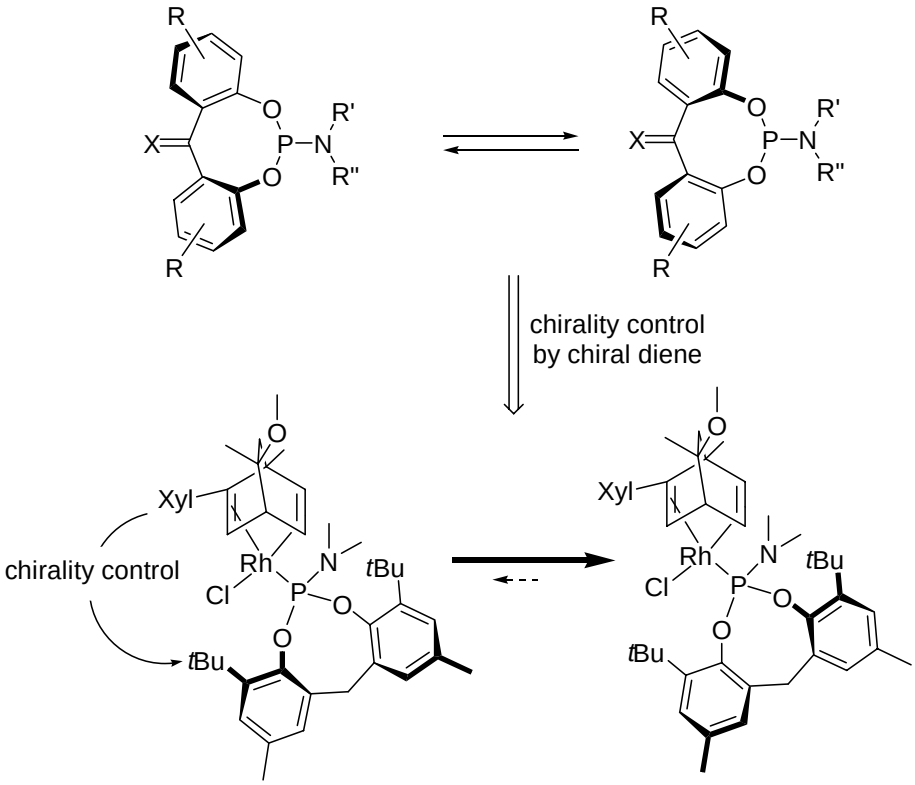

Scheme 3-12.

The complex with chirally controlled phosphoramidite could be used in the asymmetric Michael additions of α-cyano carboxylates. Particularly, the Rh complex with chiral diene **A** and achiral benzophenone-like phosphoramidite **3e**[1] gave the product in high yield and enantiomeric excess (Scheme 3-13). In the Rh complex, chiral diene **A** controlled the conformation of the achiral benzophenone-like phosphoramidite **3e**[1] to attain high catalytic activity and enantioselectivity.

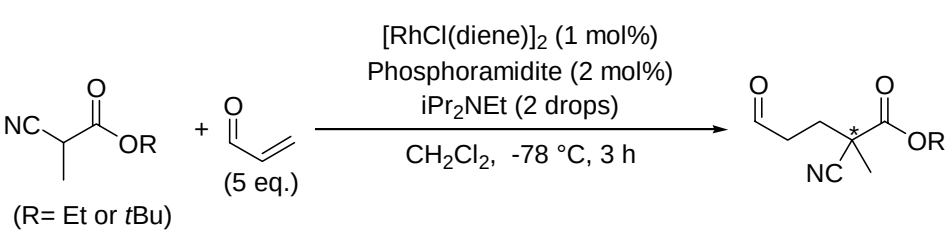

Phosphoramidite:

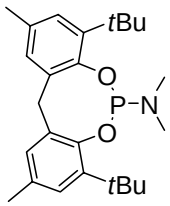

3e[1]

Phosphoramidite **(*S*,*S*)-3a**[1] & nbd: 96%, 48% *ee* (*R*) (R = Et)

Phosphoramidite **(*S*,*S*)-3a**[1] & Diene **A**: 93%, 39% *ee* (*S*) (R = Et)

Phosphoramidite 3e[1] **& Diene A**: 95%, 63% *ee* (*S*) (R = Et)

95%, 86% *ee* (*S*) (R = *t*Bu)

Diene:

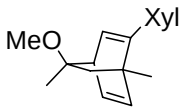

A

Scheme 3-13.

Experimental section for Chapter 3

1,5-dibromo-cycloocta-1,5-diene was prepared by previously reported method.[11] Diene ligands (2,3-Dibromo-bicyclo[2.2.1]hepta-2,5-diene (Br-nbd),[12] (2*S*,8*R*)-2-(3,5-dimethylphenyl)-8-methoxy-1,8-dimethyl-bicyclo[2.2.2]octa-2,5-diene (chiral diene **A**)[8b] and (1*S*,4*S*,8*S*)-5-Benzyl-2-phenyl-8-methoxy-1,8-dimethyl-bicyclo[2.2.2]octa-2,5-diene (chiral diene **B**)[8c]) were prepared by previously reported method. [RhCl(chiral diene **A**)]$_2$ was prepared by previously reported method.[4] 2-Cyanopropionic acid *tert*-butyl ester was prepared by previously reported method.[13]

(*S*,*S*)-*N*-(2,10-Dimethyl-12*H*-5,7-dioxa-6-phosphadibenzo[*a*,*d*]cycloocten-6-yl)-bis(1-phenylethyl) amine: Phosphoramidite 3a[1] (X = CH_2, R = 4-Me)

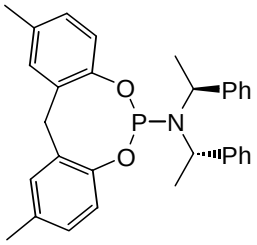

To a solution of 2,2'-methylenebis(4-methylphenol) (45.7 mg, 0.2 mmol) in toluene (2 mL) was added HMPT (hexamethylphosphorous triamide) (45 μL, 0.24 mmol) at room temperature under an argon atmosphere. After stirred for 2 h at 100 °C, toluene and excess HMPT were evaporated under reduced pressure. The residue and 1H-tetrazole (21.1 mg, 0.3 mmol) were dissolved in toluene. To the mixture was added bis[(*S*)-1-phenylethyl]amine (45 μL, 0.2 mmol) at room temperature. After stirred for 24 h at 100 °C, the reaction mixture was quenched with H_2O three times. The organic layer was dried over K_2CO_3. After concentration under reduced pressure, the residue was purified by alumina chromatography (hexane/CH_2Cl_2 = 10/1) to give phosphoramidite **3a[1]** (38.4 mg, 40% yield).

^{1}H NMR ($CDCl_3$, 300 MHz) δ 1.87 (d, 6H, *J* = 7.2 Hz), 2.32 (s, 3H), 2.33 (s, 3H), 3.48 (d, 1H, *J* = 12.9 Hz), 4.42 (dd, 1H, *J* = 12.9, 3.0 Hz), 4.94 (dq, 2H, *J* = 11.7, 7.2 Hz), 6.64 (d, 1H, *J* = 8.1 Hz), 6.93 (d, 1H, *J* = 8.1 Hz), 6.99 (s, 2H), 7.16-7.30 (m, 12H).
^{13}C NMR ($CDCl_3$, 75 MHz) δ 20.80, 22.08, 22.21, 34.08, 53.00, 53.16, 122.57, 122.61, 122.73, 122.78, 126.58, 127.80, 128.03, 128.07, 128.49, 130.22, 130.38, 133.75, 135.13, 143.55, 143.57, 149.45, 149.54, 149.71, 149.80.
^{31}P NMR ($CDCl_3$, 121 MHz) δ 142.20.
TOF-HRMS (ESI), Calcd for $C_{31}H_{32}NO_2PNa$ $[M+Na]^+$: 504.2068, Found: 504.2060.
$[\alpha]_D^{27}$ = -66 (c = 0.50 in $CHCl_3$).

(*S*,*S*)-*N*-(12*H*-5,7-dioxa-6-phosphadibenzo[*a*,*d*]cycloocten-6-yl)-bis(1-phenylethyl)amine: Phosphoramidite 3a^2 (X = CH_2, R = H)

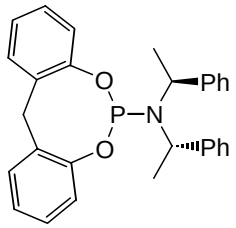

Phosphoramidite **3a^2** was prepared from bis(2-hydroxyphenyl)methane in a similar to manner as phosphoramidite **3a^1** (45% yield).

^{1}H NMR ($CDCl_3$, 300 MHz) δ 1.88 (d, 6H, *J* = 7.2 Hz), 3.58 (d, 1H, *J* = 12.9 Hz), 4.49 (dd, 1H, *J* = 12.9, 3.0 Hz), 4.95 (dq, 2H, *J* = 14.1, 7.2 Hz), 6.73 (d, 1H, *J* = 7.8 Hz), 7.00-7.30 (m, 17H).
^{13}C NMR ($CDCl_3$, 75 MHz) δ 22.00, 22.13, 34.06, 52.88, 53.04, 122.84, 122.88, 123.02, 123.06, 124.39, 126.61, 127.79, 127.96, 128.01, 128.04, 129.67, 129.83, 135.43, 143.34, 143.37, 151.65, 151.74, 151.93, 152.02.
^{31}P NMR ($CDCl_3$, 121 MHz) δ 141.80.
TOF-HRMS (ESI), Calcd for $C_{29}H_{28}NO_2PNa$ $[M+Na]^+$: 476.1755, Found: 476.1766.
$[\alpha]_D^{27}$ = -84 (c = 0.50 in $CHCl_3$).

(*S*,*S*)-*N*-(5,7,12-trioxa-6-phospha-dibenzo[*a*,*d*]cycloocten-6-yl)-bis(1-phenylethyl)amine: Phosphoramidite 3a^3 (X = O, R = H)

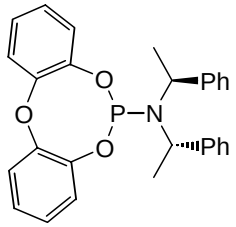

Phosphoramidite **3a^3** was prepared from 2,2'-dihydroxydiphenylether in a similar to manner as phosphoramidite **3a^1** (25% yield).

^{1}H NMR ($CDCl_3$, 300 MHz) δ 1.82 (d, 6H, *J* = 7.2 Hz), 4.79 (dq, 2H, *J* = 11.1, 7.2 Hz), 6.98-7.28 (m, 14H), 7.32-7.38 (m, 2H).
^{13}C NMR ($CDCl_3$, 75 MHz) δ 22.22, 22.41, 52.80, 52.97, 116.48, 118.18, 120.95, 121.04, 122.77, 123.09, 125.11, 126.16, 126.55, 127.80, 143.30, 147.57.
^{31}P NMR ($CDCl_3$, 121 MHz) δ 145.37.
TOF-HRMS (ESI), Calcd for $C_{28}H_{27}NO_2P$ $[M+H]^+$: 456.1728, Found: 456.1745.
$[\alpha]_D^{27}$ = -1.27 x10^2 (c = 0.60 in $CHCl_3$).

(2,10-Dimethyl-12*H*-5,7-dioxa-6-phospha-dibenzo[*a*,*d*]cycloocten-6-yl)dibenzylamine: Phosphoramidite 3c

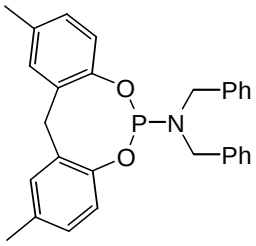

Phosphoramidite **3c** was prepared from 2,2'-methylenebis(4-methylphenol) and dibenzylamine in a similar to manner as **3a**[1] (76% yield).

^{1}H NMR ($CDCl_3$, 300 MHz) δ 2.32 (s, 6H), 3.54 (d, 1H, *J* = 12.9 Hz), 4.33 (d, 4H, *J* = 10.2 Hz), 4.35 (dd, 1H, *J* = 12.6, 3.0 Hz), 6.99 (br, 4H), 7.16 (s, 2H), 7.29-7.46 (m, 10H).

^{13}C NMR ($CDCl_3$, 75 MHz) δ 22.78, 34.13, 47.86, 48.14, 122.51, 127.11, 128.40, 128.56, 128.63, 130.40, 133.93, 134.71, 134.74, 138.38, 148.82, 148.88.

^{31}P NMR ($CDCl_3$, 121 MHz) δ 138.18.

TOF-HRMS (ESI), Calcd for $C_{29}H_{29}NO_2P$ $[M+H]^+$: 454.1936, Found: 454.1946.

(4,8-Dimethyl-12*H*-5,7-dioxa-6-phospha-dibenzo[*a*,*d*]cycloocten-6-yl)dimethylamine: Phosphoramidite 3d

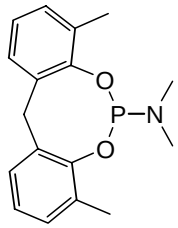

To a solution of 2,2'-methylenebis(6-methylphenol) (45.7 mg, 0.2 mmol) in toluene (2 mL) was added HMPT (45 μL, 0.24 mmol) at room temperature under an argon atmosphere. After stirred for 2 h at 100 °C, toluene and excess HMPT were evaporated under reduced pressure. The residue was purified by alumina chromatography (hexane/CH_2Cl_2 = 10/1) to give phosphoramidite **3d** (36.8 mg, 61% yield).

^{1}H NMR ($CDCl_3$, 300 MHz) δ 2.27 (s, 6H), 2.97 (d, 6H, *J* = 10.8 Hz), 3.48 (d, 1H, *J* = 12.3 Hz), 4.46 (dd, 1H, *J* = 12.3, 3.0 Hz), 6.93 (t, 2H, *J* = 7.5 Hz), 7.04 (d, 2H, *J* = 7.5 Hz), 7.19 (d, 2H, *J* = 7.5 Hz).

^{13}C NMR ($CDCl_3$, 75 MHz) δ 16.95, 16.99, 33.99, 34.53, 35.16, 35.40, 124.10, 124.12, 127.42, 127.44, 129.01, 131.10, 131.14, 135.71, 135.75, 149.34, 149.40.

^{31}P NMR ($CDCl_3$, 121 MHz) δ 138.72.

TOF-HRMS (ESI), Calcd for $C_{17}H_{21}NO_2P$ $[M+H]^+$: 302.1310, Found: 302.1298.

(4,8-Di-*tert*-butyl-2,10-dimethyl-12*H*-5,7-dioxa-6-phospha-dibenzo[*a*,*d*]cycloocten-6-yl)-dimethylamine: Phosphoramidite 3e[1] (R = R' = Me)

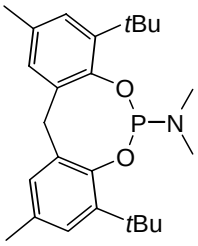

Phosphoramidite **3e[1]** was prepared from 2,2'-methylenebis(6-*tert*-butyl-4-methylphenol) in a similar to manner as phosphoramidite **3d** (90% yield).

^{1}H NMR ($CDCl_3$, 300 MHz) δ 1.40 (s, 18H), 2.30 (s, 6H), 2.96 (d, 6H, *J* = 9.3 Hz), 3.33 (d, 1H, *J* = 12.3 Hz), 4.35 (dd, 1H, *J* = 12.3, 3.0Hz), 7.02 (d, 2H, *J* = 2.1 Hz), 7.11 (d, 2H, *J* = 2.1 Hz).
^{13}C NMR ($CDCl_3$, 75 MHz) δ 21.05, 30.75, 30.81, 34.73, 35.60, 35.86, 126.39, 128.56, 132.73, 136.16, 136.20, 141.61, 141.66, 148.30, 148.40.
^{31}P NMR ($CDCl_3$, 121 MHz) δ 144.28.
TOF-HRMS (ESI), Calcd for $C_{25}H_{37}NO_2P$ $[M+H]^+$: 414.2562, Found: 414.2561.

(4,8-Di-tert-butyl-2,10-dimethyl-12*H*-5,7-dioxa-6-phospha-dibenzo[a,d]cycloocten-6-yl)dibenzyl-amine: Phosphoramidite 3e[2] (R = R' = Bn)

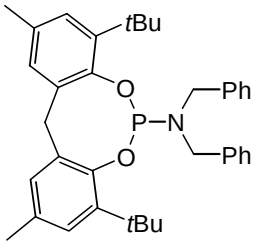

Phosphoramidite **3e[2]** was prepared from 2,2'-methylenebis(6-*tert*-butyl-4-methylphenol) and dibenzylamine in a similar to manner as phosphoramidite **3a[1]** (88% yield).

^{1}H NMR ($CDCl_3$, 300 MHz) δ 1.58 (s, 18H), 2.44 (s, 6H), 3.52 (d, 1H, *J* = 12.6 Hz), 4.53 (d, 4H, *J* = 7.2 Hz), 4.64 (dd, 1H, *J* = 12.6, 2.7 Hz), 7.19 (d, 2H, *J* = 2.1 Hz), 7.28 (d, 2H, *J* = 2.1 Hz), 7.38-7.56 (m, 10H).
^{13}C NMR ($CDCl_3$, 75 MHz) δ 21.18, 31.40, 31.47, 34.90, 35.11, 48.53, 48.79, 126.72, 127.19, 128.23, 128.59, 129.79, 133.18, 136.75, 136.78, 137.75, 137.82, 141.72, 141.77, 147.56, 147.64.
^{31}P NMR ($CDCl_3$, 121 MHz) δ 137.53.
TOF-HRMS (ESI), Calcd for $C_{37}H_{45}NO_2P$ $[M+H]^+$: 566.3194, Found: 566.3188.

(*R*)-*N*-(4,8-Di-tert-butyl-2,10-dimethyl-12*H*-5,7-dioxa-6-phospha-dibenzo[a,d]cycloocten-6-yl)(1-phenylethyl)amine: Phosphoramidite ligand 3e[3] (R = H, R' = α-methylbenzyl)

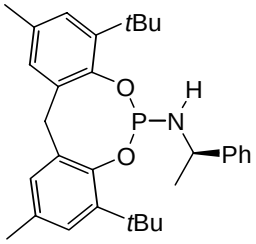

Phosphoramidite **3e**[3] was prepared from 2,2'-methylenebis(6-*tert*-butyl-4-methylphenol) and (*R*)-α-methyl- benzylamine in a similar to manner as phosphoramidite **3a**[1] (52% yield).

^{1}H NMR ($CDCl_3$, 300 MHz) δ 1.29 (s, 9H), 1.42 (s, 9H), 1.71 (d, 3H, *J* = 6.9 Hz), 2.30 (s, 3H), 2.31 (s, 3H), 3.36 (d, 1H, *J* = 12.6 Hz), 4.39 (dd, 4H, *J* = 12.6, 6.9 Hz), 6.99 (d, 1H, *J* = 1.8 Hz), 7.03 (d, 1H, *J* = 1.8 Hz), 7.11 (d, 1H, *J* = 1.8 Hz), 7.13 (d, 1H, *J* = 1.8 Hz), 7.23-7.51 (m, 10H).
^{13}C NMR ($CDCl_3$, 75 MHz) δ 14.14, 21.02, 21.07, 22.68, 26.67, 26.71, 30.77, 30.83, 30.91, 30.97, 31.61, 34.62, 34.70, 34.74, 50.19, 50.26, 126.26, 126.35, 126.40, 126.79, 128.42, 128.52, 132.94, 136.30, 136.34, 141.66, 141.71, 141.76, 146.61, 146.64, 148.17, 148.27, 148.33.
^{31}P NMR ($CDCl_3$, 121 MHz) δ 141.29.
TOF-HRMS (ESI), Calcd for $C_{31}H_{41}NO_2P$ $[M+H]^+$: 490.2875, Found: 490.2866.
$[\alpha]_D^{27}$ = +42 (c = 0.60 in $CHCl_3$).

[RhCl(chiral diene B)]$_2$

A mixture of (1*S*,4*S*,8*S*)-5-benzyl-2-phenyl-8-methoxy-1,8-dimethyl-bicyclo[2.2.2]octa-2,5-diene (chiral diene **B**) (33.0 mg, 0.1 mmol) and [RhCl(ethylene)$_2$] (21.4 mg, 0.055 mmol) in benzene (4.0 mL) was stirred under an argon atmosphere at room temperature for 24 h, and then the reaction mixture was filtered through celite. After the filtrate was evaporated under reduced pressure, the yellow residue was washed with ether. Prolonged evacuation of the product at 50 °C gave [RhCl(chiral diene **B**)]$_2$ (90% yield). The product was diastereomer mixture.

^{1}H NMR (300 MHz, $CDCl_3$) *major diastereomer* δ 0.89 (d, *J* = 13.8 Hz, 1H), 1.09 (d, *J* = 13.8 Hz, 1H), 1.14 (s, 3H), 1.78 (s, 3H), 2.91 (d, *J* = 15.9 Hz, 1H), 3.00 (d, *J* = 15.9 Hz, 1H), 3.07 (s, 3H), 3.30 (s, 1H), 3.40-3.42 (m, 1H), 4.06 (d, *J* = 5.4 Hz, 1H), 7.22-7.39 (m, 6H), 7.95-8.00 (m, 4H).
^{1}H NMR (300 MHz, $CDCl_3$) *minor diastereomer* δ 0.85 (d, *J* = 14.1 Hz, 1H), 1.03 (d, *J* = 14.1 Hz, 1H), 1.14 (s, 3H), 1.63 (s, 3H), 3.05 (s, 3H), 3.21-3.30 (m, 3H), 3.36 (s, 1H), 4.12 (d, *J* = 6.3 Hz, 1H), 7.22-7.39 (m, 4H), 7.52-7.47 (m, 2H), 7.79-7.81 (m, 2H), 7.95-8.00 (m, 2H).
^{13}C NMR (75 MHz, $CDCl_3$) *major diastereomer* δ 21.80, 41.21, 46.22 (d, J_{Rh-C} = 10.9 Hz), 47.68, 49.56, 49.76 (d, J_{Rh-C} = 3.6 Hz), 53.13 (d, J_{Rh-C} = 2.9 Hz), 55.85 (d, J_{Rh-C} = 10.8 Hz), 70.84 (d, J_{Rh-C} =

12.1 Hz), 71.46 (d, J_{Rh-C} = 11.2 Hz), 77.24, 81.10, 126.22, 127.12, 128.15, 130.41, 130.85, 131.12, 137.66, 138.39.
^{13}C NMR (75 MHz, $CDCl_3$) *mainor diastereomer* δ 21.90, 41.31, 44.90 (d, J_{Rh-C} = 11.6 Hz), 47.58, 49.46, 54.12, 55.01 (d, J_{Rh-C} = 10.1 Hz), 71.74 (d, J_{Rh-C} = 11.2 Hz), 81.03, 120.33, 127.20, 130.92, 137.72, 138.49.
Anal. Calcd for $C_{48}H_{52}Cl_2O_2Rh_2 \cdot 2H_2O$: C, 57.10; H, 5.99. Found: C, 57.10; H, 5.99. H_2O was derived from ether that washed the yellow residue (^{1}H NMR: 1.52 (s, 4H)).
$[\alpha]_D^{27}$ = -76 (c = 1.2 in $CHCl_3$).

[RhCl(Br-nbd)]$_2$

[RhCl(Br-nbd)]$_2$ was prepared from 2,3-dibromo-bicyclo[2.2.1]hepta-2,5-diene (Br-nbd) and [RhCl(ethylene)$_2$] in a similar to manner as [RhCl(chiral diene **B**)]$_2$ (40% yield).

^{1}H NMR ($CDCl_3$, 300 MHz) δ 1.20-1.27 (m, 4H), 1.58 (br, 2H), 1.76 (d, 2H, *J* = 9.6 Hz), 4.32 (br, 2H), 4.57 (br, 2H).

1,5-Dimethyl-cycloocta-1,5-diene (DM-cod)

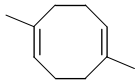

To a suspension of 1,5-dibromo-cycloocta-1,5-diene (280 mg, 1.05 mmol) and $NiCl_2$(dppp) (23 mg, 0.04 mmol) in dry Et_2O (20 mL) was added methyl Grignard reagent (1.59 mmol, 3.0M in Et_2O) under an argon atmosphere at 0 °C. The reaction mixture was stirred for 30 min at 0 °C, for 1 h at room temperature and for 2 h at reflux. H_2O (20 mL) was added and the reaction mixture was extracted with Et_2O. Combined organic layer were dried over $MgSO_4$ and solvents were removed under reduced pressure. Crude product was purified by flash chromatography over silica-gel eluted with pentane to give the product (yield 90%).

^{1}H NMR (300 MHz, $CDCl_3$) δ 0.95 (d, *J* = 6.9 Hz, 12 H), 2.29-2.38 (m, 10 H), 5.32 (t, *J* = 6.0 Hz, 2H).
^{13}C NMR (75 MHz, $CDCl_3$) δ 26.3, 33.3, 122.5, 135.8.

[RhCl(dm-cod)]$_2$

[RhCl(dm-cod)]$_2$ was prepared from 1,5-dimethyl-cycloocta-1,5-diene (DM-cod) and [RhCl(ethylene)$_2$] in a similar to manner as [RhCl(chiral diene **B**)]$_2$ (30% yield). The product was diastereomer mixture.

^{1}H NMR (300 MHz, $CDCl_3$) δ 1.50 (s, 6H, dia. minor), 1.65-1.85 (m, 8H), 1.72 (s, 6H, dia. major), 2.05-2.23 (m, 4H), 2.47-2.64 (m, 4H), 3.79 (d, 2H, *J* = 7.2 Hz, dia. minor), 3.99 (d, 2H, *J* = 6.9 Hz, dia. major).

RhCl(nbd)(3a^1): 3a^1-RhCl/nbd

To a mixture of (*S*,*S*)-*N*-(2,10-Dimethyl-12*H*-5,7-dioxa-6-phosphadibenzo[*a*,*d*]cycloocten-6-yl)-bis(1-phenylethyl)amine (**3a^1**) (9.6 mg, 0.02 mmol) and $[RhCl(nbd)]_2$ (4.6 mg, 0.01 mmol) was added CH_2Cl_2 (1 mL) at room temperature under an argon atmosphere. After stirred for 1 h, the reaction mixture was concentrated under reduced pressure to give RhCl(nbd)(**3a^1**) complex (11.8 mg, 98% yield).

^{1}H NMR ($CDCl_3$, 300 MHz) δ 1.22 (s, 2H), 1.73 (d, 6H, *J* = 7.2 Hz), 2.31 (s, 3H), 2.32 (s, 3H), 2.86 (br, 1H), 3.23 (br, 1H), 3.46 (br, 2H), 3.79 (d, 1H, *J* = 13.8 Hz), 4.58 (d, 1H, *J* = 13.8 Hz), 5.13 (br, 1H), 5.22 (br, 1H), 5.34 (dq, 2H, *J* = 14.1, 7.2 Hz), 6.81 (d, 1H, *J* = 8.1 Hz), 6.90 (d, 1H, *J* = 8.1 Hz), 7.01 (dd, 1H, *J* = 8.1, 2.1 Hz), 7.08 (d, 1H, *J* = 2.1 Hz), 7.10 (d, 1H, *J* = 2.1 Hz), 7.21 (d, 1H, *J* = 8.1 Hz), 7.30-7.40 (m, 6H), 7.51 (d, 4H, *J* = 7.5 Hz).
^{31}P NMR ($CDCl_3$, 121 MHz) δ 125.0 (d, $J_{P\text{-}Rh}$ = 266.0 Hz).
$[\alpha]_D^{27}$ = -2.4 (c = 0.25 in $CHCl_3$).
m/z (ESI): Calcd for Rh(nbd)(**3a^1**) $[M\text{-}Cl]^+$: 676.2, 677.2, 678.2, 679.2, 680.2. Found: 676.2, 677.2, 678.2, 679.2, 680.2.

RhCl(chiral diene A)(3e^1): 3e^1-RhCl/chiral diene A

RhCl(chiral diene **A**)(**3e^1**) was prepared from (4,8-di-*tert*-butyl-2,10-dimethyl-12*H*-5,7-dioxa-6-phospha-dibenzo[*a*,*d*]cycloocten-6-yl)dimethylamine **3e^1** and [RhCl(chiral diene **A**)]$_2$ in a similar to manner as RhCl(nbd)(**3e^1**).

^{1}H NMR ($CDCl_3$, 300 MHz) δ 0.90 (s, 1H), 0.94 (s, 1H), 1.15 (s, 3H), 1.31 (s, 9H), 1.34 (s, 9H), 1.39 (s, 3H), 2.26 (s, 6H), 2.29 (s, 3H), 2.31 (s, 3H), 2.72 (br, 1H), 3.22 (d, 6H, *J* = 9.0 Hz), 3.27 (s, 3H), 3.57 (br, 1H), 3.90 (d, 1H, *J* = 15.6 Hz), 4.18 (t, 1H, *J* = 6.0 Hz), 5.00 (t, 1H, *J* = 4.8 Hz), 6.83 (s, 1H), 6.98 (br, 2H), 7.01 (br, 2H), 7.07 (br, 2H).
^{31}P NMR ($CDCl_3$, 121 MHz) δ 119.5 (d, $J_{P\text{-}Rh}$ = 268.6 Hz).
$[\alpha]_D^{27}$ = -65 (c = 0.20 in $CHCl_3$).
m/z (ESI): Calcd for Rh(chiral diene **A**)(**3e^1**) $[M\text{-}Cl]^+$: 784.3, 785.3, 786.3. Found: 784.3, 785.3, 786.3.

Ir-catalyzed hydrogenation of 2-acetamidoacrylate methyl ester[6]

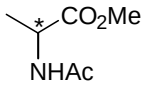

To a mixture of $[IrCl(cod)]_2$ (1.3 mg, 0.002 mmol) and (*S*,*S*)-*N*-(2,10-dimethyl-12*H*-5,7-dioxa-6-phosphadibenzo[*a*,*d*]cycloocten-6-yl)bis(1-phenylethyl)amine (**3a**[1]) (1.9 mg, 0.004 mmol) was added CH_2Cl_2 (2.0 mL) under an argon atmosphere. After stirred for 30 min at room temperature, to the solution was added 2-acetamidoacrylate methyl ester (14.3 mg, 0.1 mmol). 100-mL autoclave was charged with this reaction mixture under a stream of argon and hydrogen was introduced at a pressure of 10 atm. The solution was vigorously stirred for 3 h at room temperature. After concentration under reduced pressure, the residue was filtered through a short column of silica-gel chromatography (ethyl acetate, then methanol/dichloromethane = 1/19) to give *N*-acetylalanine methyl ester (12.4 mg, 86% yield).

^{1}H NMR ($CDCl_3$, 300 MHz) δ 1.38 (d, *J* = 7.2 Hz, 3H), 2.00 (s, 3H), 3.72 (s, 3H), 4.57 (q, *J* = 7.2 Hz, 1H), 6.21 (br, 1H).
GC (column, CP-Chirasil-Dex CB, i.d. 0.25 mm x 25 m, Chrompack; carrier gas, N_2 (75 kPa); column temp, 100 ºC; injection and detection temp, 130 ºC; split rate, 100:1), t_R = 10.8 min (*S*)/11.7 min (*R*).

Typical procedure for Rh-catalyzed Michael addition of α-cyano carboxylate

To a mixture of $[RhCl(\text{chiral diene } \mathbf{A})]_2$ (0.8 mg, 0.001 mmol) and (4,8-di-*tert*-butyl-2,10-dimethyl-12H-5,7-dioxa-6-phospha-dibenzo[*a*,*d*]cycloocten-6-yl)dimethylamine **3e**[1] (0.8 mg, 0.002 mmol) was added CH_2Cl_2 (2.0 mL) under an argon atmosphere. After stirred for 30 min at room temperature, to the solution were added 2-cyanoproionic acid *tert*-butyl ester (15.5 mg, 0.1 mmol). After cooled down to -78 °C, to the reaction mixture were added acrolein (35 μL, 0.5 mmol) and *i*Pr_2NEt (2 drops). After stirred for 3 h at -78 °C, the reaction mixture was evaporated under reduced pressure. The residue was purified by silica-gel chromatography (hexane/ethyl acetate = 3/2) to give 2-cyano-2-methyl-5- oxopentanoate acid *tert*-butyl ester (20.0 mg, 95% yield).

2-Cyano-2-methyl-5-oxopentanoate acid ethyl ester[3c]

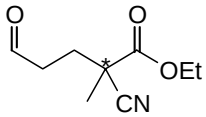

^{1}H NMR ($CDCl_3$, 300 MHz) δ 1.28 (t, *J* = 7.2 Hz, 3H), 1.57 (s, 3H), 2.05 (ddd, *J* = 14.4, 10.2, 5.7 Hz, 1H), 2.22 (ddd, *J* = 14.4, 9.9, 6.0 Hz, 1H), 2.59 (ddd, *J* = 18.6, 10.2, 6.0 Hz, 1H), 2.69 (ddd, *J* = 18.6, 9.9, 5.7 Hz, 1H), 4.21 (q, *J* = 7.2 Hz, 2H), 9.73 (s, 1H).
^{13}C NMR ($CDCl_3$, 121 MHz) δ 13.98, 23.51, 30.02, 39.76, 43.03, 63.09, 119.37, 186.71, 199.12.
$[\alpha]_D^{27}$ = +1.3 (c = 1.0 in $CHCl_3$) for a sample that is 48% *ee* (*R*).

GC (column, CP-Chirasil-Dex CB, i.d. 0.25 mm x 25 m, Chrompack; carrier gas, N_2 (75 kPa); column temp, 110 ºC; injection and detection temp, 140 ºC; split rate, 100:1), t_R = 21.2 min (*S*)/23.9 min (*R*).

2-Cyano-3-hydroxy-2-methyl-propionic acid ethyl ester[14]

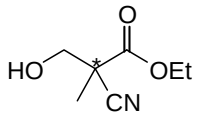

^{1}H NMR ($CDCl_3$, 300 MHz) δ 1.36 (t, *J* = 7.2 Hz, 3H), 1.60 (s, 3H), 2.60 (br, 1H), 3.92 (q, *J* = 12.6 Hz, 2H), 4.32 (q, *J* = 7.2 Hz, 2H).
^{13}C NMR ($CDCl_3$, 121 MHz) δ 13.96, 19.46, 46.17, 63.19, 66.72, 118.90, 168.47.
GC (column, ChiralDEX GTA, i.d. 0.25 mm x 25 m, Chrompack; carrier gas, N_2 (75 kPa); column temp, 130 ºC; injection and detection temp, 160 ºC; split rate, 100:1), t_R = 24.1 min/25.5min.

4-Cyano-4-methyl-2-pentenedioic acid diethyl ester[13]

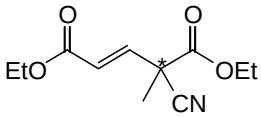

^{1}H NMR ($CDCl_3$, 300 MHz) δ 1.30 (t, *J* = 7.2 Hz, 3H), 1.33 (t, *J* = 7.2 Hz, 3H), 1.76 (s, 3H), 4.22 (q, *J* = 7.2 Hz, 2H), 4.28 (q, *J* = 7.2 Hz, 2H), 6.31 (q, *J* = 15.6 Hz, 1H), 6.88 (q, *J* = 15.6 Hz, 1H).
^{13}C NMR ($CDCl_3$, 121 MHz) δ 13.87, 14.12, 23.92, 45.98, 61.13, 63.72, 117.38, 124.37, 140.78, 166.48, 166.54.
GC (column, CP-Chirasil-Dex CB, i.d. 0.25 mm x 25 m, Chrompack; carrier gas, N_2 (75 kPa); column temp, 130 ºC; injection and detection temp, 160 ºC; split rate, 100:1), t_R = 14.8 min/15.3 min.

2-Cyano-2-methyl-5-oxopentanoate acid *tert*-butyl ester[3c]

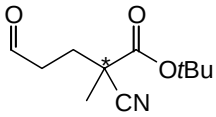

^{1}H NMR ($CDCl_3$, 300 MHz) δ 1.52 (s, 9H), 1.60 (s, 3H), 2.10 (ddd, *J* = 14.4, 10.2, 5.4 Hz, 1H), 2.23 (ddd, 1H, *J* = 14.4, 10.5, 5.1 Hz), 2.64 (dddd, 1H, *J* = 18.3, 10.2, 5.4, 0.9 Hz), 2.77 (dddd, 1H, *J* = 18.3, 10.5, 5.1, 0.9 Hz), 9.82 (s, 1H).
^{13}C NMR ($CDCl_3$, 121 MHz) δ 23.51, 27.75, 29.96, 39.84, 43.77, 84.37, 119.68, 167.67, 199.26.
$[\alpha]_D^{27}$ = -2.4 (c = 0.90 in $CHCl_3$) for a sample that is 86% *ee* (*S*).
GC (column, CP-Chirasil-Dex CB, i.d. 0.25 mm x 25 m, Chrompack; carrier gas, N_2 (75 kPa); column temp, 115 ºC; injection and detection temp, 150 ºC; split rate, 100:1), t_R = 15.7 min (*S*)/17.1 min (*R*).

Rh-Catalyzed [4+2]-cyclization of (3-hexa-2,4-dienyloxy-prop-1-ynyl)benzene[4]

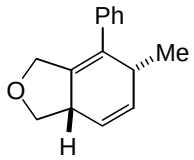

To a mixture of [RhCl(diene **A**)]$_2$ (1.2 mg, 0.0025 mmol) and (*S*,*S*)-*N*-(2,10-Dimethyl-12*H*-5,7-dioxa-6-phosphadibenzo[*a*,*d*]cycloocten-6-yl)-bis(1-phenylethyl)amine (**3a**[1]) (2.4 mg, 0.005 mmol) was added CH_2Cl_2 (1.5 mL) under an argon atmosphere. To the reaction mixture was added (3-hexa-2,4-dienyloxy-prop-1-ynyl)benzene (22 μL, 0.1 mmol). After stirred for 10 min at room temperature, $AgSbF_6$ (6.8 mg, 0.02 mmol) was added in one portion under a stream of argon. After stirred for 90 min, the reaction mixture was purified by silica-gel chromatography (pentane/diethyl ether = 10/1) to give 6-methyl-7-phenyl-1,3,3a,6-tetrahydro-isobenzofuran (20.1 mg, 95% yield).

^{1}H NMR ($CDCl_3$, 300 MHz) δ 0.94 (d, *J* = 7.2 Hz, 3H), 3.10-3.30 (m, 2H), 3.39 (dd, *J* = 11.4, 7.2 Hz, 1H), 4.15 (d, *J* = 13.5 Hz, 1H), 4.24 (d, *J* = 7.2 Hz, 1H), 4.30 (d, *J* = 13.5 Hz, 1H), 5.80 (s, 2H), 7.10-7.31 (m, 5H).
GC (column, CP-Cyclodextrin-β-2,3,6-M-19, i.d. 0.25 mm x 25 m, Chrompack; carrier gas, N_2 (75 kPa); column temp, 150 ºC; injection and detection temp, 180 ºC; split rate, 100:1), t_R = 48.5 min/50.6 min.

Computational Methods

All the calculations in Chapter 3 were performed with GAUSSIAN 03 program package. All the structures were optimized at B3LYP/631SDD (SDD for Rh, 6-31G(d) for others) level. The optimized geometries were verified as an equilibrium structures having no imaginary frequency.

RhCl(3e')(chiral diene A') (Figure 3-3 p.94)

3e': (12*H*-5,7-dioxa-6-phospha-dibenzo[*a*,*d*]cycloocten-6-yl)dimethylamine
chiral diene A': (*S*)-2-(3,5-Dimethylphenyl)-1-methylbicyclo[2.2.2]octa-2,5-diene
Charge = 0, Multiplicity = 1
SCF Done: E(B3LYP/631SDD) = -2358.51183292 a.u.

Center Number	Atomic Number	Atomic Type	Coordinates (Angstroms) X	Y	Z
1	45	0	-0.467484	0.226444	0.110569
2	17	0	-0.702947	0.531228	2.480094
3	6	0	4.557692	-0.412179	-1.076132
4	6	0	4.122801	1.031689	-1.232357

5	6	0	3.773662	1.851019	0.006375
6	6	0	-2.109814	1.691030	-0.696621
7	6	0	-0.707117	-0.282779	-1.954487
8	6	0	-0.118831	0.992254	-1.823432
9	6	0	-2.734195	0.477405	-0.883954
10	1	0	-0.146096	-1.142827	-2.309328
11	6	0	-3.961428	0.066959	-0.141006
12	1	0	-2.439387	2.394898	0.061788
13	1	0	0.915855	1.194238	-2.083294
14	6	0	4.144550	3.205293	0.030181
15	6	0	3.792825	4.053581	1.078392
16	6	0	-1.152354	2.107251	-1.812082
17	6	0	-2.229070	-0.262740	-2.148249
18	6	0	-2.771180	-1.678397	-2.346544
19	1	0	-0.708602	3.086599	-1.618667
20	6	0	3.045237	3.556698	2.147435
21	6	0	2.669677	2.215972	2.159519
22	6	0	3.035147	1.378719	1.103320
23	8	0	2.720335	0.030237	1.248440
24	6	0	-2.520967	0.660258	-3.384060
25	6	0	-1.940388	2.081054	-3.159528
26	1	0	-2.738587	2.831346	-3.121410
27	6	0	3.608372	-1.442480	-1.000839
28	6	0	3.982770	-2.785535	-0.982910
29	6	0	5.336979	-3.122034	-1.017171
30	6	0	6.302475	-2.115277	-1.067150
31	6	0	5.908820	-0.776155	-1.104000
32	8	0	2.258187	-1.107355	-0.974848
33	15	0	1.495836	-0.767158	0.485250
34	7	0	1.510175	-2.165221	1.398598
35	6	0	2.616456	-2.606153	2.247700
36	6	0	0.269801	-2.912391	1.595245
37	1	0	-0.055143	-2.852447	2.642199
38	1	0	-0.525996	-2.495542	0.973170
39	1	0	0.416190	-3.967358	1.324994
40	1	0	3.516212	-2.028530	2.043904
41	1	0	2.353841	-2.483673	3.307935
42	1	0	2.829022	-3.666985	2.060658
43	1	0	-1.268155	2.365955	-3.976981
44	1	0	-2.071225	0.189534	-4.266663
45	1	0	-3.601649	0.701637	-3.563534
46	6	0	-3.980913	-0.092744	1.247775
47	6	0	-5.168889	-0.418869	1.921242

48	6	0	-6.342013	-0.576125	1.182630
49	6	0	-6.358662	-0.410564	-0.210606
50	6	0	-5.164598	-0.093898	-0.857905
51	1	0	7.358408	-2.370202	-1.092534
52	1	0	4.102193	5.094425	1.059063
53	1	0	3.255059	1.046275	-1.905865
54	1	0	4.919069	1.567531	-1.760212
55	1	0	4.723954	3.597663	-0.802715
56	1	0	2.756386	4.204826	2.969819
57	1	0	2.077698	1.795588	2.965196
58	1	0	3.210555	-3.547110	-0.942597
59	1	0	5.633559	-4.167243	-1.005102
60	1	0	6.661874	0.006052	-1.167487
61	1	0	-3.061890	0.032230	1.811584
62	6	0	-5.159091	-0.593006	3.422978
63	1	0	-7.266948	-0.829161	1.698560
64	6	0	-7.647592	-0.567346	-0.985684
65	1	0	-5.176998	0.059484	-1.933582
66	1	0	-4.491457	-1.409451	3.724156
67	1	0	-4.797120	0.312451	3.924534
68	1	0	-6.159882	-0.816366	3.806933
69	1	0	-8.075707	-1.568714	-0.851202
70	1	0	-8.405849	0.152203	-0.651973
71	1	0	-7.492123	-0.413164	-2.058417
72	1	0	-2.601939	-2.291367	-1.454610
73	1	0	-2.253844	-2.153847	-3.188538
74	1	0	-3.842333	-1.691995	-2.563111

RhCl(3e')(chiral diene B') (Figure 3-5 p.96)

3e': (12*H*-5,7-dioxa-6-phospha-dibenzo[*a*,*d*]cycloocten-6-yl)dimethylamine

chiral diene B': (2*S*,5*S*)-5-Benzyl-1-methyl-2-phenylbicyclo[2.2.2]octa-2,5-diene

Charge = 0, Multiplicity = 1

SCF Done: E(B3LYP/631SDD) = -2550.24063124 a.u.

Center Number	Atomic Number	Atomic Type	Coordinates (Angstroms) X	Y	Z
1	45	0	-0.671154	0.187146	0.448590
2	17	0	-1.412963	-1.216696	2.237715

3	6	0	4.029316	-1.205753	-1.180490
4	6	0	2.874107	-1.787459	-1.971342
5	6	0	2.031666	-2.887960	-1.337967
6	6	0	-0.397908	0.897711	-1.536092
7	6	0	-2.705829	1.119696	-0.095541
8	6	0	-2.570678	0.053841	-0.954952
9	6	0	-0.543374	2.021413	-0.683072
10	1	0	-3.403149	1.109902	0.737014
11	6	0	0.551077	3.018216	-0.488349
12	1	0	0.552126	0.682065	-2.015772
13	6	0	-3.367285	-1.244088	-0.917662
14	6	0	1.647593	-3.980902	-2.130611
15	6	0	0.814360	-4.989746	-1.649714
16	6	0	-1.694153	0.395771	-2.158961
17	6	0	-2.040426	2.424963	-0.540608
18	6	0	-2.345668	3.568049	0.426767
19	1	0	-1.529842	-0.476467	-2.797700
20	6	0	0.337384	-4.923905	-0.339584
21	6	0	0.706451	-3.855902	0.474837
22	6	0	1.545457	-2.855020	-0.020590
23	8	0	1.954328	-1.888692	0.889926
24	6	0	-2.558364	2.766087	-1.981394
25	6	0	-2.362987	1.565948	-2.941797
26	1	0	-1.723377	1.835801	-3.790416
27	6	0	3.828296	-0.123320	-0.310760
28	6	0	4.893317	0.510266	0.329262
29	6	0	6.192150	0.040410	0.130898
30	6	0	6.415765	-1.055385	-0.704925
31	6	0	5.340874	-1.661854	-1.357129
32	8	0	2.538982	0.360649	-0.127091
33	15	0	1.468567	-0.308301	0.974052
34	7	0	2.038488	0.026035	2.507138
35	6	0	3.183695	-0.637924	3.128661
36	6	0	1.277188	0.878174	3.415796
37	1	0	2.207267	-0.960786	-2.249110
38	1	0	3.272278	-2.182515	-2.912307
39	1	0	2.016480	-4.033929	-3.152634
40	1	0	0.542696	-5.821137	-2.294243
41	1	0	-0.316048	-5.698915	0.050846
42	1	0	0.347716	-3.765635	1.494301
43	1	0	-3.321094	1.231760	-3.357260
44	1	0	-3.617541	3.039951	-1.910390
45	1	0	-2.020662	3.651807	-2.340312

46	6	0	0.834794	3.592433	0.762699
47	6	0	1.851824	4.534913	0.907883
48	6	0	2.609354	4.930531	-0.197235
49	6	0	2.337510	4.375348	-1.448052
50	6	0	1.318842	3.432365	-1.590287
51	1	0	4.688562	1.362651	0.969137
52	1	0	7.024961	0.531346	0.626947
53	1	0	7.424407	-1.426939	-0.862421
54	1	0	5.519543	-2.498896	-2.028330
55	1	0	3.698680	-1.276845	2.413130
56	1	0	2.846862	-1.259719	3.970001
57	1	0	3.893425	0.108713	3.509408
58	1	0	0.983608	0.311618	4.309063
59	1	0	0.363367	1.226747	2.932129
60	1	0	1.876909	1.745838	3.725038
61	1	0	0.265084	3.281990	1.631989
62	1	0	2.917262	4.676057	-2.316939
63	1	0	3.402039	5.665238	-0.083843
64	1	0	2.055002	4.959110	1.887933
65	1	0	1.111285	3.011768	-2.570248
66	1	0	-3.463903	-1.595516	-1.953501
67	6	0	-4.748559	-1.133852	-0.296817
68	1	0	-2.778443	-2.003439	-0.390075
69	6	0	-5.859043	-0.829850	-1.096699
70	6	0	-7.133594	-0.714019	-0.539896
71	6	0	-7.316179	-0.902058	0.831995
72	1	0	-2.052899	3.318301	1.451767
73	1	0	-3.423779	3.768530	0.430092
74	1	0	-1.831255	4.489831	0.138466
75	6	0	-6.217238	-1.207660	1.637137
76	6	0	-4.942304	-1.324822	1.078276
77	1	0	-5.725664	-0.690986	-2.168167
78	1	0	-7.983307	-0.482952	-1.177511
79	1	0	-8.307976	-0.815183	1.268181
80	1	0	-6.350016	-1.360404	2.705216
81	1	0	-4.087258	-1.557842	1.707305

References for Chapter 3

1 (a) Horner, L.; Siegel, H.; Büthe, H. *Angew. Chem.* **1968**, *80*, 1034. (b) Knowles, W. S.; Sabacky, M. J. *Chem. Commun.* **1968**, 1445. (c) Claver, C.; Fernandez, E.; Gillon, A.; Heslop, K.; Hyett, D. J.; Martorell, A.; Orpen, A. G.; Pringle, P. G. *Chem. Commun.* **2000**, 961. (d) Reetz, M. T.; Mehler, G. *Angew. Chem. Int. Ed.* **2000**, *39*, 3889. (e) Reetz, M. T.; Sell, T. *Tetrahedron Lett.* **2000**, *41*, 6333. (f) van den Berg, M.; Minnaard, A. J.; Schudde, E. P.; van Esch, J.; de Vries, A. H. M.; de Vries, J. G.; Feringa, B. L. *J. Am. Chem. Soc.* **2000**, *122*, 11539. (g) Peňa, D.; Minnaard, A. J.; de Varis, A. H. M.; de Vries, J. G.; Feringa, B. L. *Org. Lett.* **2003**, *5*, 475. (h) Monti, C.; Gennari, C.; Piarulli, U. *Chem. Eur. J.* **2007**, *13*, 1547.

2 (a) Haag, D.; Runsink, J.; Scharf, H.-D. *Organometalics*, **1998**, *17*, 398. (b) Selent, D.; Baumann, W.; Kempe, R.; Spannenberg, A.; Röttger, D.; Wiese, K.-D.; Börner, A. *Organometalics*, **2003**, *22*, 4265. (c) Huber, D.; Kumar, P. G. A.; Pregosin, P. S.; Mikhel, I. S.; Mezzetti, A. *Helv. Chim. Acta* **2006**, *89*, 1696.

3 (a) Sawamura, M.; Hamashima, Y.; Ito, Y. *J. Am. Chem. Soc.* **1992**, *114*, 8295. (b) Inagaki, K.; Nozaki, K.; Takaya, H. *Synlett* **1997**, 119. (c) Motoyama, Y.; Koga, Y.; Kobayashi, K.; Aoki, K.; Nishiyama, H. *Chem. Eur. J.* **2002**, *8*, 2968.

4 Aikawa, K.; Akutagawa, S.; Mikami, K. *J. Am. Chem. Soc.* **2006**, *128*, 12648.

5 Mikhel, I. S.; Bernardinelli, G.; Alexakis, A. *Inorg. Chim. Acta.* **2006**, 1826.

6 Giacomia, F.; Meersma, A.; Panella, L.; Lefort, L.; de Varis, A. H. M.; de Varis, J. G. *Angew. Chem. Int. Ed.* **2007**, *46*, 1497.

7 Crabtree, R. *Acc. Chem. Res.* **1979**, *12*, 331.

8 (a) Hayashi, T.; Ueyama, K.; Norihito, U.; Yoshida, K. *J. Am. Chem. Soc.* **2003**, *125*, 11508. (b) Fischer, C.; Defieber, C.; Suzuki, T.; Carreira, E. M. *J. Am. Chem. Soc.* **2004**, *126*, 1628. (c) Defieber, C.; Paquin, J.-F.; Serna, S.; Carreira, E. M. *Org. Lett.* **2004**, *6*, 3873. (d) Yokunaga, N.; Otomaru, Y.; Okamoto, K.; Ueyama, K.; Shintani, R.; Hayashi, T. *J. Am. Chem. Soc.* **2004**, *126*, 13584.

9 Stark, M. A.; Jones, G.; Richards, C. J. Organometalics, **2000**, *19*, 1282.

10 (a) Ito, Y.; Sawamura, M.; Hayashi, T. *J. Am. Chem. Soc.* **1986**, *108*, 6405. (b) Murahashi, S.; Naota, T.; Taki, H.; Mizuno, M.; Yakaya, H.; Komiya, S.; Mizuho, Y.; Oyasato, N.; Hirooka, M.;

Hirano, M.; Fukuoka, A. *J. Am. Chem. Soc.* **1995**, *117*, 12436.

11 Detert, H.; Rose, B.; Mayer, W.; Meier, H. *Chem. Ber.* **1994,** *127*, 1529.

12 Peluso, P.; Greco, C.; De Lucchi, O.; Cossu, S. *Eur. J. Org. Chem.* **2002**, 4024.

13 Wang, X.; Kitamura, M.; Maruoka, K. *J. Am. Chem. Soc.* **2007**, *129*, 1038.

14 Kuwano, R; Miyazaki, H; Ito, Y. *Chem. Commun.* **1998**, 71.

4-1. Introduction

As described in Chapter 3, achiral benzophenone-like phosphoramidite in Rh complex could be controlled in a single conformation by chiral dienes. The Rh complex with achiral phosphoramidite and chiral diene attained high catalytic activity and enantioselectivity in the asymmetric Michael addition of α-cyano carboxylate (Scheme 4-1).

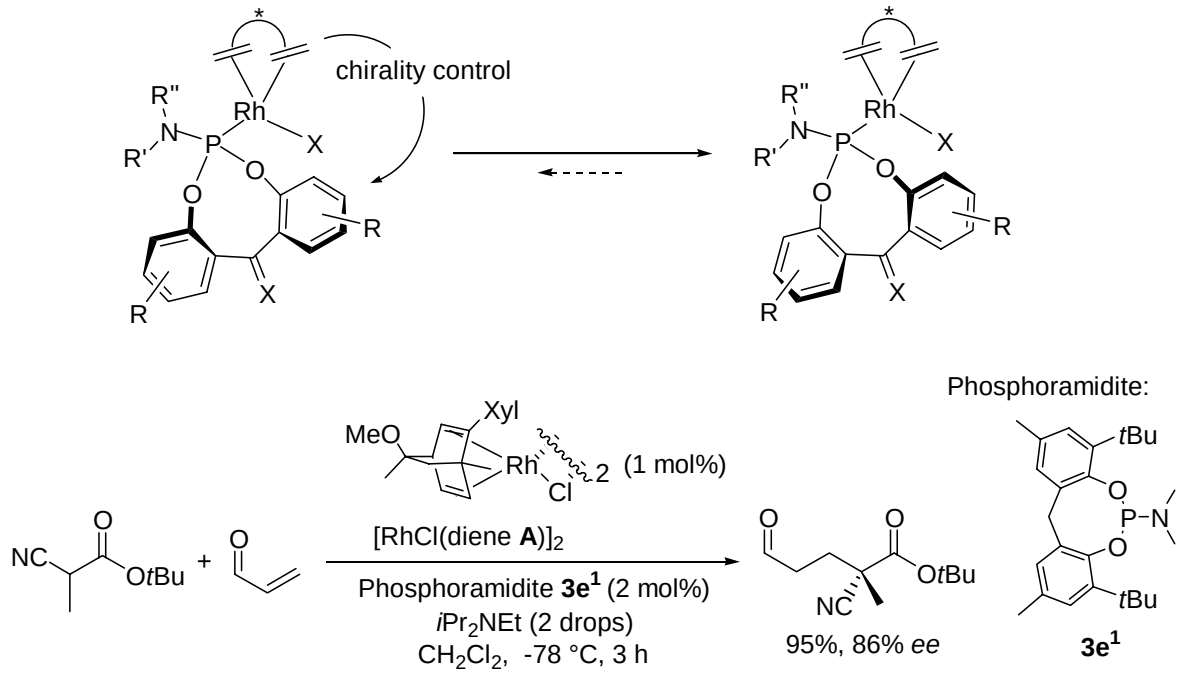

Scheme 4-1.

The conformation of benzophenone-like phosphoramidite could also be controlled by chiral amines built therein (Scheme 4-2). Similar to Rh complexes with single achiral phosphoramidites and chiral dienes, the complexes coordinated by two phosphoramidites with chiral amine part were expected to form a single conformation and attain high catalytic activity and enantioselectivity. Therefore, the complexes with benzophenone-like phosphoramidite bearing chiral amine were synthesized and used in catalytic asymmetric reactions.

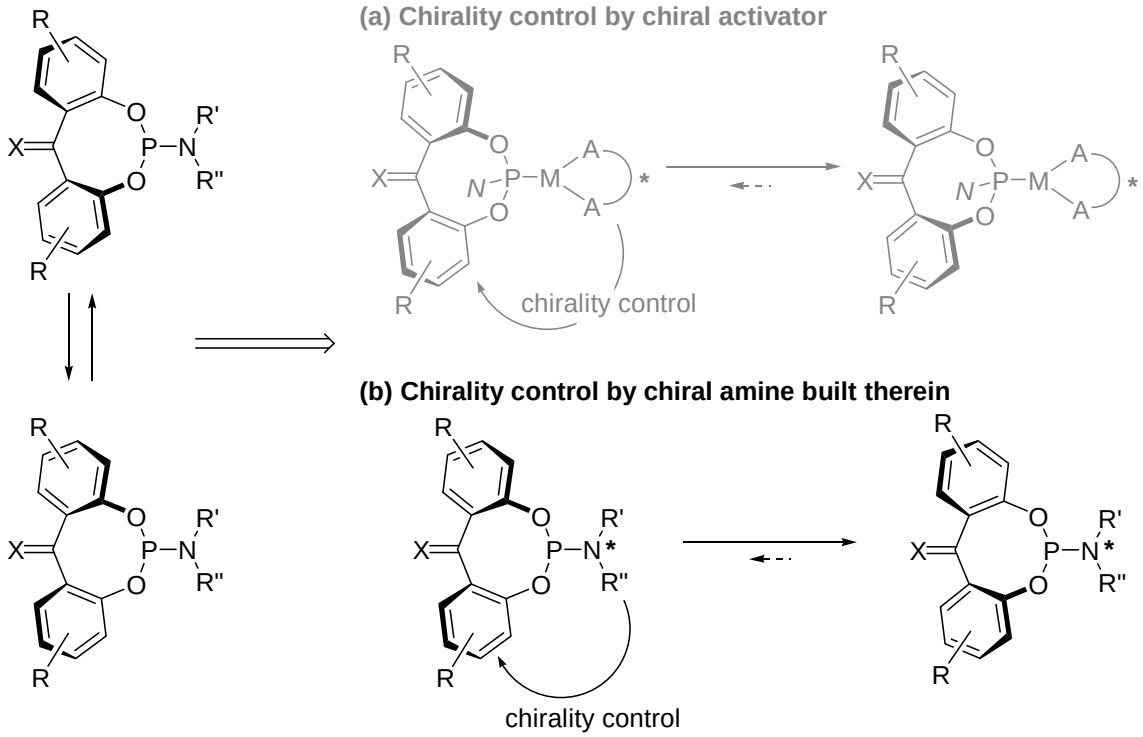

Scheme 4-2.

Recently, *atropos* BINOL-derived phosphoramidite ligands with a chiral amine were developed for catalytic asymmetric reactions.[1,2] For example, Feringa and co-workers have reported that Cu complexes with BINOL-derived phosphoramidite attains high catalytic activity and enantioselectivity in asymmetric conjugate addition to 2-cyclohexen-1-one (Scheme 4-3).[2a]

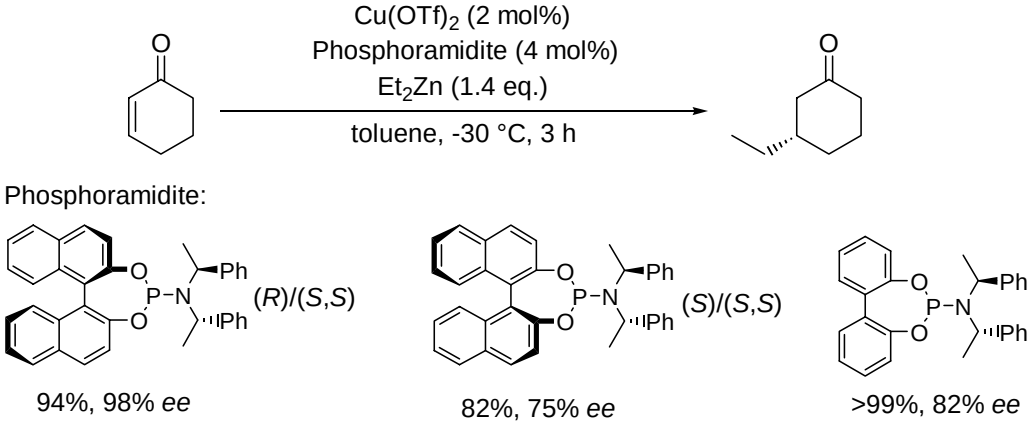

Scheme 4-3.

However, BINOL-derived phosphoramidite requires the matched combination of amine and BINOL. Phosphoramidite with (*S*)-BINOL and (*S*,*S*)-chiral amine decreased enantioselectivity. On the other hand, Alexakis and co-workers have reported that *tropos* biphenol (BIPOL)-derived phosphoramidite give the product in >99% with 82% *ee*.[2c]

Asymmetric conjugate additions were thus examined by the Cu complex of benzophenone-like phosphoramidite with a chiral amine. Particularly, the conjugate addition to nitro substrates[3] is synthetically important to provide chiral amino(acid) derivatives. For example, conjugate addition to nitroacrylate ester affords β[2]-alanine, an important chiral building blocks of natural products, such as cryptophycin C (Scheme 4-4).[4,5]

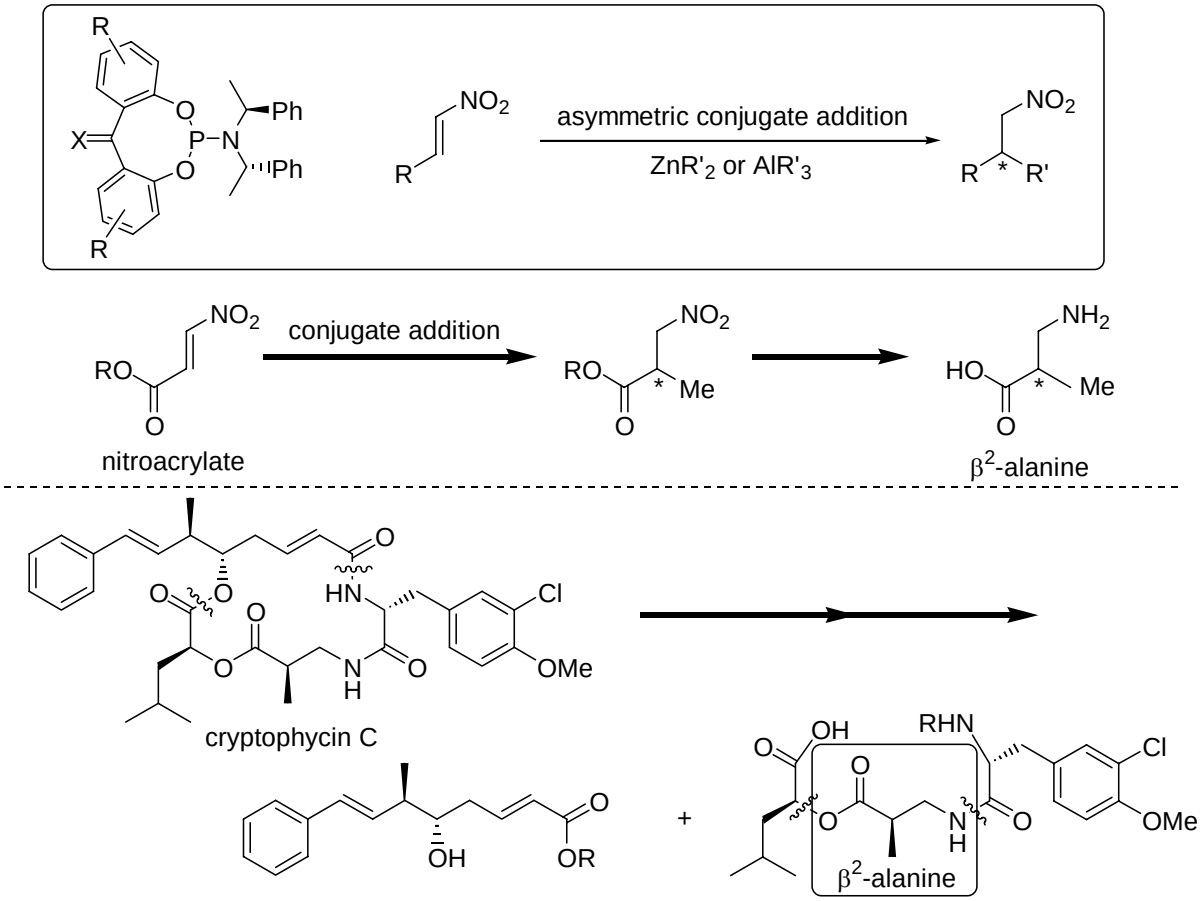

Scheme 4-4.

In Chapter 4, the author reports benzophenone-like phosphoramidite ligands in which the chirality can be controlled by a chiral amine built therein. High enantioselectivity and catalytic activity can be observed in the Cu-catalyzed asymmetric conjugate addition to nitro substrates.

4-2. Conformational analyses of complexes with benzophenone-like phosphoramidite

As described in Section 3-2, the [Rh(nbd)(**4a**)$_2$]X complexes could not be synthesized. On the other hand, the PdCl$_2$(**4a**)$_2$ complexes could be synthesized upon addition of the benzophenone-like phosphoramidite **4a** to PdCl$_2$(cod) (Scheme 4-5).

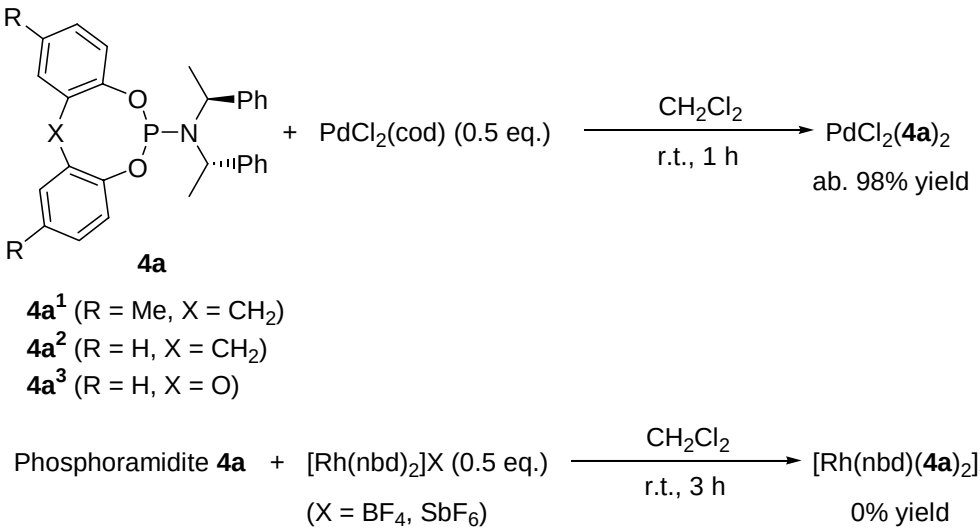

Scheme 4-5.

The conformation of PdCl$_2$(**4a^1**)$_2$ was estimated from ^{1}H and ^{31}P NMR spectra. One singlet peak of ^{31}P NMR spectrum shows that PdCl$_2$(**4a^1**)$_2$ forms a single conformation (Figure 4-1). ^{1}H NMR spectrum of 4-methylphenyl groups showed two singlets of methyl groups and two singlets and four doublets of phenyl groups. These peaks show that the bisphenyl group of **4a^1** in the Pd complex adopts non-equivalent conformation.

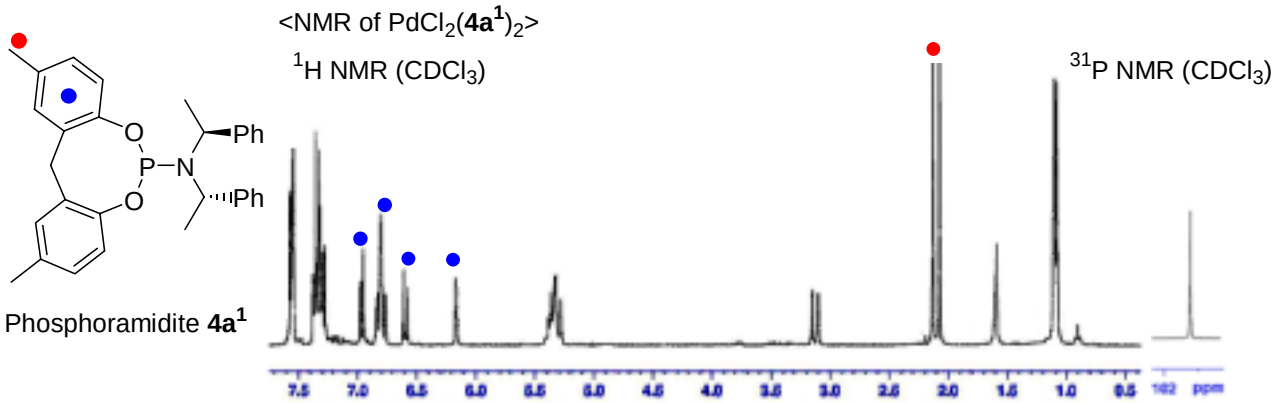

Figure 4-1. ^{1}H and ^{31}P NMR spectra of PdCl$_2$ complex with phosphoramidite **4a^1**

Conformational stability of $PdCl_2$(**4a**^{1})$_2$ was checked by VT NMR (Figure 4-2). ^{1}H NMR spectrum at 80 ˚C is similar to that of 25 ˚C; Two singlets of 4-methyl group to show the non-equivalent conformation of bisphenyl group of **4a**^{1} is kept at 80 ˚C. On the other hand, ^{1}H NMR spectrum at -80 ˚C showed that the peaks of the chiral amine became broad, while bisphenyl parts remained sharp. It is estimated that the rotation of P-N bond is slow at -80 ˚C and two α-methylbenzyl parts of the chiral amine are halfway recognized as non-equivalent.

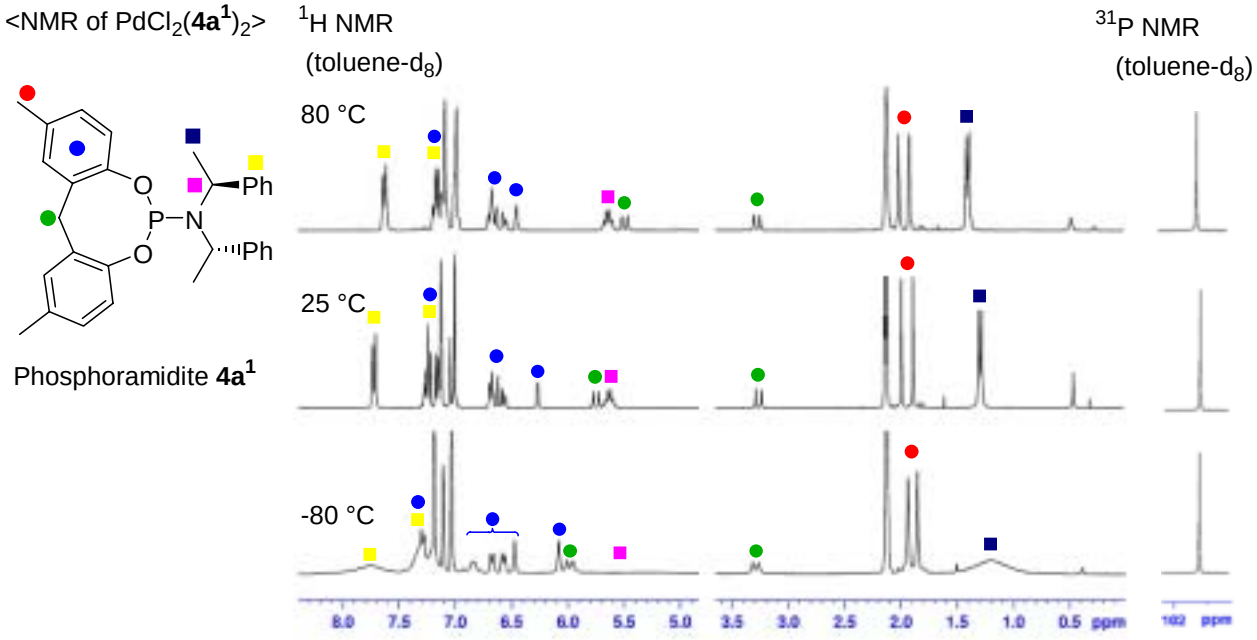

Figure 4-2. VT NMR spectra of $PdCl_2$ complex with phosphoramidite **4a**^{1}

The conformation of Pd complex with phosphoramidite was deduced by DFT calculation (B3LYP/631SDD level: SDD for Pd, 6-31G for others). Figure 4-3 shows the most stable conformation of $PdCl_2$(**4a**^{1})$_2$. The front view shows that the Pd complex of **4a**^{2} adopts C_2 conformation. As compared with the DFT calculation of *tropos* BIPOL-derived phosphoramidite, the side view of the $PdCl_2$(**4a**^{2})$_2$ complex shows the more effective shielding of phenyl rings than the BINOL or BIPOL counterparts.[6]

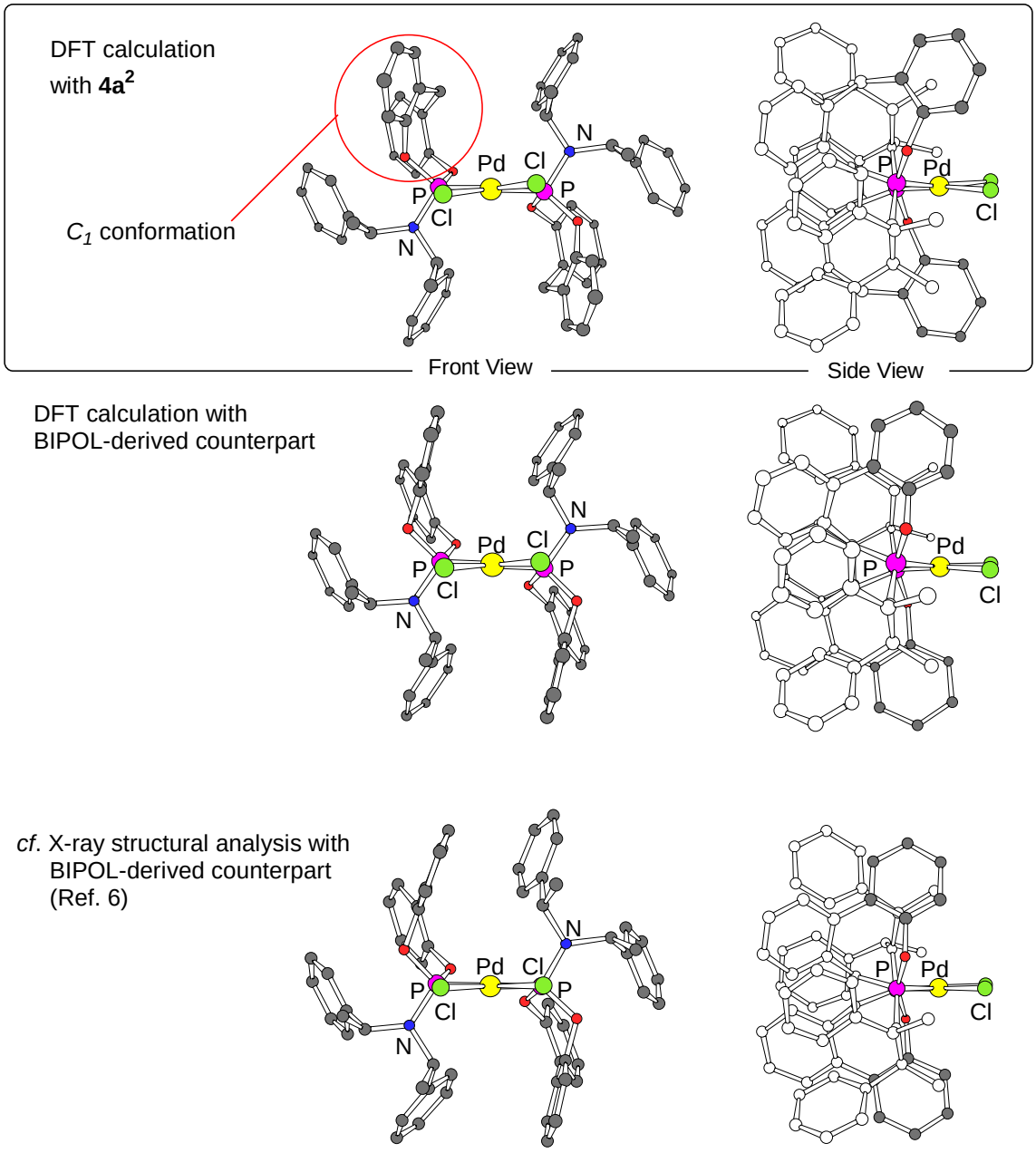

Figure 4-3. DFT calculation of $PdCl_2$ complex with phosphoramidite

This is also the case with Cu(II) complexes (Figure 4-4, B3LYP/631SDD level: SDD for Cu, 6-31G for others). Figure 4-4 shows that Cu(II) complex with **4a²** adopts C_2 conformation. In addition, the side view of the Cu complex with **4a²** shows the more effective shielding of phenyl rings than the BIPOL counterparts.

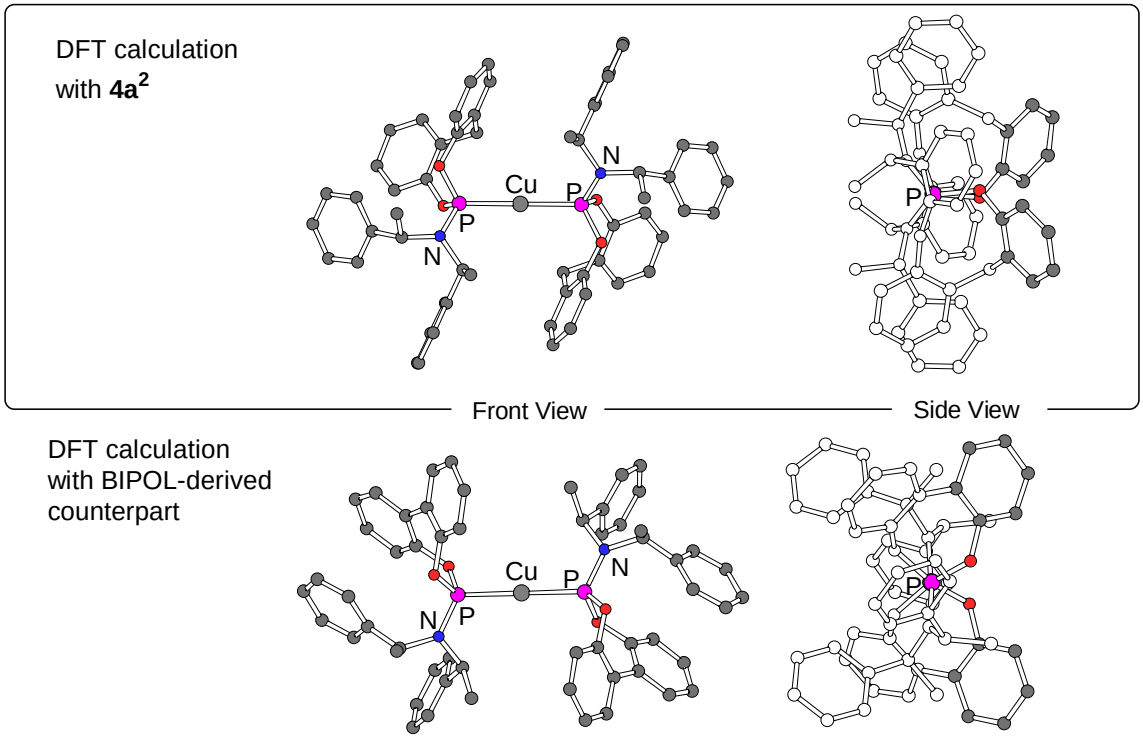

Figure 4-4. DFT calculation of Cu(II) pre-catalysts with phosphoramidite

^{1}H NMR spectrum of Pd complex with **4a¹** shows that benzophenone-like phosphoramidite in the complex adopts C_1 conformation. Therefore, Figure 4-5 exemplifies the conformation of phosphoramidite **4a²** in the Pd complex, deduced by DFT calculation. The most stable conformation of $PdCl_2$(**4a²**)$_2$ shows that the diphenylmethane part in **4a²** adopts C_1 conformation.

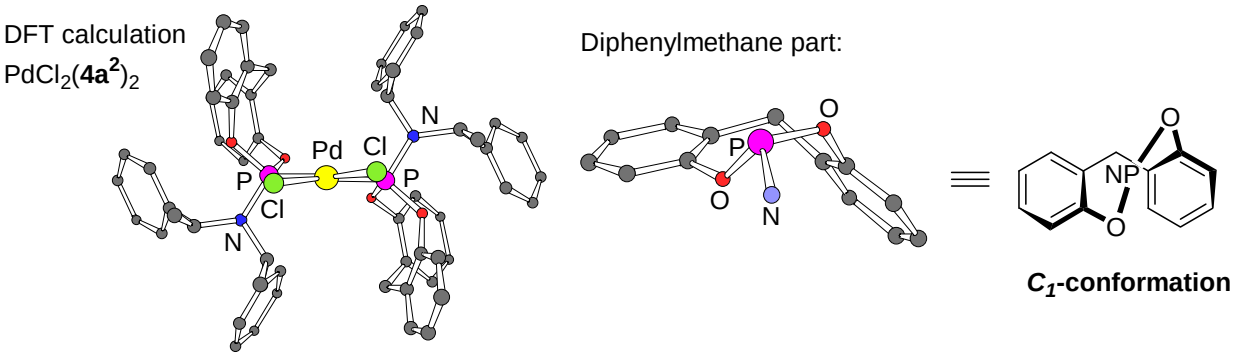

Figure 4-5. The conformation of **4a**^{2} in $PdCl_2$ complex

4-3. Cu-Catalyzed asymmetric conjugate addition

As described in Section 4-1, Cu-phosphoramidite complexes have been used in asymmetric conjugate additions. Following the previous reports, Cu complexes with **4a**^{1} were used in asymmetric conjugate addition to benzalacetone (Table 4-1). In case of $Cu(OAc)_2$ complex with **4a**^{1}, the conjugate addition proceeded at 0 °C and gave the product in 20% yield with 40% *ee*. $Cu(OTf)_2$ with **4a**^{1} provided higher catalytic activity and enantioselectivity. The conjugate addition with $Cu(OTf)_2$ complex proceeded at -40 °C and gave the product in 86% yield with 59% *ee*. However, a lower reaction temperature led to a lower reaction rate (entry 4). Not only catalytic activity and enantioselectivity, but also the absolute configuration of product was changed by copper species (entries 1 *vs.* 3).

Table 4-1. Asymmetric conjugate addition of Et_2Zn to benzalacetone

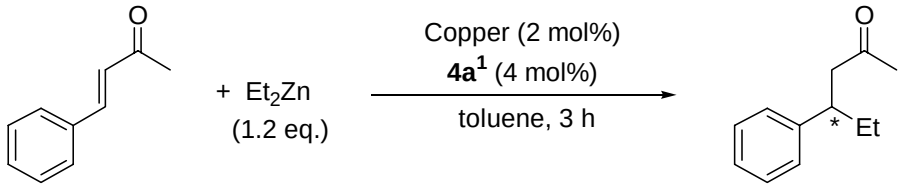

Phosphoramidite:

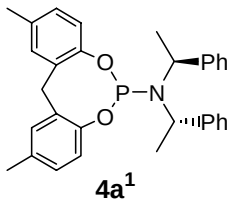

4a^{1}

Entry	Copper	Temp. (°C)	Yield (%)	*Ee* (%)
1	$Cu(OAc)_2$	0	20	40 (*R*)
2	$Cu(OAc)_2$	-30	trace	-
3	$Cu(OTf)_2$	-40	86	59 (*S*)
4	$Cu(OTf)_2$	-78	0	-

High catalytic activity of the phosphoramidite **4a** can be seen in the conjugate addition of diethylzinc to β-nitrostyrene (Table 4-2).[3] Even at -78 °C within 3 h, the $Cu(OTf)_2$ complex with phosphoramidite **4a**[1] showed remarkably high catalytic activity and enantioselectivity (>99%, 98% *ee*: entry 2).[7] Similar to Rh-catalyzed asymmetric Michael addition (see Chapter 3), phosphoramidites **4a**[1] and **4a**[2] attained almost equal enantioselectivity, and phosphoramidite **4a**[3] decreased enantioselectivity (entries 2, 3 and 4).

Table 4-2. Asymmetric conjugate addition of Et_2Zn to β-nitrostyrene

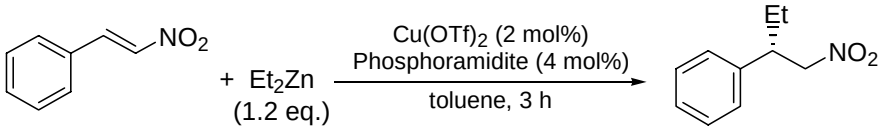

Entry	Phosphoramidite	Temp. (°C)	Conv. (%)	*Ee* (%)
1	**4a[1] (R = Me, X = CH_2)**	**-45**	**>99**	**94**
2	**4a[1] (R = Me, X = CH_2)**	**-78**	**>99**	**98**
3	**4a[2] (R = H, X = CH_2)**	**-78**	**>99**	**98**
4	4a[3] (R = H, X = O)	-78	21	88
5[a]	(*R*)/(*S*,*S*)-4b	-78	90	48
6[b]	(*R*)/(*S*,*S*)-4b	-45	>99	59
7[c]	(*R*)/(*S*,*S*)-4b	-30	>99	48
8[a]	(*S*)/(*S*,*S*)-4b	-78	80	39
9[b]	(*S*)/(*S*,*S*)-4b	-45	>99	32
10[b]	4c	-45[d]	>99	77
11[c]	4c	-30	>99	8
12[e]	4d	-65	>99	94

a. Ref 3a
b. Ref 3d
c. Ref 3c
d. Lower temperature (e.g. -78 °C) led to a lower reaction rate.
e. Ref 3e: $Cu(OTf)_2$ (1 mol%), phosphoramidite (2 mol%), reaction time (6 h)

Phosphoramidite:

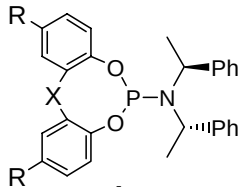

4a

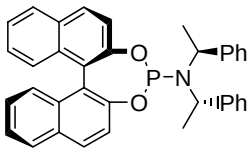

(*R*)/(*S*,*S*)-4b

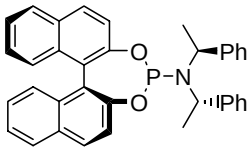

(*S*)/(*S*,*S*)-4b

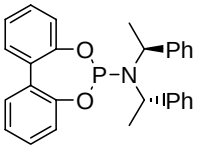

4c

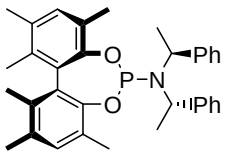

4d

The Cu-**4a**[1] catalyzed conjugate addition to β-nitrostyrene was also examined with other organometal reagents (Table 4-3). Compared to diethylzinc, the conjugate addition of dimethylzinc decreased the reactivity and enantioselectivity (entries 1 *vs.* 2). On the other hand, the conjugate addition of trimethylaluminum proceeded at -30 °C and gave 2-phenyl-1-nitropentane with 81% *ee*. In case of ethyl magnesium Grignard reagent, the conjugate addition finished within 1 h, but the product was racemic. The reactivity of ethyl magnesium Grignard reagent was too high to react to β-nitrostyrene without the Cu-**4a**[1] catalyst.

Table 4-3. Cu-**4a**[1] catalyzed asymmetric conjugate addition of organometal reagents

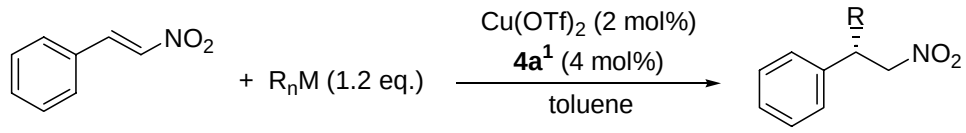

Entry	R_nM	Temp. (°C)	Time (h)	Conv. (%)	*Ee* (%)
1	Et_2Zn	-78	3	>99	98
2	Me_2Zn	0	16	89	55
3[a]	Me_3Al	-30	12	>99	81
4	EtMgBr	-78	<1	>99	0

a. Solvent was Et_2O.

Conjugate additions to other nitroalkenes were also examined with **4a**[1] to give constantly high enantioselectivities (Table 4-4). *p*-, *m*- and *o*-Methoxyphenyl, *p*-methylphenyl, *p*-trifluoro-methylphenyl, *p*-chlorophenyl, furyl and thienyl substrates were also shown to give high enantiomeric excess (91-99% *ee*). By contrast, enantioselectivity by an excellent *atropos* biphenyl phosphoramidite **4d** sharply decreased from *p*- to *o*-methoxyphenyl substrates (99% *ee* to 68% *ee*: entries 5, 7, 9). The high enantioselectivity with **4a**[1] (97% *ee* to 91% *ee*: entries 4, 6, 8) show the advantage of chirality control to fit well with the substrate change.

Table 4-4. Asymmetric conjugate addition of Et_2Zn to nitroalkenes

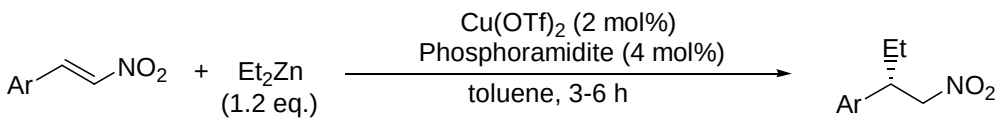

Entry	Ar	Phosphoramidite	Temp. (°C)	Conv. (%)	*Ee* (%)
1	***p*-MePh**	**4a[1]**	**-78**	**>99**	**96**
2[a]	*p*-MePh	(*R*)/(*S*,*S*)-4b	-30	>99	25
3[b]	*p*-MePh	4d	-65	>99	98
4	***p*-MeOPh**	**4a[1]**	**-78**	**>99**	**97**
5[b]	*p*-MeOPh	4d	-65	>99	99
6	***m*-MeOPh**	**4a[1]**	**-78**	**>99**	**93**
7[b]	*m*-MeOPh	4d	-65	>99	84
8	***o*-MeOPh**	**4a[1]**	**-78**	**99**	**91**
9[b]	*o*-MeOPh	4d	-65	>99	67
10	***p*-CF_3Ph**	**4a[1]**	**-78**	**>99**	**91**
11[b]	*p*-CF_3Ph	4d	-65	>99	77
12	***p*-ClPh**	**4a[1]**	**-78**	**>99**	**96**
13	**furyl**	**4a[1]**	**-78**	**>99**	**99**
14[a]	furyl	(*R*)/(*S*,*S*)-4b	-30	>99	8
15[b]	furyl	4d	-65	>99	92
16	**thionyl**	**4a[1]**	**-78**	**>99**	**98**
17[b]	thionyl	4d	-65	>99	96

a. Ref 3b
b. Ref 3e: $Cu(OTf)_2$ (1 mol%), phosphoramidite (2 mol%), reaction time (6 h)

With the great success in asymmetric conjugate addition to nitroalkenes*, conjugate addition to nitroacrylates was then examined.[8] Conjugate additions to nitroacrylates provide β-aminoacid derivatives of synthetic importance.[4,5,9]

---

* After submission of our paper, Alexakis and co-workers have quite recently (October 2007) reported the conjugate addition to 2-cyclohexen-1-one catalyzed by Cu complex with phosphoramidite **4a[2]**. However, phosphoramidite **4a[2]** afforded low enantiomeric excess (35% *ee*).[10]

Theoretical study has been showed that conjugate additions to nitroacrylate substrates proceed at β-position of nitro group.[11] In asymmetric conjugate addition of dimethylzinc to nitroacrylate ethyl ester, BINOL-derived phosphoramidite **4b** gave the product with 18% *ee* (Table 4-5, entry 7). In contrast, the conjugate addition of dimethylzinc with phosphoramidite **4a**[1] proceeded at -60 °C and gave the product with 56% *ee* (entry 3). In addition, phosphoramidite **4a**[1] gave high yield and enantioselectivity in asymmetric conjugate addition of trimethylaluminum to nitroacrylate ethyl ester (>99%, 93% *ee*: entry 1). The enantioselectivity of this Cu-catalyzed conjugate addition quite depended on the solvent employed (entries 1 *vs.* 2).[8a]

Table 4-5. Asymmetric conjugate addition of Me_3Al to nitroacrylate

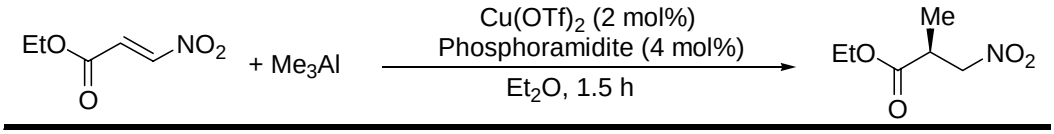

Entry	Phosphoramidite	Temp. (°C)	Yield (%)	*Ee* (%)
1	**4a**[1]	**-78**	**>99**	**93**
2[a]	4a[1]	-78	>99	38
3[b]	4a[1]	-60	>99	56
4	(*R*)/(*S*,*S*)-4b	-78	74	93
5	(*S*)/(*S*,*S*)-4b	-78	72	60
6[c]	(*R*)/(*S*,*S*)-4b	-50	85	92
7[d]	(*R*)/(*S*,*S*)-4b	-30	97	18

a. Solvent was toluene.
b. Me_2Zn was used instead of Me_3Al, reactoin time was 8 h.
c. Ref 8c
d. Me_2Zn was used instead of Me_3Al, Ref 8b

2-Methyl-3-nitropropionic acid ethyl ester, which is the product of asymmetric conjugate addition to nitroacrylate ethyl ester, can be easily transformed to β[2]-alanine ethyl ester by hydrogenation with palladium on charcoal (Scheme 4-6).[8c]

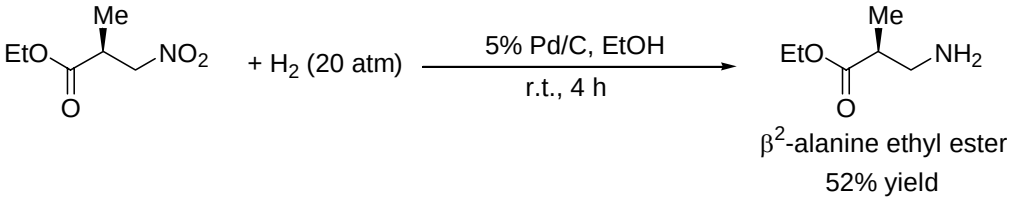

Scheme 4-6.

The *tropos* phosphoramidite **4a**[1] attained higher catalytic activity and enantioselectivity than the *atropos* BINOL counterpart not only the conjugate addition of diethylzinc but also of trimethylaluminum reagents. The Cu(I) complex with phosphoramidite have been reported to form several conplexes, such as $LCu(\mu\text{-}X)_2CuL$, $LCu(\mu\text{-}X)_2CuL_2$ and $L_2Cu(\mu\text{-}X)_2CuL_2$ (L = phosphoramidite, X = counteranion).[12] The conformation of Cu(I) complexes depends on ligand, counteranion and solvent. Therefore, several conformations of the Cu-phosphoramidite catalyst are expected to exist in the asymmetric conjugate addition to nitroalkenes and affect the catalytic activity and enantioselectivity. Mechanistic study of asymmetric conjugate addition with Cu-phosphoramidite complexes and dialkylzinc reagents has not been reported, only postulated mechanism have been reported by Alexakis and Feringa,[2a,3c] but a plausible mechanism can be proposed on the basis of non-catalytic organocuprate addition.[13] A possible pathway for the conjugate addition involves transfer of an alkyl fragment from ZnR'_2 or AlR'_3 to the Cu complex (complex(**a**) in Scheme 4-7 and 4-8).[14] The Cu(I) alkyl species (**a**) forms a π-complex (**b**) with the double bond of nitro substrates, followed by an oxidative addition to give Cu(III) species (**c**). An enantioselective insertion to the β-position of the substrate generates alkylzinc enolate, and then, upon protonation, provides the enantiomerically enriched products.

Plausible mechanism 1 (*cf*. conjugate addition to enone substrates, Alexakis, A. **2002**)[3c]

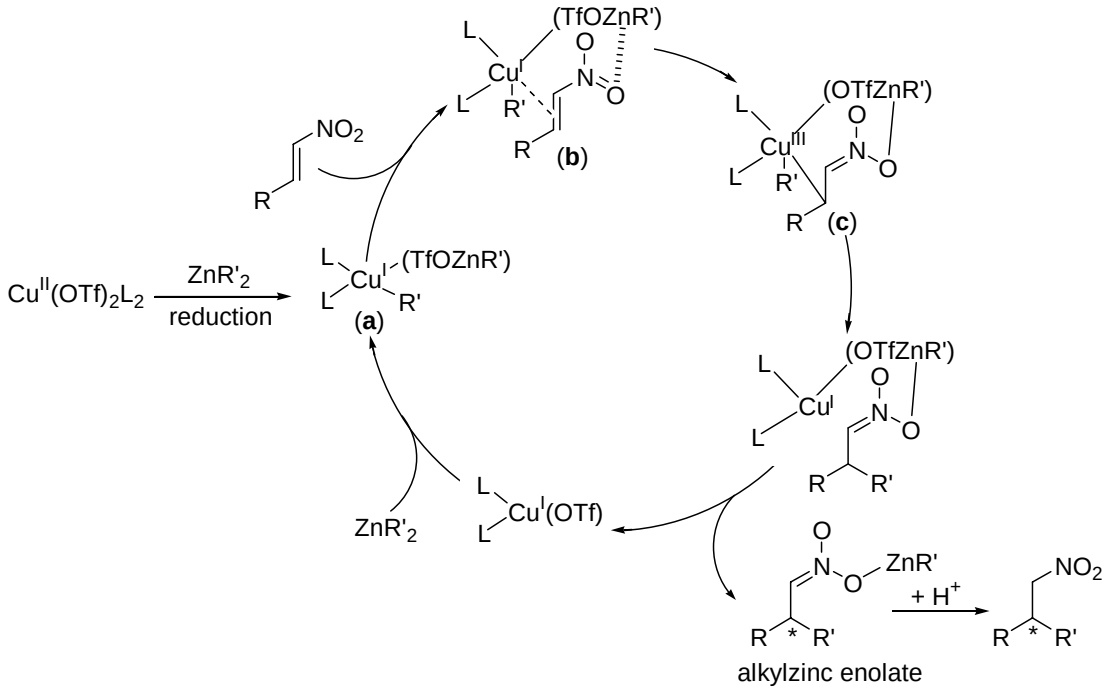

Scheme 4-7.

Plausible mechanism 2 (*cf*. conjugate addition to enone substrates, Feringa, B. L. **1997**)[2a]

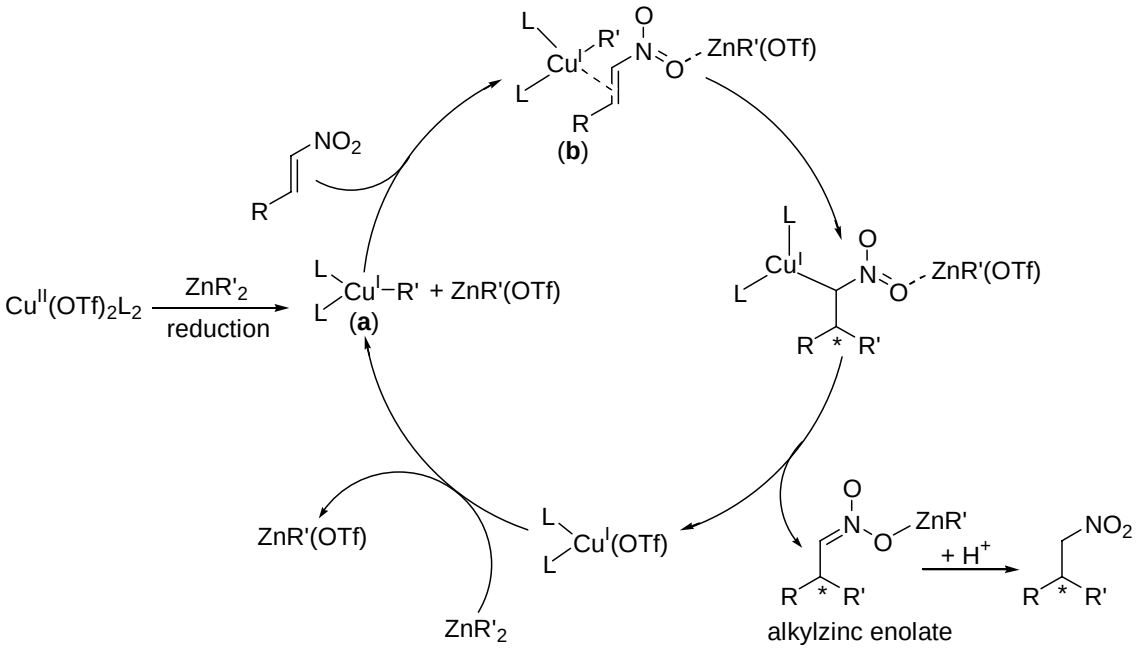

Scheme 4-8.

4-4. Conclusion

In summary, the complex with benzophenone-like phosphoramidites **4a** could be controlled to a chiral conformation by chiral amine built therein (Scheme 4-9). NMR analysis and DFT calculation of $PdCl_2$(**4a**)$_2$ complex shows that the Pd complex forms C_2 conformation, and phosphoramidite **4a** in the Pd complex adopts C_1-conformation. VT NMR analysis shows that the chiral conformation of Pd-phosphoramidite complex is kept up to 80 °C.

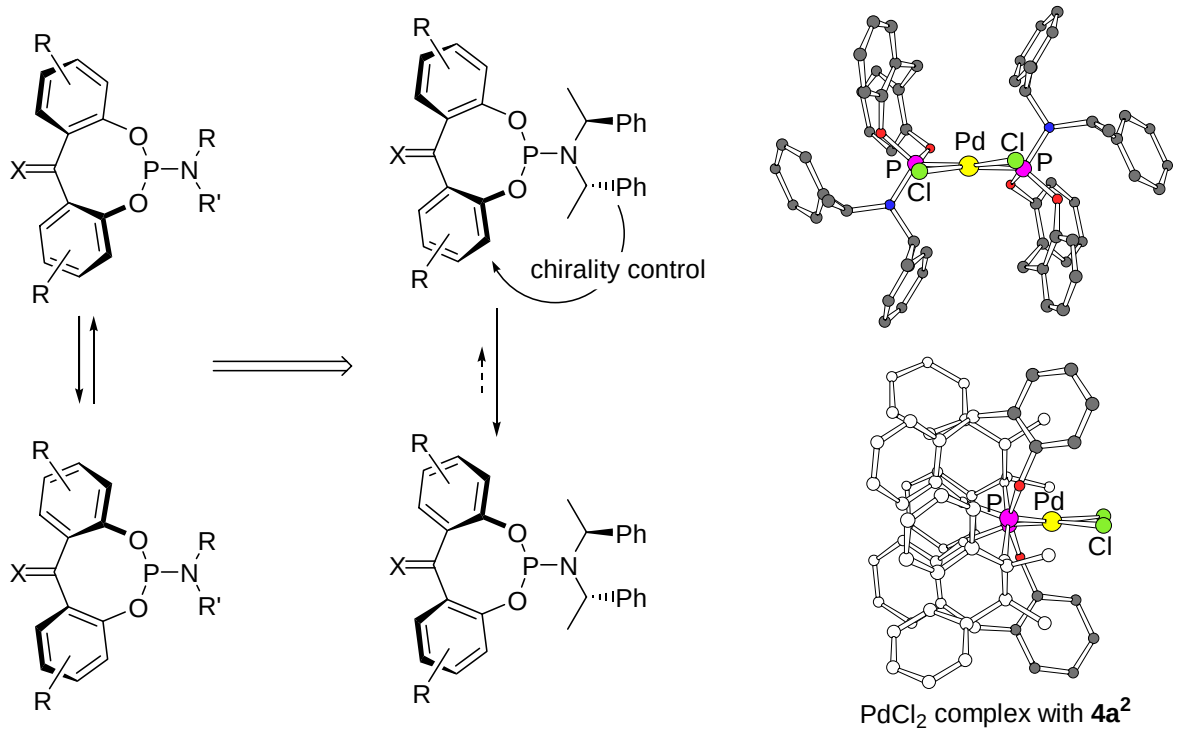

Scheme 4-9.

In addition, the benzophenone-like phosphoramidite **4a**[1] attained high catalytic activity and enantioselectivity in Cu-catalyzed conjugate addition to both nitrostyrene- and nitroacrylate-derived substrates (up to >99%, 99% *ee*). The flexible phosphoramidite **4a**[1] outperform the analogous rigid BINOL and BIPOL phosphoramidites (Scheme 4-10). These results represent emblematic cases of catalyst self-adaptation and tuning, where the highly conformationally mobile systems perform better than the rigid ones.

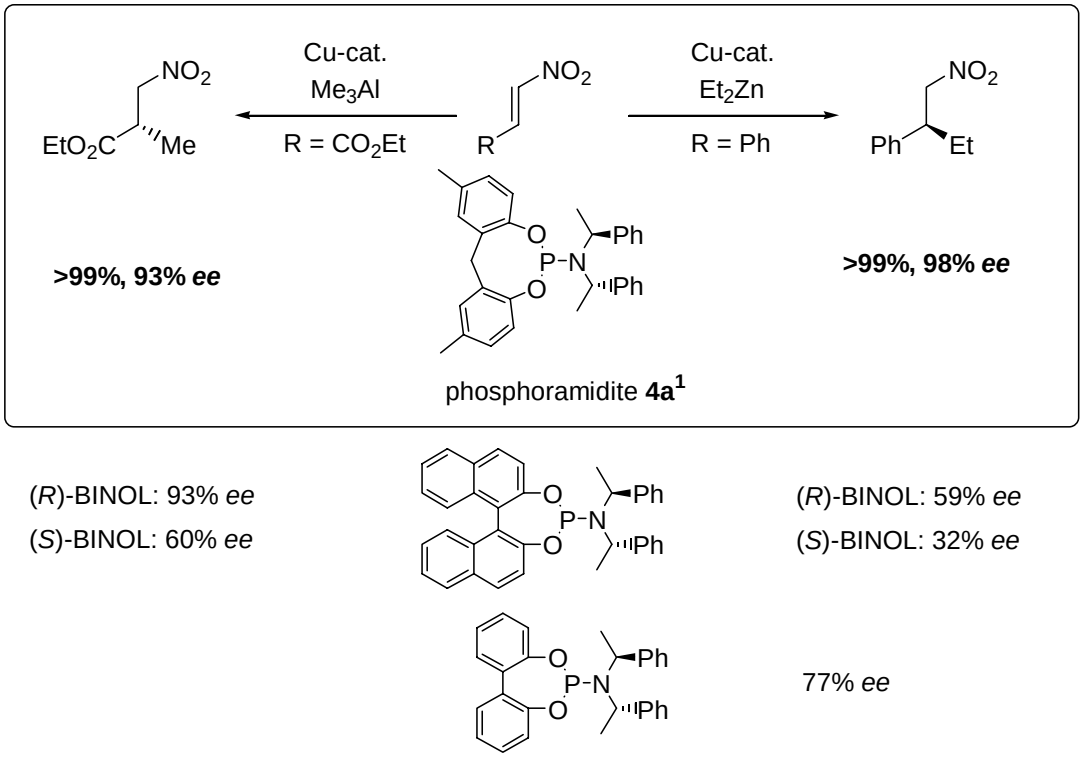
Cu-cat.
Me3Al
R = CO2Et
Cu-cat.
Et2Zn
R = Ph
NO2
EtO2C
Me
R
Ph
Et
>99%, 93% ee
>99%, 98% ee
O
P-N
O
Ph
Ph
phosphoramidite 4a1
(R)-BINOL: 93% ee
(S)-BINOL: 60% ee
(R)-BINOL: 59% ee
(S)-BINOL: 32% ee
77% ee

Scheme 4-10.

Experimental section for Chapter 4

Nitroalkene substrates were prepared by previously reported method.[15] 2,2'-methylenebis-(6-methylphenol) was prepared by previously reported method.[16]

$PdCl_2(4a^1)_2$: $(4a^1)_2$-PdCl2

To a mixture of (*S*,*S*)-*N*-(2,10-Dimethyl-12*H*-5,7-dioxa-6-phosphadibenzo[*a*,*d*]cycloocten-6-yl)-bis(1-phenylethyl)amine (**$4a^1$**) (9.6 mg, 0.02 mmol) and $PdCl_2$(cod) (2.8 mg, 0.01 mmol) was added CH_2Cl_2 (1 mL) at room temperature under an argon atmosphere. After stirred for 1 h, the reaction mixture was concentrated under reduced pressure to give $PdCl_2$(**$4a^1$**)$_2$ complex (11.1 mg, 98% yield).

^{1}H NMR ($CDCl_3$, 300 MHz) δ 1.09 (d, 12H, *J* = 7.2 Hz), 2.07 (s, 6H), 2.13 (s, 6H), 3.13 (d, 2H, *J* = 15.6 Hz), 5.31 (d, 2H, *J* = 15.6 Hz), 5.35 (q, 4H, *J* = 7.2 Hz), 6.17 (s, 2H), 6.60 (d, 2H, *J* = 8.4 Hz), 6.78 (d, 2H, *J* = 8.4 Hz), 6.81 (s, 2H), 6.82 (d, 2H, *J* = 8.4 Hz), 6.96 (d, 2H, *J* = 8.4 Hz), 7.30-7.39 (m, 12H), 7.56 (d, 8H, *J* = 6.9 Hz).
^{31}P NMR ($CDCl_3$, 121 MHz) δ 101.23.
$[\alpha]_D^{27}$ = -48 (c = 0.23 in $CHCl_3$).
m/z (ESI): Calcd for $PdHCl_2$(**$4a^1$**H)$_2$ $[M+3H]^{3+}$: 1138.3, 1139.3, 1140.3, 1141.3, 1142.3, 1143.3, 1144.3, 1145.3, 1146.3 1147.3, 1148.3. Found: 1138.2, 1139.3, 1140.3, 1141.3, 1142.2, 1143.3, 1144.3, 1145.3, 1146.3, 1147.2, 1148.3.

Cu-Catalyzed conjugate addition to benzalacetone[3c,17]

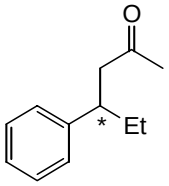

To a mixture of $Cu(OTf)_2$ (1.4 mg, 0.004 mmol) and (*S*,*S*)-*N*-(2,10-Dimethyl-12*H*-5,7-dioxa-6-phosphadibenzo[*a*,*d*]cycloocten-6-yl)bis(1-phenylethyl)amine (**$4a^1$**) (3.8 mg, 0.008 mmol) was added toluene (2 mL) at room temperature under an argon atmosphere in a Schlenk tube. After stirred for 30 min, to the solution was added benzalacetone (29.3 mg, 0.2 mmol) and cooled down to -40 °C. To the solution was added Et_2Zn (1.0 M in hexane, 240 μL, 0.24 mmol). After stirred for 12 h at -40 °C, to the reaction mixture was poured into saturated aq. NH_4Cl and the solution was extracted with Et_2O twice. The organic layer was dried over $MgSO_4$. After concentration under reduced pressure, the residue was purified by silica-gel chromatography (hexane/ethyl acetate = 4/1) to give 4-phenylhexan-2-one (30.3 mg, 86% yield).

^{1}H NMR ($CDCl_3$, 300 MHz) δ 0.82 (t, 3H, *J* = 7.5 Hz), 1.52-1.80 (m, 2H), 2.05 (s, 3H), 2.81 (d, *J* =

7.2 Hz, 2H), 2.95-3.13 (m, 1H), 7.10-7.42 (m, 5H).
HPLC (OD-H, hexanae/2-propanol = 99/1, 1.0 mL/min, detection UV = 212 nm), t_R = 7.8 min (*S*)/8.6 min (*R*).

Typical procedure for Cu-catalyzed conjugate addition to nitroalkene

To a mixture of $Cu(OTf)_2$ (1.4 mg, 0.004 mmol) and (*S*,*S*)-*N*-(2,10-Dimethyl-12*H*-5,7-dioxa-6-phosphadibenzo[*a*,*d*]cycloocten-6-yl)- bis(1-phenylethyl)amine (**4a**[1]) (3.8 mg, 0.008 mmol) was added toluene (2 mL) at room temperature under an argon atmosphere in a Schlenk tube. After stirred for 30 min, to the solution was added β-nitrostyrene (29.8 mg, 0.2 mmol) and cooled down to -78 °C. To the solution was added Et_2Zn (1.0 M in hexane, 240 μL, 0.24 mmol). After stirred for 3 h at -78 °C, to the reaction mixture was poured into saturated aq. NH_4Cl and the solution was extracted with Et_2O twice. The organic layer was dried over $MgSO_4$. After concentration under reduced pressure, the residue was purified by silica-gel chromatography (hexane/ethyl acetate = 5/1) to give 1-nitromethyl-propylbenzene (35.2 mg, 99% yield).

Typical procedure for Cu-catalyzed conjugate addition to nitroacrylate

To a mixture of $Cu(OTf)_2$ (1.4 mg, 0.004 mmol) and (*S*,*S*)-*N*-(2,10-Dimethyl-12*H*-5,7-dioxa-6-phosphadibenzo[*a*,*d*]cycloocten-6-yl)- bis(1-phenylethyl)amine (**4a**[1]) (3.8 mg, 0.008 mmol) was added Et_2O (2 mL) at room temperature under an argon atmosphere in a Schlenk tube. After stirred for 30 min, to the solution was added 3-nitroacrylic acid ethyl ester (29.8 mg, 0.2 mmol) and cooled down to -78 °C. To the reaction mixture was added Me_3Al (1.0 M in hexane, 240 μL, 0.24 mmol). After stirred for 1.5 h at -78 °C, to the reaction mixture was poured into 1*N* aq. HCl and the solution was extracted with Et_2O twice. The organic layer was dried over $MgSO_4$. After concentration under reduced pressure, the residue was purified by silica-gel chromatography (hexane/ethyl acetate = 2/1) to give 2-methyl-3-nitropropionic acid ethyl ester (32.1 mg, 99% yield).

(*S*)-2-Phenyl-1-nitrobutane[18]

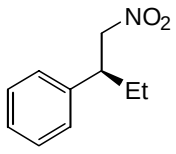

^{1}H NMR ($CDCl_3$, 300 MHz) δ 0.86 (t, 3H, *J* = 7.5 Hz), 1.59-1.82 (m, 2H), 3.31-3.43 (m, 1H), 4.56-4.60 (m, 2H), 7.13-7.39 (m, 5H).
$[\alpha]_D^{27}$ = -34 (c = 0.35 in $CHCl_3$) for a sample that is 98% *ee*.
HPLC (OD-H, hexanae/2-propanol = 98/2, 1.0 mL/min, detection UV = 212 nm), t_R = 12.3 min (*R*)/19.8 min (*S*).

(*S*)-2-Phenyl-1-nitropentane[19]

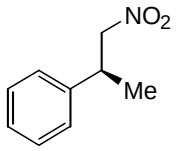

^{1}H NMR ($CDCl_3$, 300 MHz) δ 1.58 (d, 2H, *J* = 6.9 Hz), 3.36-3.53 (m, 1H), 4.48-4.55 (m, 2H), 7.10-7.38 (m, 5H).
HPLC (OD-H, hexanae/2-propanol = 98/2, 1.0 mL/min, detection UV = 212 nm), t_R = 13.6 min (*R*)/19.4 min (*S*).

(*S*)-2-(4-Methylphenyl)-1-nitrobutane[3e]

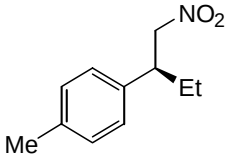

^{1}H NMR ($CDCl_3$, 300MHz) δ 0.88 (t, 3H, *J* = 7.5 Hz), 1.65-1.85 (m, 2H), 2.35 (s, 3H), 3.29-3.39 (m, 1H), 4.50-4.62 (m, 2H), 7.09 (d, 2H, *J* = 7.8 Hz), 7.16 (d, 2H, *J* = 7.8 Hz).
HPLC (OD-H, hexanae/2-propanol = 98/2, 1.0 mL/min, detection UV = 212 nm), t_R = 9.6 min (*R*)/16.3 min (*S*).

(*S*)-2-(4-Methoxylphenyl)-1-nitrobutane[19]

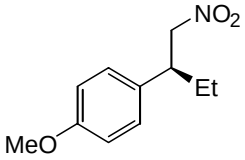

^{1}H NMR ($CDCl_3$, 300 MHz) δ 0.88 (t, 3H, *J* = 7.5 Hz), 1.59-1.78 (m, 2H), 3.28-3.38 (m, 1H), 3.81 (s, 3H), 4.48-4.61 (m, 2H), 6.89 (d, 2H, *J* = 8.7 Hz), 7.12 (d, 2H, *J* = 8.7 Hz).
HPLC (OD-H, hexanae/2-propanol = 98/2, 1.0 mL/min, detection UV = 212 nm), t_R = 13.7 min (*R*)/23.0 min (*S*).

(*S*)-2-(3-Methoxylphenyl)-1-nitrobutane[19]

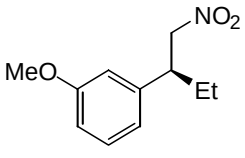

^{1}H NMR ($CDCl_3$, 300 MHz) δ 0.86 (t, 3H, *J* = 7.5 Hz), 1.67-1.84 (m, 2H), 3.30-3.40 (m, 1H), 3.82 (s, 3H), 4.55-4.59 (m, 2H), 6.73-6.85 (m, 3H), 7.25-7.30 (m, 1H).
HPLC (OD-H, hexanae/2-propanol = 98/2, 1.0 mL/min, detection UV = 212 nm), t_R = 22.6 min (*R*)/60.8 min (*S*).

(*S*)-2-(2-Methoxylphenyl)-1-nitrobutane[3e]

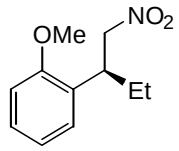

^{1}H NMR ($CDCl_3$, 300 MHz) δ 0.86 (t, 3H, *J* = 7.5 Hz), 1.70-1.91 (m, 2H), 3.65-3.82 (m, 1H), 3.86 (s, 3H), 4.58-4.73 (m, 2H), 6.89-6.97 (m, 2H), 7.11-7.14 (m, 1H), 7.24-7.27 (m, 1H).
HPLC (OD-H, hexanae/2-propanol = 98/2, 1.0 mL/min, detection UV = 212 nm), t_R = 9.3 min (*R*)/11.4 min (*S*).

(*S*)-2-(4-Trifluoromethylphenyl)-1-nitrobutane[19]

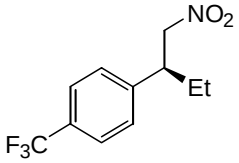

^{1}H NMR ($CDCl_3$, 300 MHz) δ 0.87 (t, 3H, *J* = 7.5 Hz), 1.67-1.87 (m, 2H), 3.42-3.52 (m, 1H), 4.54-4.68 (m, 2H), 7.11-7.14 (m, 2H), 7.24-7.27 (m, 2H).
^{19}F NMR ($CDCl_3$, 282 MHz) δ -62.61.
HPLC (OD-H, hexanae/2-propanol = 98/2, 1.0 mL/min, detection UV = 212 nm), t_R = 10.96 min (*R*)/13.73 min (*S*).

(*S*)-2-(4-Chlorophenyl)-1-nitrobutane[19]

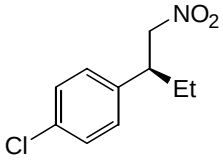

^{1}H NMR ($CDCl_3$, 300 MHz) δ 0.88 (t, 3H, *J* = 7.5 Hz), 1.65-1.84 (m, 2H), 3.32-3.42 (m, 1H), 4.49-4.63 (m, 2H), 7.14 (d, 2H, *J* = 6.6 Hz), 7.33 (d, 2H, *J* = 6.6 Hz).
HPLC (OD-H, hexanae/2-propanol = 98/2, 1.0 mL/min, detection UV = 212 nm), t_R = 12.2 min (*R*)/18.2 min (*S*).

(*R*)-2-(Furan-2-yl)-1-nitrobutane[18]

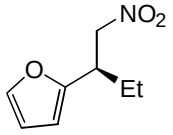

^{1}H NMR ($CDCl_3$, 300 MHz) δ 0.93 (t, 3H, *J* = 7.5 Hz), 1.70-1.84 (m, 2H), 3.49-3.59 (m, 1H), 4.52-4.68 (m, 2H), 6.16 (d, 2H, *J* = 3.0 Hz), 6.32 (dd, 1H, *J* = 3.0, 2.4 Hz), 7.37 (d, 1H, *J* = 2.4 Hz).
HPLC (OB-H, hexanae/2-propanol = 98/2, 1.0 mL/min, detection UV = 212 nm), t_R = 11.8 min

(*S*)/12.7 min (*R*).

(*R*)-2-(Thiophen-2-yl)-1-nitrobutane[18]

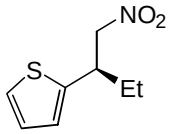

^{1}H NMR ($CDCl_3$, 300 MHz) δ 0.96 (t, 3H, *J* = 7.2 Hz), 1.59-1.85 (m, 2H), 3.68-3.79 (m, 1H), 4.52-4.64 (m, 2H), 6.90-6.92 (m, 1H), 6.96-6.99 (m, 1H), 7.23-7.28 (m, 1H).
HPLC (AD-H, hexanae/2-propanol = 98/2, 1.0 mL/min, detection UV = 212 nm), t_R = 9.5 min (*S*)/10.1 min (*R*).

(*S*)-2-Methyl-3-nitropropionic acid ethyl ester[8c]

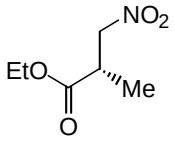

^{1}H NMR ($CDCl_3$, 300 MHz) δ 1.29 (t, 3H, *J* = 6.9 Hz), 1.30 (d, 3H, *J* = 7.2 Hz), 3.21-3.22 (m, 1H), 4.22 (q, 2H, *J* = 6.9 Hz), 4.42 (dd, 1H, *J* = 14.1, 8.1 Hz), 4.74 (dd, 1H, *J* = 14.1, 5.7 Hz).
^{13}C NMR ($CDCl_3$, 121 MHz) δ 14.05, 14.35, 37.63, 61.50, 76.42, 172.41.
$[\alpha]_D^{27}$ = -9.0 (c = 0.35 in $CHCl_3$) for a sample that is 93% *ee*.
HPLC (OD-H, hexanae/2-propanol = 98/2, 1.0 mL/min, detection UV = 212 nm), t_R = 9.5 min (*R*)/10.6 min (*S*).

(*S*)-β^2-alanine ethyl ester[8c,20]

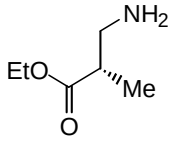

100-mL autoclave was charged with 5% palladium on charcoal (10.0 mg). After replaced by an argon, a solution of (*S*)-2-methyl-3-nitropropionic acid ethyl ester (16.1 mg, 0.1 mmol, 93% *ee*) in ethanol (2 mL) was added to the autoclave at room temperature under a stream of argon. Hydrogen was introduced at a pressure of 20 atm. After stirred vigorously for 4 h, the reaction mixture was filtered through Celite®. To the filtrate was concentrated under reduced pressure to give (*S*)-β^2-alanine ethyl ester (6.8 mg, 52% yield).

^{1}H NMR ($CDCl_3$, 300 MHz) δ 1.17 (d, 3H, *J* = 6.9 Hz), 1.28 (t, 3H, *J* = 6.9 Hz), 1.62 (br, 2H), 2.50-2.54 (m, 1H), 2.80 (dd, 1H, *J* = 12.6, 3.9 Hz), 2.97 (dd, 1H, *J* = 12.6, 7.5 Hz) 4.18 (q, 2H, *J* = 6.9 Hz).

^{13}C NMR ($CDCl_3$, 121 MHz) δ 13.82, 14.15, 34.56, 37.83, 47.59, 170.41.

Computational Methods

All the calculations in Chapter 4 were performed with GAUSSIAN 03 program package. All the structures were optimized at B3LYP/631SDD (SDD for Pd and Cu, 6-31G(d) for others) level. The optimized geometries were verified as an equilibrium structures having no imaginary frequency.

$PdCl_2$ complex with phosphoramidite 4a^2 (Figure 4-3 p.121)

4a^2: (*S*,*S*)-*N*-(12*H*-5,7-dioxa-6-phosphadibenzo[*a*,*d*]cycloocten-6-yl)bis(1-phenylethyl)amine
Charge = 0, Multiplicity = 1
SCF Done: E(B3LYP/631SDD) = -4385.45014891 a.u.

Center Number	Atomic Number	Atomic Type	Coordinates (Angstroms) X	Y	Z
1	6	0	2.595115	2.526728	1.575230
2	6	0	1.983767	3.353260	0.463394
3	6	0	2.696598	3.400900	-0.879041
4	6	0	2.900698	4.648020	-1.490088
5	6	0	3.483413	4.771162	-2.749982
6	6	0	3.878416	3.625682	-3.440818
7	6	0	3.693443	2.373091	-2.860930
8	6	0	3.111686	2.269089	-1.596858
9	8	0	3.084370	0.988328	-1.035963
10	6	0	2.285871	1.168150	1.730031
11	6	0	2.757849	0.426422	2.810850
12	6	0	3.567751	1.043139	3.763649
13	6	0	3.904175	2.390556	3.627011
14	6	0	3.417851	3.118406	2.541827
15	8	0	1.405665	0.563834	0.823808
16	6	0	-2.594624	-2.526840	1.576026
17	6	0	-1.981190	-3.354496	0.466187
18	6	0	-2.691924	-3.404297	-0.877293
19	6	0	-2.893678	-4.652347	-1.487247
20	6	0	-3.474124	-4.777605	-2.747977
21	6	0	-3.869145	-3.633362	-3.440857
22	6	0	-3.686562	-2.379907	-2.862087
23	6	0	-3.107180	-2.273802	-1.597089

24	8	0	-3.082007	-0.992265	-1.037828
25	6	0	-2.286612	-1.167822	1.729217
26	6	0	-2.760577	-0.424836	2.808313
27	6	0	-3.571318	-1.040748	3.760919
28	6	0	-3.906585	-2.388604	3.625812
29	6	0	-3.418260	-3.117704	2.542362
30	8	0	-1.405601	-0.564460	0.823085
31	1	0	0.958977	3.003849	0.303911
32	1	0	1.889386	4.383979	0.819729
33	1	0	2.589848	5.541733	-0.954108
34	1	0	3.624401	5.755268	-3.187848
35	1	0	4.324750	3.699855	-4.428015
36	1	0	3.965720	1.464735	-3.383196
37	1	0	2.496764	-0.621896	2.891583
38	1	0	3.940554	0.465523	4.604076
39	1	0	4.535036	2.875825	4.366521
40	1	0	3.662326	4.173690	2.444346
41	46	0	0.001222	-0.001555	-2.099134
42	17	0	-1.635782	0.253682	-3.790453
43	17	0	1.640416	-0.261020	-3.787702
44	15	0	1.846666	-0.005964	-0.676953
45	7	0	2.671677	-1.456858	-0.527243
46	6	0	4.152931	-1.723845	-0.611231
47	6	0	1.800004	-2.677072	-0.550176
48	6	0	4.999273	-1.172908	0.539183
49	6	0	4.753083	-1.429742	-1.994717
50	6	0	1.944847	-3.491400	0.738452
51	6	0	5.214634	-1.982180	1.665519
52	6	0	6.067246	-1.577517	2.693057
53	6	0	6.723934	-0.348583	2.612622
54	6	0	6.515554	0.468531	1.500719
55	6	0	5.664974	0.059120	0.472599
56	6	0	2.601709	-4.727509	0.782805
57	6	0	2.716237	-5.437121	1.983177
58	6	0	2.163570	-4.926413	3.156878
59	6	0	1.490003	-3.701690	3.123189
60	6	0	1.384909	-2.993915	1.926653
61	6	0	1.951638	-3.493295	-1.841316
62	1	0	4.193357	-2.808329	-0.484495
63	1	0	0.774239	-2.291920	-0.558432

64	1	0	4.817444	-0.361945	-2.201424
65	1	0	4.145985	-1.880825	-2.782285
66	1	0	5.765323	-1.848164	-2.039818
67	1	0	4.717600	-2.946375	1.732188
68	1	0	6.226230	-2.228401	3.549260
69	1	0	7.396127	-0.032441	3.406256
70	1	0	7.021441	1.427562	1.426919
71	1	0	5.527075	0.704052	-0.387262
72	1	0	3.025025	-5.153070	-0.121685
73	1	0	3.233362	-6.393081	1.994160
74	1	0	2.246979	-5.480356	4.088058
75	1	0	1.039123	-3.301223	4.027359
76	1	0	0.855326	-2.045043	1.907120
77	1	0	2.956207	-3.909552	-1.966723
78	1	0	1.243473	-4.329450	-1.832592
79	1	0	1.735038	-2.859805	-2.704826
80	15	0	-1.845506	0.003468	-0.678683
81	7	0	-2.672160	1.453717	-0.531611
82	6	0	-4.153557	1.718761	-0.619454
83	6	0	-1.801638	2.674717	-0.555903
84	6	0	-5.000228	1.176394	0.534828
85	6	0	-4.752073	1.411993	-2.000856
86	6	0	-1.950650	3.494167	0.729027
87	6	0	-5.215400	1.993272	1.655698
88	6	0	-6.067738	1.595468	2.686148
89	6	0	-6.724349	0.365960	2.614195
90	6	0	-6.515960	-0.458760	1.507919
91	6	0	-5.665535	-0.056283	0.476930
92	6	0	-2.604411	4.732180	0.765475
93	6	0	-2.722648	5.446829	1.962494
94	6	0	-2.176740	4.939343	3.140745
95	6	0	-1.506121	3.712818	3.114963
96	6	0	-1.397321	3.000065	1.921715
97	6	0	-1.950217	3.485652	-1.850720
98	1	0	-0.956266	-3.004843	0.307812
99	1	0	-1.886921	-4.384700	0.824034
100	1	0	-2.582782	-5.545106	-0.949705
101	1	0	-3.613319	-5.762384	-3.184903
102	1	0	-4.313678	-3.709163	-4.428743
103	1	0	-3.958870	-1.472424	-3.385854

104	1	0	-2.500398	0.623766	2.887927
105	1	0	-3.945697	-0.462165	4.599978
106	1	0	-4.538123	-2.873232	4.365166
107	1	0	-3.661906	-4.173290	2.446062
108	1	0	-4.195332	2.804310	-0.502860
109	1	0	-0.775548	2.290382	-0.559958
110	1	0	-4.815796	0.342434	-2.198276
111	1	0	-4.144215	1.856501	-2.791607
112	1	0	-5.764407	1.829638	-2.050741
113	1	0	-4.718381	2.957868	1.715816
114	1	0	-6.226587	2.252120	3.537961
115	1	0	-7.396360	0.055154	3.410090
116	1	0	-7.021585	-1.418423	1.440840
117	1	0	-5.527307	-0.707270	-0.378342
118	1	0	-3.022416	5.155271	-0.142638
119	1	0	-3.237315	6.404167	1.967313
120	1	0	-2.262997	5.497183	4.069337
121	1	0	-1.060311	3.314835	4.022735
122	1	0	-0.869809	2.049948	1.908338
123	1	0	-2.954714	3.900683	-1.980753
124	1	0	-1.242648	4.322319	-1.843363
125	1	0	-1.730719	2.848792	-2.711016

$PdCl_2$ with phosphoramidite 4c (Figure 4-3 p.121)

4c: (*S*,*S*)-*N*-(5,7-dioxa-6-phosphadibenzo[*a*,*c*]cyclohepten-6-yl)bis(1-phenylethyl)amine

Charge = 0, Multiplicity = 1

SCF Done: E(B3LYP/631SDD) = -4306.85463326 a.u.

Center Number	Atomic Number	Atomic Type	Coordinates (Angstroms) X	Y	Z
1	46	0	-0.000034	-0.000112	-2.317042
2	17	0	-1.678648	0.091390	-3.992425
3	17	0	1.678620	-0.091606	-3.992369
4	15	0	-1.782672	-0.121774	-0.858170
5	8	0	-1.244546	-0.730400	0.594239
6	8	0	-2.912359	-1.249188	-1.217809

7	7	0	-2.713757	1.244152	-0.668317
8	6	0	-1.994442	-1.450784	1.519494
9	6	0	-2.125800	-0.908433	2.797135
10	6	0	-2.731795	-1.652322	3.807115
11	6	0	-3.205087	-2.937455	3.534013
12	6	0	-3.077139	-3.464719	2.252049
13	6	0	-2.467785	-2.739963	1.212827
14	6	0	-2.322186	-3.337575	-0.133859
15	6	0	-2.004732	-4.699478	-0.289424
16	6	0	-1.906066	-5.283296	-1.550103
17	6	0	-2.121433	-4.513788	-2.696512
18	6	0	-2.429634	-3.159260	-2.577741
19	6	0	-2.523853	-2.591704	-1.308195
20	6	0	-4.217779	1.348850	-0.620120
21	6	0	-4.881321	0.972202	-1.953586
22	6	0	-4.874350	0.703648	0.602004
23	6	0	-4.967695	1.441636	1.792464
24	6	0	-5.631896	0.929042	2.906604
25	6	0	-6.220360	-0.335730	2.850201
26	6	0	-6.135137	-1.079780	1.673173
27	6	0	-5.469823	-0.563975	0.559127
28	6	0	-1.970288	2.549360	-0.771642
29	6	0	-2.307703	3.315693	-2.056098
30	6	0	-2.112064	3.361875	0.517382
31	6	0	-2.869979	4.536703	0.594708
32	6	0	-2.976556	5.243246	1.797739
33	6	0	-2.315809	4.790800	2.938960
34	6	0	-1.543192	3.627283	2.870425
35	6	0	-1.447254	2.921612	1.672757
36	15	0	1.782567	0.121629	-0.858140
37	7	0	2.713806	-1.244196	-0.668264
38	8	0	1.244319	0.730201	0.594235
39	8	0	2.912163	1.249129	-1.217757
40	6	0	1.994206	1.450512	1.519560
41	6	0	2.125591	0.908066	2.797155
42	6	0	2.731582	1.651899	3.807181
43	6	0	3.204832	2.937066	3.534169
44	6	0	3.076851	3.464426	2.252247
45	6	0	2.467505	2.739728	1.212983
46	6	0	2.321884	3.337418	-0.133668

47	6	0	2.004355	4.699312	-0.289154
48	6	0	1.905650	5.283197	-1.549800
49	6	0	2.121049	4.513768	-2.696255
50	6	0	2.429322	3.159249	-2.577564
51	6	0	2.523590	2.591629	-1.308051
52	6	0	4.217841	-1.348745	-0.620333
53	6	0	4.881104	-0.972191	-1.953963
54	6	0	4.874563	-0.703309	0.601590
55	6	0	4.967975	-1.441028	1.792213
56	6	0	5.632313	-0.928219	2.906173
57	6	0	6.220850	0.336503	2.849426
58	6	0	6.135563	1.080286	1.672234
59	6	0	5.470116	0.564265	0.558368
60	6	0	1.970368	-2.549447	-0.771286
61	6	0	2.307593	-3.315961	-2.055688
62	6	0	2.112327	-3.361800	0.517814
63	6	0	2.870891	-4.536195	0.595381
64	6	0	2.977624	-5.242586	1.798485
65	6	0	2.316400	-4.790418	2.939542
66	6	0	1.543143	-3.627343	2.870767
67	6	0	1.447041	-2.921823	1.673021
68	1	0	-1.748247	0.091500	2.980251
69	1	0	-2.837880	-1.225800	4.800399
70	1	0	-3.685385	-3.522284	4.313231
71	1	0	-3.470048	-4.453644	2.034651
72	1	0	-1.813545	-5.295000	0.598225
73	1	0	-1.655102	-6.336663	-1.637197
74	1	0	-2.043389	-4.961224	-3.683024
75	1	0	-2.585080	-2.527587	-3.445356
76	1	0	-4.370337	2.422925	-0.485305
77	1	0	-4.419453	1.522063	-2.776614
78	1	0	-4.786459	-0.089812	-2.181048
79	1	0	-5.946713	1.226443	-1.910413
80	1	0	-4.526162	2.432996	1.842634
81	1	0	-5.698490	1.523398	3.814435
82	1	0	-6.745441	-0.735579	3.713870
83	1	0	-6.591465	-2.064527	1.616423
84	1	0	-5.421373	-1.153864	-0.349059
85	1	0	-0.911732	2.277472	-0.846249
86	1	0	-2.092006	2.690231	-2.925974

87	1	0	-3.357855	3.620911	-2.105600
88	1	0	-1.691825	4.219905	-2.112635
89	1	0	-3.379137	4.916553	-0.285569
90	1	0	-3.573189	6.150998	1.836041
91	1	0	-2.393465	5.342971	3.871807
92	1	0	-1.007682	3.274159	3.747857
93	1	0	-0.845431	2.019024	1.624670
94	1	0	1.748071	-0.091893	2.980204
95	1	0	2.837696	1.225307	4.800433
96	1	0	3.685118	3.521851	4.313428
97	1	0	3.469726	4.453380	2.034919
98	1	0	1.813130	5.294769	0.598530
99	1	0	1.654634	6.336557	-1.636829
100	1	0	2.042971	4.961256	-3.682741
101	1	0	2.584794	2.527632	-3.445216
102	1	0	4.370537	-2.422785	-0.485415
103	1	0	4.419242	-1.522297	-2.776829
104	1	0	4.785965	0.089761	-2.181603
105	1	0	5.946562	-1.226176	-1.910897
106	1	0	4.526405	-2.432358	1.842651
107	1	0	5.698952	-1.522371	3.814134
108	1	0	6.746028	0.736523	3.712957
109	1	0	6.591952	2.064990	1.615211
110	1	0	5.421615	1.153953	-0.349944
111	1	0	0.911798	-2.277583	-0.845764
112	1	0	2.091679	-2.690662	-2.925628
113	1	0	3.357764	-3.621084	-2.105354
114	1	0	1.691794	-4.220243	-2.111952
115	1	0	3.380424	-4.915833	-0.284774
116	1	0	3.574749	-6.150007	1.836973
117	1	0	2.394173	-5.342483	3.872444
118	1	0	1.007257	-3.274453	3.748063
119	1	0	0.844710	-2.019583	1.624740

Cu(II) complex with phosphoramidite 4a^2 (Figure 4-4 p.122)

4a^2: (*S*,*S*)-*N*-(12*H*-5,7-dioxa-6-phosphadibenzo[*a*,*d*]cycloocten-6-yl)bis(1-phenylethyl)amine

Charge = 2, Multiplicity = 2

Total electronic energy: E(B3LYP/631SDD) = -3533.89831066 a.u.

Center Number	Atomic Number	Atomic Type	Coordinates (Angstroms) X	Y	Z
1	6	0	2.298246	2.774447	2.208490
2	6	0	0.923366	2.881104	1.575558
3	6	0	0.851028	3.550375	0.207906
4	6	0	-0.005493	4.642318	0.005213
5	6	0	-0.094566	5.286328	-1.230010
6	6	0	0.679543	4.842957	-2.303670
7	6	0	1.532739	3.751569	-2.136805
8	6	0	1.606016	3.124600	-0.894815
9	8	0	2.548125	2.086522	-0.771924
10	6	0	3.130454	1.652338	2.036045
11	6	0	4.354051	1.524219	2.722992
12	6	0	4.770092	2.532336	3.585596
13	6	0	3.977105	3.669422	3.749928
14	6	0	2.755553	3.777423	3.066465
15	8	0	2.762663	0.571749	1.254118
16	6	0	-2.298370	-2.774513	2.208469
17	6	0	-0.923496	-2.881222	1.575532
18	6	0	-0.851164	-3.550449	0.207854
19	6	0	0.005385	-4.642363	0.005119
20	6	0	0.094466	-5.286328	-1.230127
21	6	0	-0.679664	-4.842943	-2.303767
22	6	0	-1.532889	-3.751585	-2.136860
23	6	0	-1.606172	-3.124657	-0.894849
24	8	0	-2.548288	-2.086590	-0.771910
25	6	0	-3.130534	-1.652364	2.036053
26	6	0	-4.354108	-1.524195	2.723037
27	6	0	-4.770174	-2.532302	3.585641
28	6	0	-3.977237	-3.669427	3.749938
29	6	0	-2.755704	-3.777476	3.066445
30	8	0	-2.762739	-0.571789	1.254115
31	1	0	0.471546	1.878047	1.535974
32	1	0	0.281747	3.451118	2.254252
33	1	0	-0.606081	4.997995	0.837992
34	1	0	-0.757373	6.137840	-1.347011
35	1	0	0.630954	5.346082	-3.264428
36	1	0	2.153846	3.392939	-2.951019

37	1	0	4.945923	0.630315	2.564130
38	1	0	5.708080	2.432049	4.121904
39	1	0	4.291246	4.466621	4.416114
40	1	0	2.134202	4.654467	3.226265
41	29	0	0.000035	-0.000235	-0.332968
42	15	0	2.179682	0.564718	-0.311587
43	7	0	3.147461	-0.412824	-1.224514
44	6	0	4.531738	-0.099325	-1.751240
45	6	0	2.639093	-1.806709	-1.495993
46	6	0	5.538902	0.350022	-0.693495
47	6	0	4.475809	0.822501	-2.978347
48	6	0	3.515379	-2.861003	-0.819439
49	6	0	6.317545	-0.623778	-0.038613
50	6	0	7.322109	-0.261407	0.868717
51	6	0	7.570592	1.083563	1.131290
52	6	0	6.799285	2.061912	0.490573
53	6	0	5.793617	1.696230	-0.417392
54	6	0	4.261793	-3.796976	-1.545301
55	6	0	5.046576	-4.749696	-0.886089
56	6	0	5.089620	-4.783802	0.508866
57	6	0	4.343861	-3.858096	1.244799
58	6	0	3.567223	-2.906347	0.585650
59	6	0	2.391581	-2.022565	-2.992315
60	1	0	4.884784	-1.075024	-2.093873
61	1	0	1.655914	-1.862704	-1.006899
62	1	0	4.132671	1.827263	-2.727589
63	1	0	3.802520	0.411062	-3.735292
64	1	0	5.475661	0.903174	-3.416883
65	1	0	6.157067	-1.674769	-0.259632
66	1	0	7.920456	-1.033191	1.343640
67	1	0	8.363434	1.374116	1.813984
68	1	0	6.988064	3.114014	0.682262
69	1	0	5.227265	2.477039	-0.912411
70	1	0	4.236504	-3.800930	-2.630075
71	1	0	5.620550	-5.465873	-1.466650
72	1	0	5.696231	-5.526552	1.018309
73	1	0	4.369668	-3.877878	2.330672
74	1	0	3.005726	-2.180872	1.169694
75	1	0	3.308397	-1.969211	-3.586467
76	1	0	1.940025	-3.005892	-3.154844

77	1	0	1.702716	-1.260500	-3.370328
78	15	0	-2.179713	-0.564810	-0.311581
79	7	0	-3.147399	0.412827	-1.224494
80	6	0	-4.531696	0.099436	-1.751237
81	6	0	-2.638919	1.806679	-1.495946
82	6	0	-5.538894	-0.349871	-0.693510
83	6	0	-4.475813	-0.822395	-2.978341
84	6	0	-3.515194	2.861030	-0.819466
85	6	0	-6.317557	0.623952	-0.038685
86	6	0	-7.322144	0.261611	0.868630
87	6	0	-7.570633	-1.083350	1.131242
88	6	0	-6.799308	-2.061721	0.490577
89	6	0	-5.793615	-1.696070	-0.417370
90	6	0	-4.261556	3.796997	-1.545390
91	6	0	-5.046334	4.749765	-0.886241
92	6	0	-5.089428	4.783924	0.508711
93	6	0	-4.343723	3.858222	1.244706
94	6	0	-3.567087	2.906428	0.585620
95	6	0	-2.391289	2.022508	-2.992251
96	1	0	-0.471623	-1.878185	1.535991
97	1	0	-0.281909	-3.451290	2.254211
98	1	0	0.605985	-4.998055	0.837883
99	1	0	0.757292	-6.137821	-1.347160
100	1	0	-0.631068	-5.346035	-3.264541
101	1	0	-2.154013	-3.392945	-2.951056
102	1	0	-4.945937	-0.630259	2.564202
103	1	0	-5.708142	-2.431976	4.121977
104	1	0	-4.291397	-4.466618	4.416123
105	1	0	-2.134389	-4.654548	3.226225
106	1	0	-4.884669	1.075163	-2.093861
107	1	0	-1.655780	1.862620	-1.006773
108	1	0	-4.132697	-1.827166	-2.727584
109	1	0	-3.802528	-0.410977	-3.735303
110	1	0	-5.475676	-0.903043	-3.416854
111	1	0	-6.157069	1.674936	-0.259734
112	1	0	-7.920504	1.033410	1.343512
113	1	0	-8.363493	-1.373880	1.813925
114	1	0	-6.988094	-3.113816	0.682296
115	1	0	-5.227246	-2.476893	-0.912349
116	1	0	-4.236224	3.800910	-2.630163

117	1	0	-5.620265	5.465938	-1.466849
118	1	0	-5.696034	5.526711	1.018105
119	1	0	-4.369570	3.878045	2.330577
120	1	0	-3.005630	2.180958	1.169708
121	1	0	-3.308069	1.969210	-3.586463
122	1	0	-1.939656	3.005805	-3.154755
123	1	0	-1.702451	1.260393	-3.370211

Cu(II) complex with phosphoramidite 4c (Figure 4-4 page.122)

4c: (*S*,*S*)-*N*-(5,7-dioxa-6-phosphadibenzo[*a*,*c*]cyclohepten-6-yl)bis(1-phenylethyl)amine

Charge = 2, Multiplicity = 2

Total electronic energy: E(B3LYP/631SDD) = -3455.29849221 a.u.

Center Number	Atomic Number	Atomic Type	Coordinates (Angstroms) X	Y	Z
1	6	0	-4.137119	-2.723621	-0.119605
2	6	0	-3.339766	-2.973763	-1.331928
3	6	0	-3.125948	-4.296135	-1.781749
4	6	0	-2.417676	-4.567579	-2.946247
5	6	0	-1.900917	-3.517171	-3.712973
6	6	0	-2.090681	-2.197957	-3.297617
7	6	0	-2.791275	-1.941105	-2.122823
8	8	0	-3.030200	-0.596911	-1.806296
9	6	0	-3.818966	-1.704873	0.817373
10	6	0	-4.558827	-1.514880	1.979986
11	6	0	-5.653207	-2.335206	2.237110
12	6	0	-5.996923	-3.354199	1.330696
13	6	0	-5.247829	-3.541419	0.178316
14	8	0	-2.648757	-0.968036	0.681483
15	6	0	4.137268	2.723604	-0.119487
16	6	0	3.339917	2.973827	-1.331793
17	6	0	3.126159	4.296223	-1.781569
18	6	0	2.417891	4.567739	-2.946053
19	6	0	1.901076	3.517381	-3.712809
20	6	0	2.090781	2.198144	-3.297498
21	6	0	2.791371	1.941221	-2.122717

22	8	0	3.030234	0.597005	-1.806231
23	6	0	3.819068	1.704841	0.817462
24	6	0	4.558943	1.514760	1.980053
25	6	0	5.653376	2.335009	2.237187
26	6	0	5.997135	3.354018	1.330805
27	6	0	5.248031	3.541327	0.178446
28	8	0	2.648816	0.968079	0.681566
29	1	0	-3.508626	-5.117762	-1.185230
30	1	0	-2.270102	-5.596046	-3.259848
31	1	0	-1.362387	-3.721261	-4.633170
32	1	0	-1.731405	-1.362330	-3.890152
33	1	0	-4.262203	-0.732685	2.669622
34	1	0	-6.230513	-2.195894	3.145566
35	1	0	-6.851876	-3.992465	1.529644
36	1	0	-5.534132	-4.313812	-0.527816
37	29	0	-0.000004	0.000131	-0.541750
38	15	0	-2.242148	0.078293	-0.539469
39	7	0	-2.929317	1.577759	-0.456333
40	6	0	-4.288201	2.015862	-0.957331
41	6	0	-2.098483	2.632108	0.244842
42	6	0	-5.458998	1.215195	-0.389830
43	6	0	-4.307457	2.168340	-2.484124
44	6	0	-2.739130	3.083294	1.554442
45	6	0	-5.997849	1.587794	0.854414
46	6	0	-7.139149	0.965054	1.349522
47	6	0	-7.767212	-0.050444	0.608848
48	6	0	-7.240194	-0.433489	-0.626248
49	6	0	-6.095163	0.188643	-1.120248
50	6	0	-3.390910	4.316027	1.688464
51	6	0	-3.973562	4.685318	2.905450
52	6	0	-3.903465	3.831099	4.005601
53	6	0	-3.242312	2.604410	3.887433
54	6	0	-2.667223	2.236999	2.672155
55	6	0	-1.714321	3.761453	-0.717374
56	1	0	-4.391258	3.015769	-0.529152
57	1	0	-1.163653	2.124088	0.520294
58	1	0	-4.171214	1.217084	-3.000966
59	1	0	-3.511346	2.845021	-2.806942
60	1	0	-5.265283	2.597342	-2.796130
61	1	0	-5.536268	2.390481	1.421386

62	1	0	-7.559444	1.282183	2.299466
63	1	0	-8.671836	-0.518132	0.986119
64	1	0	-7.729611	-1.205672	-1.211832
65	1	0	-5.713285	-0.101049	-2.092577
66	1	0	-3.441664	5.007615	0.853076
67	1	0	-4.472772	5.645923	2.991477
68	1	0	-4.348192	4.122671	4.952377
69	1	0	-3.165942	1.942596	4.745607
70	1	0	-2.152255	1.281321	2.591996
71	1	0	-2.580495	4.306870	-1.101961
72	1	0	-1.072630	4.481400	-0.199826
73	1	0	-1.164168	3.358622	-1.573829
74	15	0	2.242135	-0.078184	-0.539426
75	7	0	2.929209	-1.577694	-0.456321
76	6	0	4.288057	-2.015878	-0.957346
77	6	0	2.098319	-2.631987	0.244880
78	6	0	5.458914	-1.215288	-0.389863
79	6	0	4.307277	-2.168348	-2.484140
80	6	0	2.739005	-3.083278	1.554426
81	6	0	5.997797	-1.587955	0.854346
82	6	0	7.139142	-0.965279	1.349435
83	6	0	7.767222	0.050217	0.608773
84	6	0	7.240177	0.433324	-0.626292
85	6	0	6.095100	-0.188740	-1.120270
86	6	0	3.390895	-4.315970	1.688297
87	6	0	3.973574	-4.685361	2.905239
88	6	0	3.903390	-3.831288	4.005498
89	6	0	3.242122	-2.604648	3.887483
90	6	0	2.667009	-2.237134	2.672246
91	6	0	1.713983	-3.761262	-0.717348
92	1	0	3.508880	5.117813	-1.185026
93	1	0	2.270362	5.596223	-3.259618
94	1	0	1.362548	3.721527	-4.632994
95	1	0	1.731460	1.362554	-3.890058
96	1	0	4.262286	0.732554	2.669663
97	1	0	6.230693	2.195628	3.145625
98	1	0	6.852130	3.992226	1.529762
99	1	0	5.534368	4.313727	-0.527664
100	1	0	4.391059	-3.015794	-0.529173
101	1	0	1.163560	-2.123881	0.520409

102	1	0	4.171044	-1.217083	-3.000971
103	1	0	3.511143	-2.845008	-2.806945
104	1	0	5.265086	-2.597368	-2.796171
105	1	0	5.536201	-2.390640	1.421309
106	1	0	7.559456	-1.282458	2.299353
107	1	0	8.671879	0.517853	0.986027
108	1	0	7.729608	1.205504	-1.211869
109	1	0	5.713202	0.100998	-2.092578
110	1	0	3.441716	-5.007449	0.852824
111	1	0	4.472870	-5.645932	2.991149
112	1	0	4.348137	-4.122940	4.952241
113	1	0	3.165680	-1.942952	4.745742
114	1	0	2.151947	-1.281497	2.592206
115	1	0	2.580082	-4.306735	-1.102026
116	1	0	1.072275	-4.481177	-0.199775
117	1	0	1.163794	-3.358355	-1.573744

References for Chapter 4

1 Reviews: (a) Feringa, B. L. *Acc. Chem. Res.* **2000**, *33*, 3436-3453. (b) Alexakis, A.; Benhaim, C. *Eur. J. Org. Chem.* **2002**, 3221.

2 (a) Feringa, B. L.; Pineschi, M.; Arnold, L. A.; Imbos, R.; de Vries, A. H. M. *Angew. Chem. Int. Ed.* **1997**, *36*, 2620. (b) Feringa, B. L.; Naasz, R.; Imbos, R.; Arnold, L. A. In *Modern Organocopper Chemistry*, Krause, N., Ed.; Wiley-VCH: Weinhiem, 2002; pp. 224-258. (c) Alexakis, A.; Rosset, S.; Allamand, J.; March, S.; Guillen, F.; Benhaim, C. *Synlett* **2001**, 1375. (d) Hua, Z.; Vassar, V. C.; Choi, H.; Ojima, I. *Proc. Nat. Acad. Sci. U.S.A.* **2004**, *101*, 5411.

3 (a) Sewald, N.; Wendisch, V. *Tetrahedron: Asymmetry* **1998**, *9*, 1341. (b) Alexakis, A.; Benhaim, C. *Org. Lett.* **2000**, *2*, 2579. (c) Alexakis, A.; Benhaim, C.; Rosset, S.; Humam, M. *J. Am. Chem. Soc.* **2002**, *124*, 5262. (d) Duursma, A.; Minnaard, A. J.; Feringa. B. L. *Tetrahedron* **2002**, *58*, 5773. (e) Choi, H.; Hua, Z.; Ojima, I. *Org. Lett.* **2004**, *6*, 2689. (f) Cote, A.; Lindsay, V. N. G.; Charette, A. B. *Org. Lett.* **2007**, *9*, 85.

4 Reviews: (a) Gellman, S. H. *Acc. Chem. Res*. **1998**, *31*, 173. (b) Cheng, R. P.; Gellman, S. H.; DeGrado, W. F. *Chem. Rev.* **2001**, *101*, 3219.

5 (a) Hagiwara, H.; Anthony, N. J.; Stout, T. J.; Clardy, J.; Schreiber, S. L. *J. Am. Chem. Soc.* **1992**, *114*, 6568. (b) Salamonczyk, G. M.; Han, K.; Guo, Z-.W.; Sih, C. J. *J. Org. Chem.* **1996**, *61*, 6893.

6 Mikhel, I. S.; Bernardinelli, G.; Alexakis, A. *Inorg. Chim. Acta.* **2006**, 1826.

7 Wakabayashi, K.; Aikawa, K.; Mikami, K. *54th Symposium on Organometallic Chemistry, Japan* PB 256, October 27-28, 2007.

8 (a) Rimkus, A.; Sewald, N. *Org. Lett.* **2002**, *5*, 79. (b) Eilitz, U.; Leβmann, F.; Seidelmann, O.; Wendisch, V. *Tetrahedron: Asymmetry* **2003**, *14*, 189. (c) Eilitz, U.; Leβmann, F.; Seidelmann, O.; Wendisch, V. *Tetrahedron: Asymmetry* **2003**, *14*, 3095.

9 (a) Juaristi, E. *Enantioselective Synthesis of β-Amino Acids*; Wiley-VCH: New York, 1996. (b) Appella, D. H.; Barchi, J. J., Jr.; Durell, S. R.; Gellman, S. H. *J. Am. Chem. Soc.* **1999**, *121*, 2309. (c) Hoffmann, T.; Gmeiner, P. *Synlett* **2002**, 1014.

10 Palais, L.; Mikhel, I. S.; Bournaud, C.; Falciola, C. A.; Vuagnoux-d'Augustin, M.; Rosset, S.; Bernardinelli, G.; Alexakis, A. *Angew. Chem. Int. Ed.* **2007**, *46*, 7462.

11 Chatfield, D. C.; Augsten, A.; D'Cunha, C.; Lewandowska, E.; Wunk, S. F. *Eur. J. Org. Chem.*

2004, 313.

12 (a) Zhang, H.; Gschwind R. M. *Angew. Chem. Int. Ed.* **2006**, *45*, 6391. (b) Zhang, H.; Gschwind R. M. *Chem. Eur. J.* **2007**, *13*, 6691.

13 (a) Krause, N.; Gerold, A. *Angew. Chem. Int. Ed.* **1997**, *36*, 186. (b) Nakamura, E.; Mori, S. *Angew. Chem. Int. Ed.* **2000**, *39*, 3750. (c) Woodword, S. *Chem. Rev.* **2000**, *29*, 393.

14 (a) Rimkus, A.; Sewald, N. *Org. Lett.* **2002**, *5*, 3289. (b) Rimkus, A.; Sewald, N. *Synthesis* **2004**, 135.

15 Lucet, D.; Sabelle, S.; Kostelitz, O; Le Gall, T.; Mioskowski, C. *Eur. J. Org. Chem.* **1999**, 2583.

16 Davis, T. J.; Balsells, J.; Carroll, P. J.; Walsh, P. J. *Org. Lett.* **2001**, *3*, 2161.

17 Shintani, R.; Fu, G. C. *Org. Lett.* **2002**, *4*, 3699.

18 Schäfer, H.; Seebach, D. *Tetrahedron* **1995**, *51*, 2305.

19 Mampreian, D. M.; Hoveyda, A. H. *Org. Lett*. **2004**, *6*, 2829.

20 Solymár, M.; Liljeblad, A.; Lázár, L; Fülöp F.; Kanerva L.T. *Tetrahedron: Asymmetry* **2002**, *13*, 1923.

5-1. Summary

The fundamental question about the generation of homo-chirality in Nature has long received widespread attention, and spontaneous resolution of achiral compounds has been examined by principally crystallographic analysis. Achiral compounds with free rotational bonds are conformationally mobile in a solution phase due to rapid interconversion between the conformations (Scheme 5-1). However, some conformationally mobile compounds, such as butane- and benzophenone-derived compounds, have been reported to adopt a single chiral conformation in a crystalline phase. These compounds chirally controlled can also be used as asymmetric catalysts. The catalysts chirally controlled can provide enantiomerically enriched products via enantiomeric fluctuation resulted from the external chiral bias. Therefore, the chirality control of conformationally mobile compounds is one of the most intriguing topics in view of the symmetry breaking.

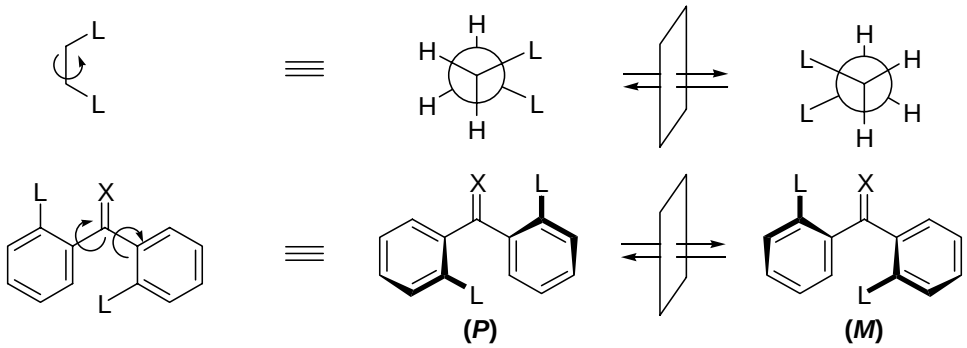

Scheme 5-1.

The author thus focused on the chirality control of conformationally mobile (*tropos*) compounds and the application to catalytic asymmetric reactions. The addition of chiral activators is useful to generate the chiral conformation of *tropos* ligands in asymmetric catalysts in a solution phase and to increase the catalytic activity and enantioselectivity of the parent asymmetric catalysts. In case of the *tropos* catalysts, the chirality control instantaneously completes and the unique chiral conformation and self-adaptation provide their great advantage over *atropos* catalysts in terms of catalytic activity and enantioselectivity in asymmetric catalyses. There are various chiral conformations in *tropos* catalysts and the chiral conformation can be changed by the chirality controlling method. Therefore, the chirality control of *tropos* catalysts is expected to be applied in various reactions.

In Chapter 2, the author has reported that Rh and Ru complexes with benzophenone-derived ligand **2a** could be instantly controlled in a single chiral conformation. Compared to one single bond rotation of BIPHEP, two single bond rotations of a benzophenone-derived ligand **2a** are more facile. The chirality control of BIPHEP complexes often needs treatment of heat for several hours. On the other hand, the chirality control of complexes with **2a** could be attained at room temperature within minutes (Scheme 5-2).

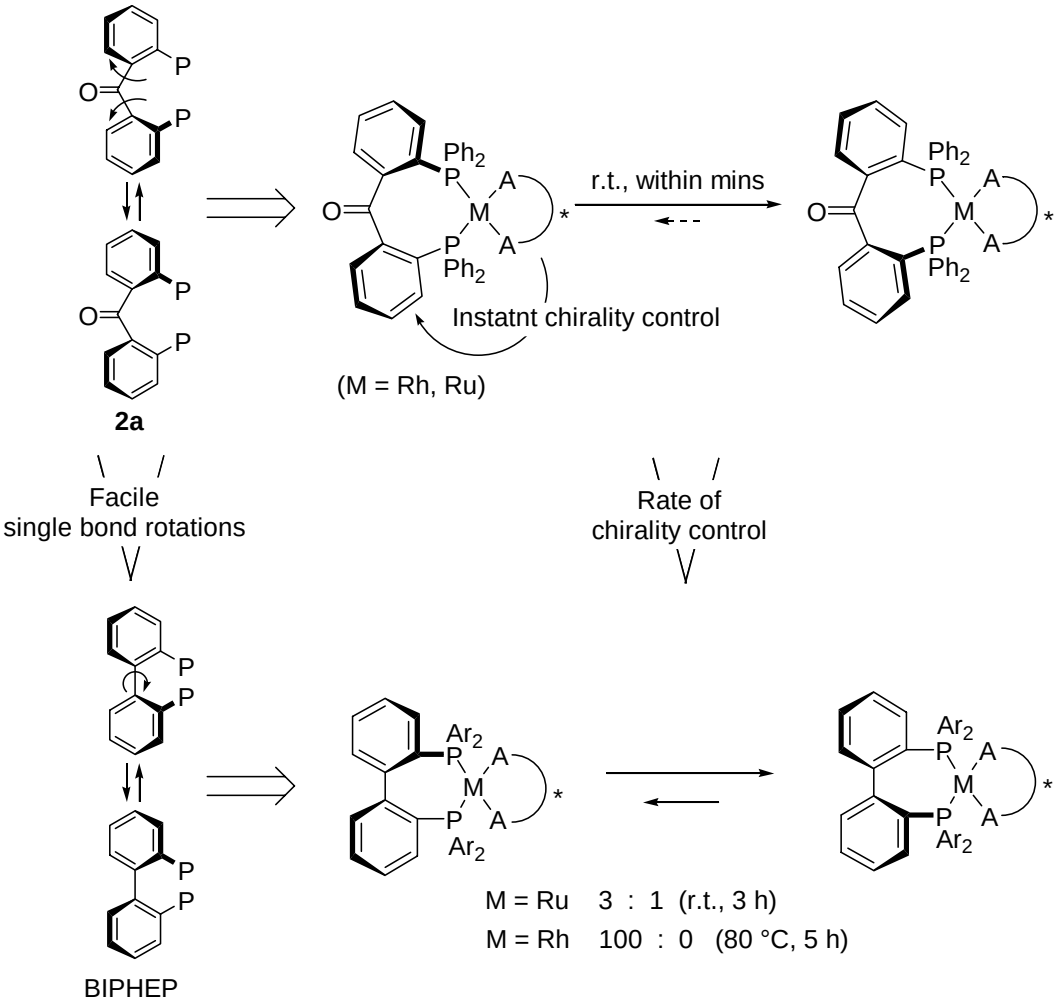

Scheme 5-2.

The X-ray structural analysis of [RuCl(OTf)(**2a**){(*S*,*S*)-dpen}]$_2$AgOTf showed the chiral conformation of **2a** in the metal complex (Figure 5-1). Figure 5-1 also shows the C_1-conformation of benzophenone skeleton of **2a**, which adopts a helical propeller conformation. The C_1-conformation can not be obtained biphenyl- and binaphthyl-derived ligands, and the complexes chirally controlled

with **2a** show distinct catalytic activity and enantioselectivity in asymmetric reactions.

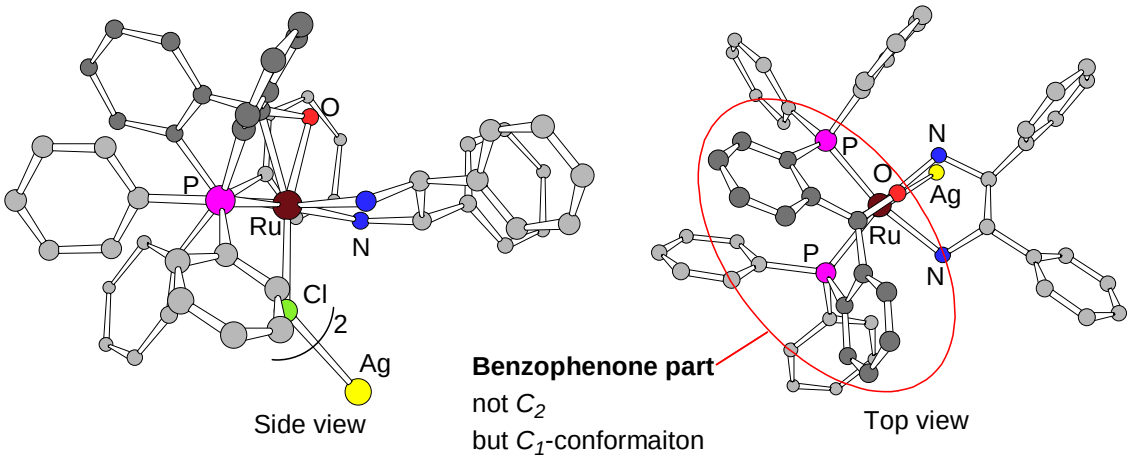

Figure 5-1. X-ray structural analysis of [RuCl(OTf)(**3a**){(*S*,*S*)-dpen}]$_2$AgOTf

The complexes with **2a** chirally controlled attained high catalytic activity and enantioselectivity in catalytic asymmetric hydrogenations. In asymmetric transfer hydrogenation of 1-acetonaphthone, the Rh-**2a** complex chirally controlled afforded higher enantioselectivity (>99%, 99% *ee*) than those attained by the enantiopure BINAP counterpart (Scheme 5-3).

Transfer hydrogention with Rh complex

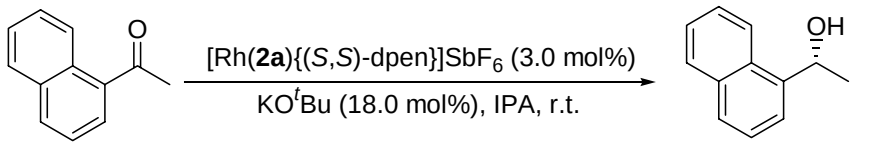

>99%, 99% *ee*

[Rh{(*R*)-binap}{(*S*,*S*)-dpen}]SbF$_6$: 98%, 72% *ee*

Scheme 5-3.

Asymmetric hydrogenation with Ru-**2a** complex chirally controlled also attained higher catalytic activity and enantioselectivity than with Ru-BINAP complex (Scheme 5-4). In addition, the Ru-**2a** complex with a silver salt attained high catalytic activity and enantioselectivity in asymmetric hydrogenations of both 1-acetonaphthone (>99%, 96% *ee*) and 9-acetylanthracene (95%, 91% *ee*). BINAP-Ru/DPEN complex had to be changed in the absolute configuration of BINAP counterpart in order to afford high enantioselectivities for both products. In sharp contrast, the Ru-**2a** complex with

silver salt is estimated to interconvert between *cis* and *trans* conformations. Each conformation was instantly controlled in a single chiral form and attained high catalytic activity and enantioselectivity to fit well with the substrate change (*trans* conformation: hydrogenation of 1-acetonaphthone, *cis* conformation: hydrogenation of 9-acetylanthracene). The high enantioselectivities with **2a** complexes exemplifies the advantage of the induced-fit catalyst with self adaptation.

(a) Hydrogention with Ru-2a complex

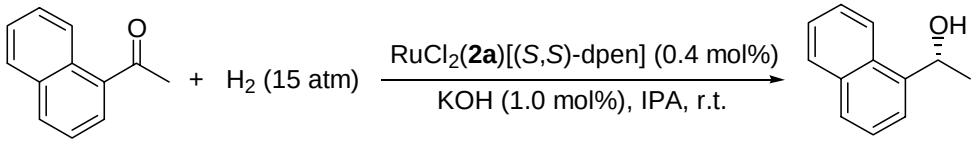

>99%, 99% *ee*

$RuCl_2$[(*S*)-tolbinap][(*S*,*S*)-dpen] : >99%, 98% *ee*

(b) Hydrogention with Ru-2a complex with silver salt

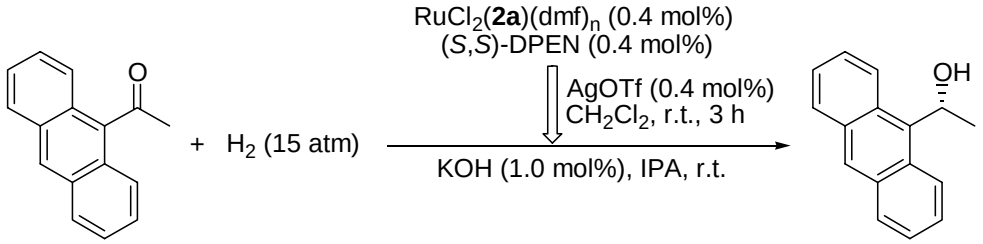

95%, 91% *ee*

$RuCl_2$[(*R*)-tolbinap][(*S*,*S*)-dpen] : 99%, 81% *ee*

Yield/*Ee*	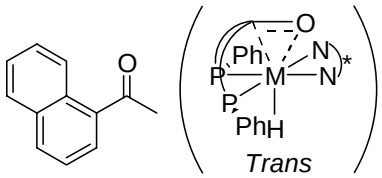 *Trans*	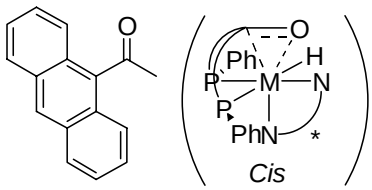 *Cis*
2a + AgOTf (1.0 eq.)	**>99%/96% *ee* (*R*)**	**95%/91% *ee* (*R*)**
(*S*)-BINAP	>99%/97% *ee* (*R*)	91%/41% *ee* (*R*)[a]
(*R*)-BINAP	>99%/14% *ee* (*S*)	99%/81% *ee* (*R*)[a]

a. tolBINAP was used instead of BINAP. Reaction temperature was 80 °C.

Scheme 5-4.

In Chapter 3, the author has reported that chirality control of achiral benzophenone-like monodentate ligands upon addition of chiral activator. Similar to the bidentate benzophenone-derived ligands, monodentate benzophenone-like ligands can be controlled in their conformations upon addition of chiral activator (Scheme 5-5).

The chirality control of achiral phosphoramidite-RhCl/chiral diene complexes was thus examined. Similar to chirality control of achiral diphosphine ligands in metal complexes upon addition of chiral diamines, chiral dienes controlled the achiral phosphoramidites in a single chiral conformation.

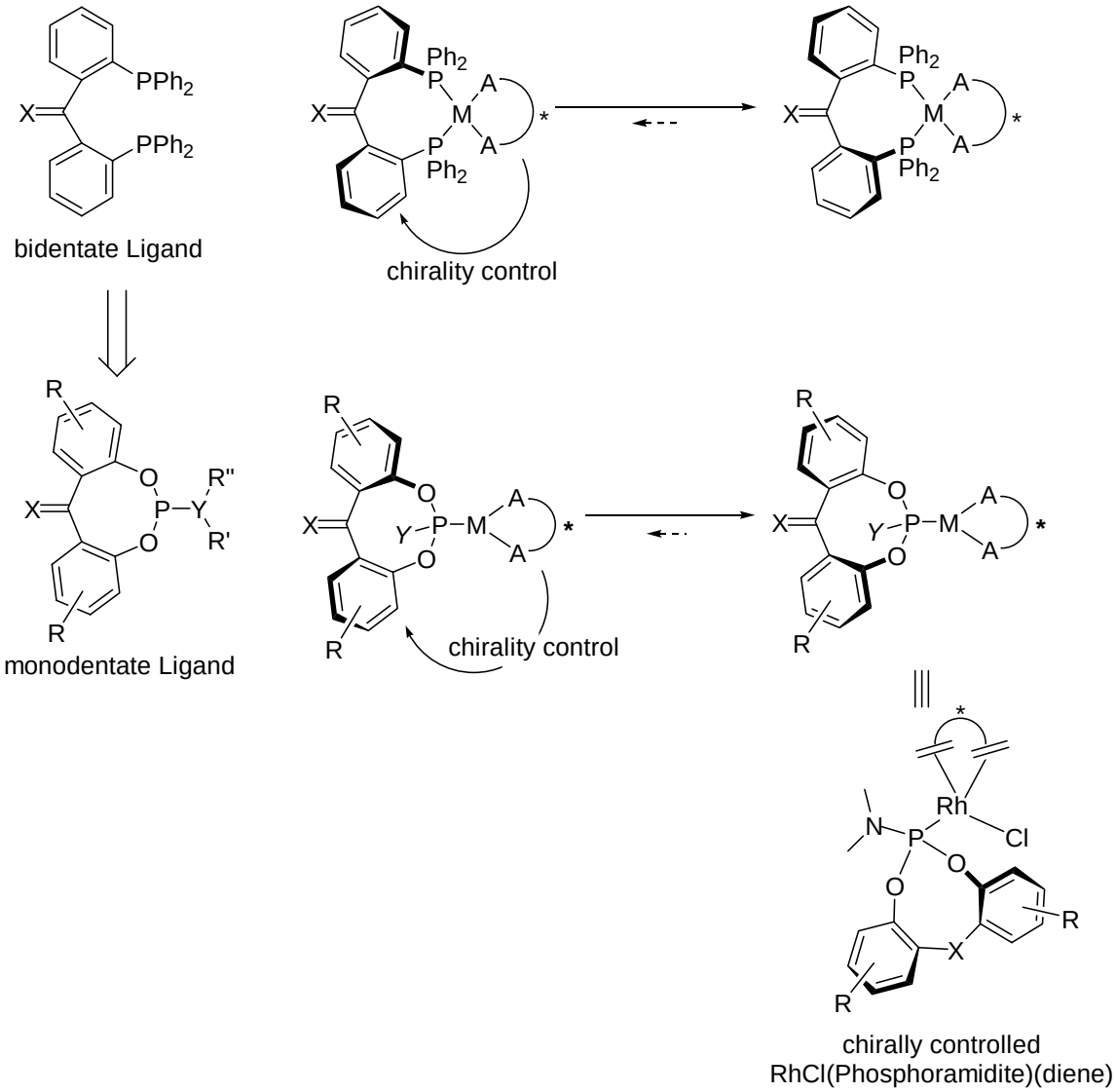

Scheme 5-5.

The most stable conformation of Rh complex with achiral phosphoramidite **3e'** and chiral diene **A'** was deduced with DFT calculations (Figure 5-2). The side view of Figure 5-2 shows that the achiral benzophenone-like phosphoramidite **3e'** adopts C_1-symmetric conformation. The front view shows that dimethylamine part of **3e'** stays away from xylyl part of **A'**.

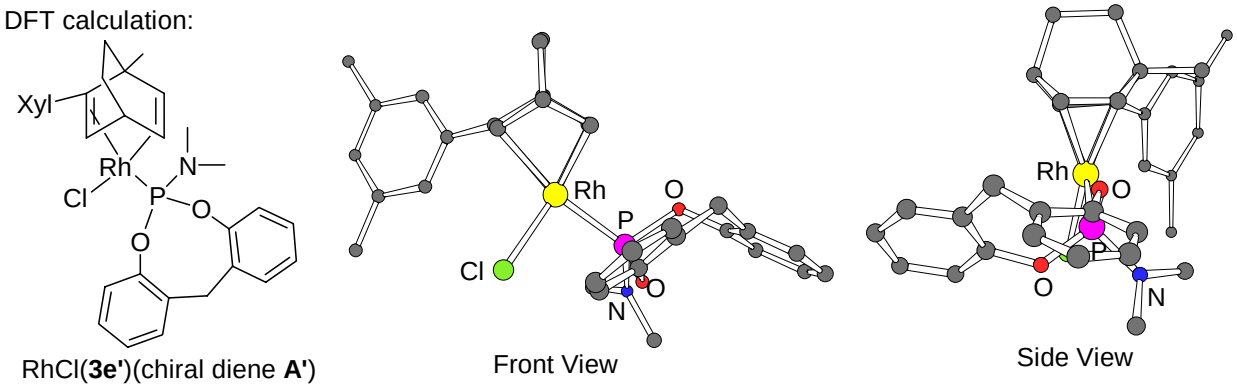

Figure 5-2. DFT calculation of RhCl(**3e'**)(chiral diene **A'**) complex

Chiral diene in Rh complex controlled the conformation of achiral phosphoramidite and afforded high catalytic activity and enantioselectivity in asymmetric Michael additions. In asymmetric Michael addition of 2-cyanoproionic acid *tert*-butyl ester, the Rh complex with chiral diene **A** and achiral benzophenone-like phosphoramidite **3e**^{1} gave the product in 95% yield with 86% *ee* (Scheme 5-6).

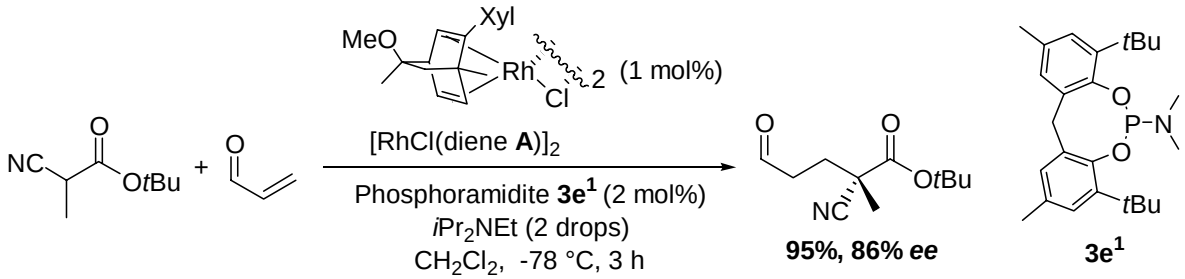

Scheme 5-6.

In Chapter 4, the author has reported that benzophenone-like phosphoramidites could be controlled to a single conformation by chiral amine built therein (Scheme 5-7), and attained high catalytic activity and enantioselectivity in asymmetric conjugate additions. The most stable conformation of the Pd complex with phosphoramidite **4a**^{2} was deduced by DFT calculations. Scheme 5-7 shows that Pd complex of **4a**^{2} adopts C_2 conformation and phosphoramidite **4a**^{2} in the Pd complex adopts C_1 conformation. These conformations were also proved from ^{1}H and ^{31}P NMR spectra.

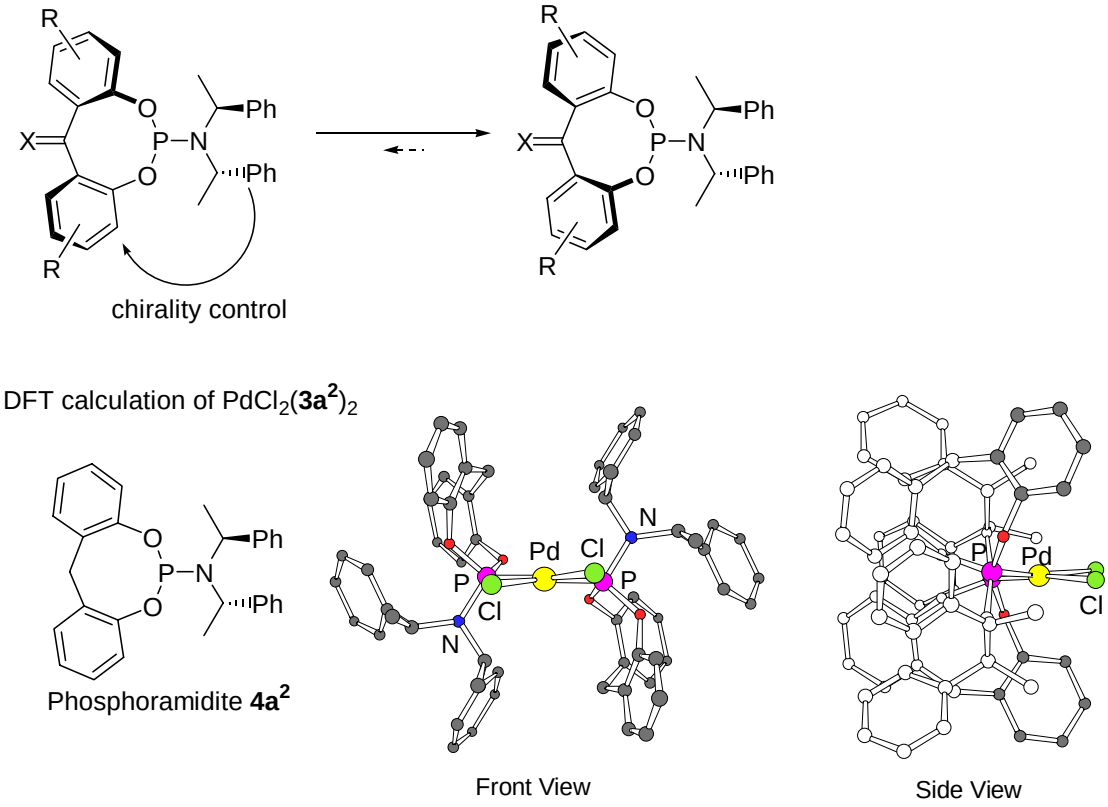

Scheme 5-7.

In the Cu-catalyzed conjugate addition to nitrostyrene- and nitroacrylate-derived substrates, phosphoramidite **4a**^{1} attained high catalytic activity and enantioselectivity (Scheme 5-8). The flexible benzophenone-like phosphoramidite **4a**^{1} outperforms the analogous rigid BINOL and BIPOL phosphoramidites.

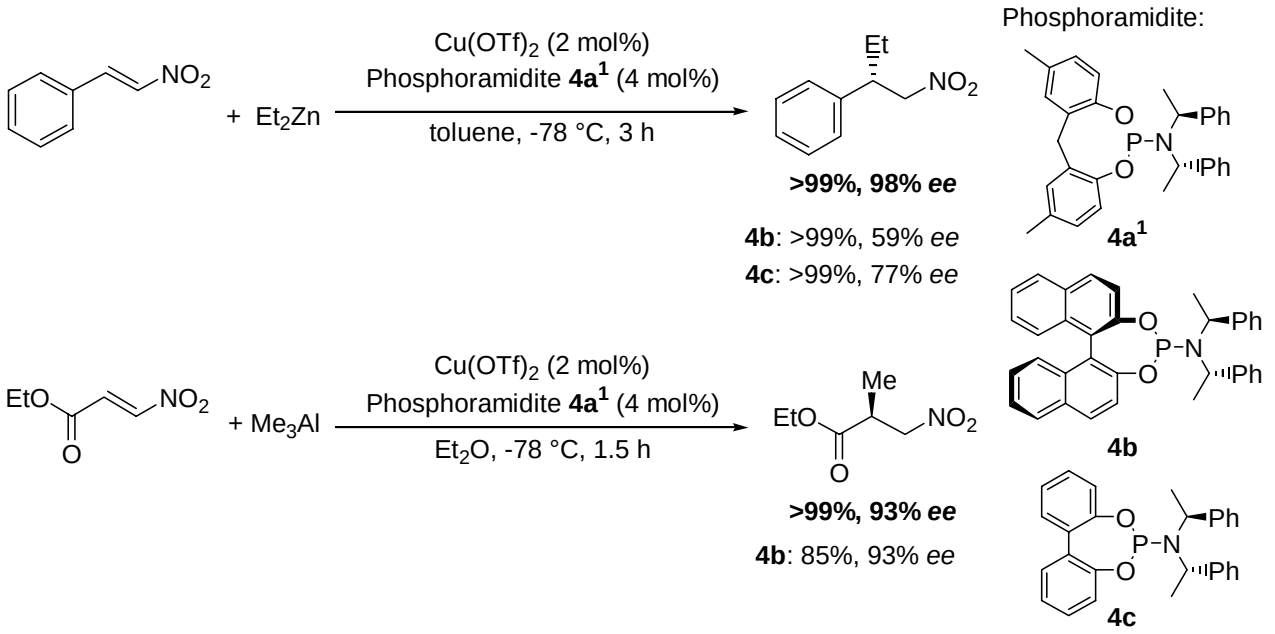

Scheme 5-8.

5-2. Outlook

In Chapter 2-4, the author has reported the chirality control of *tropos* benzophenone-derived ligands. Needless to say, other *tropos* ligands can adopt a chiral conformation in a solution phase and show advantageous properties over *atropos* ligands. In modification of benzophenone-derived diphenylphosphine ligand, the addition of one more triphenylphosphine part was also examined to synthesize C_3-symmetric *tropos* ligands (Scheme 5-9).[1] Similar to benzophenone-derived ligand **2a**, the C_3-symmetric *tropos* ligand adopts a chiral propeller conformation. The C_3-symmetric *tropos* ligand can also be controlled in a single chiral conformation upon addition of chiral activator. C_3-symmetric *tropos* ligand **5a** has three free rotational single bonds between phenyl groups, and interconvert rapidly between the chiral conformations. It has been reported that disk shaped C_3-symmetrtic ligands self-assemble to form sandwich-shaped L_2M_3 complexes with appropriate metal ions (e.g. Ag^+).[2] C_3-symmetric ligand **5a** with metal sources (M = Pd, Pt, Rh) could also synthesize L_2M_3 complexes. The L_2M_3 complexes of **5a** rapidly interconverted between chiral (*P*)- and (*M*)-helical conformations.

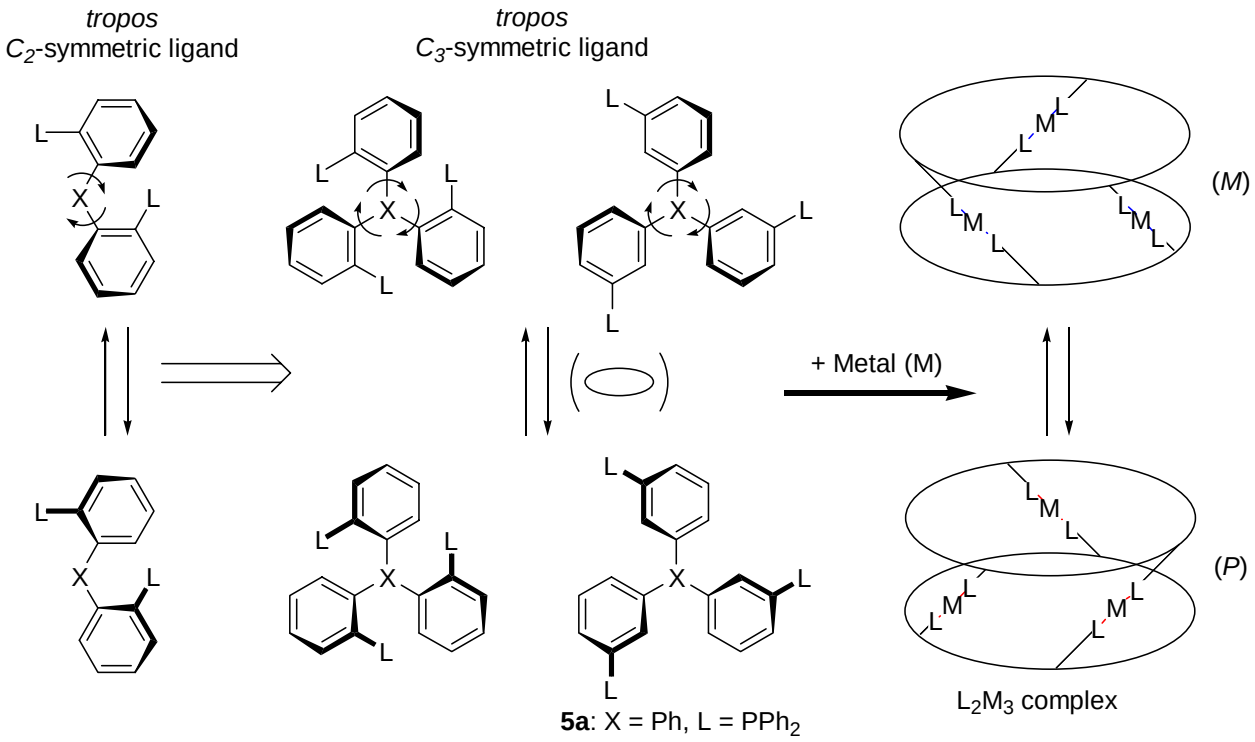

Scheme 5-9.

Although the resolution was not to good, the X-ray structural analysis of Pd_3Cl_6(**5a**)$_2$ showed that the L_2M_3 complex adopted D_3-symmetric conformation (Figure 5-3). In Figure 5-3, top view of Pd_3Cl_6(**5a**)$_2$ showed the C_3 helical conformation. On the other hand, side view of Pd_3Cl_6(**5a**)$_2$ showed the C_2-symmetric conformation around the Pd metal.

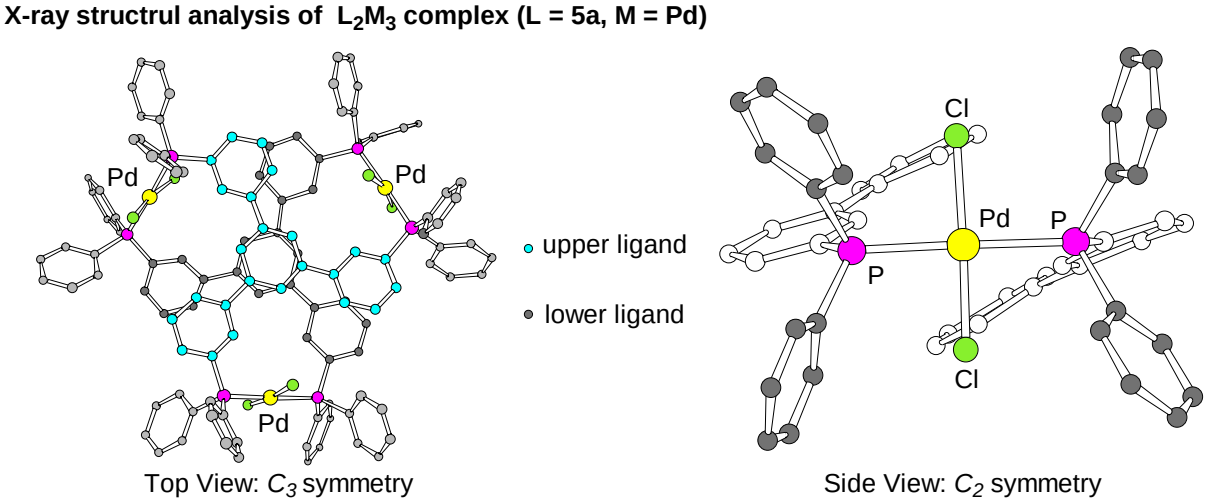

Figure 5-3. X-rat structural analysis of D_3-symmetric Pd_3Cl_6(**5a**)$_2$ complex

The chirality control of the L_2M_3 complex (L = **5a**, M = Rh) was also examined upon addition of (*S*,*S*)-DPEN. Similar to the benzophenone-derived ligand **2a**, the D_3-symmetric Rh_3(**5a**)$_2$ complex could be instantly controlled in a single chiral conformation upon addition of (*S*,*S*)-DPEN (Scheme 5-10). ^{31}P NMR spectrum of Rh_3(**5a**)$_2$ complex chirally controlled showed a doublet peak.

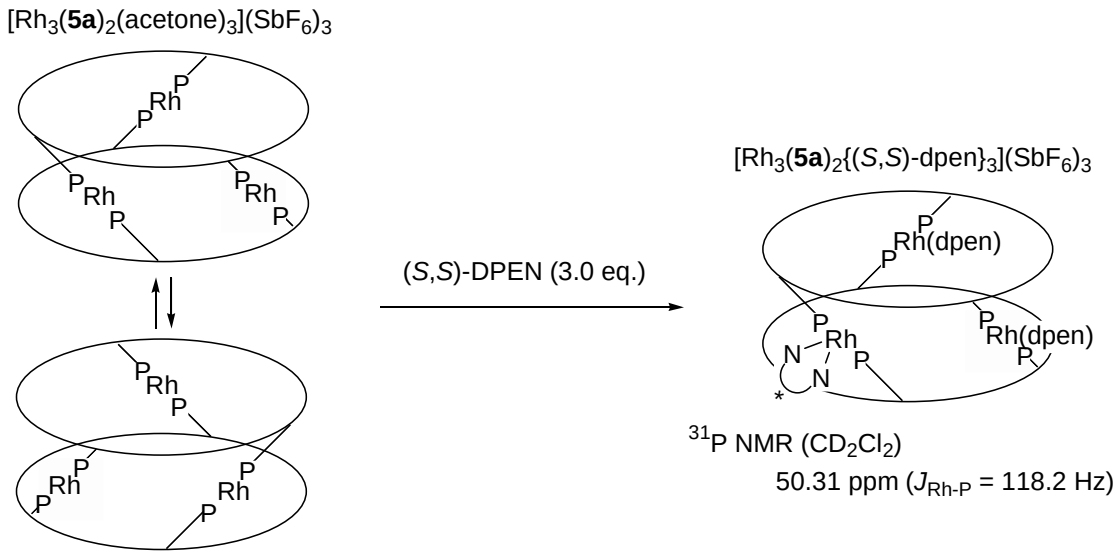

Scheme 5-10.

This result shows that C_3-symmetric *tropos* ligands can also be controlled to a single chiral conformation. Until now, the chirality control of C_3-symmetric ligands is succeeded only the L_2M_3 complex and the complex chirally controlled attains catalytic activity and enantioselectivity at a moderate level. However, chirality control of C_3-symmetric ligands is a new attempt and the C_3-helical conformation has possibility to show distinct catalytic activity from C_2-symmetric ligands, such as BIPHEP and BINAP, just like an advancement of C_1-symmetric benzophenone-derived complex.

Tropos acyclic ligands, such as chiraphos and skewphos, also show the advantage in asymmetric reactions. Chiraphos and skewphos is one of the butane and pentane-like compounds and possess two typical conformations, δ-conformation and λ-conformation.[3] The metal complexes with chiraphos and skewphos adopt δ-conformation favorably, because two methyl groups in equatorial orientation is more stable than the axial orientation in λ-conformation (Scheme 5-11).[4,5]

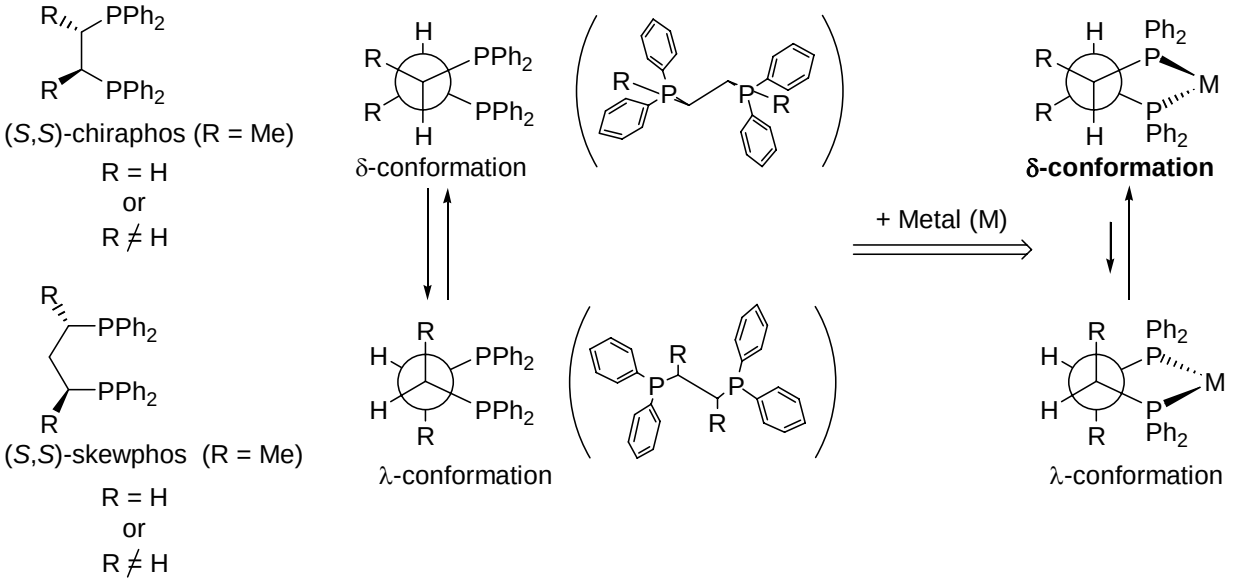

Scheme 5-11.

However, we have reported the catalytic asymmetric reactions with chiraphos and skewphos complexes to adopt λ-conformation. Heck-type reaction with (*S*,*S*)-chiraphos-Pd complex gave the product in 73% yield with 46% *ee* (*S*).[6] The sense of enantioselectivity was determined in terms of the steric repulsion between the equatorial phenyl group of chiraphos and the cyclopentene ring of the substrate. The (*S*)-enriched product should be obtained via λ-conformation, because the quadrants II and IV were occupied with equatorial phenyl groups (Scheme 5-12). When the substrate approaches to the catalyst, a steric repulsion could be maximized between equatorial methyl groups and equatorial phenyl groups in the δ-conformation of the chiraphos ligand. Therefore, the δ-conformation changes over to the λ-conformation because of the *tropos* nature of chiraphos.

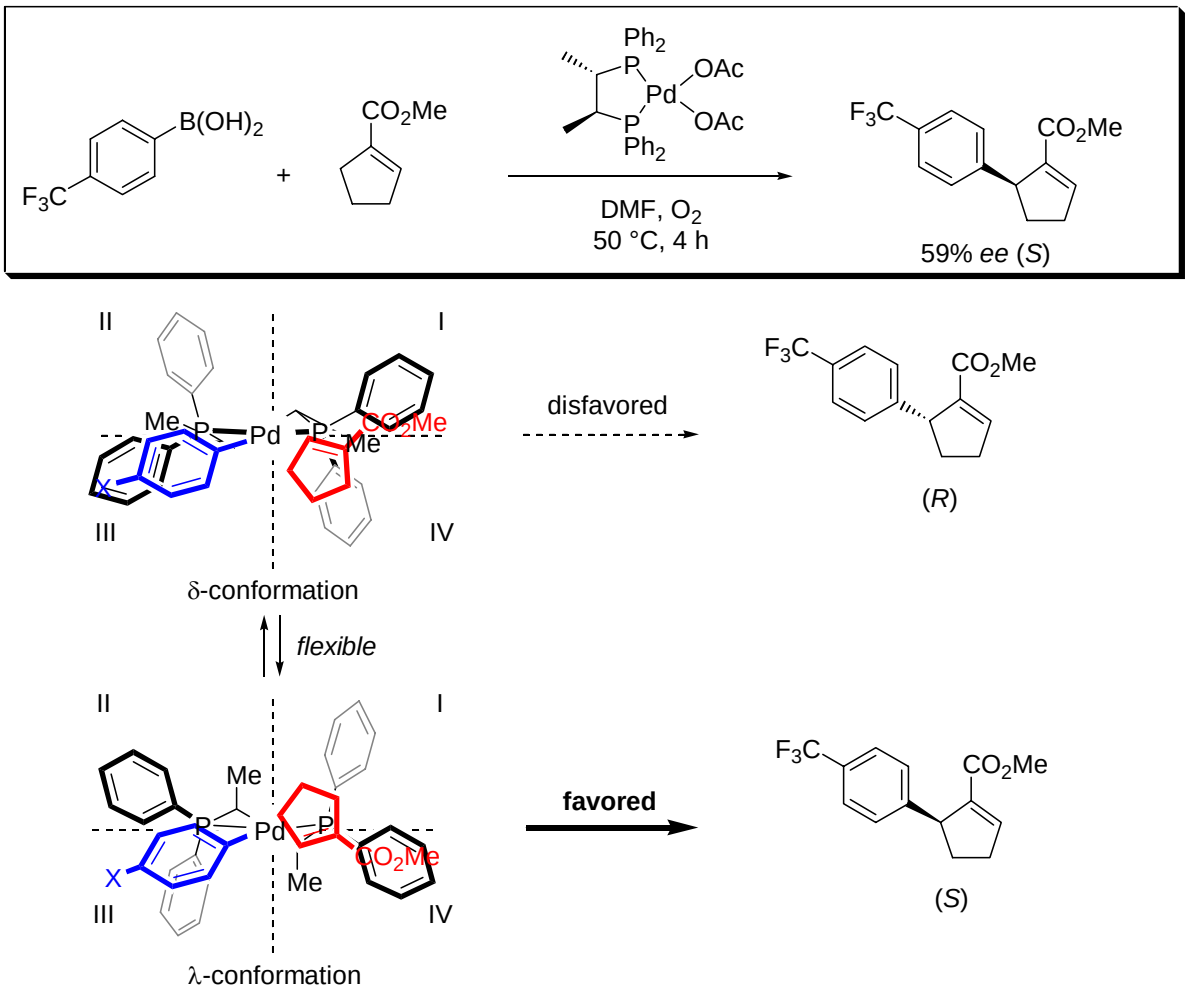

Scheme 5-12.

In case of (*S*,*S*)-skewphos-Rh complex, asymmetric ene-type cyclization of 1,6-eneyne substrate gave the product in 62% yield and 90% *ee* (*R*).[7] Similar to the Heck-type reaction with chiraphos-Pd complex, (*R*)-enriched cyclized product should be obtained via λ-conformation (Scheme 5-13). In the λ-conformation, the equatorial phenyl groups in the quadrant II and IV are in a bit horizontal because of the repulsion between two axial-methyl groups of skewphos and these phenyl groups. A vacant space is available for the bulky alkyl group of the substrate, leading to (*R*)-enriched product without conspicuous repulsions. The cyclization with (*S*,*S*)-skewphos-Rh complex also proves that (*S*)-BINAP-Rh complex, which has equatorial phenyl groups in the quadrant I and III, provides the (*S*)-enriched product (65% ee).

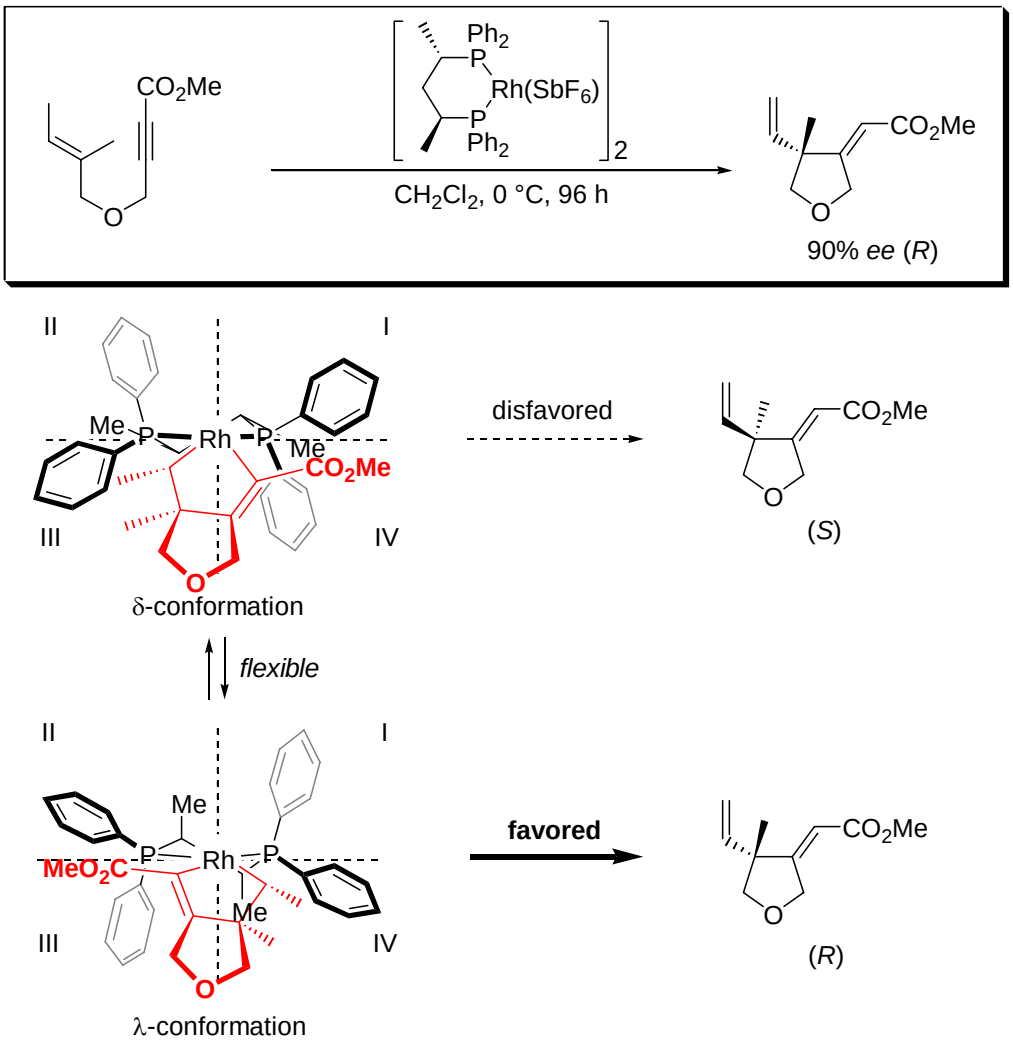

Scheme 5-13.

These results show the advantage of *tropos* acyclic ligands and the possibility to control chiraphos and skewphos complexes in disfavored λ-conformations upon addition of chiral activators. Until now, the control to λ-conformation were examine using BINOL,[8a] DM-BINOL,[8b] DABNTf and chiral diene, but unfortunately, these chiral activators could not completely control chiraphos and skewphos complexes in λ-conformation. Scheme 5-12 and 5-13 show that the λ-conformed complexes attain different chiral activity and enantioselectivity from δ-conformed complexes, because of a subtle conformational change of equatorial and axial phenyl groups. Therefore, the control to λ-conformation is an interesting topic, and the control with other chiral activators is worthwhile for further investigations.

References for Chapter 5

1 Wakabayashi, K.; Aikawa, K.; Mikami, K. *86th Spring Meeting* 2006, 3 H3-48.

2 (a) Kim, H.-J.; Moon, D.; Lah, M. S.; Hong, J.-I. *Angew. Chem. Int. Ed.* **2002**, *41*, 3174. (b) Hiraoka, S.; Harano, K.; Tanaka, T.; Shiro, M.; Shionoya, M. *Angew. Chem. Int. Ed.* **2003**, *42*, 5182. (c) Hiraoka, S.; Tanaka, T.; Shiro, M.; Shionoya, M. *J. Am. Chem. Soc.* **2004**, *126*, 1214.

3 Wakabayashi, K. *Bachelor Presentation*, Merch 3rd 2003, Tokyo Institute of Technology.

4 Chiraphos: Fryzuk, M. D.; Bosnich, B. *J. Am. Chem. Soc.* **1977**, *99*, 6262.

5 Skewphos: (a) Dehayes, L. J.; Busch, D. H. *Inorg. Chem.* **1973**, *12*, 1505. (b) Boucher, H.; Bosnich, B. *Inorg. Chem.* **1976**, *15*, 1471. (c) Bakos, J.; Tóth, I.; Heil, B.; Szalontai, G.; Párkányi, L.; Fülöp, V. *J. Organomet. Chem.* **1989**, *370*, 263.

6 Akiyama, K.; Wakabayashi, K.; Mikami, K. *Adv. Synth. Catal.* **2005**, *347*, 1569.

7 Mikami, K.; Yusa, Y.; Hatano, M.; Wakabayashi, K.; Aikawa, K. *Chem. Commun* **2004**, 98.

8 (a) Brunkan, N. M.; White, P. S.; Gagné, M. R. *Angew. Chem. Int. Ed.* **1998**, *37*, 1579. (b) Brunkan, N. M.; White, P. S.; Gagné, M. R. *J. Am. Chem. Soc.* **1998**, *120*, 11002.

List of Publication

1. Mikami, K.; Wakabayashi, K.; Aikawa, K.
   "Achiral" Benzophenone Ligand for Highly Enantioselective Ru-Catalysts in Ketone Hydrogenation
   Org. Lett. **2006**, *8*, 1517-1519.

2. Mikami, K.; Wakabayashi, K.; Yusa, Y.; Aikawa, K.
   Achiral Benzophenone Ligand–Rhodium Complex with Chiral Diamine Activator for High Enantiocontrol in Asymmetric Transfer Hydrogenation
   Chem. Commun. **2006**, 2365-2367.

3. Wakabayashi, K.; Aikawa, K.; Kawauti, S.; Mikami, K.
   Instant Chirality Control in Diphenylmethane-based Phosphoramidite Ligands: Highly Enantioselective Conjugate Addition to Nitroalkenes and Nitroacrylates
   J. Am. Chem. Soc. in press.

4. Mikami, K.; Yusa, Y.; Hatano, M.; Wakabayashi, K.; Aikawa, K.
   Enantioselective spiro ene-carbocyclization of 1,6-enynes catalyzed by *tropos* rhodium(I) complex with skewphos ligand.
   Tetrahedron **2004**, *60*, 4475-4480.

5. Mikami, K.; Yusa, Y.; Hatano, M.; Wakabayashi, K.; Aikawa, K.
   Highly Enantioselective Spiro Cyclization of 1,6-Enynes Catalyzed by Cationic Skewphos Rhodium(I) Complex
   Chem. Commun **2004**, 98-99.

6. Akiyama, K.; Wakabayashi, K.; Mikami, K.
   Enantioselective Heck-Type Reaction Catalyzed by tropos-Pd(II) Complex with Chiraphos Ligand
   Adv. Synth. Catal. **2005**, *347*, 1569-1575.

7. Mikami, K.; Kataoka, S.; Wakabayashi, K.; Aikawa, K.
   Chiral aminoalcohol NOBIN for instantaneous chirality control of racemic but tropos BIPHEP–Rh(I)-complexes: highly enantioselective ene-type cyclization of 1,6-enynes catalyzed by the Rh(I)-complexes without use of acid
   Tetrahedron Lett. **2006**, *47*, 6361-6364.

Acknowledgements

I would like to firstly thank my supervisor Professor Koichi Mikami who does deserve my greatest thanks, since he provided me with incredible support, encouragement and guidance in development of my research work for six years.

I would like to express my gratitude to Professor Masahiro Yamanaka (now in Rikkyo University) for his guidance and encouragement.

I would like to thank Dr. Kohsuke Aikawa for valuable and enjoyable discussion. And also for spending the same time in the laboratory throughout my research project.

I wish to thank Professor Susumu Kawauti for giving me the opportunity to study computational chemistry.

I am indebted to Professor Hiroharu Suzuki, Professor Takao Ikariya, and Professor Katsuhiko Tomooka (now in Kyusyu University) and their group members for providing me the chance to use their facilities.

I am much obliged to Yukinori Yusa, Katsuhiro Akiyama, Shouhei Kataoka for their assistance on the research.

This thesis was enriched significantly by valuable discussion and assistances of all the members and the foregoers in the laboratory, especially Dr. Manabu Hatano (now in Nagoya University), Yoshimitsu Ito, Satoshi Tanaka, Takashi Miyamoto, Yuichi Tomita, Isao Kaito, Hitomi Kakuno, Yuuki Takabayashi, Masahfumi Kojima, Kumiko Fujita and Martial Vallet.

I appreciate Ms. Yumi Karasawa and Reiko Takahashi for her assistance in complex office works.

And finally, I would like to thank my parents, brother, aunt, uncle and grandmother for their assistance over the last 27 years.

March, 2008

Kazuki Wakabayashi